Experimental Optimization of Process Parameters to Obtain Class A Surface Finish in Resin Transfer Molding Process

by

Mohsan Haider Raja

Department of Mechanical Engineering
McGill University, Montreal

A thesis submitted in partial fulfillment of the requirements
for the degree of Doctor of Philosophy

November, 2005

Your file Votre référence
ISBN: 978-0-494-25236-9
Our file Notre référence
ISBN: 978-0-494-25236-9

ABSTRACT

Resin transfer molding (RTM) has great potential to become an efficient and economical process for fabricating large and complicated automotive composite structures. Low capital investment, excellent mechanical properties, closed mold processing, low pressure equipment, short cycle times and process versatility in component integration and assembly, make RTM very attractive for high volume automotive applications. However, a high class surface finish, required for exterior car body panels, is difficult to achieve with RTM. There are several material and process parameters that severely affect the surface quality of RTM molded components. One of the major contributing factors is the shrinkage related to the curing of thermoset resins. A volumetric shrinkage of 7-10% is common for polyester resins, which breaks the material's contact with the tool, resulting in poor surface finish. Low profile additives (LPA) are added to the polyester resin for shrinkage compensation; however the effects of LPA content on thermal, rheological and morphological properties of polyester resins, as well as surface finish aspects of resulting composites, are not well understood.

In this research, the influence of material and processing parameters on the surface finish is characterized through experimental design techniques. Analytical, experimental and numerical methods are employed to optimize processing conditions for class A finish quality and shorter cycle times. Specifically, the effects of LPA content on cure kinetics, cure shrinkage and morphological changes are investigated through differential scanning calorimetry (DSC), rheological and optical microscopic techniques. Models are developed to predict cure shrinkage, LPA expansion, cure kinetics and viscosity variations of the resin. These models are then incorporated in commercial software to predict resin flow, degree-of-cure evolution and pressure variations during cure. Analytical and numerical simulation results are then validated with the experimental data. Processing windows defined for different process parameters based on analytical and numerical analyses are further used in the test matrices designed through the Taguchi

method. Analysis of variance (ANOVA) and multiple regression analyses are carried out on the surface roughness of test samples molded under varying conditions. The relative influence of the most significant parameters is characterized and empirical models are developed to predict surface roughness. The effect of post-cure shrinkage on the surface roughness of the test samples is also investigated. Levels of the most significant process parameters are then set for a high class surface finish, minimum cost and short cycle times.

The results show that the LPA content had no significant effect on the cure kinetics; however cure shrinkage decreased non-linearly with increasing LPA content. LPA content at 10% was found to be the minimum amount for shrinkage compensation. LPA content ($\geq$10%) resulted in pressure increase and morphological changes during RTM manufacturing. A cure gradient was observed for low pressure injections which had a significant effect on the resin pressure and roughness. LPA was found to be the most influential parameter affecting surface finish. A minimum of 10% LPA was required for class A surface finish. Higher injection pressures and filler content improved surface quality, whereas styrene content, cure rate and temperature gradient had no effect on the surface roughness in the range tested. A direct relationship was observed between LPA content, final cure shrinkage, resin pressure and surface finish.

RÉSUMÉ

La fabrication de pièces de grande dimension à géométrie complexe pose un défi de taille aux fabricants de pièces en matériaux composites pour l'industrie automobile. Le procédé d'injection sur renforts (RTM) permet de fabriquer de telles pièces de façon économique. En effet, ce procédé requiert un investissement initial faible, utilise une pression d'injection relativement basse et produit des pièces ayant de bonnes propriétés mécaniques. De plus, le procédé RTM devient intéressant pour la production de pièces automobiles car il permet d'atteindre des temps de production très courts et nécessite un moule fermé qui peut être aisément modifié. Cependant, les pièces de carrosseries pour l'automobile doivent avoir un fini de surface parfait. Les matériaux utilisés et les paramètres de moulage influencent la qualité du fini de surface. Un des facteurs les plus importants pour la qualité du fini de surface est le retrait obtenu lors de la polymérisation de la résine thermodurcissable. En effet, le retrait d'une résine polyester peut varier de 7% à 10%. Ce phénomène crée un espace entre le moule et la surface de la pièce et par ce fait produit un mauvais fini de surface. Afin de diminuer le retrait, des agents thermoplastiques (LPA) sont ajoutés à la résine polyester. L'efficacité et les effets des agents thermoplastiques sur les propriétés thermiques, rhéologiques et morphologiques de la résine polyester sont peu connus.

Ce travail porte sur l'influence de la formulation des matériaux utilisés et des paramètres de moulage RTM sur la qualité du fini de surface. Des méthodes analytiques, expérimentales et numériques sont utilisées pour atteindre un fini de surface de classe A tout en réduisant les temps de cycle. L'effet de la concentration en LPA sur la cinétique de réticulation, le retrait et les changements morphologiques sont étudiés par calorimétrie différentielle à balayage (DSC), rhéologie et microscopie optique. Des modèles sont établis afin de prédire le retrait de la résine et la dilatation produite par les agents thermoplastiques. La cinétique de réticulation et l'évolution de la viscosité de la résine sont également modélisées. Ces modèles sont utilisés dans des logiciels

commerciaux pour prédire la l'écoulement de la résine dans le renfort, l'évolution du degré de polymérisation de la résine et l'évolution de la pression hydrostatique de la résine pendant la polymérisation. Les résultats des simulations sont comparés aux résultats expérimentaux ce qui permet de valider les modèles développés. La méthode Taguchi est utilisée pour définir une matrice d'essais d'après un groupe de paramètres choisis. Des analyses de variation (ANOVA) et de régression linéaire sont effectuées afin d'isoler les paramètres ayant le plus d'influence sur la rugosité de surface. Les conditions de moulage optimales permettant de réduire le temps de cycle et les coûts de moulage sont ensuite déterminées.

Les résultats confirment que le pourcentage en agents thermoplastiques (LPA) influence peu la cinétique de réticulation. De plus, le retrait diminue de façon non-linéaire avec une augmentation du pourcentage de LPA. Une concentration en LPA minimale de 10% est nécessaire pour compenser le retrait. Un pourcentage plus élevé entraîne une augmentation de la pression entre la pièce et le moule ainsi que d'importants changements morphologiques durant l'injection. Un gradient de polymérisation est observé pour des injections à basse pression ce qui influence la rugosité de surface de la pièce. Les résultats démontrent que paramètre ayant le plus d'influence sur la qualité de surface est la concentration du LPA. Un pourcentage minimale en LPA de 10% est nécessaire pour obtenir un état de surface de classe A. De plus, une augmentation de la pression d'injection et du pourcentage en charges améliore la qualité de l'état de surface. D'autres paramètres comme la concentration en styrène, la vitesse de réticulation et le différentiel de température des plateaux ont été étudiés. Ces paramètres n'ont pas contribué à des améliorations notables du fini de surface. Enfin, un lien direct a été observé entre la concentration du LPA, le retrait de la résine, la pression de la résine et le fini de surface.

ACKNOWLEDGEMENTS

First of all, I would like to express my sincere gratitude towards my supervisors; Dr. Pascal Hubert and Dr. Larry Lessard for their supervision, guidance, encouragement and kindness throughout this work. Thanks for being outstanding supervisors and cool guys. You helped me in understanding both the processing and manufacturing aspects of composite materials. I am grateful to Dr. Michael Debolt and Dr. Francois Trochu for their technical support and expert opinion during the course of this work. I am also thankful to Dr. Edu Ruiz and Eric St-Amant for their technical assistance on this project.

The Auto21 Network of Centers of Excellence and Ford Motor Inc. are gratefully acknowledged for the financial support. I would also like to thank students and staff at Ecole Polytechnique de Montreal and AMTC-NRC for their help with the equipment and measurements. Technical assistance from the members of McGill Composite Materials and Structures Laboratory is gratefully appreciated as well.

I would also like to thank Dr. Musa Kamal, Dr. Young-Mi Chung, Mr. Danny and Mr. Ed Siliauskus of McGill Chemical Engineering for providing lab facilities and assistance with the measurements and Mr. Michael Rioux of ETS for his expert opinion. I would like to express my extended and special thanks to my uncle Mr. Safdar Raja for helping me achieve my goals and the rest of my family and friends for their support, understanding and patience.

CONTRIBUTIONS OF THE AUTHORS

This is a manuscript-based thesis consisting of four journal papers. Titles of the research articles, names of authors and their contributions are listed below:

Cure Shrinkage Characterization and Modeling of a Polyester Resin Containing Low Profile Additives

Mohsan Haider, Pascal Hubert, Larry Lessard

This manuscript is the original work of Mohsan Haider, with the following exceptions. Dr. Pascal Hubert supervised the research, provided technical advice with the equipment setup and contributed in the analysis of data and manuscript editing. Dr. Lessard provided expert advice, supervised the work and contributed to the manuscript editing.

An Experimental Investigation for Class A Surface Finish in Resin Transfer Molding Process

Mohsan Haider, Pascal Hubert, Larry Lessard

This article is the original work of Mohsan Haider. Dr. Pascal Hubert supervised the research, provided technical advice and contributed in manuscript editing. Dr. Lessard provided expert advice, technical support with experimental setup, supervised the work and contributed to the manuscript editing.

Numerical Simulations for Class A Surface Finish in Resin Transfer Molding Process

Mohsan Haider, Eduardo Ruiz, Pascal Hubert, Larry Lessard

This manuscript is the original work of Mohsan Haider, with the following exceptions. Dr. Edu Ruiz contributed towards numerical modeling and assistance with the software. Dr. Pascal Hubert and Dr. Larry Lessard supervised the research, provided expert opinion and contributed in the editing process.

Optimization of RTM Processing Parameters for Class A Surface Finish

Mohsan Haider, Pascal Hubert, Larry Lessard

This manuscript is the original work of Mohsan Haider, with the following exceptions. Dr. Pascal Hubert and Dr. Larry Lessard supervised the research, provided expert opinion and contributed in the editing process.

TABLE OF CONTENTS

LIST OF FIGURES

LIST OF TABLES

LIST OF SYMBOLS

A	Constant
A_p, A_d	Reaction constants in free radical formulation
B	Constant
C_1, C_2	Constants
E	Activation energy
E_1, E_2	Activation energies in Kamal formulation
E_p, E_d	Activation energies in free radical formulation
E_m	Elastic modulus of the mold
E_r	Elastic modulus of the resin
[E]	Polyester concentration
F	Filler properties
f	Efficiency of the initiator
G_f	Shear modulus of the fibers
Hp	Hydrostatic pressure
[I]	Initiator concentration
$[I]_0$	Initial concentration of the initiator
K	Permeability of the porous media
k(T)	Rate constant
k_o	Arrhenius frequency factor
k_1,k_2	Arrhenius constants
k_p, k_d, k_z	Free radical frequency factors
k_{p0}, k_{d0}	Free radical constants
MSD	Mean-squared deviation
[M]	Unsaturated group concentration
$[M]_0$	Initial concentration of the monomer
m, n	reaction orders
n	Number of measurements

P	Pressure
∇P	Pressure gradient
Q	Heat generated during chemical reaction
Q_o	Total heat-of-reaction
dQ/dt	Rate of heat generation
R	Universal gas constant
[R]	Concentration of free radicals
R_a	Roughness
R_q	Square root of the arithmetical mean
R_y	Distance between highest and lowest point
S/N	Signal-to-noise ratio
[S]	Styrene concentration
T	Absolute Temperature
T_b	Constant
t	Time
t*	Gel time
v	Resin velocity
V_o	Original volume
V_{filler}	Volume fraction of filler
V^T	Total volumetric shrinkage for fully cured resin
ΔV	Change in volume
dV/dt	Rate of volume change
v_r	Poison's ratio of the composite
v_f	Fiber volume fraction
w_f	Weight fraction of the fibers
Y_i	Roughness profile deviation from the mean
Y_{max}	Highest point from the mean in roughness profile
Y_{min}	Lowest point from the mean in roughness profile
y_i	Output parameter for trial i in statistical calculations
$\bar{y}$	Mean of all y_i values
[Z]	Concentration of inhibitor

GREEK SYMBOLS

α	Degree-of-cure
α_f	Final degree-of-cure
α_G	Degree-of-cure at gelation
α_{max}	Maximum degree-of-cure
$\Delta\alpha$	Change in resin degree-of-cure
$d\alpha/dt$	Rate of cure
β_m	Volumetric thermal expansion coefficient of uncured resin
β_p	Volumetric thermal expansion coefficient of cure resin
$\dot{\gamma}$	Shear rate
$d\gamma/dt$	Shear rate
η	Viscosity
η_0	Initial viscosity
η_c	Viscosity under cure effects
η_f	Viscosity under filler effects
η_{sr}	Shear rate effects on viscosity
σ	Standard deviation
ϕ	Porosity of the reinforcement

CHAPTER 1

INTRODUCTION & MOTIVATION

1.0 Background

The automotive sector is facing the tough challenge of producing high quality, fuel efficient cars with a minimum impact on the environment. Government regulations are pushing car manufacturers to reduce fuel emissions and give higher mileage per unit of fuel used. These objectives are being achieved through three methodologies: by changing the engine and its assemblies to incorporate low emission fuels and bio-gases, by producing electric cars and by reducing the ultimate weight of the car. However, the weight reduction should not be accompanied by a loss of ultimate strength and stiffness.

The application of lightweight materials has shown significant possibilities for meeting the needs of auto designers. It is now, thus, essential to look upon the weight-to-power ratio as a fuel economy factor in addition to the vehicle performance index. In lightweight materials technology, plastics and polymer composites are finding growing importance in automobiles due to safety regulations, legislations on emission control and recent noise, vibration & harshness requirements [1]. Recently, the development of lighter automobiles has been of eminent importance for environmental preservation and reduced fuel consumption. By developing lighter materials for automobiles, engineers

and scientists hope to lessen the burden on engines. The result is more economical fuel use for better mileage and reduced carbon dioxide and nitrogen oxide emissions, leading to a lessened greenhouse effect.

1.1 Automotive Materials

These efforts in light weight materials have led to the introduction and continued implementation of plastics and a host of various composite materials. Much of this started in the early 1990s when the United States Council for Automotive Research [2] was developed as a consortium between automakers Chrysler, Ford and General Motors. Major shifts in the materials making up automobiles are not only of great importance to technologists in the raw materials industry, but it is also of keen interest to part suppliers. The challenge for automakers is to produce inexpensive, environmentally conscious vehicles that are safe, attractive and economical to operate.

Along with advances in tooling, machinery, component design and developments in fabrication methodology, come technological advances in materials. Composite materials have had the largest impact on how automotive designers select their materials. Resin producers are continually developing both new resins and variations on existing resins. One area getting particular attention today is the use of nano-composite technology to improve plastic performance in both physical properties such as stiffness and toughness as well as in scratch and fire resistance. Regardless of the promises, such new materials will be added to the production cycle only when they reduce costs and create competitive advantages. With massive investment in current manufacturing machinery primarily for use with metals, it is incumbent on alternative material industries to demonstrate that their materials and processes make economic and performance sense.

A major focus of automotive scientists is on developing new lightweight, high-strength materials and manufacturing technologies since fuel efficiency increases as a vehicle's weight decreases. In fact, researchers are aiming to cut vehicle weight by up to 40 percent or almost 600 kg from the weight of a current average mid-sized sedan.

- Current aluminum technology can cut half the weight out of a conventional body structure, although cost reduction is a major challenge.

- Polymer composites (any kind of plastics reinforced with glass, textile or other materials) offer design flexibility, strength, durability and significant weight savings. However, engineers still need to develop low-cost manufacturing technology.

1.1.1 Composites in Automotive Industry

The automotive sector is one of the major consumers of plastics and consumes over 8% of total domestic/engineering plastics manufactured in the world. The automotive engineers, designers and specifiers look at plastics as alternate materials, not simply as replacement materials. A consensus view of the automotive industry, based on technical merits, cost and benefits, makes plastics and composite materials a suitable candidate due to factors such as economy, weight reduction, styling potential, functional design, new effects, reduced maintenance and superior corrosion and chemical resistance.

In the automobile industry today, composite materials are used in applications as varied as car body panels (doors, roofs) [3-8], semi-structural parts (front bumpers) [9], and engine parts (cylinder-head covers) [7, 8]. The use of thermoplastic composite materials in the automotive industry, already used for under-the-hood components (radiator-tanks, heater-fan housings, cooling fans) [10], has recently witnessed a strong growth, with new applications such as intake manifolds, rocker covers, and engine thermostat parts [10]. Structural parts for front-ends and tailgate frames, mainly molded through the injection-compression or other injection technology, have also benefited from the advantages provided by composites. Most of the composites used for these applications are based on polyamide or polypropylene. The future of composites in car body panels lies in the improvement of conductive sheet molding compound (SMC) and surface varnishes that will make it possible to paint an entire body frame on the assembly line. Sandwich structures, based on composites are being tested and developed to replace metal structural parts. Composite materials remain well positioned in the heavy vehicle sector, as

transformation processes are more efficient and production costs lower, relative to those for automobiles.

1.2 Problem Statement

One low cost manufacturing process used to produce composite parts is Resin Transfer Molding (RTM). This process consists of injecting a thermoset resin at low pressure through a fibrous reinforcement placed in a mold cavity. Once the resin has impregnated the reinforcement, it goes through exothermic chemical reaction and the part can be de-molded at the end of this polymerization cycle. Although widely used in the aerospace industry, RTM is still not economical and feasible for high volume automobile industry. This is partly due to the difficulties related with process optimization, which requires an appropriate resin formulation for short cycle times, mold design, proper molding parameters selection and warpage prediction after molding. Also, for exterior car body panels it is difficult to achieve aesthetic appeal or surface quality in compliance with the industry specifications and standards without sacrificing the stiffness and strength of the part. Some of the common surface defects and possible contributing factors are listed in Table 1.1.

The automotive industry mainly uses unsaturated polyester (UP) resins because of low costs and fast reaction rates allowing short cycle times and economical high volume production. Unfortunately, a significant amount of chemical shrinkage is related with the curing of such resins, which is one of the major factors contributing towards poor surface finish. Seven to ten percent volumetric shrinkage has been reported for polyester resins, which, when used in actual manufacturing, leads to the material's loss of contact with the tool (mold). That is why the material is unable to achieve the surface quality of the mold and results in poor surface finish.

Table 1.1 Common surface defects and possible causes

Defects	**Possible Contributing Factors**
Pinholes	Coarse particles, particle agglomeration
Ripple or long range waviness	Resin shrinkage, glass fiber dispersion
Sink marks	Resin shrinkage, fiber distribution, fiber length, fiber orientation
Fabric print through	Resin shrinkage, fiber bundle integrity, strand dimensions, fiber distribution, high fiber volume fraction
Variable localized fiber volume fraction	Fiber washout due to high flow rates and injection pressures
Dark areas	Styrene loss from the surface
Pop up blisters in painted surfaces	Subsurface voids due to trapped air and volatiles
Dimensional inaccuracy	Warpage and resin shrinkage
Dry spots	Poor resin flow and impregnation, race tracking and edge flow, sharp corners in the mold
Resin overflow	Irregular resin film on the surface due to cure gradient
Rough surfaces	Poor mold finish
Dull surfaces	Mold coated with too much release agent or mold sealant

This shrinkage also results in fabric print through on the surface, which is another major contributing factor towards poor surface quality. These defects make it impossible to achieve high class finish and tight tolerances on car body panels in compliance with industry specifications and standards (known as class A surface finish) and thus makes RTM less attractive to the automobile industry. In order to increase the use and application of the RTM process and composite materials in the automotive sector, it is necessary to optimize the process to increase its competitiveness.

1.3 Project Objectives

The main objective of this study is to optimize material and processing conditions to obtain high class surface finish in RTM molded composite material components for the automotive industry. To control chemical shrinkage in unsaturated polyester resins, thermoplastic additives or low profile additives (LPA) are incorporated in the resin. However, this does not completely solve the problem of shrinkage. The formulation of low profile resins is difficult to optimize (based on the choice and proportion of the low profile additive), and the mechanism that compensates shrinkage is still not well-understood. Another objective of this research is to find an optimum type and quantity of LPA, which will compensate for cure shrinkage. Other technological problems related to the RTM process can be decomposed into four key areas; they all need to be optimized:

1. The understanding and modeling of thermal and resin cure kinetics phenomena during polymerization helps to predict the evolution of the chemical reaction and to optimize the cure of the resin. The two phenomena, respectively of physical and chemical in nature, are intimately connected. Temperature initiates and catalyzes the exothermic chemical reaction, which in turn modifies the heat transfer, and therefore changes the temperature.

2. A basic knowledge of viscosity and gel time variations under changing processing conditions is very crucial. Equally important is the understanding of resin shrinkage behavior with various amounts of LPA during isothermal cure cycles. A study of

these problems must be conducted to predict consequences of shrinkage and to optimize the process.

3. To obtain a part of good quality, without defects, successful injection of the resin through the reinforcement is essential. For this reason, the optimization of the resin injection and curing and mold pre-heating process is of paramount importance. Commercially available software PAM-RTM will be employed to model these problems.

4. Finally effects of processing parameters on the manufacturing cycles, cycle times and surface roughness need to be studied and optimized. Experimental design techniques offer promising results and will be employed.

1.4 Structure of the Thesis

This is a manuscript-based dissertation consisting of four journal articles. Material presented in these publications is in a logical flow sequence.

Literature review (chapter 2) presents a concise and complete bibliographic review of the recent research work in the area of RTM manufacturing and process simulations, thermal and rheological characterization and modeling of thermoset resins with and without various ingredients, statistical process optimization, the Taguchi method and measurement techniques for surface finish characterization.

Cure Shrinkage Characterization and Modeling of a Polyester Resin Containing Low Profile Additives (chapter 3) describes analytical techniques, measurement procedures, data and results for the thermal, rheological, morphological and cure shrinkage characterization and modeling of a polyester resin. Models developed, their estimated parameters and LPA shrinkage-expansion mechanisms are also described in this chapter.

An Experimental Investigation for Class A Surface Finish in Resin Transfer Molding Process (chapter 4) relates analytical results of previous chapter with manufacturing aspects of low profile based resins. This chapter explores the effects of LPA content and cure gradient on pressure variations during RTM manufacturing. The effects of the amount of accelerator and catalyst on the gel time variations are also presented here.

Numerical Simulations for Class A Surface Finish in Resin Transfer Molding Process (chapter 5) enlists simulations of complete RTM cycle. Mold pre-heating, mold filling, resin curing and pressure variation simulations are done under identical processing conditions are that of actual manufacturing discussed in chapter 4. The experimental validation of numerical results is also presented here.

Optimization of RTM Processing Parameters for Class A Surface Finish (chapter 6) outlines the test matrices designed based on design-of-experiment statistical procedures. Surface finish measurement technique is also presented in this chapter along with the analysis and optimization procedures and the results of DOE and multiple regression analysis.

Conclusion (chapter 7) gives a brief summery of this work. Conclusions are drawn based on the outcome of this study and future work in this area is proposed.

CHAPTER 2

LITERATURE REVIEW

2.0 Introduction

The fiber reinforced composite manufacturing process generally known as liquid composite molding (LCM) is a family of versatile processes to manufacture composite parts in the automotive, aerospace, railroad, marine and sports industries. It consists of three main sub-categories: resin transfer molding (RTM), structural reaction injection molding (SRIM) and compression molding. Of these, RTM is the focus of this study.

Resin transfer molding (RTM) is one of the most efficient, attractive and economical processes for high performance composite materials with low cost manufacturing. During the process, a thermoset resin is injected at low pressures (<700 kPa) into a mold cavity containing a pre-placed fiber preform or a stack of fiber mats of reinforcing material in the shape of the desired part. The resin impregnates the mold cavity to occupy the empty spaces between the fibers. The mold is usually heated to initiate a curing reaction, which is an exothermic resin polymerization phenomenon that cross-links the resin and results in a composite structure. A step-by-step diagram of the RTM process is shown in Figure 2.1. This process has been improved over the past years through automation and better control. RTM's ability to produce a wide variety of shapes at moderate cost makes it a very attractive process.

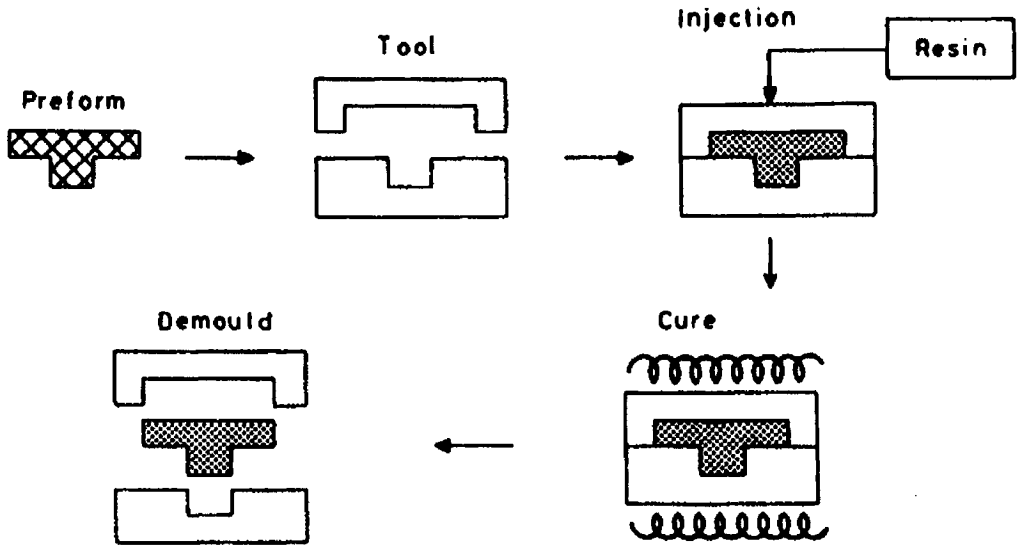

Figure 2.1 The RTM process (adapted from Strong [11]).

The main difference between RTM and SRIM is the resin system used by each process. SRIM uses a mixing activated resin system in which two or more reactive polymers are mixed in a mixing chamber and then injected into a mold. The resin reacts rapidly and forms a solid part immediately after the mold is filled with the resin. Therefore, the resin injection is performed under high pressure with mold filling times less than one minute. However the resin system used in RTM is activated thermally. Cross-linking between resin molecules takes place at a certain temperature. The temperature depends on the initiator system and may vary from one initiator to another. The mold filling time in RTM is of the order of minutes enabling one to use relatively low-pressure equipment for manufacturing. The RTM process has been successfully used in the development of various products for applications in automotive, marine, aerospace, defense, electrical, electronics and consumer product industries [11-25].

RTM has become an interesting method for producing high quality fiber reinforced composite parts because of its capabilities such as non-expensive process equipment, excellent control on mechanical properties, closed mold process, low filling pressure, incorporation of metal inserts and attachments, possibility of producing large and complex parts, and low labor cost [13-25]. The sophistication in resin transfer molding

process comes form many material and processing parameters. Researchers have been trying to optimize this process though experimental work and numerical simulations. A number of studies have been done in the area of mathematical modeling and numerical simulations [26-38].

2.0.1 Objectives and Structure of this Chapter

The objective of this study is to provide a brief and comprehensive review of the literature in the area of RTM processing with relation to process optimization for surface quality improvement. Achievement of class A surface finish in RTM is a multifaceted, complex problem. Several areas need to be explored to understand and optimize material, process and equipment variables that affect the surface quality of components. That is why this chapter is divided into several sub-sections, each addressing a specific area of interest.

- Recent work done in the area of RTM including resin flow characterization, simulation and modeling is presented in section 2.1. Void formation, which affects physical and mechanical properties of parts, through-thickness temperature variation in thick RTM molded components and their effects on properties are also discussed in this section.

- Section 2.2 gives a brief introduction to class A surface finish and techniques that can be used to achieve it. The measurement of surface quality is very important for relative assessment of test samples. A review of the available roughness measurement techniques and methods for quantifying different surfaces is also presented in this section.

- A polyester resin is used in this research. A brief review on cure kinetics characterization, modeling and experimental methods available, is presented in sections 2.3. This section also enlists several empirical cure kinetics models available in the literature for polyester resins.

- Rheological behavior of polyester resins is discussed in detail in section 2.4. This section also includes chemorheological models and effects of curing on viscosity variations of polyester resins.

- A detailed review of the literature on shrinkage-expansion behavior of polyester resins containing low profile additives is presented in section 2.5. The LPA action mechanism, effects of LPA on cure kinetics and shrinkage and comparison of different LPA is discussed in detail in this section. Inorganic fillers are added to polyester resins for several reasons. Effects of fillers on mechanical properties, cure kinetics and cure shrinkage are also presented in this section.

- Several experimental design techniques available in the literature are presented in section 2.6. However, the Taguchi method, which is used for RTM process optimization, is discussed in detail. Equations for the analysis of the results and recent applications of the Taguchi methods are also discussed in this section. Recent work done on the optimization of the RTM process for class A surface finish is also presented in this section.

2.1 Research in the Area of RTM

For a composite part to meet the quality control requirements and have the desired properties and dimensions, several manufacturing hurdles faced during RTM processing need to be overcome during the mold filling and the curing stage. First, during the mold filling stage, the resin should occupy all available space between the fibers. Any spaces uncovered by the resin are known as voids or dry spots and will be detrimental to the mechanical properties of the composite [39]. In the last decade, modeling and simulation tools for the mold filling stage have helped significantly to design the complete filling of the mold by optimizing the injection location for the resin and manipulating the flow rates or the pressure of the resin [39–49].

The curing stage requires invoking the initiation of the cure reaction and then managing the heat evolved from the part to avoid large thermal gradients and consequently residual

stresses that could lead to shrinkage and warpage and lack of dimensional tolerance. Models for resin cure have been developed and applied to predict the curing and temperature history of the composite during the curing stage [48–52]. In situations where cycle times are of paramount concern, the mold is usually pre-heated to aid the resin flow, the filling process itself could be non-isothermal, coupling the flow and cure behavior. Models and simulations for coupled situations are complicated but have been addressed in the literature [53–59].

2.1.1 Void Formation

Voids are formed due to the mechanical entrapment of the air during resin flow. The resin travels in between the fiber tows and within the fiber tows. The applied pressure, fiber-preform permeability, fiber volume fraction and resin properties govern the flow speed within each avenue. An irregular flow front can lead to the trapping of air pockets in the preform. Another form of voids is caused by the gas created by reactions taking place within the resin. Voids can also be introduced in the system in the form of bubbles, when the resin, prior to injection, is insufficiently degassed. The presence of voids inside the composite structure is highly undesirable since they adversely affect physical and mechanical properties and result in poor surface finish.

The void formation and development depends on a number of factors, such as injection pressure, outlet pressure, resin/mold temperature during injection and curing, packing, pressure during curing, resin properties (viscosity, surface tension, etc.), fiber type (distribution, orientation, surface treatment, etc.), and wetting angle between resin and fiber. There appears to be no proven way to eliminate voids completely. Thus, the understanding of the void formation is necessary for obtaining good surface finish.

Howe, Paton, and Goodwin studied the effect of the voids on the mechanical properties of the laminates [60]. They found that the level of porosity was several times greater at the surface than internally. It was thought to be because of higher amount of free space (space between the tows) at the mold surface. In the interior of the laminate, the fiber

tows are able to intermingle to reduce the available free space that resin or void can occupy.

Lundstrom and coworkers [61-62] reported that void content was decreased by increasing vacuum assistance. Young [63] reported that the injection pressure had large influence on void content, and low pressure generally resulted in better wetting. Hayward and Harris [64] reported that significant improvements were found in the mechanical properties and in the void content for products made with vacuum assistance, compared with those produced without vacuum assistance under otherwise identical conditions. Patel et al. [65] reported that merging took place at flow front because the permeabilities in the fiber tows and the gap between the fiber tows were different. They concluded that void formation was correlated to the capillary number and the liquid-fiber-air contact angle.

Chen et al. [66] reported that low viscosity, high mold temperature and high injection pressure could improve RTM quality. Having vacuum assistance or increasing fiber volume content will reduce the quantities of voids entrapped. Mahale et al. [67] reported that void content was a function of the capillary number characterizing the flow process. A critical value of capillary number $C_a = 2.5x10^3$ identified a zone below which void content increased exponentially with the decrease of the capillary number. Above this critical value, negligible entrapment of voids was observed. Because of the very small interstitial spaces within fiber tows, the permeability is much less in the tows than in the gap between the fiber bundles. Flow led in the gap between the fiber bundles and this is the potential for void formation within fiber bundles [66, 68].

Chan et al. [69,70] and Phelan et al. [71] developed a model to predict the air entrapment in fiber tows. Chan et al. [70] pointed out that as the macro-flow velocity (flow around the fiber bundles) was sufficiently low, the micro-flow front (flow around the fibers inside the fiber bundle) might advance ahead of the macro-flow front by the action of the capillary force. A wicking flow in the fiber bundles was experimentally observed by Patel [72] also. Patel reported that a slower resin injection favored wetting of individual fibers and high temperature led to better bonding and wetting.

2.1.2 Through Thickness Temperature Gradient

Lebrun et al. recorded through thickness temperature profiles in the mold cavity of a flat steel RTM mold at different locations and under different conditions [73]. A significant influence of the type and insertion method of thermocouples was observed on the precision of temperature recorded. Steel-sheathed thermocouples were found practically more reliable compared to thermocouples wires. Large temperature variations during impregnation and cure phases were observed under the same processing conditions for thicker cavities. Also, a significant viscosity difference was observed because of the temperature difference between the mid-thickness and the mold surface. (higher velocity of the resin on the surface of the mold compared to the mid-plane). Because of the viscosity variation, air entrapment was observed at the mid span in the absence of a pressure gradient. The authors suggest that precautions must be taken to mold thick laminates in heated tools. They say that these defects (entrapped air) appear when mats are used as reinforcements; larger defects could be expected when fabrics, having low permeabilities, are used.

In another publication, Lebrun et al. looked at the influence of the through thickness temperature variation on the generation of defects [74]. It was observed that the heat transfer reduced because of the void formation. An increase in pressure above the injection pressure was observed and related to the thermal expansion of the resin. Large bubbles were found at the mid-section of the panels because of the entrapped air due to the faster resin flow on the mold surface compared with the mid-plane.

2.2 Class A Surface Finish

The term used for acceptable surface roughness for exterior car body panels in auto industry is known as class A surface finish. Unfortunately a clear definition of class A surface finish is absent in the literature. However, Dutiro [75] and Bayldon [76] define class A surface finish as the one which exhibits aspects of flatness, smoothness and light reflection similar to that of finished stamped steel sheeting, typically with a DOI

(distinctness-of-image) values between 60 and 90, as measured with D-sight optical enhancement techniques. Neitzel et al. define class A surface finish as: "a substrate made of composite material represents a class A surface, if its optical appearance is identical to an adjacent steel panel" [77].

Class A finish is a perfectly polished, high luster surface, free of porosity and scratches of any kind. The term originated in the marine and automotive industries. Examples of such a finish can be found on high quality boat hulls and automobiles. However, those finishes are achieved through two different procedures. Cars have primers and paint systems sprayed over medium quality metal surfaces. The paint flows into a self-leveling thin film and requires polishing to achieve a true Class A surface. The boat hull, however, receives its finish directly from the mold itself. The mold quality is the limiting case for the part quality. If the mold has a Class A finish, the parts produced from it have the possibility of having a similar high quality finish. Construction of quality molds can decrease final finishing time and increase overall part quality. Specular gloss (brightness, shine) can be measured using a gloss meter with reference to a standard surface, a viewing angle and a material color. There are several different techniques, which can be employed to achieve a high class surface finish in composite materials. They include:

1. **Resin formulation:** By finding the optimum chemical composition of the resin in order to reduce the shrinkage and ultimately reducing the defects on the surface of the part. The types and quantities of resin, styrene, catalyst, accelerator, internal de-molding agent, external de-molding agent, filler, low profile additives and degassing agent have to be found for optimum chemical composition of the matrix. In recent years, resins with low profile additives have been introduced for reducing shrinkage and enhancing product surface finish [78-86]. A detailed discussion about the effects of LPA on cure kinetics and cure shrinkage of polyester resins is presented in section 2.5.

2. **Part and tool design:** Quality and surface finish of the part highly depends on its design and on the design and surface finish of the mold. The mold should be designed in such a way to eliminate sharp edges and corners where it is difficult for the resin to

reach. Gates and vents locations must be optimized in order to remove trapped air and allow smooth flow of the resin. Several studies have been conducted to optimize gate and vent locations [87-90].

3. **In mold coatings (IMC):** In mold coatings and gel coat techniques are being used to achieve optimum surface finish. However, these materials are expensive and hence add more to the manufacturing cost and process time [91].

4. **Process parameters:** Optimization of the molding process parameters such as molding temperature, upper and lower mold temperatures, injection rate or pressure, rate of cure and injection temperature [92-93] can be performed to obtain a set of optimum levels of these parameters for high class surface quality.

5. **Secondary polishing:** Secondary and finishing operations [94-95] are performed to improve dimensional accuracy and surface finish of molded components. These operations are labor intensive and in most cases increase process cycle times and manufacturing costs and hence are not desirable in high volume, low cost automotive applications.

Research efforts need to be directed towards improving surface finish quality through optimization of material and processing parameters for making RTM a feasible, economical and cost effective process for high volume auto industry.

2.2.1 Surface Roughness Measurements

Surface finish also known as surface texture or roughness is a quality characteristic, which represents the degree-of-smoothness of a surface. The methods for the quantitative measurement of surface quality in metal surfaces are well established. Unfortunately, due to the lack of a clear definition of class A surface finish in automotive applications, a standard method or procedure for class A finish is absent in the literature. However, work is in progress and researchers are trying to establish a standard for these measurements [96]. There are several types of equipment and techniques available in the literature to quantify finish quality. Methods for measuring surface quality can be divided into contact

and non-contact measurement techniques. For contact measurements, a stylus is used, which scans the surface. Displacement signals are then transformed into electrical signals, which are processed using a microprocessor, and hence ultimately a surface profile is obtained. For non-contact measurements, optical microscope, electronic microscope or optical sensors are used for measuring the surface and hence ultimately surface parameters are obtained.

Typical measurement systems used in automotive sector are quality measurement system (QMS), BYK wave-scan, D-sight and the ONDULO quality control systems [97]. These systems are based on the light reflection principle. QMS and BYK wave-scan can be used to get gloss, distinctness-of-image (DOI) and orange peel. Gloss refers to the shine of the sample surface and is obtained from the intensity of the reflected light. DOI evaluates structure size, brilliance and smoothness of the surface, whereas orange peel values measure the severity of the visible surface dimples by analyzing the degree of distortion of the reflected image of the lamp. ONDULO can be used for scanning the parts, which reflects the structured grid line. Defects are visualized through ONDULO software. However, the main drawback of all these techniques is that they can only be used with a high level of gloss, which is absent in most composite surfaces. Many of the RTM and SMC surfaces do not have a high enough gloss to be measured with the techniques mentioned earlier [96]. However contact and non-contact surface profilometry have great potential to be used as a standard method for the measurement of composite surfaces [96-97].

A surface profilometer maps surface topography by dragging a sharp probe across a sample surface. A profilometer typically uses a mass cantilever system to keep the tip force constant while scanning. Profilometers utilize the same imaging fundamentals as a scanning probe microscopy, but with a much larger tip (2.5 microns in diameter). The larger tip limits the vertical and horizontal resolution. The probe tip is usually made of diamond to reduce tip wear. Profilometers are typically used to measure surface roughness or film thickness. Modern Profilometers are capable of creating 3-dimentioal

topographical surface maps rather than traditional line scans (single horizontal direction scans while measuring feature height).

2.2.2 Parameters for Surface Quality Characterization

There are many parameters that can be defined from the surface profile of a surface. Three of the most common one-dimensional parameters used for quantitative analysis of surface roughness are R_a, R_q and R_y [98-99]. A typical profilometer scan signal for a composite panel is shown in Figure 2.2 [100].

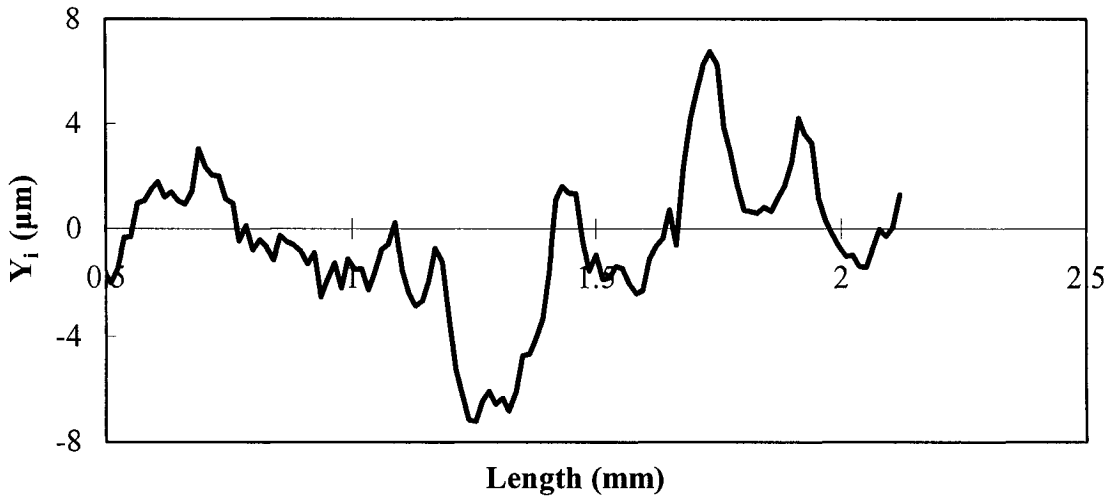

Figure 2.2 A typical scan obtained with a surface profilometer (adapted from Hu [100]).

The most common parameter used for surface profiling is R_a and is defined as "the arithmetical mean of the absolute values of the profile deviations (Y_i) from the mean line" [98-99]. R_a is represented by Equation 2.1.

$$R_a = \frac{1}{n}\sum_{i}^{n}|Y_i| \qquad (2.1)$$

Surface roughness can also be characterized by using R_q and R_y response values. R_q is the square root of the arithmetical mean of the squares of profile deviations (Y_i) from mean line and is represented by Equation 2.2.

$$R_q = \left[\frac{1}{n}\sum_{i}^{n} Y_i^2\right]^{1/2} \tag{2.2}$$

R_y is the difference in the elevation between the highest point from the mean line Y_{max} and the depth Y_{min} of the lowest point from the mean line.

$$R_y = Y_{\max} - Y_{\min} \tag{2.3}$$

Generally one of three parameters defined above is used as a quality characteristic of a surface. Debolt [96] described a procedure to quantify surface roughness for class A finish using roughness parameter R_a. A non-contact profilometer was used and an analysis procedure was developed. This procedure employed band-pass filtering and Fourier Transforms for extracting regions of particular wavelength. Calculations were performed to determine surface roughness for each of the wavelength regions. The method developed was found very efficient in quantifying the differences in plaques molded under varying processing conditions. Unfortunately, a standard definition of class A surface finish in terms of roughness parameters (R_a, R_q and R_y) is not available in the literature.

2.3 Cure Kinetics of Polyester Resins

The cure reaction of unsaturated polyester resins is a free radical chain growth polymerization. The uncured system contains styrene monomer, unsaturated polyester molecules, and curing agents. The reaction starts with the decomposition of initiator molecules into free radicals, which trigger the polymerization. The free radicals link adjacent unsaturated polyester units and form primary polymer chains through connecting styrene monomers [101]. This reaction is highly exothermal and can be monitored with

differential scanning calorimetry (DSC), Fourier Transform Infrared Spectroscopy (FTIR), dielectric measurements and rheo-kinetic measurements.

Gelation and vitrification are important stages in the curing of thermosetting resin systems. Gelation corresponds to the formation of the first insoluble fraction of polymer of infinite molecular weight. From processing point of view, the gel point represents the state beyond which the material no longer flows. It is generally accepted that gelation occurs at a fixed degree-of-cure, which is independent of the curing temperature [101].

Vitrification is a reversible transition from the liquid or rubbery state to the glassy state due to reaction. It occurs when the increasing glass transition temperature of the reacting system becomes equal to the cure temperature. As of this moment, curing within the glassy state becomes extremely slow and the reactive process changes from chemical control to diffusion control [102]. Since up to vitrification the reaction is controlled mainly chemically and gelation does not involve any change in the cure kinetics, it is possible to carry out a kinetic study using a single rate equation [103].

A comprehensive review of literature on cure kinetics of thermoset resins in general has been performed by Yousefi et al. [104] and a number of cure kinetics models are given by Halley et al. [105].

2.3.1 Cure Kinetics Modeling

In the literature, two forms of cure kinetics models are used to describe thermoset curing reaction. Empirical models assume an overall reaction order that fit cure kinetics data. This kind of model provides no information on the reaction kinetics mechanism and is predominantly used in numerical simulations. This model was first introduced by Kamal and Sourour in 1973 [106-107]. Mechanistic models are derived from an analysis of the individual reactions involved during curing and require detailed measurement of the concentration of reactants, intermediates and products. Hence, mechanistic models are more complex; however they give more detailed information about the reaction kinetics.

This approach was first introduced by Stevenson in 1986 [108]. Empirical models are much simpler than mechanistic models and hence are extensively used for cure kinetics modeling of polyester resins.

2.3.1.1 Empirical Models

A number of variations of Kamal and Sourour model [106-107] have been proposed to describe the cure kinetics of various resin systems. In general, the reaction rate can be expressed as a function of processing temperature T and degree-of-cure α as:

$$\frac{d\alpha}{dt} = k(T)f(\alpha) \tag{2.4}$$

where the dependence of the rate constant $k(T)$ on the temperature is assumed to follow the Arrhenius law:

$$k(T) = k_o \exp\left(\frac{-E}{RT}\right) \tag{2.5}$$

where k_o is the Arrhenius frequency factor, E is the activation energy, and R is the universal gas constant. With regard to $f(\alpha)$, two functions are used to characterize the curing of a thermoset resins: the n^{th}-order function and the auto-catalyzed mechanism [101]. For polyesters, which usually contain an inhibitor that results in an induction time at the beginning of the cure, the auto-catalyzed function is more reasonable. For an auto-catalytic reaction in which the initial rate is not zero, the reaction rate can be expressed as [107]:

$$\frac{d\alpha}{dt} = (k_1 + k_2\alpha^m)(1-\alpha)^n \tag{2.6}$$

where $k_{1,2}$ are Arrhenius constants and m and n are reaction orders. The sum (m+n) is generally assumed to be 2 to express a pseudo second-order mechanism [109]. If the initial rate is zero, the rate equation becomes:

$$k_1 = 0;\ k_2 = k$$

and $$\frac{d\alpha}{dt} = k\alpha^m(1-\alpha)^n \tag{2.7}$$

Since the reaction process stops once the resin vitrifies, several models were proposed to fulfill the condition of zero reaction-rate at vitrification [101]:

$$\frac{d\alpha}{dt} = k\alpha^m(\alpha_{\max} - \alpha)^n \tag{2.8}$$

$$\frac{d\alpha}{dt} = k\left(\frac{\alpha_{\max} - \alpha}{\alpha_{\max}}\right)^x \alpha^m(\alpha_{\max} - \alpha)^n \tag{2.9}$$

where α_{max} is the maximum degree-of-cure achieved for each isothermal experiment and x is an adjustable parameter. A detailed list of cure kinetics models used for epoxy and various other resin systems is given by Halley and Mackay [105].

2.3.1.2 Free Radical Models

The reactive components in a commercially available unsaturated polyester (UP) resin system consist of an unsaturated polyester [E], the styrene [S], an inhibitor [Z] and an initiator [I]. The cure kinetics of a UP resin, initiated with an initiator, can be approached by a mechanism of free radical polymerization. This consists of a sequence of steps: initiation, inhibition, propagation and termination [110]. The equations for the free radical polymerization are complex. The details of these equations are given elsewhere [108,111]. These equations can be simplified by introducing lumped concentrations for the unsaturated groups [M] = [E] + [S] and for the free radicals [R] = [E] + [S] + [I]. With these simplifications and some assumptions, [111-112], the system of equations describing the curing process can be written as:

Inhibitor: $$\frac{d[Z]}{dt} = -k_z[Z][R] \tag{2.10}$$

Initiator: $$\frac{d[I]}{dt} = -k_{dj}[I_j] \qquad \text{where j = 1, 2, 3, ... N} \tag{2.11}$$

Monomer: $$\frac{d[M]}{dt} = -k_p[M][R] \tag{2.12}$$

Radical: $$\frac{d[R]}{dt} = 2\sum_{j=1}^{N} f_j k_{dj}[I_j] + k_z[Z][R] - k_t[R]^2 \tag{2.13}$$

Where [Z] is the inhibitor concentration, [I_j] is the concentration of the j^{th} initiator, [M] refers to the total monomer concentration that is the sum of the concentrations of the polyester resin [El and styrene [S], [R] refers to the radical concentration that is the sum of the concentrations of polyester radical [E], styrene radical [S], and the initiator radical [I] (i.e., [R] = [E] + [S] + [I]), k_z is the rate constant of the inhibition reaction, k_{dj} is the rate constant of the decomposition reaction of the j^{th} initiator, k_p is the rate constant of the propagation reaction, k_t is the rate constant of the termination reaction, and f_j is the efficiency of the j^{th} initiator. Several empirical models have been proposed by the researchers to estimate these rate constants and efficiency factors [108-113]. However, as can be seen from Equation 2.10 through 2.13, free radical models are very complex and require an experimental tracking of the conversion of several species during the cure reaction and hence are not feasible when an overall reaction kinetics is desired.

2.3.2 Experimental Methods for Cure Characterization

Although several experimental techniques are available to characterize curing reaction of thermoset resins, differential scanning calorimetry (DSC) is the most popular technique because of its simplicity. DSC measures the rate of heat generated (dQ/dt) during a chemical reaction. The basic assumption in DSC cure kinetics measurements is that the change in heat flow is proportional to the change in the degree-of-cure α, that is

$$\frac{dQ}{dt} \propto \frac{d\alpha}{dt}$$

or $$\frac{1}{Q_o}\frac{dQ}{dt} = \frac{d\alpha}{dt} \tag{2.14}$$

where Q_o is the overall heat-of-reaction, which can be estimated from a non-isothermal temperature scan that can take the reaction to a complete cure. The extent of cure can then be evaluated as a function of time by integration. There are two experimental techniques for DSC measurements; isothermal and non-isothermal tests. In an isothermal test, the rate of energy released is measured at constant temperature and the extent of reaction is calculated from Equation 2.14. The major assumptions in this type of test are that the total heat-of-reaction can be determined accurately, and that all reactions contributing to the overall reaction have the same enthalpy.

Curing behavior of an unsaturated polyester resin with varying amounts of initiator (MEKP) at various processing temperatures was investigated by Vilas et al. [101]. Typical heat flow curves as function of time at different processing temperatures obtained with DSC are shown in Figure 2.3. The interesting thing to note in Figure 2.3 is the effect of processing temperature on the reaction rate. The increase in processing temperature not only increased the reaction rate but also it increased the total heat flowing out of the resin sample, which is given by the area under the heat flow curves. The variation in heat flow was integrated based on the total heat flow and is plotted in Figure 2.4. From this Figure, it is apparent that the level of temperature is crucial in achieving higher degrees-of-cure. Higher the temperature level, higher is the reaction rate and maximum degree-of-cure, however higher temperature levels reduced the inhibition time. Resin took much longer time to start reacting at 30°C as compared with 80°C [101].

Kamal and Sourour [106-107] reported isothermal kinetic data for epoxy-aromatic diamine systems that agreed with proposed auto-catalytic kinetics models. Lee [114] used isothermal testing of a polyester-styrene system to determine its kinetic parameters and rate constants of inhibitors and initiators. Work by Hsieh and Su [115] showed isothermal DSC results could be used to predict the kinetics of an epoxy molding compound and agreed well with non-isothermal tests (in the absence of vitrification).

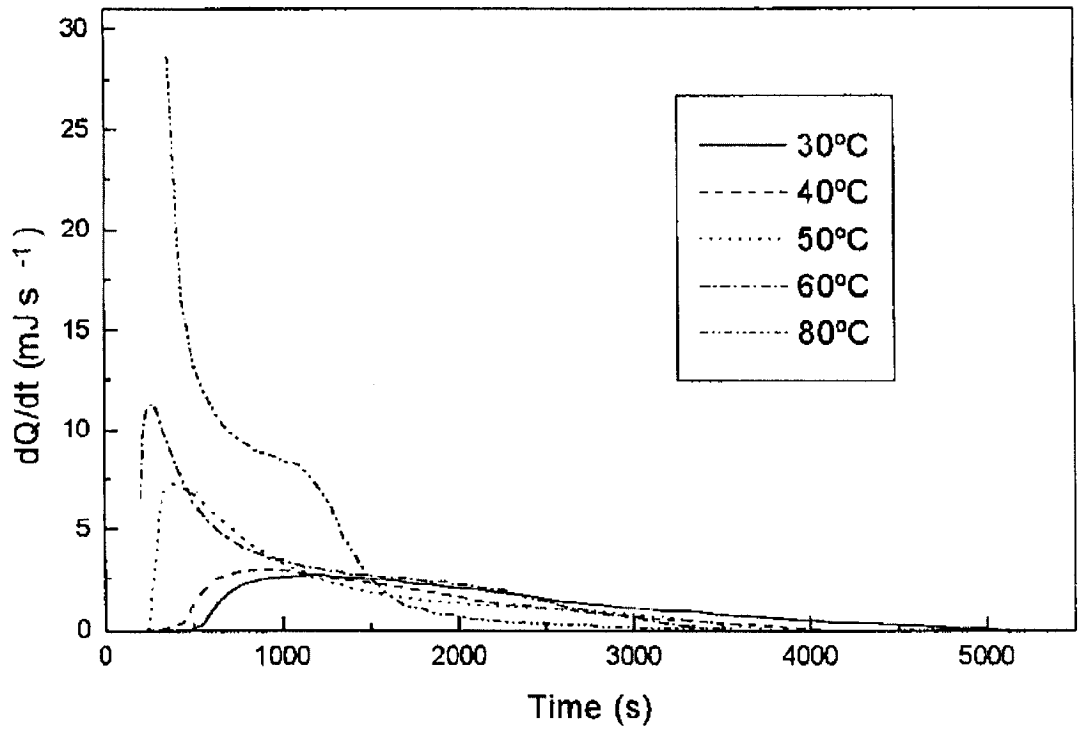

Figure 2.3 Exothermic heat flow at different isothermal temperatures (adapted from Vilas et al. [101]).

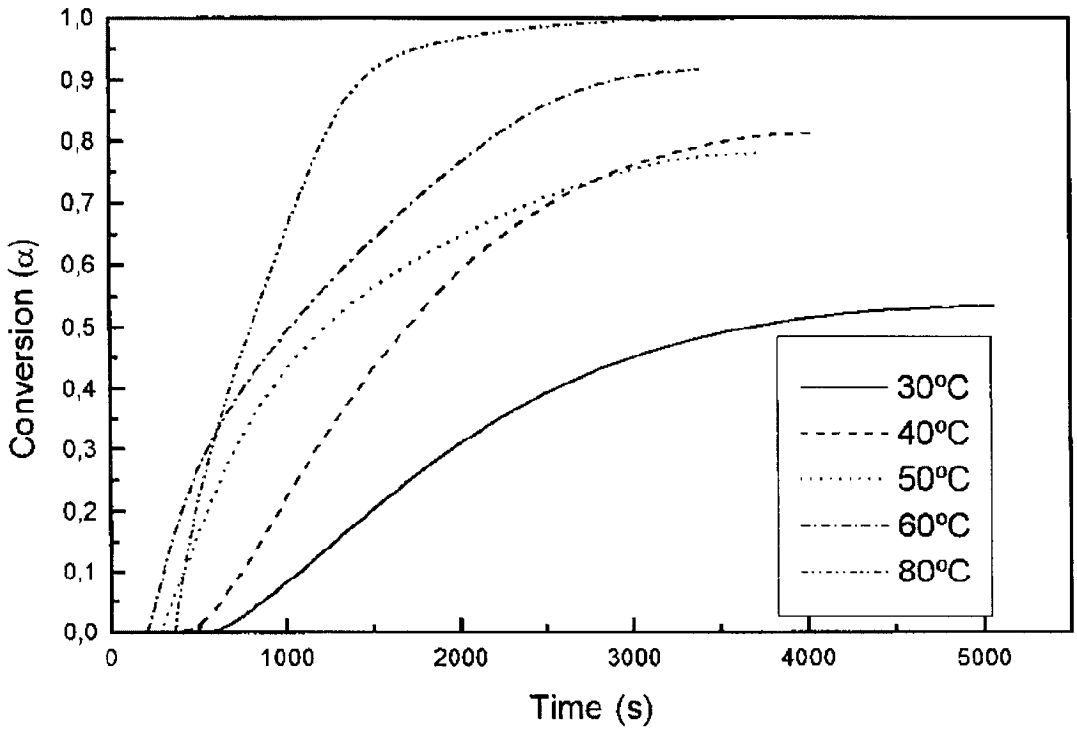

Figure 2.4 Degree-of-cure as a function of time (adapted from Vilas et al. [101]).

Gonzalez-Romero and Casillas [116] noted that isothermal tests were time consuming and had insufficient accuracy in the initial stages of the tests at high temperatures due to significant exotherms prior to thermal equilibrium. However, results from both isothermal and non-isothermal tests using methyl methacrylate-based resins agreed with each other and were well represented by a phenomenological model.

In non-isothermal tests the heat-of-reaction is monitored over a linearly increasing temperature scan and kinetics data is obtained via various analyses of the DSC curve produced. Ng and Zloczower [110] monitored kinetics of unsaturated polyesters via non-isothermal DSC measurements and noted that non-isothermal tests provided kinetics data over a wider temperature range and were more easily related to processing conditions. Khanna et al. [117] used non-isothermal DSC tests to determine the kinetics of a phenolic triazine resin system. Prime [118] has argued that data from non-isothermal and isothermal tests are inherently different and has proposed methods to relate results from each test. Recent advances in analyses of non-isothermal data includes work by Chiou and Letton [119] that de-convoluted DSC data into separate peaks to account for different reactions.

2.4 Chemorheology of Polyester Resins

Chemorheology is defined as the study of visco-elastic behavior of reacting systems. This study encompasses knowledge of the variations in viscosity due to chemical reactions and processing conditions and characterization of the growth of the infinite molecular network. The viscosity of thermosetting resins is affected by several variables. Ryan [120] expressed viscosity (η) as a function of pressure (P), temperature (T), time (t), shear rate ($\dot{\gamma}$) and filler properties (F). The relationship is given in Equation 2.15.

$$\eta = \eta(T, P, \dot{\gamma}, t, F) \tag{2.15}$$

The effects of each variable on the viscosity are usually examined by separate tests. The models derived from these separate tests are then recombined to provide an overall viscosity variation model used in processing applications. The effect of pressure on viscosity has not been studied extensively. The cure effects on the viscosity are two-fold; the viscosity will initially decrease due to increased thermal effects and will eventually increase due to formation of the cross-linked network via the curing reaction. This phenomenon is shown in Figure 2.5. In this Figure, stage I refers to the decrease in resin viscosity due to thermal effects. As the temperature or time increases the curing reaction begins and the decrease in viscosity due to heating is compensated by the increase in viscosity due to the curing process. At the point of minimum viscosity (stage II) the polyester is injected into the mold. Finally, the viscosity of the resin increases as the material is transformed from liquid state to the sold state (stage III).

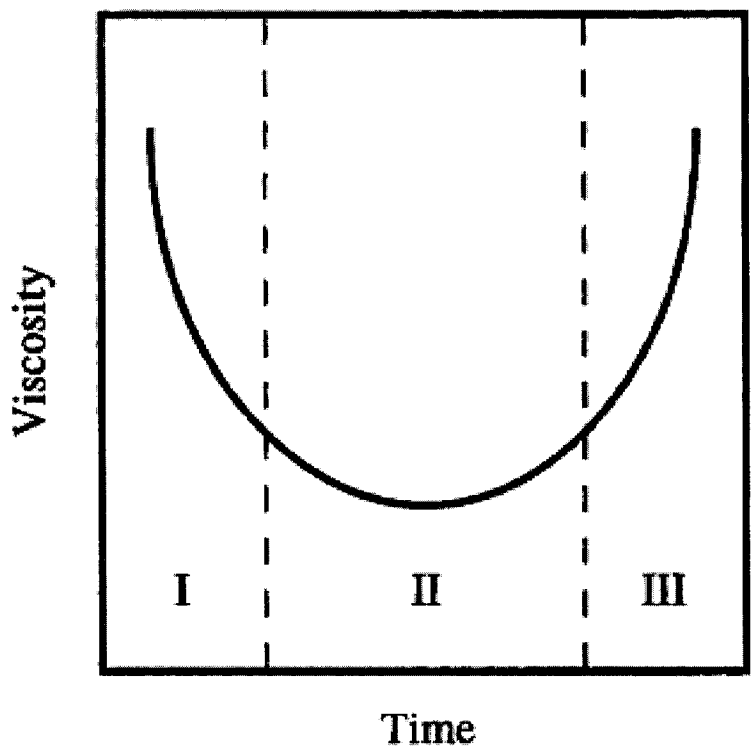

Figure 2.5 Viscosity variations in polyester resins during processing (adapted from Halley et al. [105]).

2.4.1 Chemorheological Models

The effects of temperature and time on the viscosity can also be described explicitly in terms of the extent of cure (α) from knowledge of the kinetics of the cure i.e. α(T, t) and temperature by the following equation,

$$\eta_c = \eta_c(T, \alpha) \tag{2.16}$$

Models, which examine the effects of cure on the viscosity, range from simple empirical models used for epoxy and polyurethane systems [121-126], probability based and molecular models used for polyurethane and epoxy systems [127-130], gelation models used for polyester, epoxy, and melamine systems [121,131-132], Arrhenius models used for many thermosets including epoxies and polyimides [133-137], and detailed models based on free volume analyses used for epoxy systems [119, 138]. Further reviews of curing effect models are given by Ryan [120] and Roller [139]. Halley and Mackay listed a detailed set of viscosity variations models including effects of curing, shear rate, and filler content along with a list of standard procedures for their measurements [105].

Yang and Suspene [122] proposed a micro-gel model for unsaturated polyester resins with non-homogeneous reaction. This model (Equation 2.17) was purposed for resin systems with three distinct stages during cure: micro-gelation, transition and macro-gelation.

$$\begin{aligned} \ln(\eta_s) &= A + B(t/t^*) \\ \eta_s &= \frac{\eta_c}{\eta_0} - 1 \end{aligned} \tag{2.17}$$

where η_c is the viscosity at any given time t, t^* is the gel time, η_0 is the initial viscosity and A and B are constants obtained from curve fit of experimental data. Castro and Macosko [140] studied the kinetics and rheology of a polyurethane system and came up with a relationship between viscosity and degree-of-cure. This relationship is referred as Macosko's model and is given in Equation 2.18.

$$\eta(\alpha,T) = \eta_0(T)\left(\frac{\alpha_G}{\alpha_G - \alpha}\right)^{(C_1+C_2\alpha)} \tag{2.18}$$

where $\eta_0(T) = B\exp\left(\frac{T_b}{T}\right)$

In this model, η is viscosity, T is temperature, α is degree-of-cure, α_G is degree-of-cure at gelation and C_1, C_2, B and T_b are all fitting constants. These constants are determined through regression techniques applied to experimental data. These models (Equation 2.17 and 2.18) can be used to predict viscosity variations as a function of time, temperature and degree-of-cure in a polyester resin.

2.4.2 Cure Effects on Viscosity

Isothermal and non-isothermal tests are used to study the effect of cure on the viscosity of thermoset resins. For an isothermal test, the sample is dynamically sheared at a low oscillation rate and strain. The strain may be initially high to determine the viscosity of the resin, as the viscosity may be quite low, and a higher strain will increase the accuracy of the instrument. However, the strain must be reduced once curing has begun to ensure that the test is conducted in the linear visco-elastic region. Isothermal test is used to determine the changes in viscosity over time at a fixed frequency and at various constant temperatures.

ASTM 4440-84/90 recommends a procedure for determining the curing viscosity of thermoset resins via isothermal tests. Isothermal tests have also been carried out in steady state condition, which is used to determine the change in viscosity as a function of time at a given shear rate. However, the effects of shear rate on network formation of the resin must be evaluated in order to validate these tests. Mussati and Macosko [131] measured the curing viscosities of a phenolic resin, an epoxy resin, and an EPDM rubber as a function of time at various temperatures.

Malkin and Kulichikin [141] and Lane et al. [142] measured the changes in complex viscosity for DGEBA/DCA and TGDDM/DDS epoxy resin systems via isothermal tests using parallel plate rheometer. These studies also incorporated dielectric measurements during the curing in an attempt to find a correlation between complex viscosity and dielectric measurements and to relate these measurements to the degree-of-cure. Kojima et al. [143] measured the cure effects on the viscosity of a polyimide fiber resin through isothermal tests. Pahl and Hesekamp [144] also monitored the viscosity of filled epoxy resins with the same technique.

Work by Han and Lem [145-148] investigated the effects of curing on the chemo-viscosity and normal stresses of filled polyesters. Non-isothermal tests defined as dynamic temperature ramps are used to measure the changes in viscosity during an imposed temperature ramp at a given oscillatory frequency and strain. This ramp may be linear or non-linear in order to derive curing viscosity information or to model processing conditions. Also, the strain may be changed during the ramp, yet, must be within the linear visco-elastic region and not interfere with the network formation.

Martin et al. [121, 132, 134] measured the viscosity of epoxy resins during various linear temperature ramps to evaluate curing model parameters. A typical graph from this research is shown in Figure 2.6. In the beginning, the viscosity of the epoxy resin decreases with the increase in temperature and then it starts increasing due to the polymerization and formation of long molecular chains. Authors [121, 132, 134] noted a relative decrease in viscosity with increasing ramp rates at a given temperature. Chiou and Letton [119] investigated the curing of a three-component epoxy resin system in order to evaluate the curing effects on the viscosity. Tajima and Crozier [149] evaluated the curing models for various epoxy resin systems using temperature ramp tests on samples partially reacted to various initial degrees-of-cure.

Lane et al. [142] and Kenny et al. [150] examined the relationship between viscosity and dielectric properties through temperature ramp tests. A standard procedure for non-isothermal tests is given in ASTM 4440-84/90, where ramp rates of 3 to 5°C/min are

recommended in order to minimize thermal inertia effects. Although most industrial ramp rates are non-linear, this linear rate is representative of typical curing rates used. An inherent assumption when using the above dynamic techniques is that the complex viscosity gives a good representation of the viscosity during the curing reaction. This has been validated for many systems. However, care should be taken when relating the effects of cure on complex viscosity to the processing viscosity. Steady temperature ramp tests are used to monitor the change in steady shear viscosity at a given shear rate during a linear or non-linear temperature ramp.

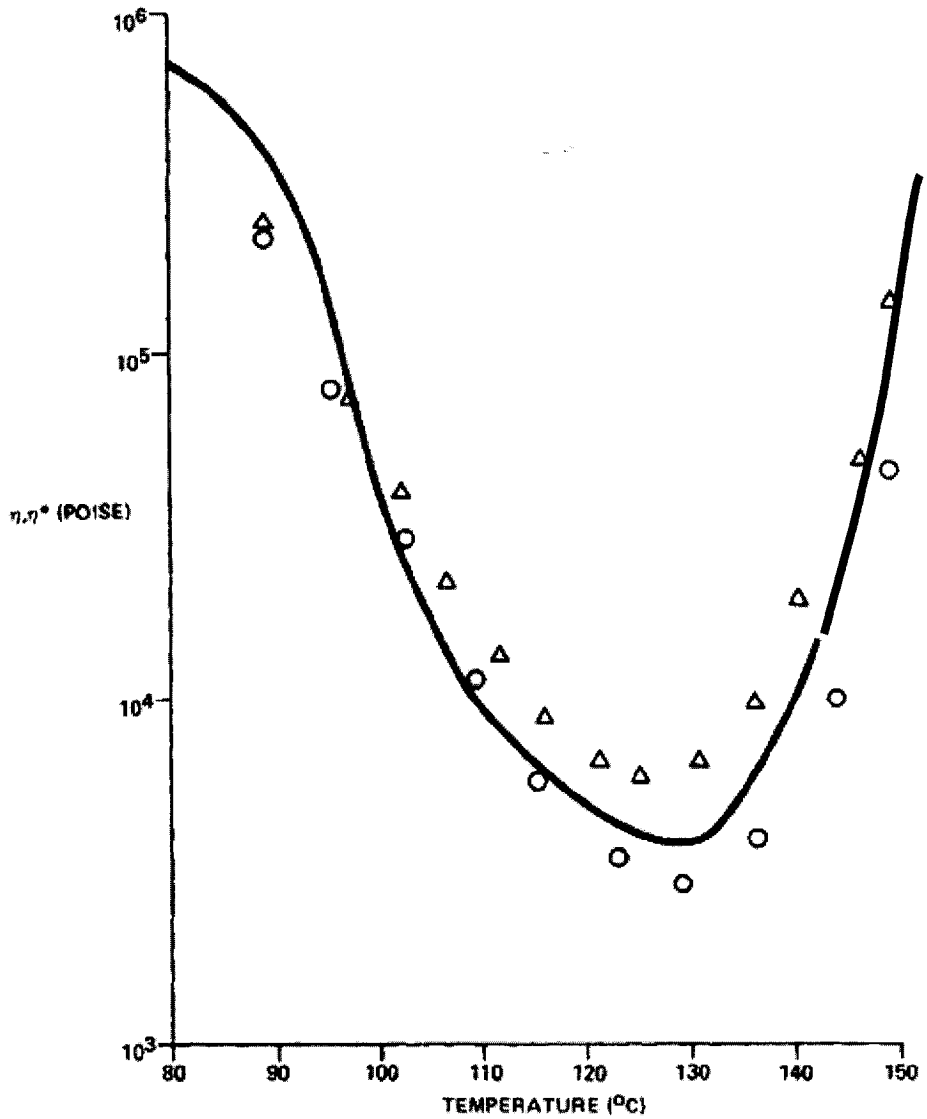

Figure 2.6 Viscosity variations in an epoxy resin as a function of temperature (adapted from Martin et al. [132]).

Complex viscosity (η^*) represents the total resistance to the dynamic shear. The complex viscosity function can be broken down into two components: dynamic viscosity (η') or the real components and out-of-phase viscosity (η'') or imaginary component as follows:

$$\eta^* = \eta' - i\eta'' \tag{2.19}$$

Martin et al. [132,134] used a squeezing flow viscometer to measure the change in viscosity during a linear temperature ramp of an embedded epoxy resin and developed a model for the curing viscosity using an optimization technique. The most common geometry used for the determination of the cure viscosity is the parallel plate rheometer [85-86,121,132,134,143,150-151]. This rheometer may be operated at low shear rates (< $0.01 sec^{-1}$) under isothermal and non-isothermal conditions. Other geometries such as slit [84], cone and plate [145-148], eccentric disc [152], capillary, squeezing flow and sliding plate have also been used. Other measurement systems and procedures have also been employed to measure effects of cure on the viscosity, and a detailed list is given by Halley and Mackay [105].

2.5 Cure Shrinkage of Polyester Resins

When thermoset resins go through exothermic cure reaction, their molecules rearrange themselves, the state is changed from liquid to solid, the density increases and hence they shrink in volume. This volumetric shrinkage breaks the material's contact with the mold and results in poor surface finish. Some of the common manufacturing and surface finish quality problems arising from resin cure shrinkage are fabric print though, ripple or long range waviness, sink marks and dimensional inaccuracy. A volumetric shrinkage of 7-10% has been reported for polyester resins [153-158], which makes it difficult to achieve a good surface finish in automotive applications. However, a lower volumetric shrinkage (1-3%) is reported for epoxy resins [159-161].

Bogetti and Gillespie [157] proposed a processing model, which gives cure shrinkage as a function of degree-of-cure. In this model, the incremental volume shrinkage is assumed to be proportional to the incremental change in degree-of-cure as follows:

$$\Delta V = \Delta\alpha * V^T \tag{2.20}$$

where ΔV is change in volumetric shrinkage, $\Delta\alpha$ is the change in resin degree-of-cure and V^T is the total volumetric shrinkage for fully cured resin. Total volume shrinkage of 6% has been reported by Bogetti and Gillespie for polyester resins [157].

Hill et al. proposed two models to predict volume changes during the cure of unsaturated polyester (UP) resin [158]. These models are able to account for both thermal expansion and polymerization shrinkage during processing. The first model, which is based on degree-of-cure, was developed by combining experimental results from differential scanning calorimetry (DSC) and dilatometry. The second model is based on radical concentration. The model based on the degree-of-cure is simpler and easy to use and it is explained here. The overall volumetric changes of a thermoset resin during cure can be considered to be a combination of thermal expansion/contraction and polymerization shrinkage as:

$$\left(\frac{1}{V_o}\frac{dV}{dt}\right)_{overall} = \left(\frac{1}{V_o}\frac{dV}{dt}\right)_{Thermal} - \left(\frac{1}{V_o}\frac{dV}{dt}\right)_{Shrinkage} \tag{2.21}$$

where

$$\left(\frac{1}{V_o}\frac{dV}{dt}\right)_{Thermal} = \left(\beta_m(1-\alpha)+\beta_p\alpha\right)\left(\frac{dT}{dt}\right)$$

$$\left(\frac{1}{V_o}\frac{dV}{dt}\right)_{Shrinkage} = B\frac{d\alpha}{dt}$$

where

β_m - volumetric thermal expansion coefficient of uncured resin

β_p - volumetric thermal expansion coefficient of cure resin

B - constant

α - degree-of-cure

T - absolute temperature

t - time

Hill et al. [158] found polymerization shrinkage in a linear relationship with the degree-of-cure. Total volumetric shrinkage of about 9% was observed in unsaturated polyester resin containing a 1:1 mixture of maleic anhydride and propylene glycol containing 35% wt. of styrene. Li et al. reported cure shrinkage of 6% for MY750 epoxy resin (unmodified diglycidyl ether of bisphenol-A epoxy resin) using density difference method [162]. The shrinkage was found to be a linear function of the degree-of-cure and was independent of time and temperature.

Researchers have used several techniques to measure cure shrinkage. Some of those techniques employ volume change, such as those based on capillary dilatometer [158], or direct measurement of sample dimensions. Others measure a linear shrinkage, such as those using thermo-mechanical analyzer, density difference method [162] and dynamic mechanical analyzer [163].

2.5.1 Shrinkage Compensation through Low Profile Additives

Low profile additives (LPA) are thermoplastic materials that generally serve as non-reactive additives in unsaturated polyester and vinyl ester resins. These materials are initially soluble or form a stable dispersion in the styrene and resin mixture before cure, but become incompatible with the cured resin during the curing process. Common LPA include poly vinyl-acetate, poly methyl-methacrylate, polystyrene, thermoplastic polyurethanes and polyesters. LPA have been found to be highly effective in eliminating the polymerization shrinkage of unsaturated polyester resins in high temperature molding processes.

2.5.1.1 LPA Action Mechanism

Unfortunately, a detailed and well understood LPA mechanism through which shrinkage compensation takes place is still a matter of argument and controversy. Several mechanisms have been suggested in the literature. Researchers have tried to explain LPA expansion through free monomer boiling and exerting pressure [164], strain-relief cracking mechanism [165], LPA thermal expansion mechanism [166], phase separation and micro-void formation [167-173] and nucleation and expansion of styrene in LPA rich phase [169]. However, a general explanation of LPA mechanism is given by Li et al. [168] as follows:

Step 1: System starts as a homogeneous mixture containing unsaturated polyester (UP), LPA, styrene and initiator. When this resin system is injected in the hot mold, its temperature rises and it expands thermally. The rise in temperature causes initiator to decompose and cure starts.

Step 2: As the cure reaction progresses the LPA become incompatible and start to form a second phase. Un-reacted styrene and UP resin start to collect in the thermoplastic phase and localized phase separation occurs.

Step 3: Temperature and degree-of-cure continue to increase. As the degree-of-cure increases, the UP phase shrinks. As the temperature increases, the volume occupied by the LPA and un-reacted monomer increases due to thermal expansion and compensates for the polymerization shrinkage.

Step 4: Resin gels, viscosity increases exponentially and the resin keeping shrinking.

Step 5: A two phase structure builds up as the cure and shrinkage progresses.

Step 6: Stresses build up internally because of the possible difference of the two phases in reaction rate and modulus. Micro-voids are formed and stress is released; consequently, the polymerization shrinkage is compensated. Here, the reaction mixture turns opaque and expansion starts.

This mechanism is shown in Figure 2.7. The LPA mechanism for low temperature cure is reported as slightly different from high temperature cure and is investigated by Lee and coworkers [169-173].

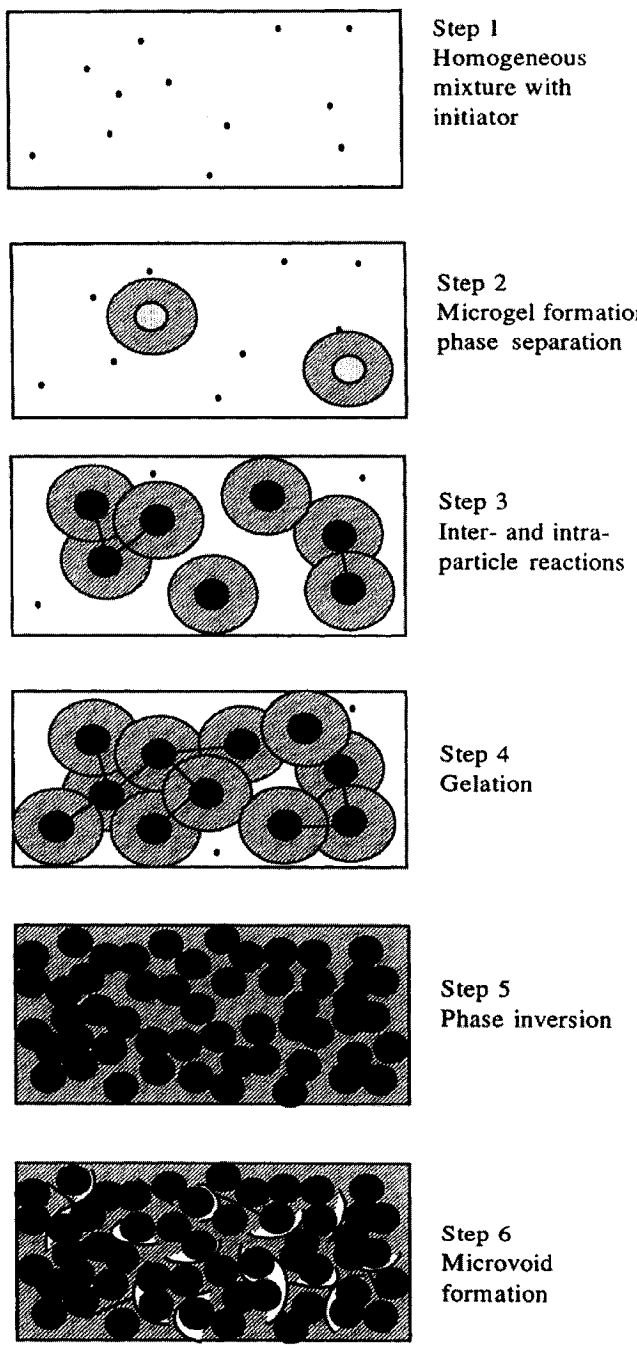

Figure 2.7 LPA expansion mechanism (adapted from Li et al. [168]).

Lee et al. [169-173] concluded that a co-continuous or LPA-rich phase dominated structure was essential for thermoplastics to be effective as shrinkage control additives at low temperature cure. Phase separation and micro-void formation were found to be two most critical steps for shrinkage control. Micro-cracking was found to occur when the stresses generated by polymerization shrinkage became greater than the 'resistance' force possessed by the interface or LPA-rich phase.

During the cure of low profile resins, a certain critical amount of LPA is needed in the resin to form a two phase structure, which is essential for shrinkage compensation mechanism. Bucknall, Davies and Partridge explored the phase separation involved when resin mixed with PVAc was cured [174]. It was found that a phase inversion from a dispersion of PVAc particles in a resin matrix to a co-continuous phase structure occurred at PVAc concentrations between 8 and 16%. Even further, a combination of $CaCO_3$ filler with 16% PVAc resulted in the best shrinkage control. During curing, the filler resisted shrinkage and induced internal stresses in the polymer, which caused cavitations in the PVAc and shear deformation in the resin. This mechanism was found effective in reducing shrinkage when the concentration of PVAc was high enough to provide a co-continuous structure. Further research by Bucknall, Partridge and Phillips [175] reported on the independent variations in polyester, PVAc and styrene concentrations. It was found that PVAc provided a low energy pathway for fracture and energy absorption was reduced when the structure became co-continuous.

Micro-void formation during LPA expansion in unsaturated polyester resin cure was investigated in detail by Zhang and Zhu [176]. Micro-void formation was observed to be controlled by the amount of LPA and styrene. Increase in LPA content increased the volume fraction of voids. Other parameters with significant effect on the formation and size of micro-voids were processing temperature, type and quantity of initiator, filler content and external pressure. Higher processing temperature and filler content results in bigger volume fraction of voids.

Suspene et al. [177] investigated phase diagrams as a mean to explain the low profile shrinkage control mechanism. A low profile mechanism was developed based on the idea of micro-void formation. The authors explained that phase separation takes place when cure reaction causes gelation. At gelation, high molecular weight of long chains of polymer decreases the miscibility of LPA in the resin and hence phase separation occurs. Molecular chains grow larger to form the micro-particles of the macro-network. The styrene rich phase eventually becomes an LPA-rich phase due to consumption of the reactants. During the maximum reaction rate the reaction takes place very quickly and creates large shrinkage forces. The shrinkage stress passes through the interfacial area and into the LPA phase. Because LPA is a weak thermoplastic, the shrinkage stress tears off the LPA phase and forms micro-voids. The formation of micro-voids thus provides the volume compensation.

2.5.1.2 Effects of LPA on Cure Kinetics

Effects of LPA on exothermic reaction kinetics, cure rate, final degree-of-cure and total enthalpy of reaction are somewhat controversial. Some researchers have found no significant effect of LPA on reaction kinetics and cure rate [168-173,178]. However, some others suggest a slower reaction rate as a result of LPA inclusion into the resin [179].

Li et al. [168] studied the cure and shrinkage behavior of Q6585 polyester resin, from Ashland Chemical Inc., with different types and amounts of LPA. It was found that the amount of LPA had a minor effect on cure kinetics, rheological behavior and gel time of a polyester resin, as shown in Figure 2.8. Li et al. [168] also observed that the LPA changed the resin from transparent to opaque. Two distinct regions were observed in micrographs referred as the UP rich structure and a co-continuous structure formed by UP and LPA. Micro-void formation was observed at a later stage in resin cure. Researchers also observed that a relatively low LPA content gave better shrinkage control [168].

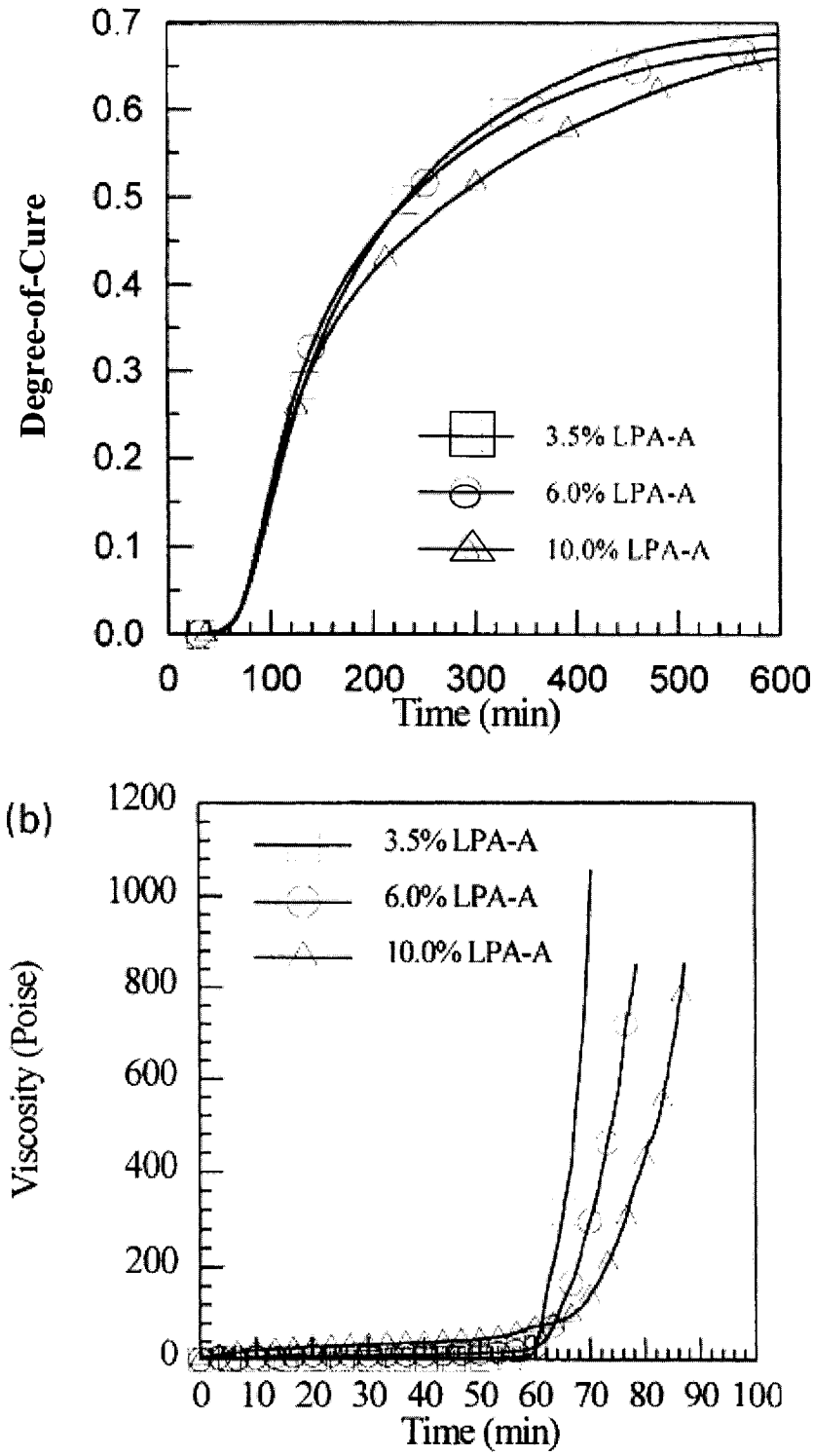

Figure 2.8 (a) Degree-of-cure as a function of time (b) Viscosity variations as a function of time (adapted from Li et al. [168]).

Lucas et al. in 1992 [178] investigated the effects of PVAc and $CaCO_3$ on the cure kinetics, mechanical properties, and surface finish of a UP resin. More specifically, they studied the effect of PVAc and $CaCO_3$ on the cure kinetics while keeping the ratio of styrene to C=C double bonds of unsaturated polyester resin constant. It was found that the final degree-of-cure of double bonds did not depend on the PVAc content, which means there was no significant influence of LPA on cure kinetics. Also, the glass transition temperature was not affected by the addition of PVAc. However, filler content decreased the induction time and increased the rate of cure. Compared to pure resin alone, the addition of LPA and filler had the affect of higher elastic modulus but a decrease in both flexural strength and impact energy. The addition of filler and LPA also resulted in better shrinkage control; however it gave a rough surface on the panels manufactured.

Hsu et al. [179] examined the effects of different LPA systems and their effects on the reaction kinetics. It was found that PVAc had the best shrinkage control followed by PMMA and polystyrene (PS). The study found that the PVAc provided larger interfacial areas than PMMA and PS and therefore gave better shrinkage control. Polar thermoplastics were found to give better control over shrinkage than non-polar thermoplastics. Study also suggested that the addition of LPA decreased total heat-of-reaction and final degree-of-cure. Models were developed to predict volume change during cure.

Huang and Su [180] studied the effects of different low profile additives on the morphological changes during the cure of unsaturated polyester resins. PVAc and PMMA were examined with different molar ratios of styrene to C=C bonds of polyester. Huang and Su also examined the influence of temperature, molar ratio of styrene to polyester C=C bonds and LPA content on phase characteristics prior to reaction [181]. They found that the addition of LPA reduced both the reaction rate and the heat-of-reaction. Also, a reduction in induction time and time to reach maximum reaction rate was observed.

2.5.1.3 Shrinkage Control of LPA

In the past, the effects of LPA concentration, LPA types, LPA molecular weights, polyester resin structure and processing conditions on polymerization shrinkage have been investigated. However, experimental results concerning the effects of LPA concentration and LPA molecular weights are quite controversial, where the effectiveness of shrinkage control performance in the cure of UP resins has been reported to be independent of, decreasing with, or increasing with various LPA concentrations. Also, in-depth analysis for the shrinkage control action of LPA over the whole cure process still remains less than satisfactory.

Li and Lee [169] studied the effects of LPA type and concentration and chemical structure of the resin on its shrinkage behavior. For low temperature cure, a range of LPA concentration was found for which LPA were most effective. A volumetric shrinkage of about 10% was also found for Q6585 neat polyester resin from Ashland Chemicals. Cao and Lee [171] found that final degree-of-cure and residual styrene was greatly improved by using a dual initiator system. Cao and Lee also studied the effect of different co-promoters and secondary monomers on the shrinkage behavior of low profile resins [172]. It was found that low promoter and high styrene level resulted in late volume expansion and hence poor shrinkage control. Researchers have found that the resins with a co-promoter gave higher reaction rates and better shrinkage control.

Liu et al. [182] examined the shrinkage behavior of unsaturated polyester (UP) resin with varying amounts of LPA. A volumetric shrinkage of approximately 10% was observed for an unsaturated polyester resin without any low profile additive. A graph adapted from this research is given in Figure 2.9, which shows the effect of amounts of LPA on the shrinkage behavior of polyester resin. An increase in the amount of LPA, reduces the final cure shrinkage of polyester resin.

Kinkelaar et al. [183] used a dilatometer to study the effect of low profile additives and cure temperature on shrinkage control. The formulation involved only unsaturated polyester, styrene, LPA and initiator. For isothermal curing, the optimum concentration

of LPA was found to be 2.5%. At higher concentrations, the LPA structure was observed to become more spherical and tightly packed and began to act as non-reactive filler. Hsieh et al. reported on the effect of the rate of exothermic heat released from the curing reaction on the morphology of the cured resin [184].

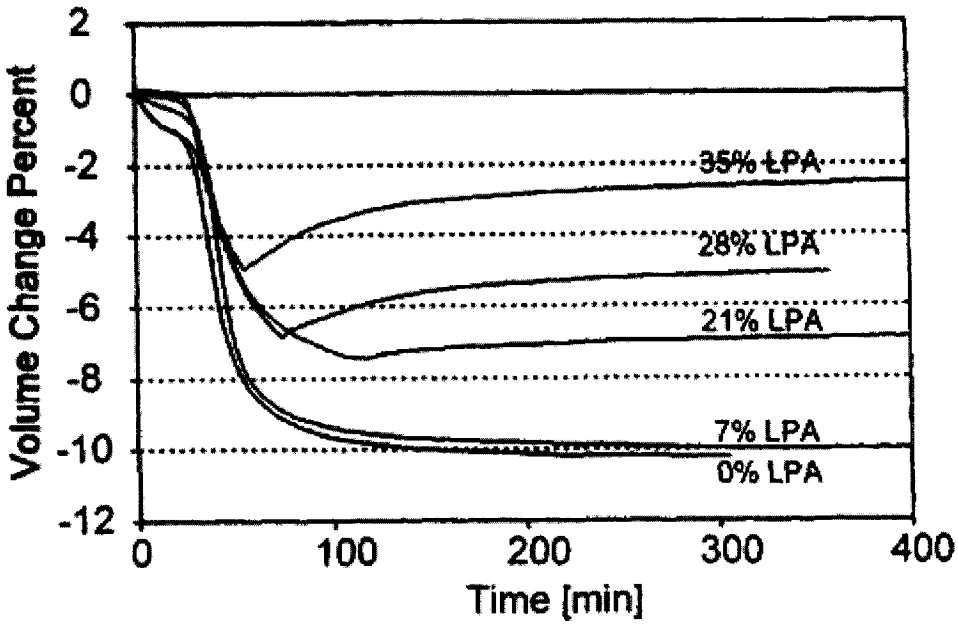

Figure 2.9 Volumetric shrinkage as a function of time for various amounts of LPA (adapted from Liu et al. [182]).

Boyard and coworkers [185] investigated the relationship between shrinkage and degree-of-cure. A net shrinkage of 9% was observed in unsaturated polyester resins. Shrinkage and shrinkage compensation in neat and low profile resins was found to be linear with the degree-of-cure [185]. A minimum amount of LPA (15%) was used for shrinkage compensation. Adding filler and fibers decreased the final shrinkage in neat resins.

Huang et al. [186] reported effects of four low profile additives, namely poly vinyl-acetate (PVAc), poly methyl-methacrylate (PMMA), thermoplastic polyurethane (PU) and polystyrene (PS), on the volume shrinkage of unsaturated polyester resins. The

results showed that the volume shrinkage generally decreased linearly with increasing LPA concentration. The effectiveness of volume shrinkage control was best for PVAc, followed by PMMA and PS.

Effects of inclusion of nano-clay particles on the shrinkage control of low profile unsaturated polyester resins have also been studied. Xu and Lee [173] reported that the addition of a small amount (1-3%) of nano-clay particles in unsaturated polyester resins, gave better shrinkage control. Some other researchers have tried to modify chemical substances like styrene-butadiene to make them work as low profile additives [187]. LPA actions in resins are very complex and models to predict their behavior during curing are non-existent. An objective of this study is to model the behavior of LPA during the cure cycle.

2.5.1.4 Effectiveness of LPA

There are several types of commercially available LPA but their shrinkage compensation behavior and final shrinkage volume differ from each other. Gordon et al. [153] stated compatibility, molecular weight, di-polar moment and glass transition as major factors influencing the choice and actions of LPA. Optimum LPA concentration was optimized based on the criteria of minimum final shrinkage and residual stresses in a completely cured resin. It was also found that an addition of 1% wt. accelerator strengthened the shrinkage compensation effects of poly vinyl-acetate (PVAc) low profile additives. Phase separations and micro-void formation were found to be the shrinkage compensation driving mechanisms [153].

The most common LPA are PVAc and PMMA. The type and amount of LPA depends on the application. The optimum amount varies for different LPA based on the chemical composition of resin and the processing conditions. Other factors to consider in selecting an additive include molecular weight, compatibility, dipole moment and glass transition temperature. For PVAc, the useful range of molecular weight is from 10,000-250,000

g/mol. Good shrinkage control has been correlated with the dipole moment of the LPA [179].

2.5.2 Effects of Fillers

Fillers are added to a polymer matrix for several reasons. Fillers reduce the cost of the resin since they are cheaper than the matrix. Fillers increase the matrix modulus and reduce resin shrinkage. In addition, fillers provide control over viscosity and improve the appearance of the surface. The most common fillers are calcium carbonate ($CaCO_3$), clay and polyethylene powder. Inorganic fillers also work as heat sinks to achieve a better temperature control across a molded part during curing. The effect of particulates on the curing kinetics of unsaturated polyester resin was investigated by Han and Lem [145-148]. For the investigation, $CaCO_3$, clay and polyethylene powder were used as fillers. It was found that the presence of the particulates increased the curing rate.

A reduction in cure shrinkage of polyester resins has been reported when fillers were added into the resin [165]. Even further, a better shrinkage control was achieved when fillers were used in combination with LPA. Filler was observed as resisting cure shrinkage and inducing internal stresses in the polymer matrix [174]. Lucas et al. [178] reported a decrease in the induction time of cure reaction and an increase in the cure rate when LPA were used in the resin formulation. Compared to the pure resin, the addition of LPA and filler had the affect of higher elastic modulus but a decrease in both flexural strength and impact energy. The addition of filler and LPA also resulted in better shrinkage control; however it gave a rough surface on the manufactured panels. Surface roughness measured was in the following order (neat resin < neat resin + filler < neat resin + filler + LPA).

Micro-void formation during LPA expansion in unsaturated polyester resins cure, which is very important in shrinkage compensation mechanism of LPA, was investigated in detail by Zhang et al. Filler content was observed to favor micro-void formation. Higher filler content resulted in higher micro-void volume fraction. However, effects of filler on

micro-void formation were found to be inter-coupled with the amount of LPA [176]. Dutiro et al. studied effects of various factors including filler content, on the degree of surface finish [188]. Gloss, surface roughness and mold fill times were taken as the response values. Higher filler content was observed to reduce gloss; however it also reduced roughness.

2.6 Design of Experiments

Experimentation has always been very important in manufacturing processes. Experimentation has been defined as "an operation carried out under controlled conditions in order to discover an unknown effect or establish a hypothesis or to illustrate a known law" [189]. Experiments are done by the scientists and engineers alike to advance their understanding about a particular phenomenon. Scientists try to establish cause-effect relationships and conduct experiments to identify the truth about such a relationship, whereas engineers conduct experiments to improve the quality of products and processes. In brief, experiments are generally performed to explore, estimate and confirm.

Design of experiments (DOE) or statistically designed experiments (SDE), is a scientific approach, which allows to understand a process and to determine how the input variables (factors) affect the output or quality characteristics. It is a systemic approach to process optimization. Experiments are designed and planned through DOE for appropriate data collection, which are then analyzed through statistical methods. Statistical design of experiments is an alternative to the traditional, inefficient one-factor-at-a-time experimentation, where one factor is varied at a time while keeping all the other factor levels constant [190].

For industrial experiments, factors can be classified into two types: qualitative and quantitative. Qualitative factors are those where there is no numerical hierarchy to separate the two levels: for example, good and bad, two brands of chemicals etc. Quantitative factors, on the other hand, are those that are measurable and continuous, for

example, the thickness of a wafer, the diameter of spindle, the strength of steel etc. The response is the quantity measured in an experiment. When the response relates to some measure of quality, then it is called a quality characteristic.

There are three different design of experiment approaches for improving product and process quality: classical design of experiments, the Shainin method and the Taguchi method.

2.6.1 Classical Approach to Experimentation

Classical design of experiments technique was first developed by Fisher et al. for applications in agricultural field in early 1920's [191]. In this approach, while experimenting with several factors, the strategy consists of selecting a starting point or baseline set of levels for each factor, then successively varying each factor over its range with the other factors held constant at the baseline level. After completing all trials, a series of graphs are usually plotted showing the effect on the response of varying each factor with all other factors held constant. Since only one factor is varied at a time, this strategy is also known as one-factor-at-a-time method. Along with many benefits, there are major disadvantages related with this technique. For example,

- No predictive knowledge of the system being studied is given. Response values can not be predicted or estimated at factor levels at which trials have not been conducted.

- Possible interactions existing between factors are not taken into account, where interaction is the dependence of one factor on the other. In the presence of interactions a factor fails to produce the same effect on a response at different levels of another factor. Interactions between factors are common in industrial experiments; as a result implementations based on one-factor-at-a-time strategy usually are less efficient and produce poor results. It is shown that such a technique does not give any information about the position of the optimum in cases where interactions exist between factors.

Nevertheless, researchers have shown practical applications of this technique for industrial and non-industrial problems [192-197].

2.6.2 The Shainin Method

Dorian Shainin, another expert in the filed of quality engineering, developed a different approach to experimental design in 1952. Shainin has developed a variable alternative to both the Taguchi and the classical approach, by adopting simple but statistically powerful techniques. Bhote states "within the world of design of experiments, the Shainin methods are the simplest, easiest and the most cost effective ways to get to the finish line" [198-199]. But researchers [200] found that Shainin's approach also suffered from the same problems as that of one-factor-at-a-time experimentation. Nevertheless, it was found to be a useful technique for engineers for identifying few critical factors with their best or worst levels and some industries like Motorola are practicing it [201-202]. A detailed description and applications of this method are given by Anthony et al. [203].

2.6.3 The Taguchi Method

The Taguchi method, developed by Dr. Genichi Taguchi, refers to a technique of quality engineering that includes both statistical process control and new quality related management techniques. It is a method for designing and performing experiments to investigate processes where the output depends on many input variables, without having tediously and uneconomically run the process using all possible combinations of values of those variables. By systematically choosing certain combinations of variables through this method, it is possible to separate their individual effects [204-205].

The Taguchi approach to quality engineering places a great deal of emphasis on minimizing variations as the main mean of improving quality. The idea is to design products and processes whose performance is not affected by outside conditions. The method uses a set of tables (known as orthogonal arrays) that enable main variables and interactions to be investigated in a minimum number of trials [204-206].

2.6.3.1 Robust Design

The most important contribution of the Taguchi technique is the concept of robust design. Robust design is the approach for determining the optimum configuration of design parameters for performance, quality and cost. The robust design method provides a systematic and efficient way for finding the near-optimum combination of design parameters so that the product is functional, exhibits a high level of performance, and is robust to noise factors. Noise factors are those parameters that are uncontrollable or are too expensive to control [206].

In order to determine and subsequently minimize the effect of factors that cause variation, the design cycle is divided into three phases: system design, parameter design, and tolerance design. In the first, the designer uses knowledge of the process being investigated to produce an initial design of a product or process. The objective of the second phase is to choose suitable values for the parameters of a product or process. In tolerance design, higher quality parts replace less reliable components, improving the quality of the product or process [207-208].

2.6.3.2 Statistical Analysis of Experiments

The Taguchi method employs orthogonal arrays to design and execute experimental plans. Orthogonal arrays are a special set of matrices, constructed to lay out product design experiments. An orthogonal array is a set of experiments in which values of a number of parameters are simultaneously changed in each of the experiment. The orthogonal array stipulates the way of conducting a minimal number of experiments, which, in most of the cases, gives full information of all factors that affect performance parameters. A detailed discussion and a list of orthogonal arrays for different design conditions is given by Roy [209]. Roy also enlisted the formulae and procedures for ANOVA (analysis of variance) calculations, which are performed on the results obtained from the Taguchi method.

A powerful tool in the Taguchi method is the inclusion of the variability of data from multiple trials, in the analysis of results. Taguchi came up with formulae to calculate the variation in multiple data sets using, what is called, mean-squared deviation (MSD). MSD formulae are different based on the quality characteristics of the product. Formulae for mean-squared deviation for different quality characteristics are given in Equations 2.22-2.24.

Smaller: $$MSD = \frac{1}{n}\sum_{i=1}^{n} y_i^{\,2} \tag{2.22}$$

Nominal: $$MSD = \frac{1}{n}\sum_{i=1}^{n} \left(y_i - \bar{y}\right)^2 \tag{2.23}$$

Bigger: $$MSD = \frac{1}{n}\sum_{i=1}^{n} \frac{1}{y_i^{\,2}} \tag{2.24}$$

where n is the number of trials, y_i is the value obtained during each trial and $\bar{y}$ is the average value. MSD values are then used to calculate, what is called, a signal-to-noise (S/N) ratio. Formulae for S/N ratio are given in Equations 2.25-2.27.

Smaller: $$\frac{S}{N} = -10\log_{10}(MSD) \tag{2.25}$$

Nominal: $$\frac{S}{N} = 10\log_{10}\left(\frac{\bar{y}^2}{\sigma^2}\right) \tag{2.26}$$

Bigger: $$\frac{S}{N} = -10\log_{10}(MSD) \tag{2.27}$$

where σ is the standard deviation in the results. MSD and S/N ratios are yardsticks for the analysis of the variability in experimental results obtained under identical processing conditions. A smaller value of MDS and a bigger value of S/N is desirable and represent minimum variability in the measurements [209].

2.6.3.3 Applications of the Taguchi Method

The Taguchi method has been applied successfully in various fields of study, including all branches of engineering along with applied and pure sciences. However industrial and manufacturing product-and-process improvement has been the focal point of Taguchi method's application. Jean et al. reported the application of the Taguchi method for process optimization in high energy electron beam case hardening of cast iron [210]. The Taguchi method was compared with multiple regression techniques in predicting the response values. Both methods were found to be very compatible; however multiple regression resulted in less average error. Most-significant factors were identified with the Taguchi method. Predicted S/N ratio was very close to the measured ratio [210].

Tsai et al. [211] investigated the application of the Taguchi method in simulation and optimization of a manufacturing system. Most recently, the Taguchi method has been successfully applied in process parameter optimization of a welding process [212], coil spring manufacturing process [213], hot forming process [214], injection molding process [215], die casting process [216], blow molding process [217], turning [218] and drilling operations [219]. The Taguchi method of experimental design and analysis is a powerful tool, which offers simultaneous improvements in quality and cost [220-222].

Hence, the Taguchi method is a powerful statistical tool for product and process improvement. In this approach, the quality is evaluated at every stage of the product-design process aiming to reduce variations and quality problems. It is an efficient tool to determine optimum process conditions for better performance, higher quality and reduced cost. Some of benefits of the Taguchi method are reduced noise or variance around the target value, cost effective determination of important factors affecting quality characteristic and emphasis on quality improvement in the product design stage.

2.6.4 Optimization of Process Parameters

Lin et al. state that optimization of RTM process consists of widely different objective functions and design variables [93]. Objectives are to minimize cycle time, void content,

temperature gradient, injection pressure, temperature overshoot and reduce tooling cost, labor required for lay up or performs assembly and volatile emissions. Common design variables are gate location, number of gates, placement of high permeability layers, injection pressure, mold temperature, tooling geometry and material choice. A great deal of work has been done in the area of numerical modeling and simulation of RTM process [39-59]. However class A surface finish is still absent in the parts manufactured with RTM process because of the manufacturing and processing problems related with this process. Some of processing problems can be addressed through simulations like mold design, mold heating, filling and resin curing. However, there are neither mathematical nor empirical models available in the literature to predict the surface quality of resulting part as a function of processing parameters and the work in the area of experimental process optimization for class A surface finish is limited and rare. Only a few researchers [75-76,96,178,224-225] have tried to address this industrial problem and even then, only at a very basic level.

Dutiro et al. used statistical experimental design (SED) techniques to study the effect of various factors on surface finish [75,92]. Gloss, surface roughness and mold fill times were taken as the response values. Roughness was measured using a laser profilometer. Fabric print through, shrinkage trenches, surface flow lines, filler filtration patches and pinholes were found to be the common problems contributing towards poor surface finish. This research established that gloss increased with the lower filler content, V_f[1], mold temperature and higher injection pressure. Whereas roughness reduced with higher filler content, injection pressure and with lower V_f and mold temperature. This work was further verified by Bayldon [76]. Higher filler content and injection pressures were confirmed to result in better surface finish.

Lucas et al. studied the effects of LPA and fillers on polymerization reaction, mechanical properties and surface rugosities. Surface rugosity (surface quality) was measured using the Talysurf-120 device [178]. A glass plaque was used as a reference with $R_a = 0.05$ μm. Without the addition of LPA, the rugosity was measured to be $R_a = 0.29$ μm in the neat

[1] V_f refers to volume fraction of fibers in the composite part.

resin. For PVAc concentrations that resulted in shrinkage compensation, the measurements were reported between R_a = 0.06-0.08 μm. By adding both filler and PVAc, there was an improvement in surface finish. The surface finish was reported in the following order (neat resin < neat resin + filler < neat resin + filler+ LPA). Lucas et al. also found a critical concentration (8%) of LPA, which was needed for shrinkage compensation. No further improvement in the surface finish was observed when LPA level was increased above 8%.

Karbhari et al. [223] studied the effect of material, process and equipment variables on the mechanical performance of RTM molded parts using the Taguchi method. Eight experiments were carried out to check the effect of seven 2-level factors. Parts were analyzed based on tensile failure stress, shear strength and maximum stress quality characteristics. Optimum levels of process parameters were determined and set and validation experiments were carried out. The quality characteristics were found to be very close to theoretical values at optimum levels of control factors. The Taguchi method was found to be an efficient and economical method for evaluating the relative importance and interaction of both process and performance related parameters.

Vallat et al. [224] reported on the effects of internal de-molding agents and $CaCO_3$ fillers on the surface roughness of bulk molding compounds. No significant different in the surface roughness was observed by increasing the amount of internal de-molding agent in the resin. The resin morphology was found to be different on the surface and in the bulk of the material. No LPA were found on the surface leaving a thin film of the resin; however fillers and LPA were well dispersed in the bulk through the thickness. Kim and Lee [225] investigated effects of stacking sequence and fiber volume fraction of glass fiber mat on the surface quality of composite panels. Three different types of mats were used. A Satin weave on the outside gave better finish. Ultimately a composite bus housing panel was designed and manufactured by RTM and a stacking sequence of the fiber mat was determined, which minimized fabric print through on the surface.

2.7 Conclusion

A brief review of the recent work in the area of resin transfer molding, cure kinetics, viscosity variations and cure shrinkage measurement and modeling of polyester resins, low profile additives, surface finish issues, manufacturing problems in RTM processing, effects of fillers, surface roughness measurements, design of experiments and particularly the Taguchi method is presented here. Composite materials and their processing techniques are relatively new to the manufacturing sector and processes like RTM are still not fully optimized. There is a great deal of interest in the development of analytical, mathematical, numerical and statistical tools to enhance understanding and further the knowledge of composite processing. As discussed earlier, there is not much research work done in the area of class A RTM manufacturing, which is very important to promote the wide spread use of low cost fiber glass composites in the automotive industry. Effects of low profile additives on cure kinetics and chemorheology of polyester resins are not well understood and standard methods for characterization are still a matter of argument. Even further, research on the behavior of LPA during actual manufacturing and their effects on resulting finish quality of composite structures are altogether absent. There is need to study the effects of LPA and other processing parameters on cure kinetics, cure shrinkage and resulting surface finish of RTM molded components using analytical, numerical and statistical tools and that is the objective of this research.

2.8 Optimization Methodology

The RTM process involves several parameters that potentially affect the quality of RTM molded components. The parameters can be divided in to two categories: Material parameters and process parameters. Material parameters include types of quantities of resin, styrene, low profile additive, catalyst, accelerator, inhibitor, internal and external de-molding agents, filler, reinforcement, wetting agent and air release agent. Process parameters include molding temperature, temperature gradient between the mold platens, injection pressure, flow rate and injection temperature. A systematic approach is needed to choose significant parameters and their levels to be used in experimental test matrices

and statistical analysis. Hence, the research for the optimization of processing parameters is divided into four key areas: material characterization (chapter 3), RTM manufacturing (chapter 4), numerical simulations (chapter 5), and statistical analysis (chapter 6). A flow chart of the research is presented in Figure 2.10.

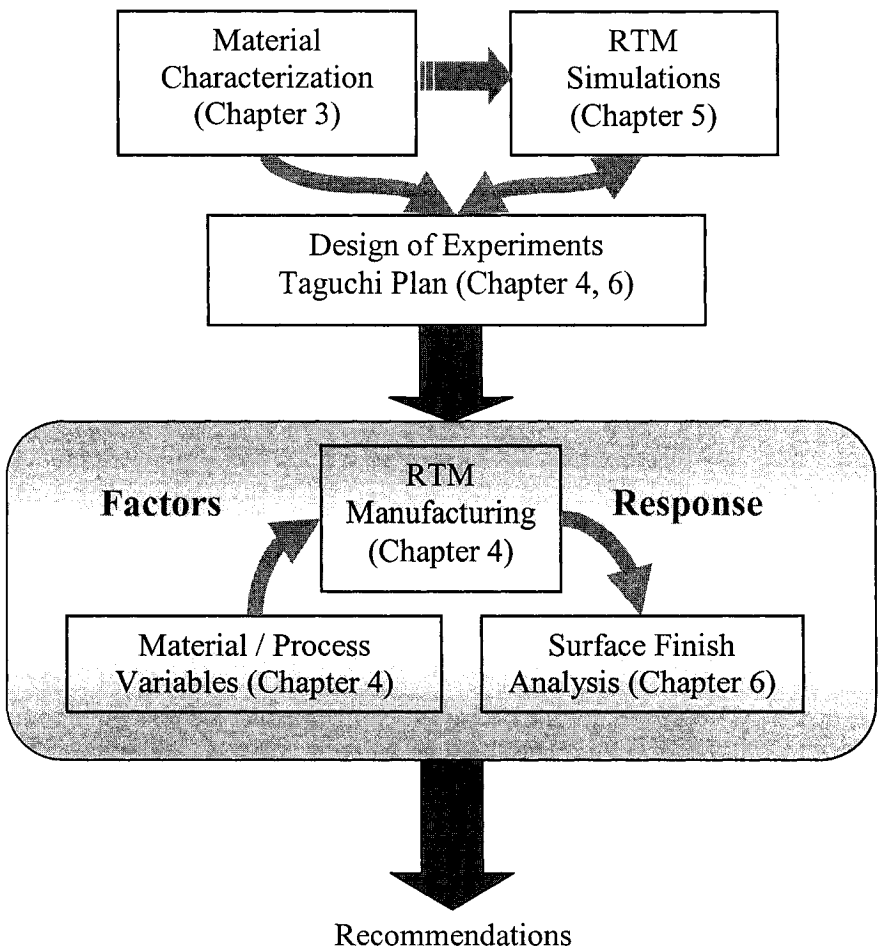

Figure 2.10 The flow chart of the proposed research

CHAPTER 3

CURE SHRINKAGE CHARACTERIZATION AND MODELING OF A POLYESTER RESIN CONTAINING LOW PROFILE ADDITIVES

Mohsan Haider, Pascal Hubert*, Larry Lessard

Department of Mechanical Engineering, McGill University
817 Sherbrooke Street west, Montreal H3A 2K6, Quebec, Canada

(Prepared for Composites Part A. Applied Science and Manufacturing)

Abstract

Resin Transfer Molding (RTM) has great potential as an efficient and economical process for fabricating large and complicated composite structural components. The low capital investment cost required and process versatility in component integration and assembly make RTM very attractive for high volume automotive applications. One of the challenges facing the automotive field is the resulting surface finish of manufactured components. The shrinkage associated with the curing of thermoset resins contributes to the poor surface quality. Low profile additives (LPA) are added to the resin to

* Corresponding author:
E-mail: pascal.hubert@mcgill.ca
Tel.: 1(514) 398-6303

compensate for the cure shrinkage; however their effects on the thermal, rheological and morphological properties of polyester resins are not well understood. In this paper, the effect of LPA on cure kinetics, cure shrinkage and viscosity of a polyester resin is studied through differential scanning calorimetry (DSC) and special rheological techniques. Models are developed to predict cure shrinkage, LPA expansion, cure kinetics and viscosity variations of the resin as a function of processing temperature. Finally, morphological changes in the resin with and without LPA, during isothermal cure, are studied with hot stage optical microscopy. The results show that the LPA content in the range tested had no significant effect on the cure kinetics. However, higher LPA content reduced cure rate and cure shrinkage. A minimum of 10% LPA was required to compensate for cure shrinkage. Shrinkage behavior of all formulations was similar until a degree-of-cure of 0.5. However, resin formulations with higher LPA content showed expansion at later stages during curing.

Keywords: B. Curing- chemical shrinkage, B. Rheological properties, D. Thermal analysis, E. Resin transfer molding (RTM)

3.1 Introduction

Polymer composites are increasingly used in automotive applications because of their light weight, corrosion resistance, superior fatigue resistance, energy absorption and noise suppression capabilities. However, the resulting aesthetic appeal or surface finish is a critical issue particularly for car body panels. Class A surface finish is difficult to achieve with RTM molded components. Some of most common surface finish quality problems like fabric print through, ripple or long range waviness, sink marks and dimensional inaccuracy are caused principally by the resin cure shrinkage. Cure shrinkage of 7-10% typically reported for standard polyester resins [1-8] makes it difficult to achieve surface finish qualities and tight tolerances on car body panels in compliance with industry specifications and standards. Thermal, rheological and morphological characterization techniques can be employed to understand the shrinkage

behavior of low cost unsaturated polyester resins which are commonly used in automotive applications. With proper material characterization, resin cure kinetics, rheological and cure shrinkage models can be developed. The models can then be implemented in composite processing simulation tools in order to define the best resin formulation that would improve surface finish of composite automotive parts.

Cure shrinkage behavior of unsaturated polyester resins has been studied by several researchers. Bogetti and Gillespie [9] measured volumetric shrinkage of a polyester resin and derived a model (Equation 3.1) giving the cure shrinkage as a linear function of degree-of-cure.

$$\Delta V = \Delta\alpha * V^T \tag{3.1}$$

where ΔV is change in volumetric shrinkage, $\Delta\alpha$ is the change in resin degree-of-cure and V^T is the total volumetric shrinkage for fully cured resin. Volume shrinkage of 6% was reported by Bogetti and Gillespie for a standard polyester resin [9]. Hill et al. also proposed two models to predict volume changes during the cure of unsaturated polyester resin [10]. The first model, which is based on conversion, was developed by combining experimental results from differential scanning calorimetry (DSC) and dilatometry. The second model was based on radical concentration. The overall volumetric change of resin during cure was considered to be a combination of thermal expansion/contraction and cure shrinkage as:

$$\left(\frac{1}{V_o}\frac{dV}{dt}\right)_{overall} = \left(\frac{1}{V_o}\frac{dV}{dt}\right)_{Thermal} - \left(\frac{1}{V_o}\frac{dV}{dt}\right)_{Shrinkage} \tag{3.2}$$

where

$$\left(\frac{1}{V_o}\frac{dV}{dt}\right)_{Thermal} = \left(\beta_m(1-\alpha)+\beta_p\alpha\right)\left(\frac{dT}{dt}\right)$$

$$\left(\frac{1}{V_o}\frac{dV}{dt}\right)_{Shrinkage} = B\frac{d\alpha}{dt}$$

where

β_m - volumetric thermal expansion coefficient of uncured resin

β_p - volumetric thermal expansion coefficient of cure resin

B - constant

α - degree-of-cure

T - absolute temperature

t - time

A total volumetric shrinkage of about 9% was observed for unsaturated neat polyester resin containing a 1:1 mixture of maleic anhydride and propylene glycol containing 35% wt. of styrene [10]. A cure-shrinkage of 6% was reported for MY750 epoxy resin (unmodified diglycidyl ether of bisphenol-A epoxy resin) by Li et al. using a density difference method. The shrinkage was found to be a linear function of degree-of-cure and was independent of time and temperature [11]. Several cure shrinkage measurement techniques using capillary dilatometer [10], density difference method [11], thermo-mechanical analyzer and dynamic mechanical analyzer [12-13] have also been developed.

Low Profile Additives

Low profile additives (LPA) are thermoplastic materials such as poly methyl-methacrylate (PMMA), poly vinyl-acetate (PVAc) and polystyrene (PS) added into thermoset resins and generally serve as non-reactive additives in unsaturated polyester and vinyl ester resins. LPA have been found to be highly effective in eliminating the polymerization shrinkage of unsaturated polyester resins in high-temperature molding processes. Research has been conducted to study the effects of LPA type, molecular weight and concentration on cure shrinkage [14-20]. The effects of cure conditions on LPA behavior including temperature, pressure and thermal history have also been investigated [14-20]. The LPA mechanism, through which the shrinkage is compensated, has been under investigation for many years; however it has not been fully understood. Researchers have employed various analytical techniques such as DSC, dilatometry,

Fourier transform infrared spectroscopy (FTIR), scanning electron microscope (SEM) and optical microscopy to evaluate the influence of LPA concentration on cure kinetics, cure shrinkage and morphological changes in polyester resins [14-20]. However, the most common technique used for cure kinetics characterization is DSC, and for cure shrinkage characterization is dilatometry.

Effects of LPA on Cure Kinetics

Effects of LPA on exothermic reaction kinetics, cure rate, final degree-of-cure and total enthalpy of reaction are somewhat controversial. Some researchers have found no significant effect of LPA on reaction kinetics and cure rate [14-20]. However, some others suggest slower reaction rates as a result of LPA inclusion into the resin [21]. Li et al. [14] studied the cure and shrinkage behavior of Q6585 polyester resin, from Ashland Chemical Inc., with different types and amounts of LPA. It was found that the amount of LPA had a minor effect on cure kinetics, rheological behavior and gel time of a polyester resin. Li et al. [14] also observed that the LPA concentration changed the resin from transparent to opaque. Lucas et al. in 1992 [20] investigated the effects of PVAc LPA on the cure kinetics of unsaturated polyester resin while keeping the ratio of styrene to C=C double bonds constant. It was found that the final degree-of-cure of double bonds did not depend on the PVAc content, which means there was no significant influence of LPA on cure kinetics. Hsu et al. [21] however reported that the addition of LPA decreased the total heat-of-reaction and final degree-of-cure in a polyester system. Models were developed to predict volume change during cure. This result was further confirmed by Huang and Su [22] who studied the effects of different low profile additives on the morphological changes during the cure of unsaturated polyester resins. They found that the addition of LPA reduced both the reaction rate and the heat-of-reaction. Also, a reduction in induction time (time to start the chemical reaction) and time to reach maximum reaction rate was observed at higher LPA levels.

Effects of LPA on Cure Shrinkage

The effects of LPA concentration, LPA types, LPA molecular weights, polyester resin structure and processing conditions on polymerization shrinkage have also been investigated. Li and Lee [14] studied the effects of LPA type and concentration and chemical structure of the resin on its shrinkage behavior. For low temperature cure, a range of LPA concentration (3.5-5% by weight) was found for which LPA were most effective. A volumetric shrinkage of about 10% was also found for Q6585 neat polyester resin from Ashland Chemicals which reduced to 4% for an addition of 3.5% of LPA. Cao and Lee [17] found that final degree-of-cure increased from 0.87 to 0.96 and residual styrene reduced from 10% to 0% when a dual initiator system was used for an isothermal cure at 60°C. Kinkelaar et al. [23] used a dilatometer to study the effect of low profile additives and cure temperature on shrinkage control. The formulation involved only unsaturated polyester, styrene, LPA and initiator. For isothermal curing, the optimum concentration of LPA was found to be 2.5%. At higher concentrations, the LPA structure was observed to become more spherical and tightly packed and began to act as non-reactive filler. Huang et al. [24] reported effects of four low-profile additives like poly vinyl-acetate (PVAc), poly methyl-methacrylate (PMMA), thermoplastic polyurethane (PU) and polystyrene (PS), on the volume shrinkage of unsaturated polyester resins using a dilatometer. The results showed that the volume shrinkage generally decreased linearly with increasing LPA concentration. The effectiveness of volume shrinkage control was best for PVAc, followed by PMMA, PS and PU. Liu et al. [25] examined the shrinkage behavior of unsaturated polyester (UP) resin with varying amounts of LPA (PVAc). A volumetric shrinkage of approximately 10% was observed for an unsaturated polyester resin without any low profile additive. Increase in the LPA content (from 0-35%) resulted in a relative decrease in the final cure shrinkage (from 10-2%) of the polyester resin.

Boyard and coworkers [26] investigated the relationship between shrinkage and degree-of-cure. A net shrinkage of 9% was observed in unsaturated polyester resins. Shrinkage in the neat resin was found to be linear with the degree-of-cure [26]. A minimum amount of LPA (15%) was used for shrinkage compensation. Adding filler and fibers decreased

the final shrinkage in neat resins. Effects of inclusion of nano-clay particles on the shrinkage control of low profile unsaturated polyester resins have also been studied. Xu and Lee [19] reported that the addition of a small amount (1-3%) of nano-clay particles in unsaturated polyester resins, gave better shrinkage control. Some other researchers have tried to modify chemical substances like styrene-butadiene to make them work as low profile additives [27].

LPA Expansion Mechanism

Unfortunately, a detailed and well understood LPA mechanism through which shrinkage compensation takes place is still absent from the literature. Several mechanisms have been suggested by the researchers which explain LPA expansion through phase separation and micro-void formation [14-19], free monomer boiling and exerting pressure [28], strain-relief cracking mechanism [29], LPA thermal expansion mechanism [30] and nucleation and expansion of styrene in LPA rich phase [31]. However, it is generally accepted that the shrinkage control of LPA is based on thermal expansion during high temperature cure, phase separation between LPA and unsaturated polyester (UP) resins and micro-void formation on the interface between UP and LPA phases [14-19]. Lee et al. [15-19] concluded that a co-continuous or LPA-rich phase dominated structure was essential for thermoplastics to be effective as shrinkage control additives at low temperature cure. Phase separation and micro-void formation were found to be two most critical steps for shrinkage control. Micro-cracking was found to occur when the stresses generated by polymerization shrinkage became greater than the 'resistance' force possessed by the interface or LPA-rich phase. Micro-void formation during LPA expansion in unsaturated polyester resin cure was investigated in detail by Zhang and Zhu [31]. Micro-void formation was observed to be controlled by the amount of LPA and styrene. Increase in LPA content increased the volume fraction of voids. Other parameters with significant effect on the formation and size of micro-voids were processing temperature, type and quantity of initiator, filler content and external pressure. Higher processing temperature and filler content resulted in bigger volume fraction of the

voids. There are several types of commercially available LPA but their shrinkage compensation behavior and final shrinkage volume differ from each other. Gordon et al. [32] stated compatibility, molecular weight, di-polar moment and glass transition as major factors influencing the choice and actions of LPA. Optimum LPA concentration was optimized based on the criteria of minimum final shrinkage and residual stresses in a completely cured resin. It was also found that an addition of 1% wt. accelerator strengthened the shrinkage compensation effects of poly vinyl-acetate (PVAc) low profile additives. Phase separations and micro-void formation were found to be shrinkage compensation driving mechanisms [32]. Despite these research efforts, a broad-based knowledge and experience about the way shrinkage and shrinkage compensation occurs in low profile resins over the entire cure cycle during manufacturing, is still absent. Also, missing is the basic understanding of the effects of LPA content on surface quality of molded components.

Most of the previous work on the study of LPA in polyester resins was focused on the experimental observation of the morphology and shrinkage evolution during cure. In this paper, a comprehensive investigation of the shrinkage of LPA modified resins is conducted. A direct method for the measurement of shrinkage-expansion behavior of LPA based resin systems is presented and differential scanning calorimetry (DSC) techniques are used for cure kinetics characterization. Then models are developed to characterize cure kinetics, shrinkage and viscosity variations during cure. Finally, morphological cure changes in the resin with and without LPA during isothermal cure are studied with hot stage optical microscopy. The effects of the amounts of LPA and fillers on the cure kinetics morphology, viscosity variations and cure shrinkage are investigated.

3.2 Materials

Scott Bader's PD9551 polyester resin [33] was used in this research. The resin was supplied with a standard amount (10% by weight of resin) of LPA. Resin batches without LPA and with varying amounts of LPA (5, 8, 10, 20, 40%) were also tested. Low profile

additive added to the resin was Scott Bader PD9419 polymer solution, which contained PVAc and PMMA low profiles additives. OMYA BLR2 calcium carbonate filler was added to the resin and standard accelerator (cobalt 2-ethylhexanoate) and catalyst (tert-butyl peroxybenzoate) were used. Table 3.1 summarizes the resin formulations, ingredients and their weight fractions based on the weight of the resin. The resin was mixed with the accelerator first, then the filler was mixed well with the resin mixture. The catalyst was added into the resin-filler mixture and mixed again. At this point the resin was ready for testing. At least five samples were tested for each resin formulation.

3.3 Experimental Setup and Procedures

3.3.1 Differential Scanning Calorimetry

A TA Instruments Q100 differential scanning calorimeter was used for isothermal and non-isothermal scans on the resin samples. The weight of each sample was less than 10 mg and aluminum hermetic pans were used. The variation among the sample weights was within 1 mg. Non-isothermal scans were carried out from room temperature to 240°C with ramp rates of 10, 20 and 30°C/min. The total heat-of-reaction was obtained from the area under the exothermic peak. The total heat-of-reaction was used to calculate the degree-of-cure during isothermal scans and typical cure cycles. For isothermal scans, the DSC cell was pre-heated to the desired temperature. The samples were kept at isothermal temperatures of 80°C and 90°C for 45 minutes, cooled down to room temperature and re-heated at a rate of 10°C/min to 240°C to measure the residual heat-of-reaction. The isothermal temperature levels were chosen to result in a gel time range of 2-4 minutes, which is required for short cycle times. Five experiments were carried out for each test condition to verify the repeatability of the results.

3.3.2 Combined Rheology and Shrinkage Measurements

The shrinkage and rheological behavior of the resin was measured using a TA Instruments AR2000 rheometer. Forty millimeter diameter disposable aluminum parallel plates were used in oscillation mode. The experimental setup for rheology experiments is shown in Figure 3.1. This setup consisted of two plates where the bottom plate was fixed and a known amount of torque was applied on the top plate. The gap between the plates was kept constant to measure the viscosity under isothermal and non-isothermal conditions. The normal force F_z shown in Figure 3.1 is the amount of force applied by the top plate on the resin sample. This force is defined as positive when the resin sample is in compression. These tests were done in torque or strain controlled mode at a constant angular velocity (ω).

To determine viscosity variations of the resin sample during a temperature ramp, the resin sample was poured between the plates at room temperature. The gap was set at 500 μm and the temperature was increased at a slow ramp rate of 2°C/min. The rheometer was programmed in oscillation mode with a maximum angular strain of 15% at a frequency of 0.2 Hz. The variation of the gel time was studied under isothermal condition of 80°C, 90°C and 100°C. The rheometer chamber was pre-heated to the desired temperature before pouring the resin between the plates. The gel point was calculated based on the cross-over point of elastic modulus G′ and loss modulus G″. The same oscillation parameters were used for the isothermal tests.

A special test procedure based on the rheometer normal force control was developed to study the cure shrinkage of the resin. The cure shrinkage tests were performed under 80°C, 90°C and 100°C isothermal temperatures. The rheometer was programmed with two segments. In segment I, the gap between the plates was kept constant at 500 μm. The maximum strain was fixed at 15% with an oscillation frequency of 0.2 Hz. In this segment, since the resin was in liquid state no normal force was applied. At resin gelation, the rheometer was controlled according to the following settings (segment II): a maximum torque of 500 μNm at a frequency of 30 Hz was applied and the normal force

applied to the sample was kept constant at 0.1 N in compression. In this segment, when the normal force changed because of resin shrinkage or expansion, the gap changed to compensate for the change in normal force induced by the dimensional change of the sample. The equipment was set to compensate the gap for a normal force change of ±0.1N. A typical variation in normal force during the curing of a low profile resin at 90°C is plotted in Figure 3.2 and Figure 3.3 presents the corresponding gap change. As can be seen from these graphs when the resin is in the liquid state, the gap is constant and normal force is zero (segment I). The gel point which marks the end of segment I and the beginning of segment II occurs at approximately 1 minute. Then the normal force becomes negative (in tension), which corresponds to the shrinkage of the sample as the gap starts to decrease (1 minute - 4 minutes). After 4 minutes, the resin starts to expand and the normal force becomes positive (in compression). At this point, the gap between the parallel plates increases to compensate for the positive normal force. The difference between the target normal force and the measured value is due to the response time of the rheometer contact system. Five experiments were carried out for each test condition to verify the repeatability of the results.

3.3.3 Hot Stage Optical Microscopy

An Olympus BX-60 optical microscope equipped with bright-field, dark-field, fluorescence and differential interference contrast modes of operation was used to observe resin morphological changes during cure. This microscope was equipped with 10, 20 and 50X magnification objectives. A Sony 3CCD color camera and Flashpoint frame grabber were used to capture high-resolution color optical micrographs using Image Pro Plus running on a PC. A Linkam THMS 600 hot stage was used to study the in situ measurements of morphological changes in the resin during curing. The resin sample was placed between two very thin glass plates and heated at a very fast rate of 50°C/min to the desired isothermal temperatures and then the temperature was kept constant for 30 minutes in the hot stage accessory. Resin morphology was recorded with the camera at 80°C and 90°C isothermal temperatures and was later compared with degree-of-cure variations from DSC under same conditions.

3.4 Resin Cure Kinetics

Table 3.2 shows the total heat-of-reaction for all resin formulations under non-isothermal cure conditions. The values for average heat-of-reaction are between 401 and 427 J/g and the largest standard deviation is 25 J/g. The variation in average heat-of-reaction for different formulations is within a single standard deviation which makes the difference statistically insignificant. The heat flow measured during the non-isothermal scans is plotted in Figure 3.4 for a typical heating rate of 10°C/min. The onset of reaction, peak and end of reaction temperatures summarized in Table 3.3 are very close for all resin formulations (variation less than 6%). However, the resin with 40% LPA has a slower reaction rate as shown in Figure 3.5 which presents the variation in cure rate as a function of degree-of-cure. The formulations with 5, 10 and 20% LPA follow the same curve; however the reaction rate is relatively slower for the resin without LPA. Thus the amount of LPA in the range from 0-20% has no significant effect on the reaction rate; however the extreme case at 40% LPA slows down the reaction rate. In Figure 3.6, variation in degree-of-cure is plotted as a function of temperature for a heating rate of 10°C/min. The degree-of-cure curve for all formulations follows the same path; however for the extreme case of LPA (40%) the reaction starts later compared with other formulations.

The evolution of degree-of-cure of resin D (10% LPA) cured at different heating rates is plotted in Figure 3.7. The curves are shifted with respect to the temperature due to the thermal inertia of the resin. A similar trend was observed for other resin batches under identical processing conditions. This means that heating rate is an important factor which affects the degree-of-cure variation. It also shows that although faster heating rates result in faster cure rates, they delay the degree-of-cure evolution when plotted as a function of temperature.

Table 3.4 lists the isothermal heat-of-reaction, residual heat-of-reaction, isothermal final degree-of-cure and gel time for all the resin formulations under 80°C and 90°C isothermal cure conditions. The gel time is calculated based on a degree-of-cure of 0.055 obtained from rheology tests conducted under identical processing conditions. As can be seen from

Table 3.4, isothermal heat-of-reaction (between 356-388 J/g for 80°C and 353-380 J/g for 90°C), residual heat-of-reaction (20-31 J/g for 80°C and 10-20 J/g for 90°C), final degree-of-cure (0.85 – 0.91) and gel times (3.8-4.4 min for 80°C and 2-2.2 min for 90°C) for all formulations are close as the variation among isothermal heat-of-reaction and final degree-of-cure values is less than 10%. The variability among the values does not have any trend and seems to be independent of the amount of LPA. However, the LPA content has a significant effect on the cure rate, which is apparent from Figures 3.8 and 3.9. The cure rate is plotted as a function of degree-of-cure for 80°C and 90°C isothermal temperature in Figure 3.8 and 3.9, respectively. The curves for different formulations follow the same trend for both temperature levels; however the elevation of the curves is much higher at 90°C compared with 80°C due to the increase in reaction rates with increase in processing temperature. The cure rate evolution is identical for 0% and 5% LPA resins (Figures 3.8 and 3.9). These two formulations show highest reaction rates compared with other formulations, which result in a faster degree-of-cure evolution as shown in Figure 3.10. The resins with 10% and 20% LPA content have identical cure rate evolution. The slowest cure rate is observed for 40% LPA resin. The slow reaction rates result in a relatively late degree-of-cure evolution as shown in Figure 3.10. This means that although the LPA content, in the range tested, does not change heat-of-reaction, final degree-of-cure and gel times, it has a significant effect on the cure rates. Reaction rate slows down with increasing LPA content. Hence, to obtain a higher reaction rate during RTM processing of PD9551 polyester resin, a least amount of LPA content and higher temperature levels are recommended based on its shrinkage compensation properties.

A cure kinetics model was developed from the DSC measurements for the resin with 10% LPA which corresponds to the standard resin formulation used in automotive applications. The model used was developed by Kamal and Sourour [34] and is given by:

$$\frac{d\alpha}{dt} = \left(K_1 + K_2\alpha^m\right)\left(\alpha_{max} - \alpha\right)^n \tag{3.3}$$

$$K_i = A_i \exp\left(-\frac{E_i}{RT}\right) \quad i = 1,2 \tag{3.4}$$

where α is the degree-of-cure, α_{max} is the maximum degree-of-cure achieved in an isothermal scan, R is the universal gas constant, T is the temperature, E_1 and E_2 are activation energies, A_1 and A_2 are frequency factors and m and n are kinetic exponents. The model parameters presented in Table 3.5 were obtained from fitting Equation 3.3 to the measured rate of cure using a linear regression. Figure 3.11 shows the good agreement between the measured and predicted resin degree-of-cure under isothermal curing conditions. The percent error between experimental and numerical results was about 5% for 80°C and about 3% for 90°C, which indicates that the model is relatively accurate to predict the evolution of degree-of-cure for the selected temperature range.

3.5 Resin Viscosity

Figure 3.12 shows the variation in resin viscosity as a function of time at 80°C processing temperature for different formulations. As can be seen from this graph, the viscosity variation curves are nearly identical for all resin formulations before the gel point and the gel point is virtually independent of the LPA content in the range from 0-40%. By comparing this data with DSC results, a degree-of-cure of 0.055 was calculated corresponding to the gel point.

Macosko's viscosity model (Equation 3.5 and 3.6) was fitted to the experimental data to model viscosity variations for the standard resin (10% LPA) as a function of time and temperature [35].

$$\eta_O(T) = B\exp\left(\frac{T_b}{T}\right) \tag{3.5}$$

$$\eta(\alpha,T) = \eta_O(T)\left(\frac{\alpha_G}{\alpha_G - \alpha}\right)^{(C_1+C_2\alpha)} \tag{3.6}$$

where $\eta_o(T)$ is the viscosity at a given temperature, T is temperature in Kelvin, α is the degree-of-cure, α_G is the degree-of-cure at gelation, T_b B, C_1 and C_2 are model

parameters obtained from curve fitting Equation 3.5 and 3.6 in experimental data and are listed in Table 3.6. This model predicts the variation in viscosity as a function of process temperature and degree-of-cure under isothermal and non-isothermal curing conditions. Experimental and numerical variations in viscosity under non-isothermal conditions for a standard resin (10% LPA) are shown in Figure 3.13. As the temperature of the resin increases, the viscosity decreases due to thermal effects. The viscosity keeps decreasing until a temperature of about 90°C, and then the cure reaction starts which increases the viscosity exponentially. There is a sharp contrast between the two regions which suggests that the resin gels very fast once the cure reaction begins. Hence, it is important to determine the time window for resin injection into the mold cavity, which can be obtained from the viscosity variation curves under isothermal conditions as shown in Figure 3.14. Figure 3.14 also gives the viscosity variation predicted by the model in Equation 3.6. As can be seen from Figure 3.14, processing windows of 4, 2 and 1 minutes are available for 80°C, 90°C and 100°C isothermal temperatures, respectively. Figures 3.13 and 3.14 also show the good agreement between experimental and numerical modeling results.

3.6 Cure Shrinkage

3.6.1 Resin without LPA

Figure 3.15 shows the cure shrinkage measured for the resin without LPA (resin A) with the technique discussed in Section 3.3.2. The average measured cure shrinkage after gelation was 9.5% which is comparable to the published data for polyester resin (7-10%) [1-8]. The slight different among shrinkage values for different isothermal temperatures is due to the experimental variability. This result confirms that the technique developed in this work is in the right range for this type of resin. The curves in Figure 3.15 have two regions referring to the two segments in the experimental procedure. In the first region, the resin is in liquid state and there is no shrinkage (segment I). This region ends at gelation. Once the resin has solidified, it starts to shrink in the second region (segment II). It is important to note that the technique measures shrinkage after gelation only. The

shrinkage behavior of the neat resin is plotted as a function of degree-of-cure in Figure 3.16, where evolution of degree-of-cure for this resin is obtained from DSC experimental results. The cure shrinkage behavior of the neat resin is a linear function of degree-of-cure and is relatively independent of the processing temperature in the range tested. This result is consistent with the work by Bogetti and Gillespie [9] and Hill et al. [10].

The filler was added to the resin at a volume fraction of 11%. The cure shrinkage behavior of resin with and without filler is plotted in Figure 3.17. The addition of filler did not change the evolution of cure shrinkage as a function of degree-of-cure. However, 13% less shrinkage was observed for the resin with filler. This result is consistent with the addition of filler of 11%, which confirms that the rule of mixtures can be used to predict the cure shrinkage of a filled resin as a function of the total resin shrinkage of the neat resin and percentage of filler.

From the results at 80°C and 90°C for the resin without LPA, a resin shrinkage model [9] was modified and fitted to the experimental data. The model is given by Equation 3.7.

$$\begin{aligned}
\left(\frac{\Delta V}{V}\right)_{Shrinkage} &= 0 \quad \alpha \le \alpha_G \\
\left(\frac{\Delta V}{V}\right)_{Shrinkage} &= \left(\frac{\alpha - \alpha_G}{\alpha_M - \alpha_G}\right)\left(\frac{\Delta V}{V}\right)_{Total}\left(1 - V_{Filler}\right) \quad \alpha_G < \alpha < \alpha_M \\
\left(\frac{\Delta V}{V}\right)_{Shrinkage} &= \left(\frac{\Delta V}{V}\right)_{Total}\left(1 - V_{Filler}\right) \quad \alpha \ge \alpha_M
\end{aligned} \tag{3.7}$$

where α is the resin degree-of-cure, $(\Delta V/V)_{Total}$ is the total volumetric shrinkage of the resin, α_G is the degree-of-cure at gelation; α_M is the degree-of-cure corresponding to the total cure shrinkage and V_{filler} is the volume fraction of the filler. For the resin without LPA, α_G is 0.055, α_M is 0.8 and $(\Delta V/V)_{Total}$ is 0.095. The shrinkage model (Equation 3.7) was in good agreement with the experimental data as shown in Figure 3.18.

3.6.2 Resin with LPA

The shrinkage-expansion data for all formulations cured at 90°C is plotted in Figure 3.19 as a function of degree-of-cure. The resin without LPA and resin with 5% LPA had the same shrinkage behavior. Resin with 8% started showing some expansion after shrinkage; however this resin formulation was unable to completely compensate for the shrinkage. The final shrinkage in this formulation was about 4.5 percent. When the LPA amount was raised to 10%, the LPA not only compensated for the shrinkage but also expanded (-2%). Similar result was obtained for the 20% formulation (-2%). However, the resin with 40% LPA although compensated for the initial cure shrinkage, it showed no further expansion (0%). As can be seen from Figure 3.19, the shrinkage behavior of all the resin formulations is similar until a degree-of-cure of 0.5. However, there are three distinct regions in Figure 3.19 for resin formulations with 10% and higher LPA levels. The resins show a shrinkage behavior until a degree-of-cure of 0.5 and then expansion starts which goes on until a degree-of-cure of 0.9. There is no further expansion after a degree-of-cure of about 0.9.

A graph is plotted in Figure 3.20 to show the final cure shrinkage at the end of the isothermal cure and the amount of LPA in the formulation. It is apparent from this graph that the resin shows a net final cure shrinkage below an LPA content of 10%, whereas 10% and 20% LPA resins have identical shrinkage-expansion behaviors and show a net final expansion of about 2%. Resin with 40% LPA although completely compensates for the shrinkage, it does not show any further expansion. From the graph in Figure 3.20, it can be deduced that 10% is the critical amount of LPA needed to compensate for the shrinkage. This is the minimum amount needed to achieve phase separation and micro-void formation necessary to compensate for the shrinkage. Increasing LPA levels above 10% did not result in further expansion.

An empirical model is developed to predict shrinkage and shrinkage compensation behavior of the standard low profile resin (10% LPA). The model of combined shrinkage-

LPA action is given by Equation 3.8. This model adequately predicts the shrinkage and expansion behavior of the standard resin as shown in Figure 3.21. The model parameters obtained from experimental data are given below;

$$
\begin{aligned}
\left(\frac{\Delta V}{V}\right)_{Shrinkage} &= 0 \quad \alpha \le \alpha_G \\
\left(\frac{\Delta V}{V}\right)_{Shrinkage} &= \left(\frac{\alpha - \alpha_G}{\alpha_C - \alpha_G}\right)\left(\frac{\Delta V}{V}\right)_{TSH} \quad \alpha_G < \alpha < \alpha_C \\
\left(\frac{\Delta V}{V}\right)_{Shrinkage} &= \left(\frac{\alpha - \alpha_C}{\alpha_M - \alpha_C}\right)\left(\frac{\Delta V}{V}\right)_{TEX} + \left(\frac{\Delta V}{V}\right)_{TSH} \quad \alpha_C < \alpha < \alpha_M \\
\left(\frac{\Delta V}{V}\right)_{Shrinkage} &= \left(\frac{\Delta V}{V}\right)_{TEX} + \left(\frac{\Delta V}{V}\right)_{TSH} \quad \alpha \ge \alpha_M
\end{aligned}
\tag{3.8}
$$

where $\alpha_G = 0.055$, $\alpha_C = 0.5$, $\alpha_M = 0.9$, $\left(\frac{\Delta V}{V}\right)_{TSH} = 4.8$ and $\left(\frac{\Delta V}{V}\right)_{TEX} = -6.8$

$(\Delta V/V)_{TSH}$ corresponds to the shrinkage of this resin and $(\Delta V/V)_{TEX}$ corresponds to the LPA expansion. This model assumes that the resin shrinkage and expansion is not significantly affected by the processing temperature in the temperature range tested. As shown in Figures 3.19 and 3.21, the degree-of-cure at 0.5 is a critical value, where resin expansion starts. The model in Equation 3.8 can be extended to other low profile resin systems with linear shrinkage-expansion regions.

3.7 Resin Morphology Observations and Discussion

The resin without LPA was transparent throughout the cure as observed with optical microscopy. As shown in Figure 3.22, a few air bubbles are visible throughout the cure cycle. Air bubbles became more pronounced at higher degree-of-cure because of the solidification of resin molecules at the boundary. However, no major significant morphological change was observed during the complete cure cycle for the resin without LPA. The results for the resin with 10% of LPA are shown in Figure 3.23. The resin

remained transparent until gelation which occurred at a degree-of-cure of 0.055. Then a two phase structure started to form as shown in Figure 3.23(c). The two phase structure was very well formed and visible at a degree-of-cure of 0.2 (Figure 3.23(d)). The two phase structure kept expanding until a degree-of-cure of 0.52. Then micro-crack propagation was observed at a degree-of-cure of 0.65. Micro-crack propagation kept on going until a degree-of-cure of 0.9. This two phase structure and micro-cracking turned the transparent resin into an opaque material.

In Figure 3.24, shrinkage-expansion behavior, elastic modulus (G′) development and morphological variations are plotted as a function of degree-of-cure for the standard resin with 10% LPA during an isothermal cure at 90°C. There is a direct relationship between the shrinkage-expansion behavior and elastic modulus development. The expansion in the resin does not start until the resin has become fully elastic. The elastic modulus starts to develop after gelation and keeps increasing very fast until a degree-of-cure of 0.5 and in this region the resin shows shrinkage behavior. From a degree-of-cure of 0.5 until the end of cure cycle, the elastic modulus is fully developed and hence the micro-void formation process starts and resin expands in this region as shown in Figure 3.24. Although stresses are incurred in the resin before this critical point (α = 0.5) but since the resin has a viscous component, these stresses are dissipated.

Based on these results, the LPA mechanism can be divided into three major stages. The first stage starts when the resin is in liquid state and ends at gelation ($\alpha \approx 0.055$). The second stage starts at gelation and ends at a degree-of-cure of 0.5. The third stage starts at a degree-of-cure of 0.5 and keeps going until a degree-of-cure of 0.9. The first two stages are the same for all formulations as observed through rheological experiments. However, only the first stage has similar morphology. Resin shrinkage in the first stage is insignificant from a manufacturing point of view, since more resin can be pumped into the RTM mold before gelation. Phase separation between unsaturated polyester (UP) resin and LPA takes place during the first stage. Phases are fully separated by the end of gelation. In the second phase, phases keep expanding as can be seen by the microscopy data. Micro-void formation also starts in this stage; however the stresses developed at the

interface of two phases are dissipated because of the visco-elastic behavior of the resin. That is why the resin keeps shrinking in this phase. In the third phase, the resin is fully elastic with developed elastic modulus. Stresses are developed at the interface in the fully elastic resin between shrinking resin and expanding LPA because of the difference in the thermal expansion coefficients and elastic moduli of the two phases at the micro-level. The ultimate result is resin expansion because of the micro-voids and micro-cracks at the interface of UP resin and LPA phase. Micro-void formation continues until the end of cure cycle. Resin with LPA tested under a microscope showed global crack propagation at a degree-of-cure of 0.65. This is because of coalescence of micro-voids. LPA expansion and crack propagation continued until the end of cure cycle. The two phase structure made it impossible for light to pass through which made this resin opaque. Micro-voids interconnected only because of the small thickness of the resin layer tested with optical microscopy. However that would not be the case in actual manufacturing where composite panels have fibers and are very thick.

3.8 Conclusion

The objective of this study was to investigate the effects of LPA content on cure kinetics, cure shrinkage and morphology of a polyester resin. The following inferences can be drawn from the results:

- LPA content, in the range tested, had no significant affect on the total heat-of-reaction and gel time. The onset of reaction temperatures, peak temperatures, degree-of-cure evolution, maximum degree-of-cure and cure rates of the polyester resins were identical for resin formulations with LPA content between 0 and 20%. However, the resin formulation with an extreme case of LPA (40%) showed a relatively slower reaction rate under isothermal and non-isothermal cure conditions compared to other formulations.

- The final polymerization shrinkage/expansion of the resin was highly dependent on the amounts of LPA. The resin showed a final shrinkage (10%) for the resin formulations with LPA content less than 10%, shrinkage compensation and expansion (-2%) for LPA contents between 10-20%, and shrinkage compensation for LPA content of 40%. The shrinkage-expansion behavior of polyester resins was found to be a linear function of the degree-of-cure.

- The LPA content had a significant affect on the morphology of the resin. No changes in the structure and its transparency were observed for the resin without LPA; however resin with 10% LPA showed a co-continuous structure development during cure which turned the transparent resin into opaque solid. Micro-cracking was observed in the resin with LPA at a later stage in cure due to micro-void formation. The same phenomenon has also been reported by Lee et al. [15]. The LPA expansion mechanism was highly dependent on the development of elastic modulus during cure. The LPA expansion started only after the resin became fully elastic.

The combination of resin shrinkage, LPA expansion and resin morphological changes with reaction kinetics under identical process conditions provided a better understanding of the shrinkage and LPA expansion mechanism. Phase separation which resulted in a co-continuous structure and micro-void formation thereafter, were found to be two critical steps for shrinkage control. LPA level at 10% was found to be the ideal amount needed for phase separation, micro-void formation and minimum cost. The procedure developed for cure shrinkage measurements of polyester resins based on normal force control principle in rheological experimentations agreed well with the published data and hence can be extended towards other resin systems. The models developed for cure shrinkage and LPA expansion were in good agreement with the experimental results.

3.9 Acknowledgements

This research was made possible by the financial support of Auto21 Network of Centers of Excellence and the Ford Motor Company. Authors would like to acknowledge Scott Bader Company for the resin and OMYA for the filler used in this work. We would also like to gratefully acknowledge the significant interaction and support from Dr. Michael DeBolt of the Ford motor company and Eric St-Amant of McGill Composite Materials and Structures Laboratory.

References

1. Kinekelaar M, Wang B, Lee LJ. Shrinkage behavior of low profile unsaturated polyester resins. Polymer 1994;35(14):3011-3022.
2. Huang Y, Liang C. Volume shrinkage characteristics in the cure of low shrink unsaturated polyester resins. Polymer 1996;37(3):401-412.
3. Hill RR, Muzumdar SV, Lee LJ. Analysis of volumetric changes of unsaturated polyester resin during curing. Polymer Engineering and Science 1995;35(10):852-859.
4. Li C, Potter K, Wisnom MR, Stringer G. In-situ measurement of chemical shrinkage of MY750 epoxy resin by a novel gravimetric method. Composite Science and Technology 2004;64:55-64.
5. Han S, Wang KK, Hieber CA. Characterization of the rheological properties of a fast curing epoxy molding compound. Journal of Rheology 1997;41(2):177-195.
6. Ninan NK, Reghunadhan CP. Rheological cure characterization of Phosphate –Triazine polymers. Journal of Applied polymer Science 2003;88:908-914.
7. Rocks J, Halter M, George G, Vohwinkel F. Calorimetric and rheological characterization of a high performance epoxy curable at low temperatures. Polymer International 2003;52:1749-1757.
8. Kinkelaar M, Muzumdar S, Lee LJ. Dilatometric study of low profile unsaturated polyester resins. Polymer Engineering and Science 1995;35(10):823-836.
9. Bogetti TA, Gillespie JW Jr. Process-Induced Stress and Deformation in Thick-Section Thermoset Composite Laminates. Journal of Composite Materials 1992;26: 626–660.
10. Hill RR Jr, Muzumdar SV, Lee LJ. Analysis of Volumetric Changes of Unsaturated Polyester Resins During Curing. Polymer Engineering and Science 1995;35(10):852-859.
11. Li C, Potter K, Wisnom MR, Stringer G. In-Situ Measurement of Chemical Shrinkage of MY750 Epoxy Resin by a Novel Gravimetric Method. Composite Science and Technology 2004;64:55-64.
12. Lee H, Veville K. Handbook of Epoxy Resins, McGraw-Hill, New York, 1967, 11-17.
13. Schoch KF, Panackal PA, Frank PP. Real Time Measurement of Resin Shrinkage during Curing. Thermomechanica Acta 2004;417:115-118.
14. Li W, Lee JL. Shrinkage control of low profile unsaturated polyester resins cured at low temperatures. Polymer 1998;39(23):5677-5687.

15. Li W, Lee JL. Low Temperature Cure of Unsaturated Polyester Resins with Thermoplastic Additives. I. Dilatometry and Morphology Study. Polymer 2000;41:685-696.
16. Li W, Lee JL. Low temperature cure of unsaturated polyester resins with thermoplastic additives II. Structure formation and shrinkage control mechanism. Polymer 2000;41:697-710.
17. Cao X, Lee LJ. Control of Shrinkage and Residual Styrene of Unsaturated Polyester Resins Cured at Low Temperature: I. Effects of Curing Agents. Polymer 2003;44:1893-1902.
18. Cao X, Lee LJ. Effect of Co-promoter and Secondary Monomer on Shrinkage Control of Unsaturated Polyester (UP)/Styrene (St)/Low-Profile Additive (LPA) Systems Cured at Low Temperatures. Journal of Applied Polymer Science 2001;82:738-749.
19. Xu L, Lee LJ. Effect of Nanoclay on Shrinkage Control of Low Profile Unsaturated Polyester (UP) Resin Cured at Room Temperature. Polymer 2004;45:7325-7334.
20. Lucas J, Borrjo J, Williams R. Cure of Unsaturated Polyester Resins: 2. Influence of Low Profile Additives and Fillers on the Polymerazation Reaction, Mechanical Properties and Surface Rugosities. Polymer 1993;34(9):1886-1890.
21. Hsu CP, Kinkelaar P, Lee LJ. Effects of Thermoplastic Additives on the Cure of Unsaturated Polyester Resins. Polymer Engineering and Science 1991;31(20):1450-1460.
22. Huang YJ, Sue CC. Effect of Polyvinyl Acetate and Polymethyl Methacrylate Low Profile Additives on the Curing of Unsaturated Polyester Resins. Morphological Changes during Cure. Journal of Applied Polymer Science 1995;55(2):323-342.
23. Kinkelaar M, Muzumdar S, Lee LJ. Dilatometric Study of Low Profile Unsaturated Polyester Resins. Polymer Engineering and Science 1995;35(10):823-836.
24. Huang Y, Liang C. Volume Shrinkage Characteristics in the Cure of Low Shrink Unsaturated Polyester Resins. Polymer 1996;37(3):401-412.
25. Liu CJ, Kiasat MS, Nijhof AH, Blokland H, Marissen R. The Effect of the Addition of a Low Profile Additive on the Curing Shrinkage of an Unsaturated Polyester Resin. Polymer Engineering and Science 1999;39(1):18-25.
26. Boyard N, Vayer M, Sinturel C, Delaunay D. Modeling PVTX Diagrams: Application to Various Blends Based on Unsaturated Polyester—Influence of Thermoplastic Additive, Fillers, and Reinforcements. Journal of Applied Polymer Science 2004;92:2976-2988.
27. Chan-Park MB, McGarry FJ. Tough Low Profile Additives in Sheet Molding Compound. Polymer Composites 1996;17(4):537-547.
28. Bartkus EJ, Kroekel CH. Low Shrink Reinforced Polyester Systems. Applied Polymer Symposia 1970;15:113-135.
29. Pattison VA, Hindersinn RR, Schwartz WT. Mechanism of Low-Profile Behavior in Single-Phase Unsaturated Polyester Systems. Journal of Applied Polymer Science 1975;19(11):3045-3050.
30. Atkins A.E., in Paul D.R., Newman, S., editors. *Polymer Blends*, Academic Press, New York, 1978, 391-400.
31. Zhang Z, Zhu S. Microvoids in Unsaturated Polyester Resins containing Poly (vinyl acetate) and Composites with Calcium Carbonate and Glass Fibers. Polymer 2000;21:3861-3870.
32. Gordon S, Boukhili R, Trochu F. The Effect of Low Profile Additives on the Surface Aspects of RTM Molded Composites, Proceedings of third Canadian International Composite Conference, 21st –24th August, 2001, Montreal, Canada.
33. Scott Bader, Provisional Data Sheet PD9551 - R&D Group, Fax transmission, August 2002.
34. Kamal MR, Sourour S. Kinetic and thermal characterization of thermoset cure. Polymer Engineering and Science 1973;13(1):59-64.
35. Castro JM, Macosko CW. Kinetics and Rheology of typical polyurethane reaction injection molding systems. SPE technical papers 1980;26:434-438.

Table 3.1 Materials used and weight fractions (based on the weight of the resin)

Materials	**Type (Manufacturer)**	**Weight Fraction (%)**
Resin	PD9551 (Scott Bader)	-----
LPA	PD9419 (Scott Bader)	0 (Resin A) 5 (Resin B) 8 (Resin C) 10 (Resin D) 20 (Resin E) 40 (Resin F)
Filler	Calcium carbonate (Omya)	30*
Catalyst	Tert-Butyl peroxybenzoate (Akzo Chemicals)	2.6*
Accelerator	Cobalt 2-ethylhexanoate (Akzo Chemicals)	0.5*

* based on the weight of the resin and LPA

Table 3.2 Total heat-of-reaction (J/g) for non-isothermal cure scans.

LPA Content (%)	10°C/min	20°C/min	30°C/min	Average (σ*)
0	400	407	400	402 (4)
5	424	439	420	427 (10)
8	420	410	415	415 (5)
10	424	422	407	417 (9)
20	423	415	410	416 (6)
40	415	387	402	401 (25)

*** Standard deviation**

Table 3.3 Curing parameters for 10°C/min non-isothermal scans.

LPA Content (%)	Onset of Reaction Temperature (°C)	Peak Temperature (°C)	End of Reaction Temperature (°C)	Heat-of-Reaction (J/g)
0	97	113	171	400
5	96	110	167	424
8	97	110	170	420
10	97	112	170	424
20	97	111	165	423
40	100	116	167	415
Maximum Variation	4%	5%	3%	6%

Table 3.4 Results of DSC tests for isothermal cure scans.

LPA Content (%)	Isothermal Temperature (°C)	Isothermal Heat-of-Reaction (J/g)	Residual Heat-of-Reaction (J/g)	Isothermal Final Degree-of-cure	Gel Time (min)
0	80	356	31	0.89	4.4
5	80	383	30	0.90	4.0
8	80	375	25	0.90	4.2
10	80	370	22	0.89	4.0
20	80	388	20	0.90	3.9
40	80	367	22	0.92	3.8
Maximum Variation	80	8%	35%	3%	12%
0	90	356	20	0.89	2.0
5	90	360	20	0.85	2.1
8	90	365	18	0.85	2.2
10	90	353	19	0.85	2.1
20	90	380	15	0.90	2.0
40	90	363	10	0.91	2.2
Maximum Variation	90	7%	50%	7%	9%

Table 3.5 Parameters for the cure kinetics model (Equation 3.3).

Parameters	A_1 (sec^{-1})	E_1 (kJ mol^{-1})	A_2 (sec^{-1})	E_2 (kJ mol^{-1})	m	n	α_{max}
Values	$1.07x10^{13}$	149.7	$7.20x10^{10}$	87.54	0.711	1.464	0.9

Table 3.6 Parameters for the viscosity model (Equations 3.5, 3.6)

Parameters	C_1	C_2	α_G	B (Pa.s)	T_b (^oK)
Values	1.502	1.01	0.055	$1.51x10^{-4}$	2701

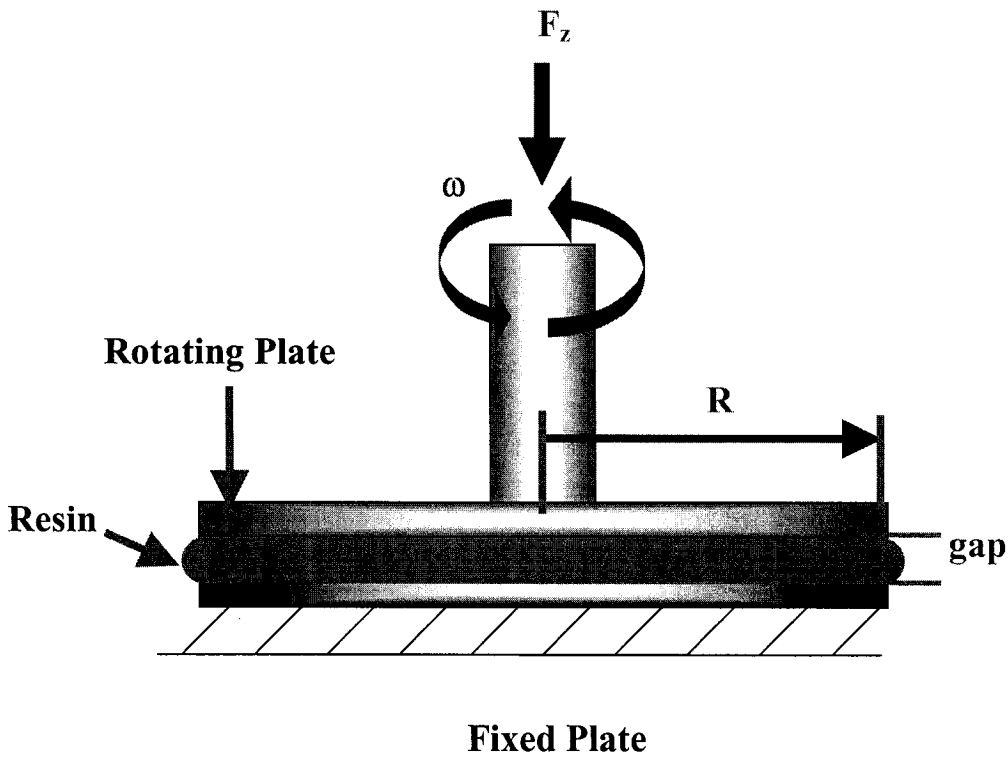

Figure 3.1 Parallel plate geometry setup

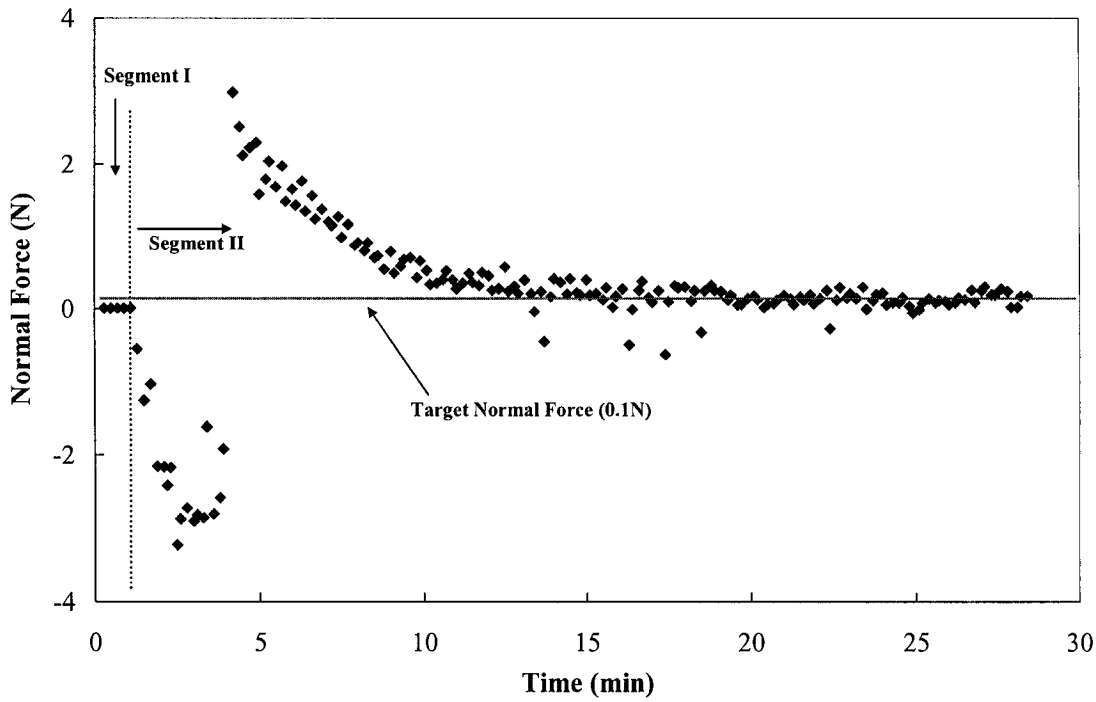

Figure 3.2 The change in normal force as a function of time

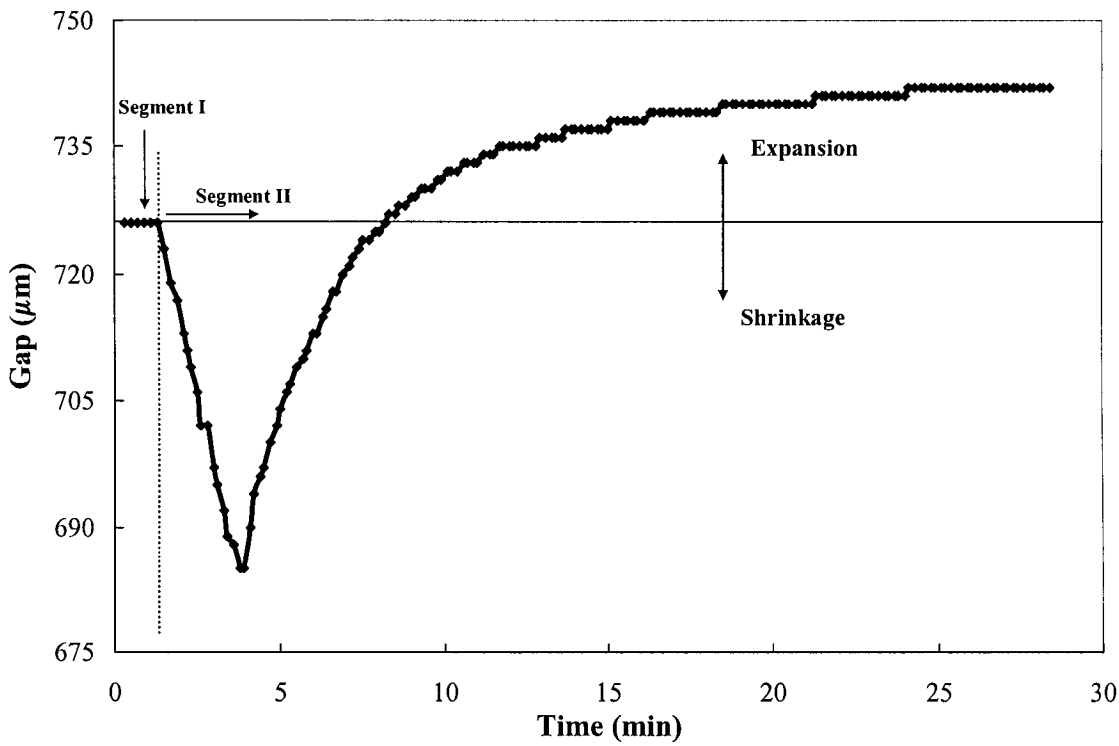

Figure 3.3 The change in gap to compensate for changes in normal force

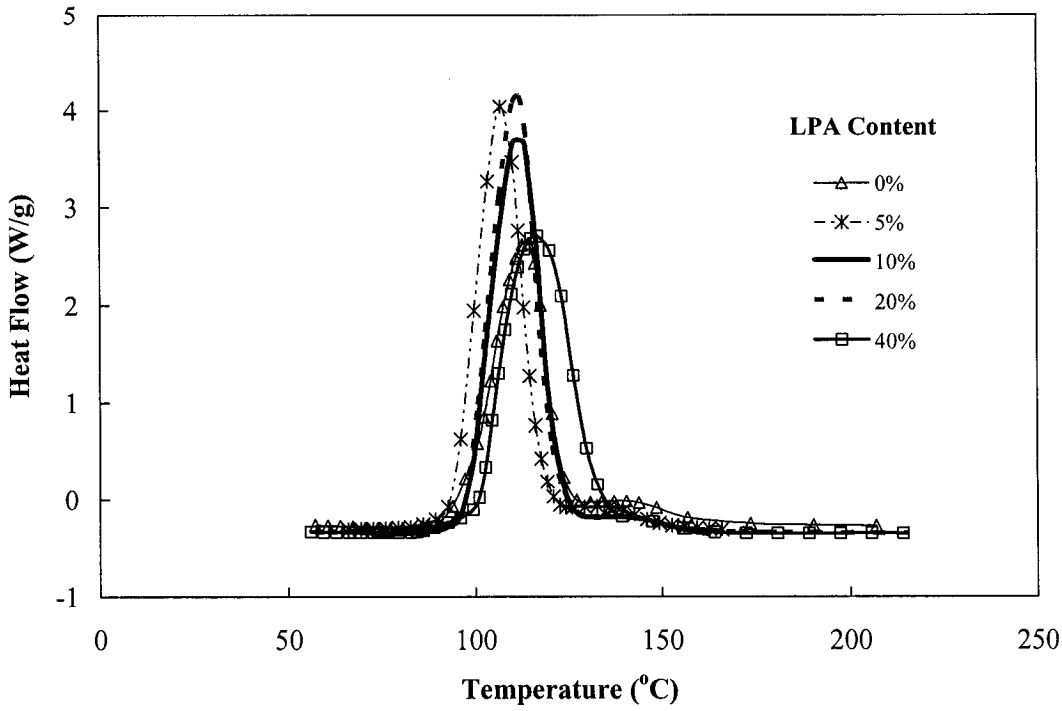

Figure 3.4 Variation in heat flow for different amounts of LPA under 10°C/min non-isothermal conditions.

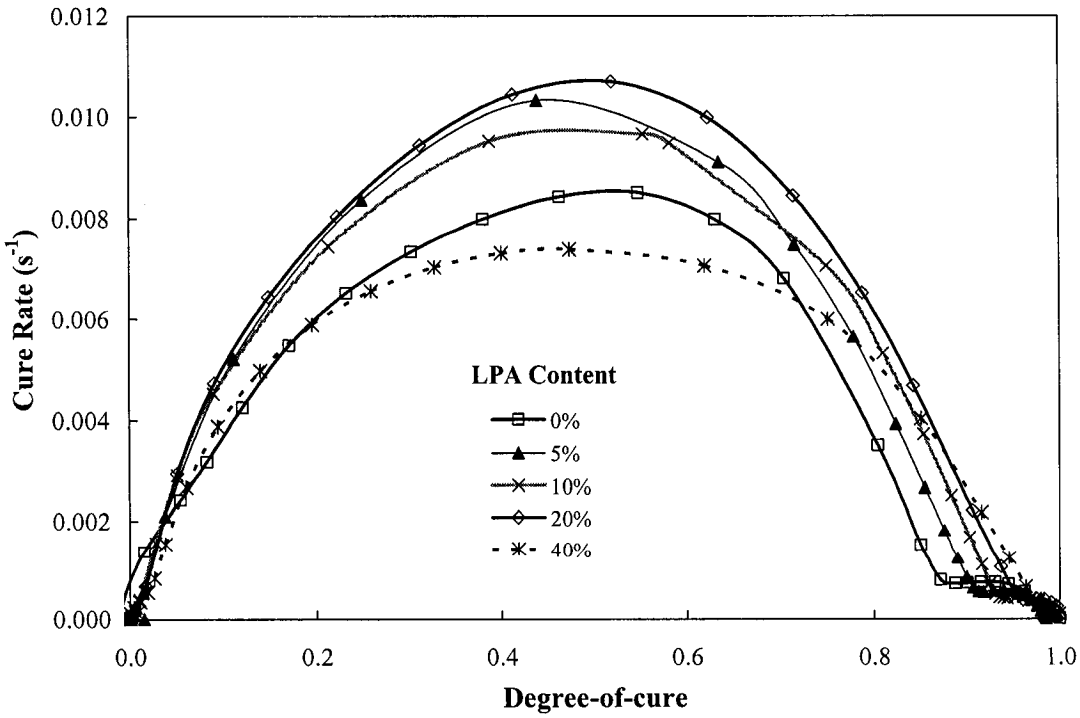

Figure 3.5 Variation in cure rate as a function of degree-of-cure under 10°C/min non-isothermal conditions.

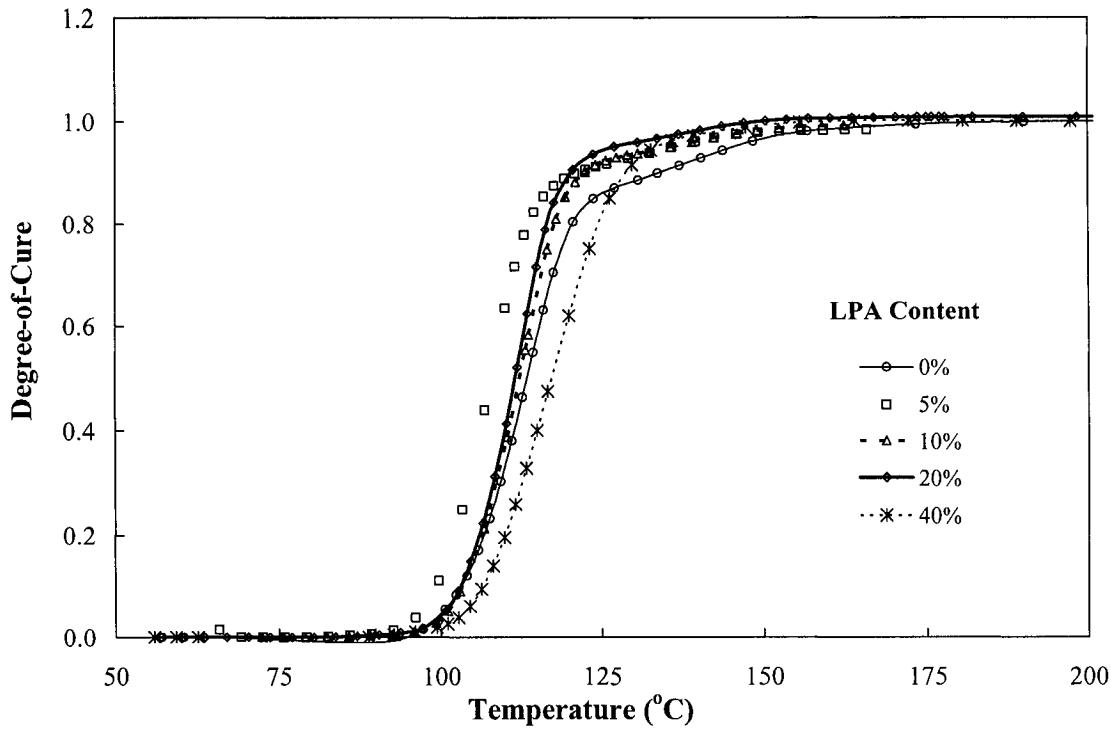

Figure 3.6 Degree-of-cure variation of all types of resins under 10°C/min non-isothermal conditions.

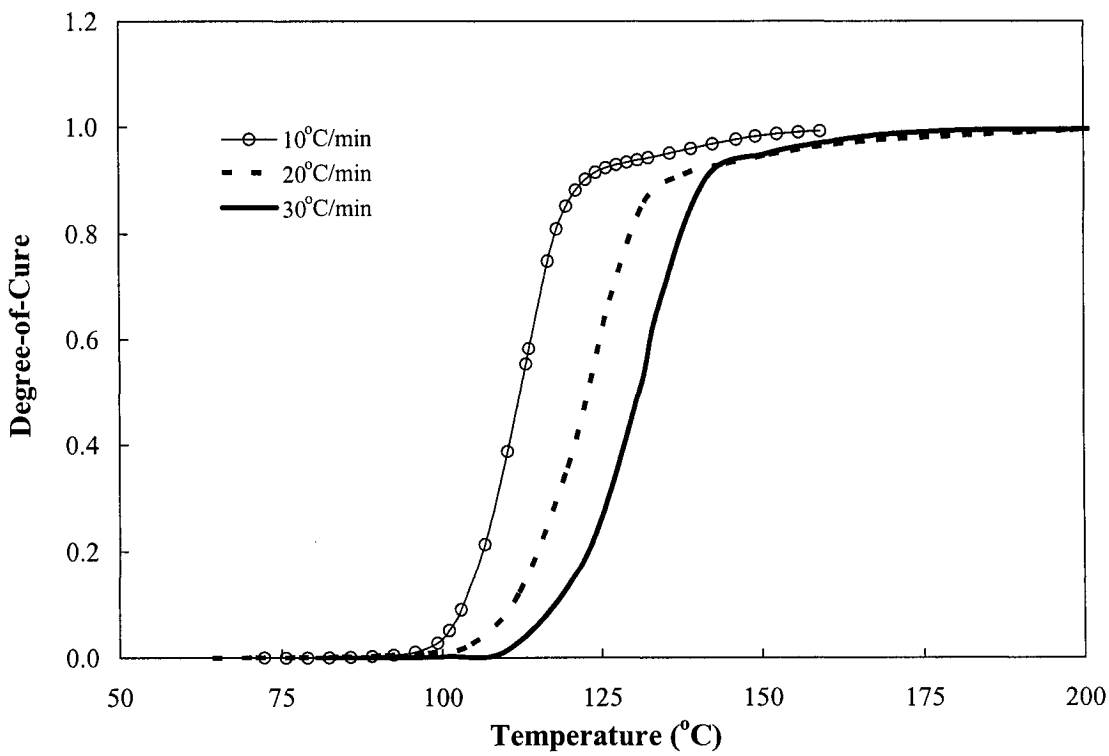

Figure 3.7 Degree-of-cure variation for 10% LPA resin under non-isothermal conditions

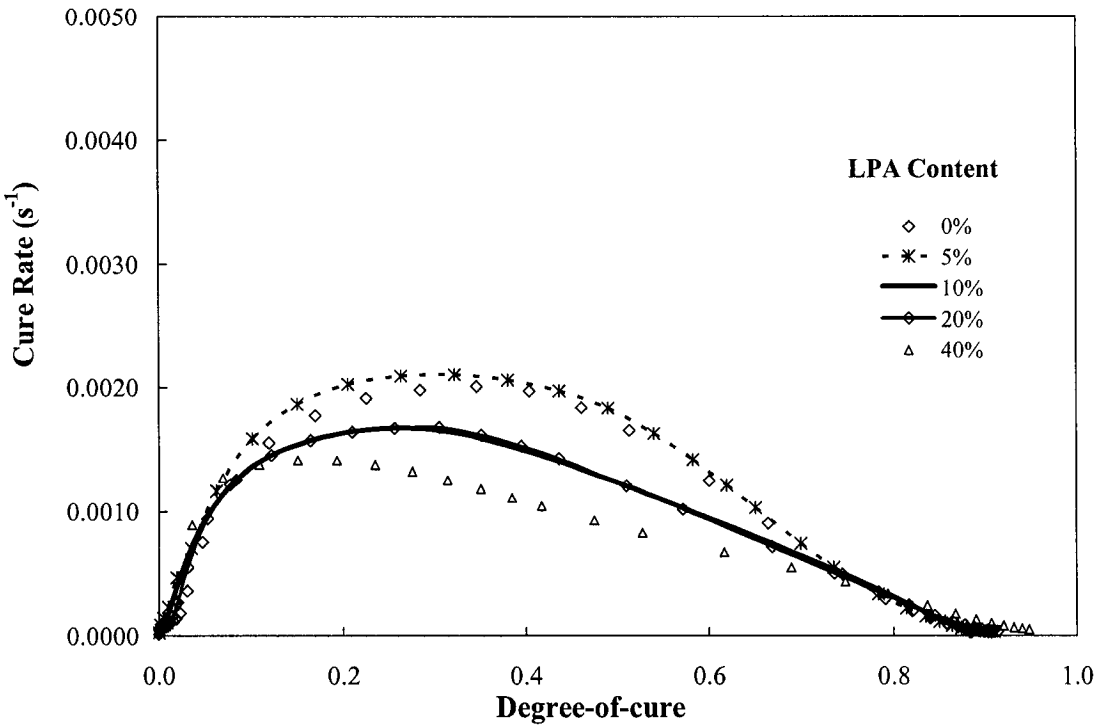

Figure 3.8 Variation in cure rate as a function of degree-of-cure under 80°C isothermal cure.

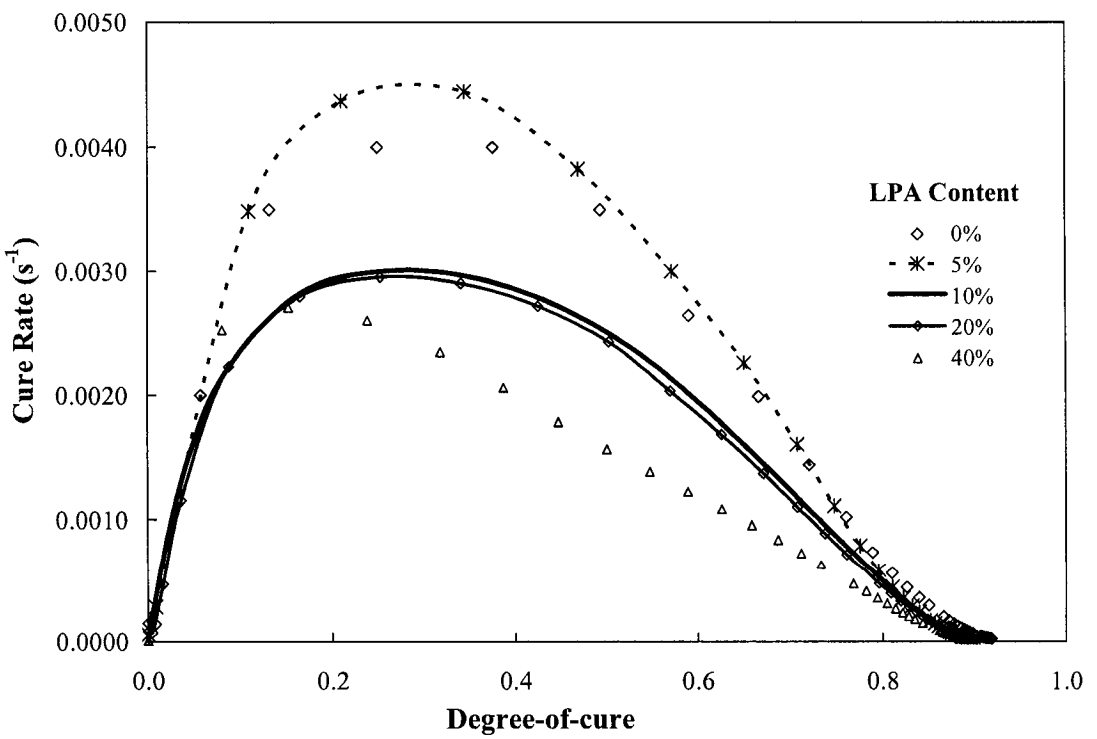

Figure 3.9 Variation in cure rate as a function of degree-of-cure under 90°C isothermal cure.

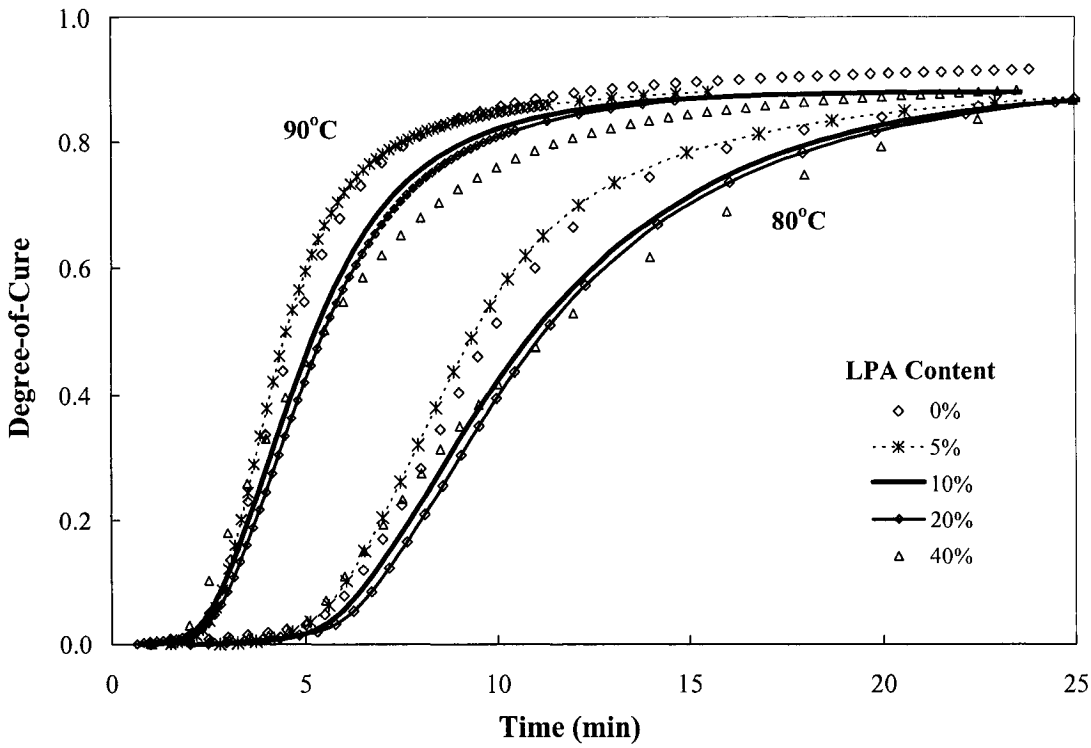

Figure 3.10 Degree-of-cure variations of all resins under 80°C and 90°C isothermal conditions.

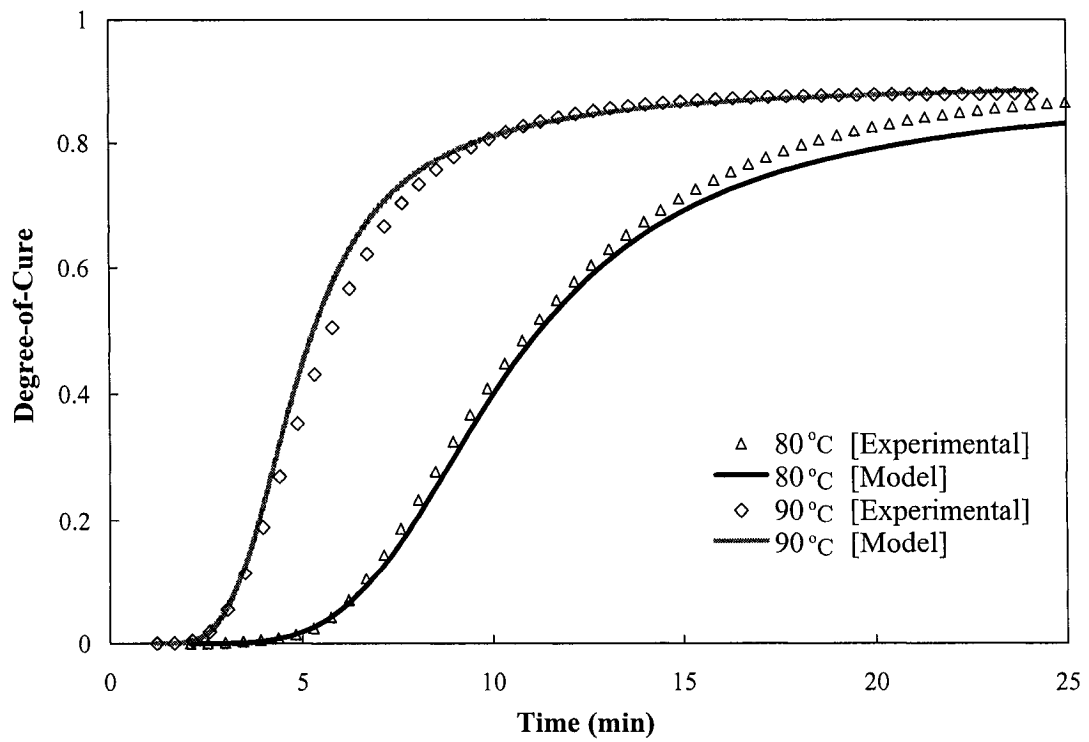

Figure 3.11 Experimental and predicted degree-of-cure for resin with 10% LPA at 80°C and 90°C isothermal cure.

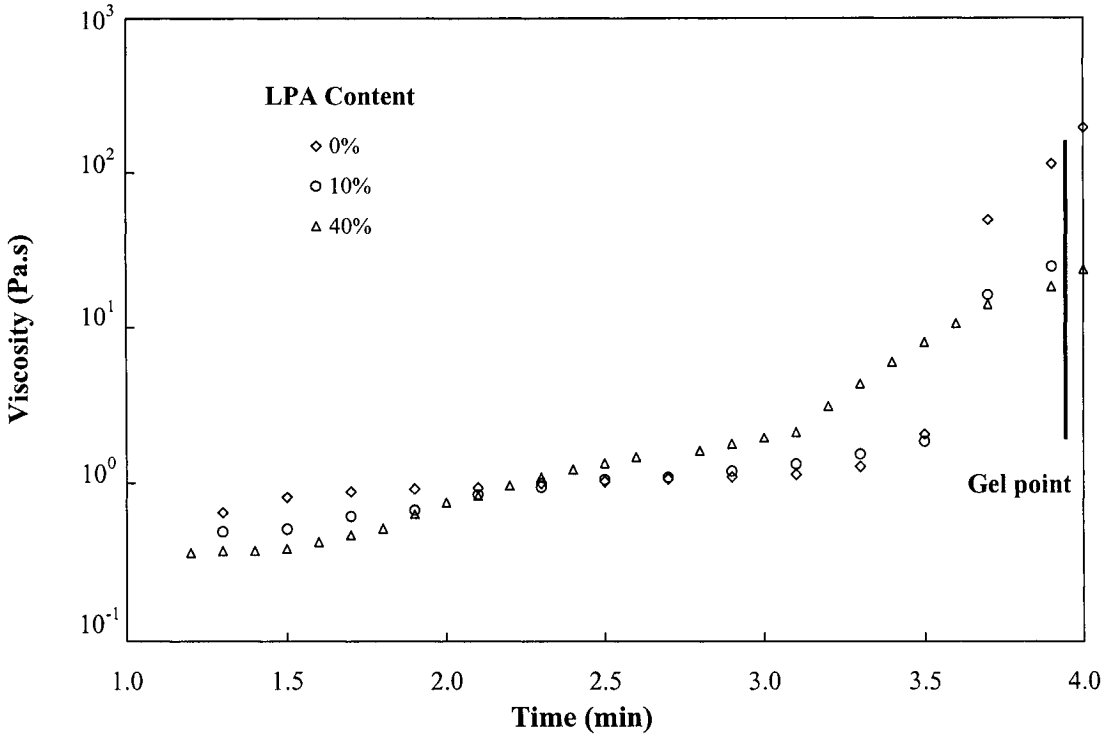

Figure 3.12 The variation in viscosity as a function of time for different formulations under 80°C isothermal cure.

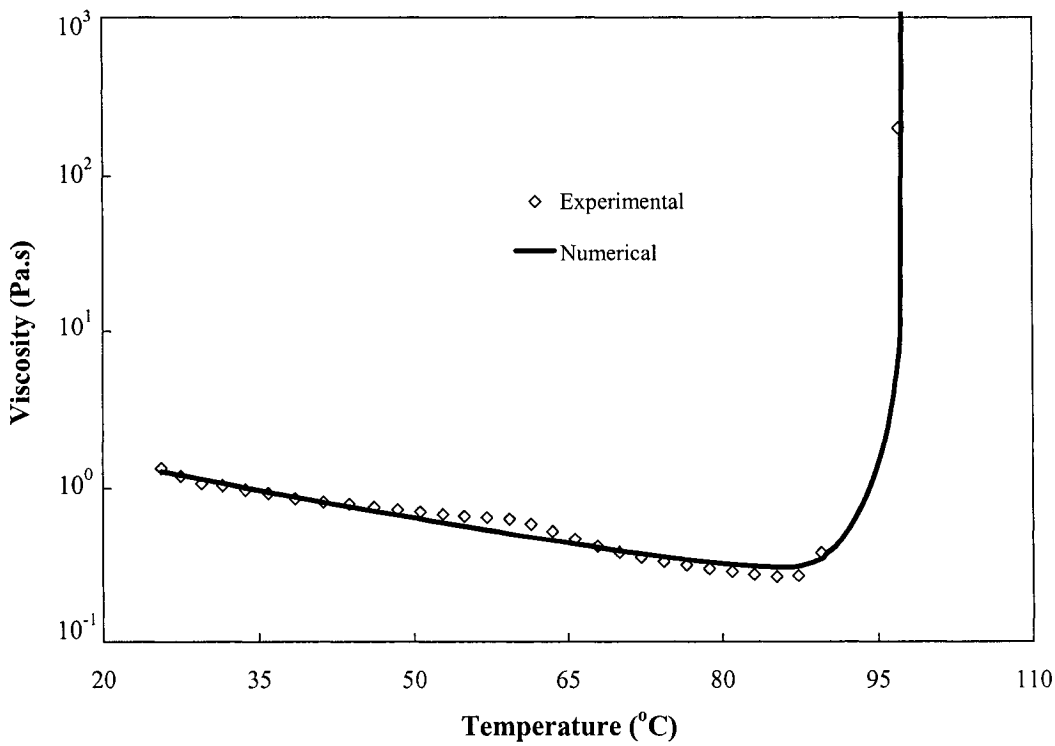

Figure 3.13 Viscosity variations in 10% LPA resin as a function of temperature under non-isothermal conditions (Equation 3.6).

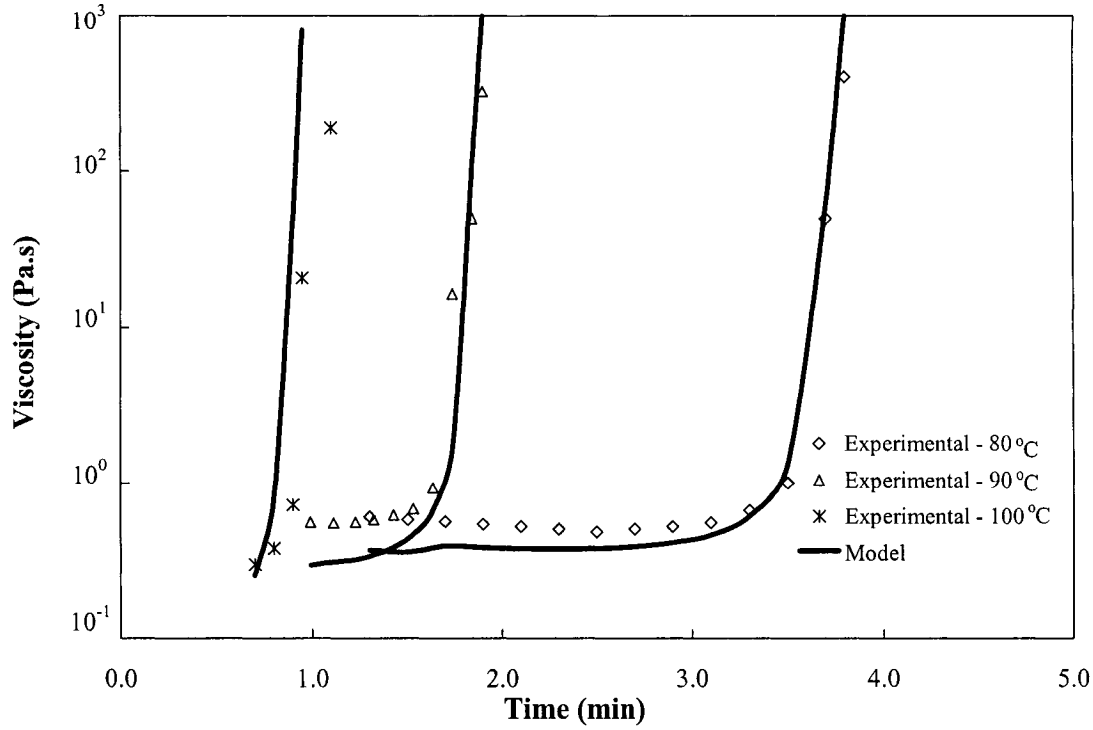

Figure 3.14 Viscosity variations in 10% LPA resin as a function of time under isothermal conditions (Equation 3.6).

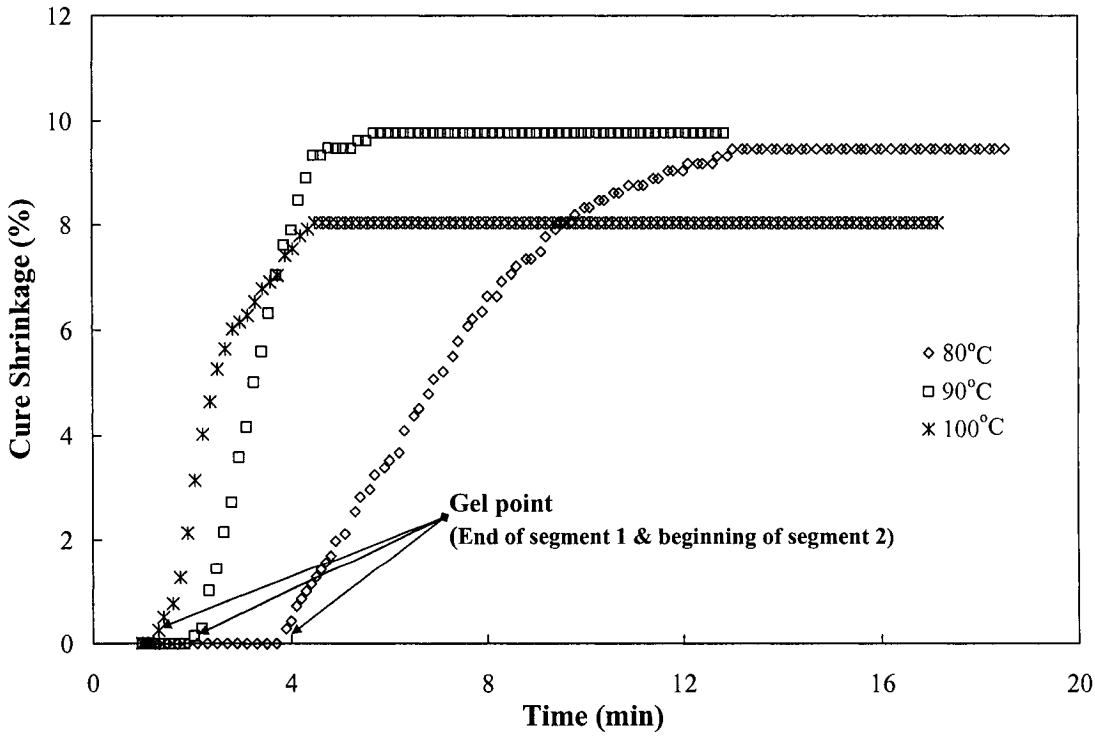

Figure 3.15 Cure shrinkage in the neat resin under isothermal conditions.

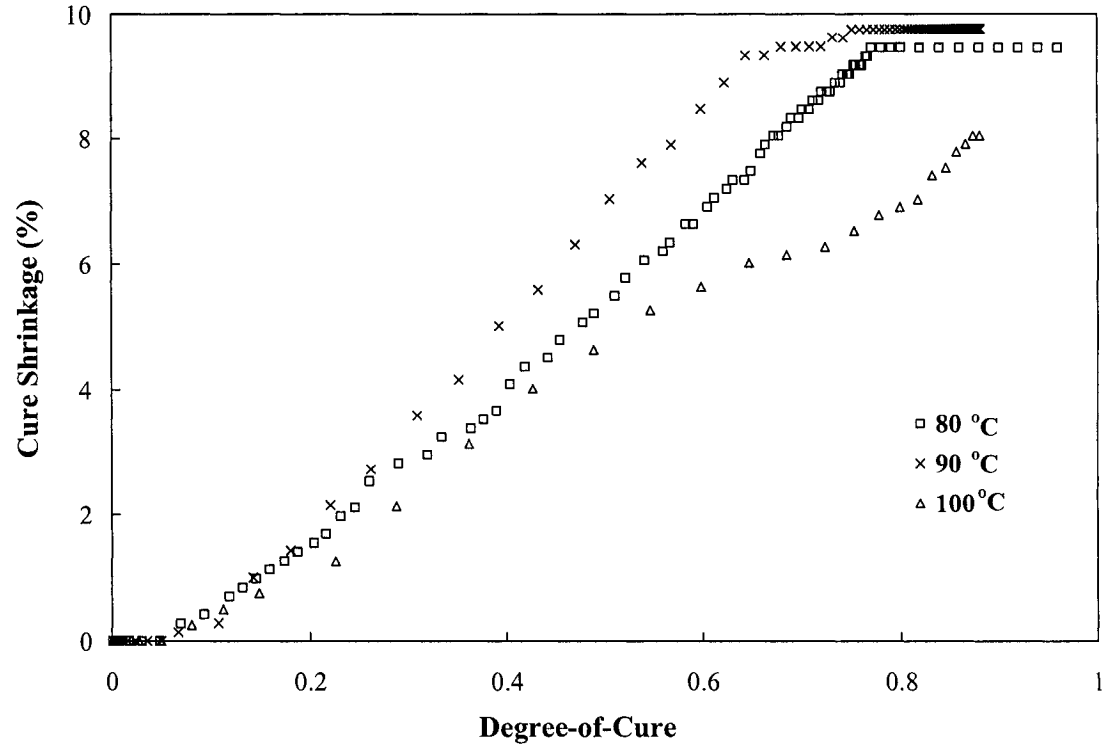

Figure 3.16 Cure shrinkage in the neat resin under isothermal conditions as a function of degree-of-cure.

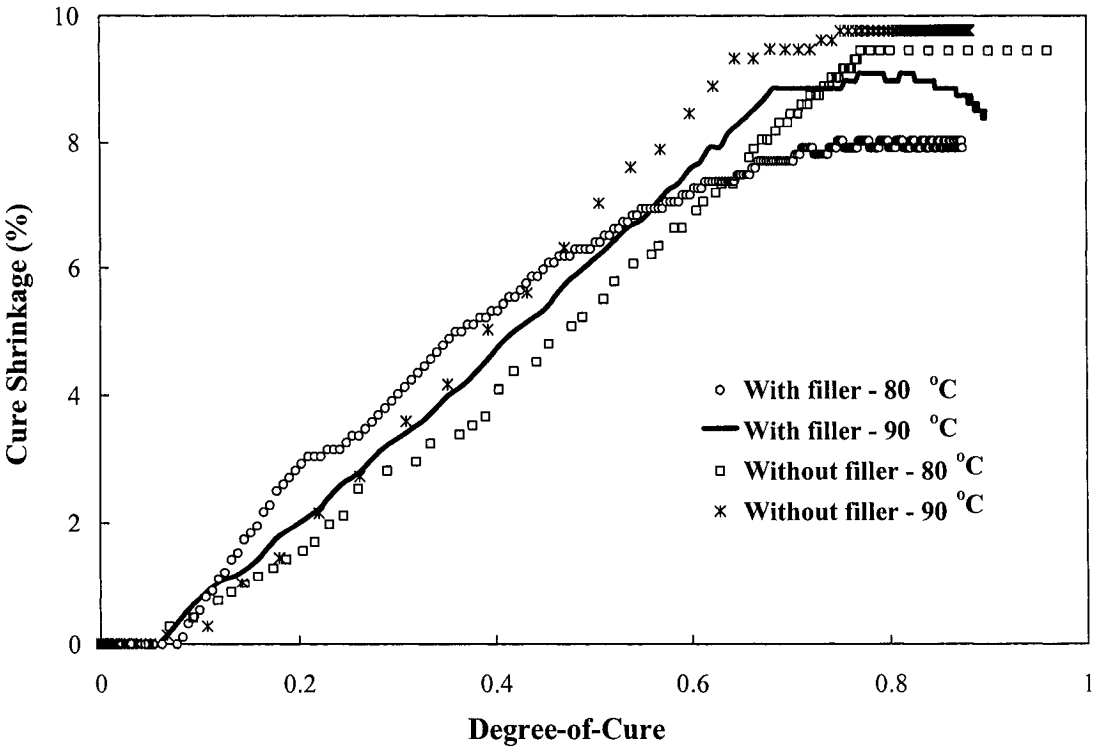

Figure 3.17 The effects of filler on the cure shrinkage behavior of resin without LPA (resin A).

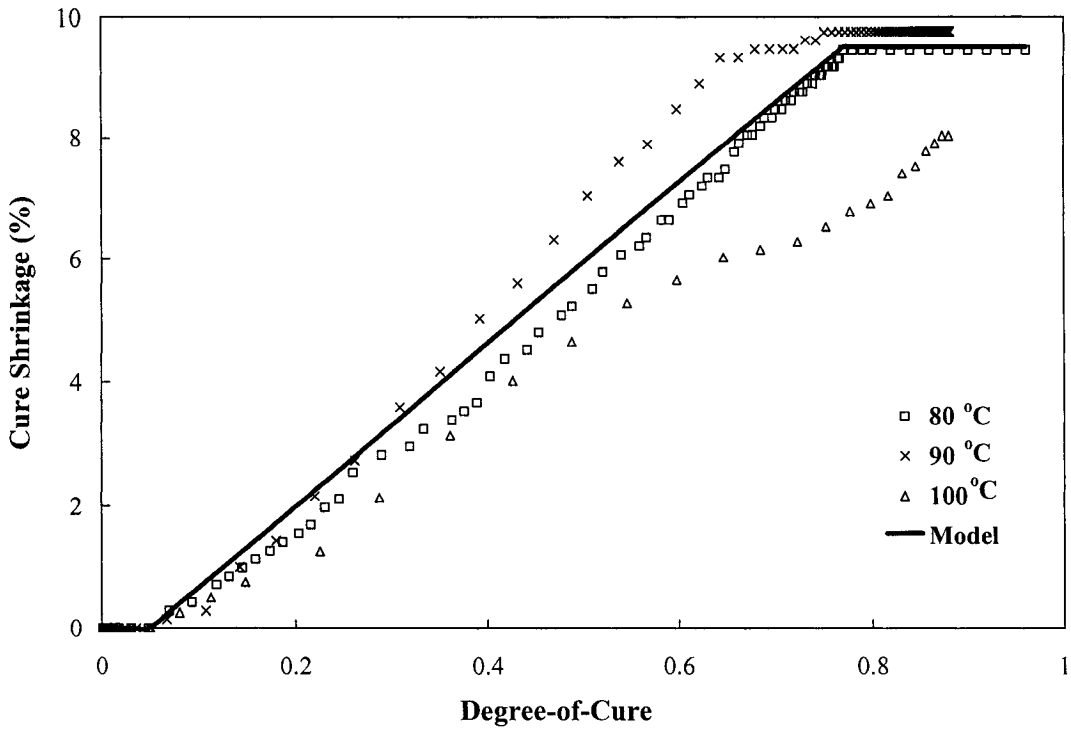

Figure 3.18 Experimental results and numerical validation of shrinkage model (Equation 3.7) for a neat resin.

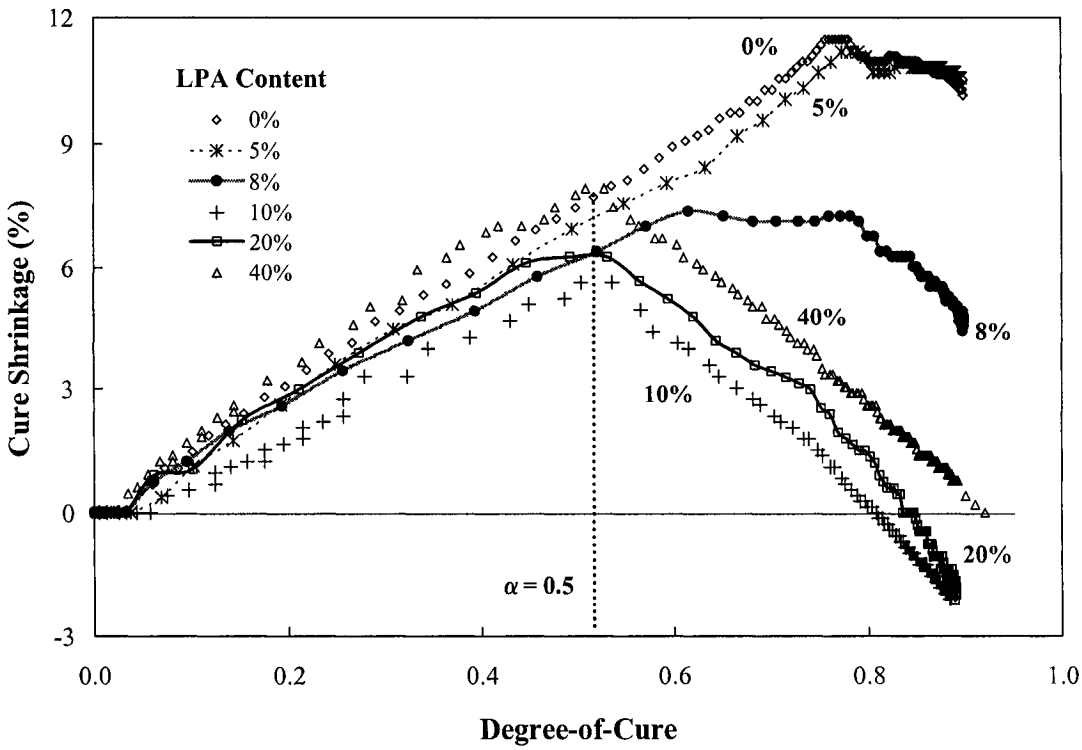

Figure 3.19 Cure shrinkage and LPA expansion under 90°C isothermal cure in different formulations.

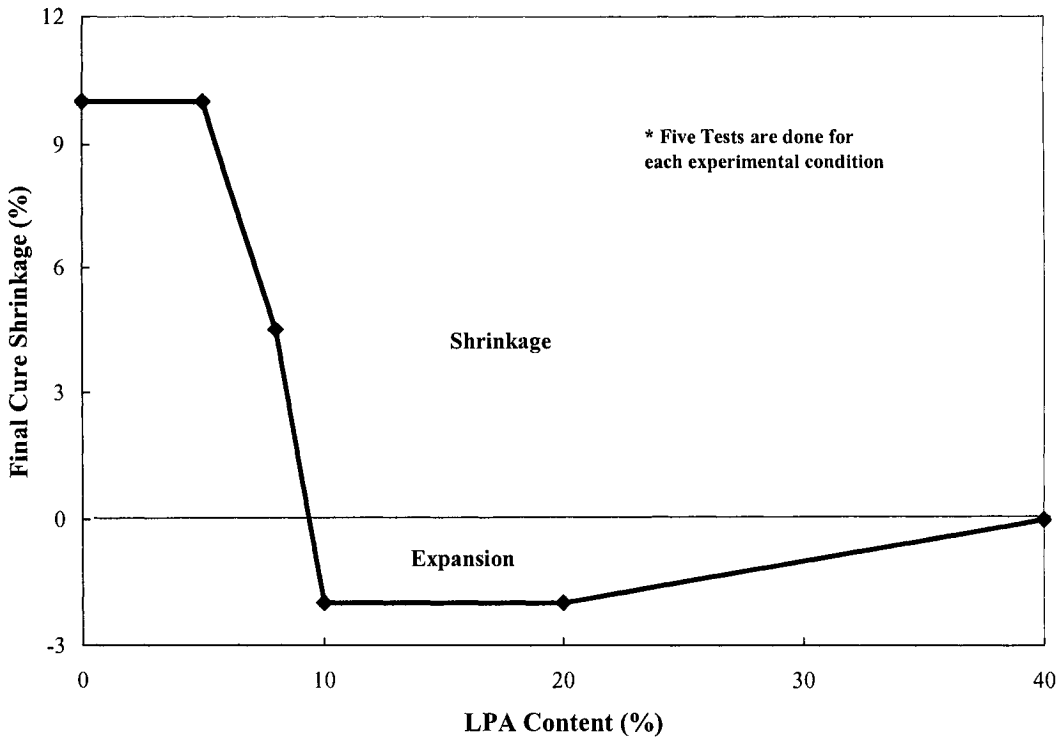

Figure 3.20 Reduction in final cure shrinkage as a function of LPA content.

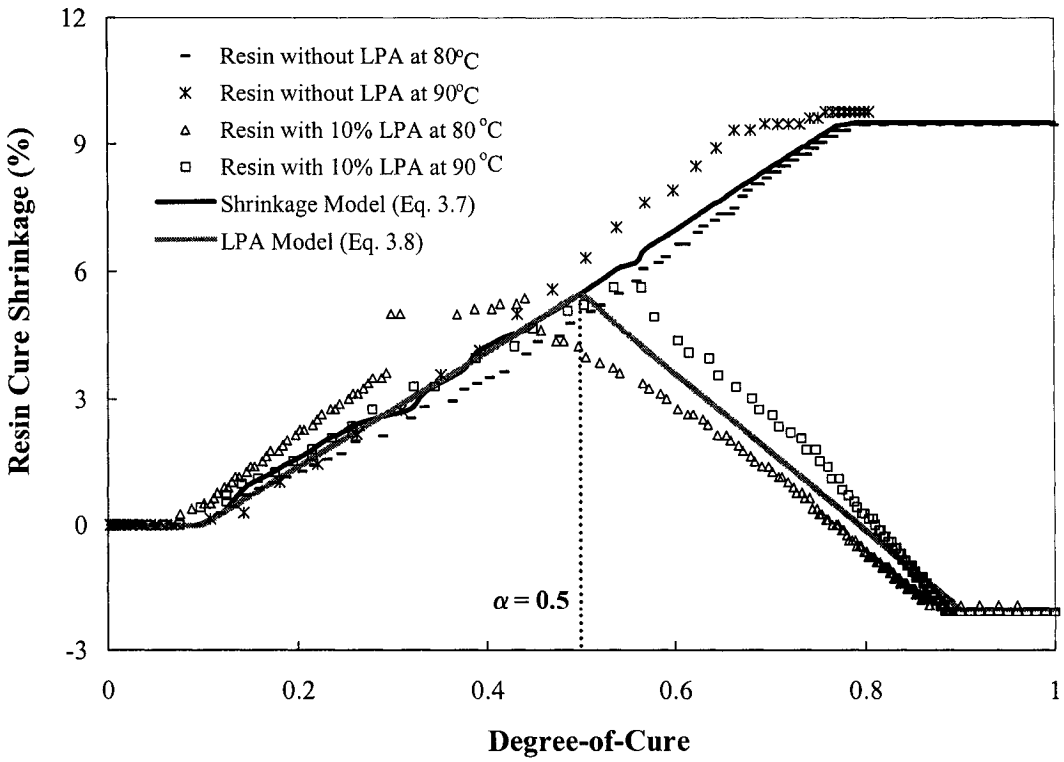

Figure 3.21 Experimental results and numerical validation of cure shrinkage and LPA expansion (Equation 3.7 and 3.8).

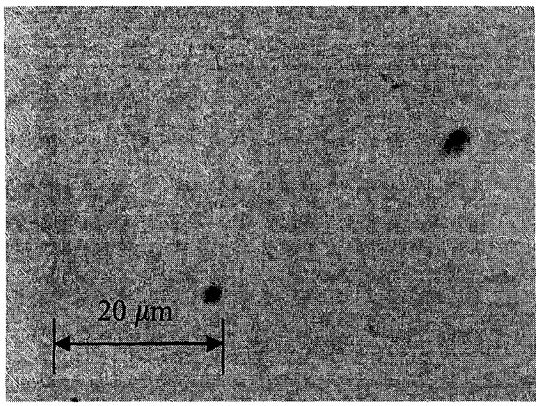

(a) $\alpha = 0$

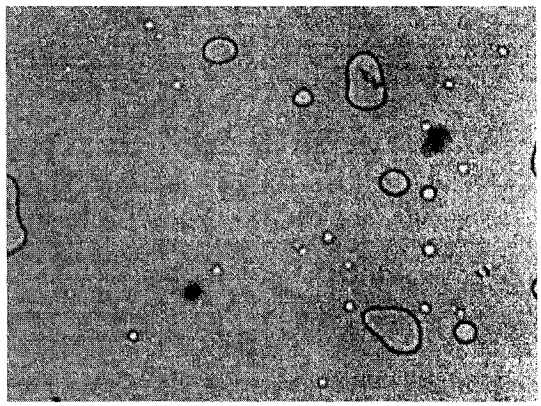

(b) $\alpha = 0.055$ (gelation)

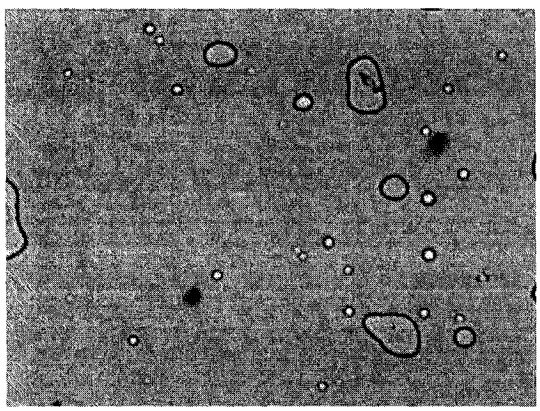

(c) $\alpha = 0.35$

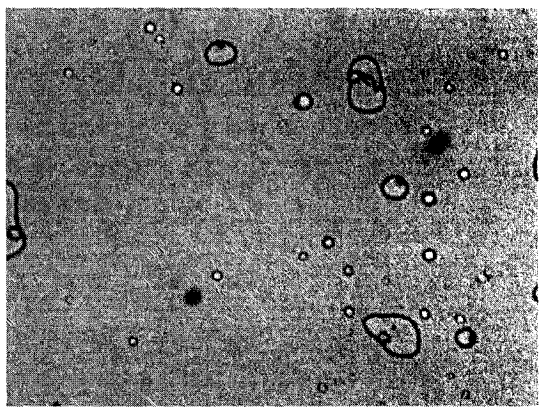

(d) $\alpha = 0.70$

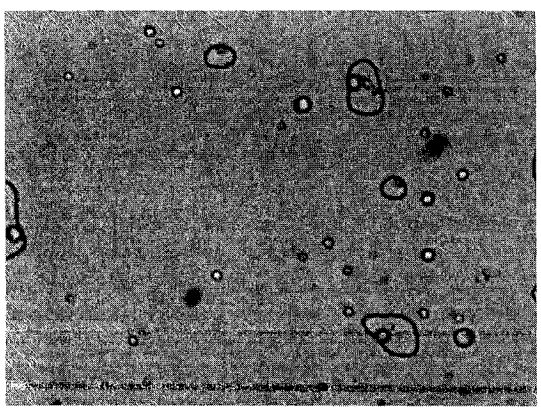

(e) $\alpha = 0.85$

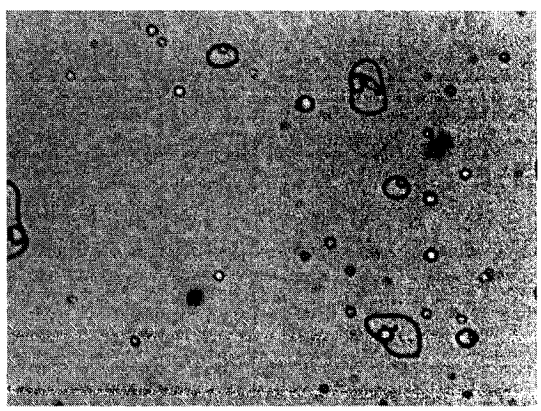

(f) $\alpha = 0.89$

Figure 3.22 Morphological changes in the neat resin (without LPA) under 90°C isothermal cure at different degrees-of-cure.

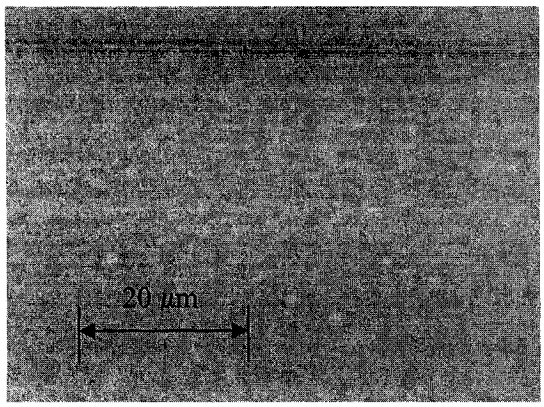

(a) $\alpha = 0$

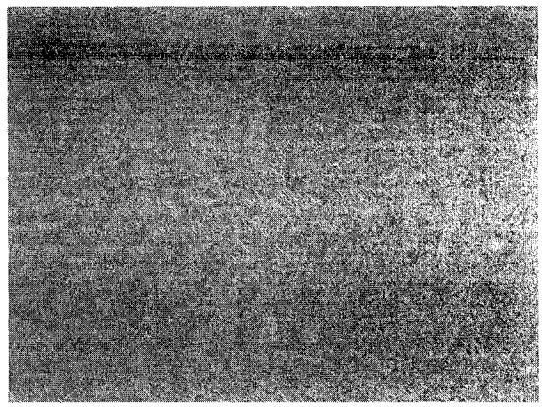

(b) $\alpha = 0.005$

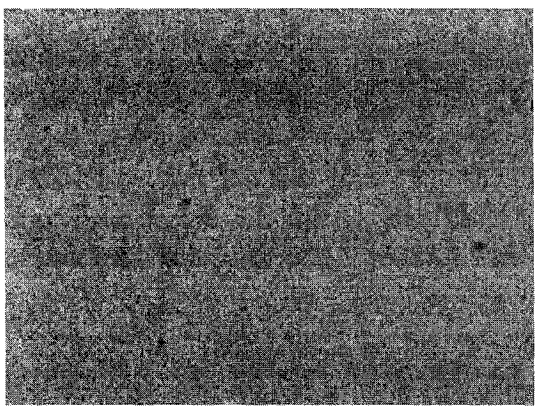

(c) $\alpha = 0.055$ (gelation)

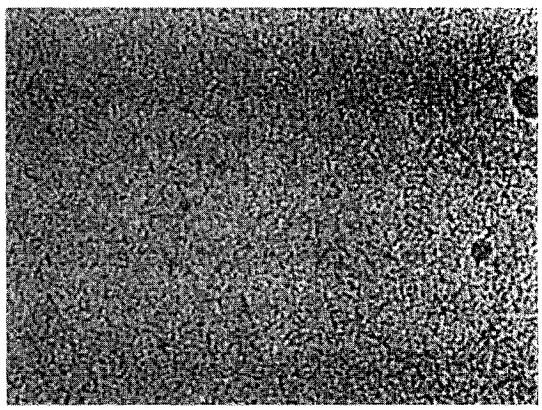

(d) ($\alpha = 0.20$)

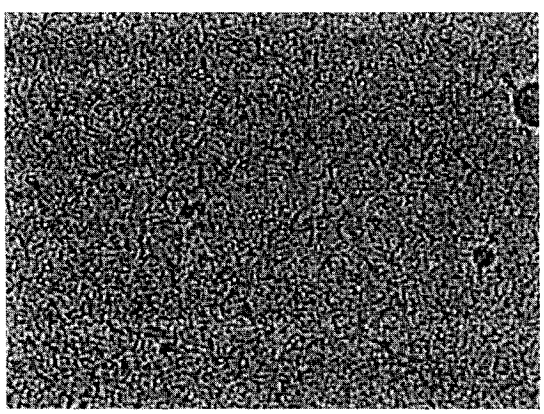

(e) $\alpha = 0.37$

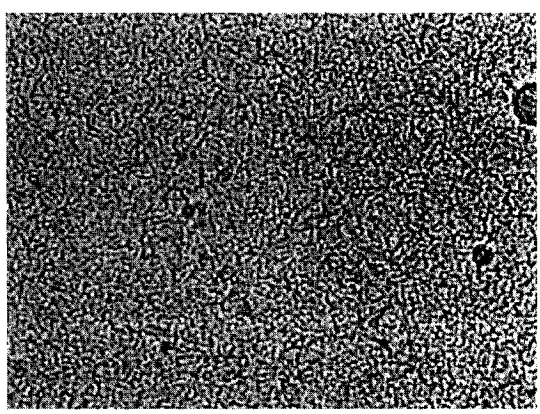

(f) $\alpha = 0.52$

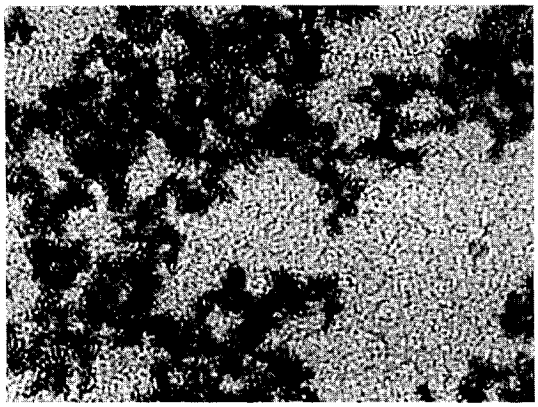

(g) $\alpha = 0.65$

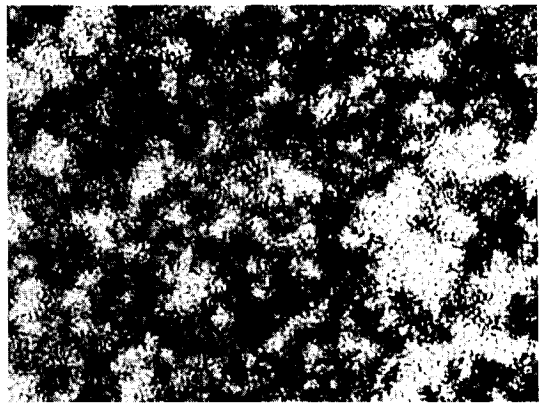

(h) $\alpha = 0.73$

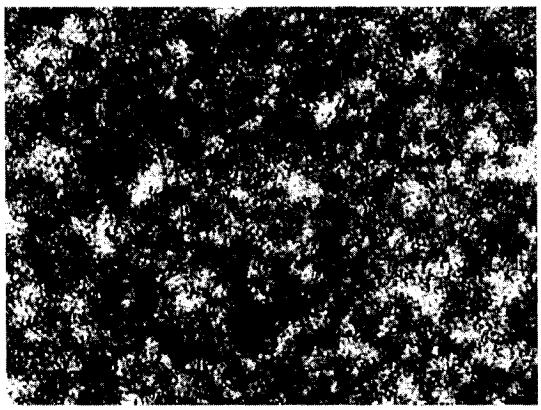

(i) $\alpha = 0.83$

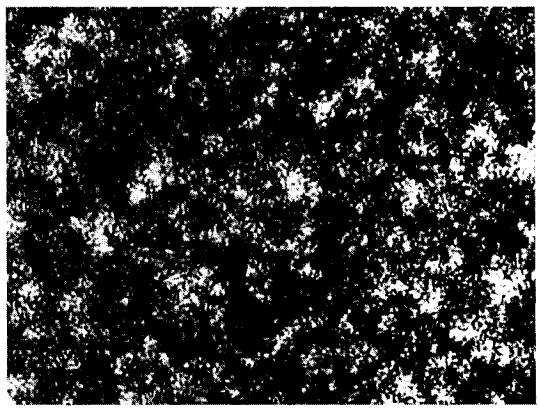

(j) $\alpha = 0.86$

Figure 3.23 Morphological changes in resin with 10% LPA under 90°C isothermal cure at different degrees-of-cure.

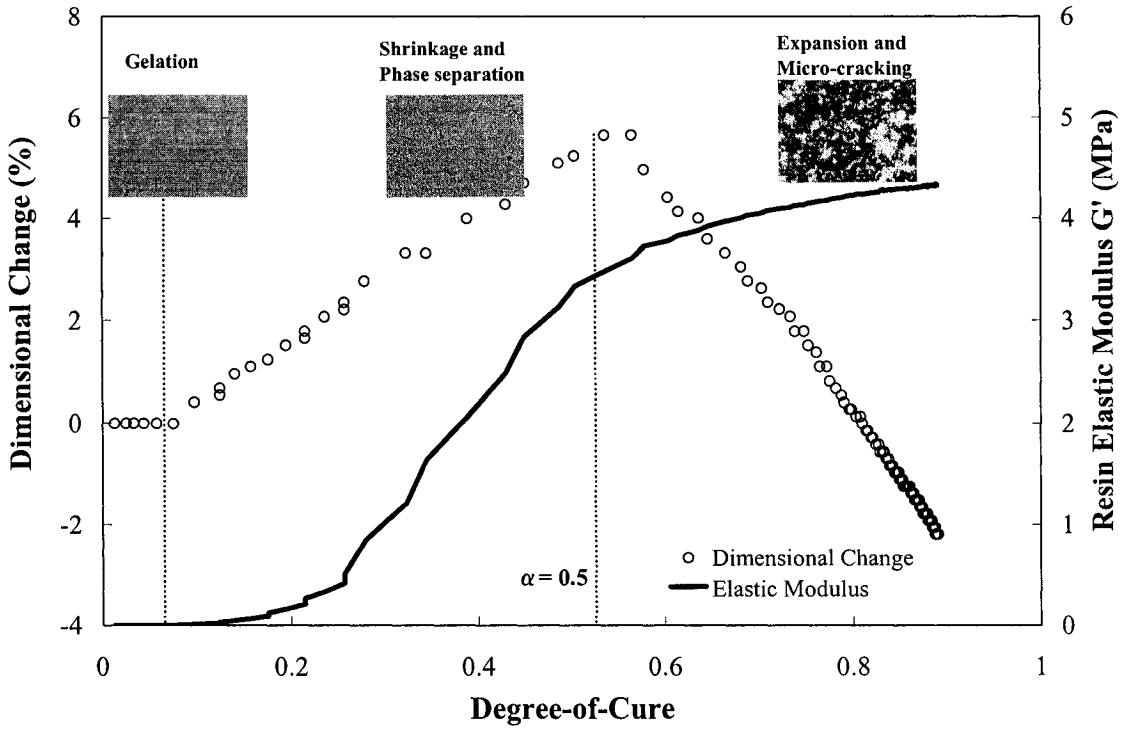

Figure 3.24 Shrinkage and morphological variations, and elastic modulus development during 90°C isothermal curing in 10% LPA resin.

LIST OF SYMBOLS

A_1, A_2	Frequency factors
B	Constant
C_1, C_2	Constants
E_1, E_2	Activation energies
K_1, K_2	Arrhenius constants
m, n	reaction orders
R	Universal gas constant
T	Absolute Temperature
T_b	Constant
t	Time
V_o	Original volume
V^T	Total volumetric shrinkage for fully cured resin
V_{filler}	Volume fraction of filler
ΔV	Change in volume
dV/dt	Rate of volume change

GREEK SYMBOLS

α	Degree-of-cure
α_G	Degree-of-cure at gelation
α_m	Degree-of-cure at maximum shrinkage and expansion
α_{max}	Maximum degree-of-cure
$\Delta\alpha$	Change in resin degree-of-cure
$d\alpha/dt$	Rate of cure
β_m	Volumetric thermal expansion coefficient of uncured resin
β_p	Volumetric thermal expansion coefficient of cure resin
η	Viscosity
η_0	Initial viscosity
σ	Standard deviation

Link between Material Characterization (chapter 3) and RTM Manufacturing (chapter 4)

Chapter 3 presents the analytical characterization of material parameters. This chapter sets the basis for material parameter selection for subsequent numerical simulations, design-of-experiments, RTM manufacturing and statistical analysis. This chapter provides degree-of-cure evolution, viscosity variations, shrinkage and expansion data and morphological changes in the resin. This chapter also provides crucial information on the gel time of resin formulations under different processing conditions, which is important for complete resin infiltration inside the mold. Test matrices in chapter 4 are designed based on the analytical characterization of material parameters in chapter 3. The levels of LPA, styrene, processing temperature and temperature gradients are chosen for minimum shrinkage, maximum expansion, minimum viscosity, minimum gel times and processing times. The shrinkage-expansion behavior of resin formulations observed with rheology experimentation is verified with pressure variations observed during RTM manufacturing.

CHAPTER 4

AN EXPERIMENTAL INVESTIGATION FOR CLASS A SURFACE FINISH IN RESIN TRANSFER MOLDING PROCESS

Mohsan Haider, Pascal Hubert*, Larry Lessard

Department of Mechanical Engineering, McGill University
817 Sherbrooke Street West, Montreal H3A 2K6, Quebec, Canada

(Prepared for Composite Science and Technology)

Abstract

Achievement of high class surface finish is important to the high volume automotive industry when using the Resin Transfer Molding (RTM) process for exterior body panels. Chemical cure shrinkage of the polyester resins has a direct impact on the surface finish of RTM molded components. Therefore, resins with Low Profile Additives (LPA) are used to reduce cure shrinkage and improve surface quality of the composite parts. However, a little is known about the behavior of low profile resins during RTM manufacturing and their ultimate effects on the surface quality of molded plaques. In this work, the effects of controlled material and processing parameters on the pressure variations, process cycle times and ultimately on the surface quality of RTM molded components were investigated. Taguchi experimental design techniques were employed to design test matrices and optimization analysis was performed. Test panels were

* Corresponding author:
E-mail: pascal.hubert@mcgill.ca
Tel.: 1(514) 398-6303

manufactured using a flat plate steel mold mounted on a press. Pressure sensors were inserted in the mold cavity to monitor pressure variations during different stages of cure reaction and at various locations in the mold cavity. It was found that a critical amount of LPA (10%) was required to push the material against the mold cavity and to compensate for the resin cure shrinkage. A significant increase in pressure was observed during later stages in resin cure due to the LPA expansion. The pressure increase had a significant effect on the surface roughness of the test samples with higher pressures resulting in better surface finish. A cure gradient was observed for low pressure injections which significantly reduced the maximum pressure levels. Process cycle times were found to be dependent on the amounts of accelerator and catalyst in the resin, and processing temperatures.

Keywords: A. Polymer-matrix composites (PMCs), B. Thermal properties, C. Pressure variations, E. Resin transfer molding (RTM)

4.1 Introduction

The automotive industry is aiming to replace conventional materials with polymer composites because of their beneficial properties such as higher stiffness and strength, lightweight, fire, corrosion and impact resistance [1-2], and noise suppression capabilities. Out of many composite manufacturing processes available, resin transfer molding (RTM) is one of the most efficient and economical process for high volume automotive applications due to its capabilities such as non-expensive process equipment, excellent control on mechanical properties, closed mold process, low filling pressures, incorporation of metal inserts and attachments, possibility of producing large and complex parts and low labor costs [3-11].

However, one of the major issues in using this process for automotive applications is the resulting surface quality. A high class surface finish is difficult to achieve for RTM

molded components due to various process and material related issues. Some of most common surface finish quality problems like fabric print through, ripples or long range waviness, pinholes, sink marks and dimensional inaccuracy are caused by resin cure shrinkage. A significant amount (7-10%) of cure shrinkage is associated with the cure reaction of standard polyester resins [12-13], which makes it difficult to achieve surface finish qualities and tight tolerances on car body panels in compliance with industry specifications and standards.

The addition of low profile additives (LPA) in the unsaturated polyester resin can potentially reduce the cure shrinkage. Low profile additives (LPA) generally serve as non-reactive additives in unsaturated polyester and vinyl ester resins to compensate for chemical cure shrinkage. These materials are initially soluble or form a stable dispersion in the styrene and resin mixture before cure, but become incompatible with the cured resin during the curing process. The most common LPA include poly vinyl-acetate (PVAc), poly methyl-methacrylate (PMMA), polystyrene (PS), thermoplastic polyurethanes (PU) and polyesters. LPA have been found to be effective in eliminating the polymerization shrinkage of unsaturated polyester resins in high temperature molding processes. In the past, much of the research efforts were focused on characterization of low profile based unsaturated polyester resins during curing using techniques like differential scanning calorimetry (DSC), scanning electron microscope (SEM), Fourier transform infrared spectroscopy (FTIR), optical microscopy and rheology [12-20]. The effects of LPA content on cure kinetics, reaction rates have been reported by many researchers. Some researchers have found no significant effect of LPA on reaction kinetics and cure rate [17, 21-24], whereas some others suggest slower reaction rates and relatively lower final degrees-of-cure as a result of LPA inclusion into the resin [25].

The effects of LPA concentration on cure shrinkage of unsaturated polyester resins have also been investigated [12-29]. A volumetric shrinkage of approximately 10% is reported for unsaturated polyester resins without any low profile additives. Researchers observed decrease in final cure shrinkage as a function of LPA content; however the shrinkage compensation depended on the LPA type, concentration, compatibility and

molecular weights [19-29]. Optimum concentrations of various LPA which result in minimum cure shrinkage in polyester resins have been reported by Liu et al. [14], Cao and Lee [17], Kinkelaar et al. [25] and Boyard et al. [26]. Boyard et al. [26] also observed reduction in cure shrinkage of neat polyester resins by adding filler and fibers. Huang et al. [27] investigated the shrinkage compensation effects of four LPA in an unsaturated polyester resin. The results showed that the volume shrinkage generally decreased linearly with increasing LPA concentration. The effectiveness of volume shrinkage control was best for poly vinyl-acetate (PVAc), followed by poly methyl-methacrylate (PMMA) and polystyrene (PS). Effects of inclusion of nano-clay particles on the shrinkage control of low profile unsaturated polyester resins have also been studied. Xu and Lee [28] reported that the addition of a small amount (1-3%) of nano-clay particles in unsaturated polyester resins, gave better shrinkage control. The effects of the LPA content (between 0 and 40%) on cure kinetics, cure shrinkage and morphological changes in Scott Bader PD9551 unsaturated polyester resin used in this research were studied and have been presented in [20]. A volumetric shrinkage of 9.5% was found in the resin without low profile additives. LPA content had no significant effect on the cure kinetics; however increasing LPA content reduced the cure shrinkage. LPA content at 10% was found to be the minimum amount for complete shrinkage compensation. The shrinkage and shrinkage compensation was found to be a linear function of degree-of-cure.

In short, LPA based resins show expansion during exothermic cure reaction. The effects of resin expansion during RTM manufacturing need to be investigated. Hence, RTM molds instrumented with thermocouples and pressure transducers are required for process monitoring during RTM processing of low profile resins. In the past, researchers have used instrumented RTM molds to monitor temperature and pressure variations during RTM manufacturing. Lebrun et al. [30] investigated temperature and pressure variations during filling and curing in a heated RTM mold. An increase in resin pressure was observed after impregnation due to the thermal expansion of the resin followed by a sharp drop in resin pressure due to curing and shrinkage. Researchers also observed a cure gradient along the length of the part with resin curing at different times at different locations. Lynch and coworkers [31] reported on the development of a special pressure

transducer accessory to monitor pressure variations during the curing of carbon fiber epoxy laminates. Pressure transducers have also been employed to study pressure variations during RTM resin injection phase and in the study of the effects of injection pressure on mechanical properties [32-33].

Despite research efforts on thermal, rheological and morphological characterization of LPA based resin systems, a little is known about the behavior of LPA based resins during RTM cure cycles and their ultimate effects on the surface finish of RTM molded components. The objectives of this paper are to investigate the effect of resin dimensional changes observed in polyester resins containing LPA on pressure variations during RTM processing. The ultimate goal is to determine the optimum process conditions for short cycle times and best surface finish. Furthermore, this paper presents pressure sensor data and discusses how the manufacturing process can be monitored in order to get class A finish panels for automotive applications. The effects of mold temperature, temperature gradient and injection pressures are also characterized through experimental design techniques.

4.2 Materials

Scott Bader PD9551 unsaturated polyester resin [34] was used in this research. The resin was supplied with a standard amount of LPA (10% wt. of resin). The low profile additive used in the resin was Scott Bader PD9419 polymer solution which contained poly vinyl-acetate (PVAc) and poly methyl-methylacrylate (PMMA) low profile additives. OMYA BLR2 calcium carbonate filler was added to the resin and standard accelerator (cobalt 2-ethylhexanoate) and catalyst (tert-butyl peroxybenzoate) were used. Composite panels were manufactured by RTM with F3P glass fiber preforms. The preform structure consisted of three layers of glass fibers as shown in Figure 4.1. The top layer (side-A) had a surface veil consisting of thin continuous glass fibers of an average diameter of 20 μm. The center layer consisted of chopped fiber bundles and the bottom layer (side-B) also had thin continuous individual glass fibers of an average diameter of 20 μm. The difference between side-A and side-B was that relatively higher binder

concentration was present on side-B of the preform which could potentially affect the surface quality of the test samples. Hence, side-A was used for all the surface finish measurements. The weight fraction (w_f) of surface veil (9.2%) was much smaller compared to the weight fraction of structural mat (81.6%) in the preform. Table 4.1 summarizes the materials used and their weight fractions based on the weight of the resin. The resin was mixed with the accelerator first and then the filler was added into it. The filler was mixed well with the resin mixture. At the end, the catalyst was added into the resin-filler mixture and mixed again. At this point the resin was ready for injection.

4.3 RTM Setup and Test Matrix

Composite plates were manufactured using a heated steel mold mounted on a hydraulic press. The mold had a mirror like polished finish and was instrumented with type J thermocouples and Dynisco PT422 pressure sensors connected to a Vishay's System 6000 data acquisition system. The mold platens were heated to the required temperatures with a Conair circulating water heating system. Thermocouples were attached to the top and bottom mold platens to record variations in the mold temperature. The picture of the mold with its mounting on the press is shown in Figure 4.2. The resin at room temperature was injected into the mold cavity with a Radius Engineering constant pressure pneumatic-controlled injector [35]. The 3.175 mm thick picture frame was sealed using a Gore-Tex joint sealant gasket. A temperature gradient was created by moving the top and bottom platens away from each other and setting them at two different temperatures (in a range from 75°C to 90°C). The bottom mold was always kept at 90°C whereas the temperature of the top mold was adjusted to achieve the required gradient. The 24 cm by 26 cm F3P glass fiber preform was cut and placed inside the mold just before injection. Side-A of the preform was placed towards the hottest mold platen. The injection and vent ports were designed to create a uniform linear flow front though the fiber preform. The pressure sensors (referred as PS1, PS2, PS3 and PS5) were located near the injection and vent ports and PS4 was mounted on the injection pump to measure injection pressure. The injections were performed at different injection pressure levels ranging from 200 to 650 kPa. The mold surfaces were cleaned with acetone and coated

with a single layer of Chemlease 41-90 mold release agent. Manufactured composite panels were kept inside the mold until the resin achieved the maximum pressure level. A schematic and photograph of the picture frame, fiber preform, injection port, vent port and location of the pressure sensors (PS) is given in Figure 4.3. Resin tracers were used to verify the uniformity of the flow front.

4.3.1 Determination of Processing Window

Differential scanning calorimetry (DSC) tests performed in [20] showed that LPA content (in the range from 0-20%) and styrene content (in the range from 0-8%) did not significantly affect the cure kinetics; hence these levels were used for the experimental test matrix of Table 4.2. However, the amounts of accelerator and catalyst which would result in a processing window of 1, 3 and 10 minutes (which are the three levels of gel time in the test matrix) are unknown. Hence, DSC and rheology tests were performed to determine the resin formulation which would result in processing windows of 1, 3 and 10 minutes at a processing temperature of 90°C. The processing parameters that affect gel times and cure rates are the amount of accelerator, catalyst and the curing temperature. Six resin formulations given in Table 4.3 were tested with DSC and rheology to determine the processing window (gel times) at 80°C, 90°C and 100°C isothermal temperatures. The formulations contained accelerator in a range from 0.05 – 1% and catalyst in a range from 0.4 – 3%. At least three DSC and rheology scans at 80°C, 90°C and 100°C isothermal temperatures were performed on each resin formulation of Table 4.3 to determine the gel time and verify the consistency of the results. Gel time was calculated based on the cross over point of the resin elastic modulus G′ and loss modulus G″. The rheometer chamber was pre-heated to the desired temperature and then resin was poured on the parallel plates of the equipment. The gel times for different formulations at different temperatures are given in Table 4.4 and are plotted in Figure 4.4.

Based on processing temperature and gel time required, formulations can be chosen from Table 4.4. Resin formulations can be chosen from Figure 4.4 to result in a gel time range of 1-30 minutes for the processing temperature range of 80-100°C. From Table 4.4

and Figure 4.4, accelerator can be added at 0.05, 0.2 and 1% and catalyst can be added at 0.4, 1.6 and 3% to results in a gel time range of 10, 3 and 1 minute at a processing temperature of 90°C, respectively. It is apparent from Table 4.4 that gel times do not change significantly when accelerator level is increased above 0.25%. Also, the temperature has a major effect on the curing of this resin where an increase of 10°C in the processing temperature decreases gel time significantly for any given formulation. For the chosen formulations (1, 4, 6) the variation in cure rate is plotted as a function of degree-of-cure in Figure 4.5 and the variation in degree-of-cure as function of time is plotted in Figure 4.6 for a processing temperature of 90°C. As can be seen from Figure 4.5, the cure rate is the slowest for the resin formulation with least amount of accelerator and catalyst (formulation 1) and hence takes longer time to reach a maximum degree-of-cure of 0.9. The cure rate increases significantly when accelerator level is increased from 0.05% to 0.2% and hence reduces the time to reach maximum degree-of-cure from 70 to 20 minutes. The time to reach maximum degree-of-cure reduces even further (20 to 10 minutes) and cure rates increase when accelerator is increased from 0.2% to 1% as shown in Figures 4.5 and 4.6.

4.3.2 Experimental Test Matrix

The parameters that can affect surface finish quality during RTM are divided in two categories. Material parameters include LPA, solvent (styrene), filler, catalyst, accelerator, internal and external de-molding agents and reinforcement. Processing parameters include mold temperature, temperature gradient between the mold platens, injection pressures and injection rates. These parameters can be controlled while room temperature, humidity level, condition and aging of the equipment and mold preparation variations arising from different experimenters are parameters which are often not controlled in a production environment. The effects of humidity level and room temperature are minimal in resin transfer molding since it is a closed mold process and injections are performed at higher temperature levels.

It is unrealistic, uneconomical and impossible to optimize all process parameters simultaneously; in addition some parameters need to be fixed based on the requirements of the process, cost, compatibility issues and limitations of the equipment capabilities. Hence, material parameters: LPA, styrene, filler, accelerator and catalyst (combined in gel time) are chosen to investigate their effects on the surface finish quality. Processing parameters: injection pressure and temperature gradient are also chosen. These six parameters are thought to be the most important parameters which can potentially affect the surface quality of the RTM molded components, cost and cycle times.

An experimental test matrix of eighteen trials was designed to investigate the effects of six parameters (LPA, styrene, filler, gel time, temperature gradient and injection pressure), each at three levels on the surface finish, process cycle time and pressure variations using the Taguchi method [36-38]. The levels of processing parameters are listed in Table 4.2. The levels of LPA, styrene and process temperatures were chosen based on the resin characterization discussed in [20]. LPA content at 0% and 5% resulted in the same final cure shrinkage [20]; hence only one level (5%) was used in the test matrix. The levels of gel times were chosen to investigate the effects of reaction rate on the surface finish of molded test panels. Injection pressure levels were chosen to determine the effect of flow rate on the surface quality of the molded components. Table 4.5 tabulates all the experiments with each process parameter at a given level. The test panels were manufactured using the experimental setup discussed earlier. The fiber volume fraction for all the experiments was kept constant at 0.2, which was later verified with the ratio of the volume of fibers used and the volume of the finished plate.

4.4 Resin Pressure Profile Analysis

Pressure variations observed during an RTM cure cycle for a resin with 10% LPA are shown in Figure 4.7 (experiment # 4 Table 4.5). As can be seen from Figure 4.7, since the resin was injected at a relatively high pressure level (621 kPa) it infiltrated through the fibers within ten seconds. The mold was then clamped and pressure was maintained until gelation at about five minutes. The interesting thing to note in Figure 4.7 is the

simultaneous drop in pressure levels due to gelation at all locations. This is due to the higher injection pressure which results in a very fast filling of the mold cavity and resulting in a minimum cure gradient along the length of the test sample; however it is not the case for low pressure injections where resin takes relatively longer time to infiltrate through the fibers and hence induces a significant cure gradient. In Figure 4.7, the pressure dropped down to zero and stayed at zero for another four minutes. Then the pressure started to increase due to the LPA expansion.

The pressure variation observed at sensor location PS2 is further plotted in Figure 4.8, where four stages can be identified. Stage 1 corresponds to the resin injection where the resin pressure increases gradually until resin starts to flow out of the vent port. During Stage 2, the vent port is closed and the resin pressure is maintained at the injection pressure until resin gelation. Stage 3 starts as the resin pressure quickly drops to zero indicating that the resin starts to gel and shrink. During this stage, the panel loses contact with the mold surface until the LPA expansion induces a significant increase in resin pressure. Stage 4 corresponds to the LPA expansion where the panel makes good contact with the mold surfaces. RTM panels manufactured under various processing conditions were kept inside the mold until the resin pressure measured in Stage 4 became constant. Process cycle time is defined as the time from the start of the injection until the resin achieves maximum pressure level in Stage 4.

All the sensors inserted in the mold showed an increase in pressure during Stage 4; however the maximum pressure observed at each sensor was different. The sensors closest to the injection port showed the highest pressure whereas the sensors farthest showed relatively low pressure. The same phenomenon was observed for other injections. However, this relative pressure decrease was smaller for high pressure injections and was larger for low pressure injections. As shown in Figure 4.9, the relative decrease in the pressure level of sensor PS1 and sensor PS5 is almost 1 MPa (injection pressure 207 kPa) compared with only 0.6 MPa pressure decrease between these two sensors in Figure 4.7 (injection pressure 621 kPa). Also a prominent cure gradient can be seen at different sensor locations from Figure 4.9.

The relative decrease in pressure at different sensor locations is due to the fact that the cure starts at the vent port and travels towards the injection port. As can be seen from Figure 4.10, the resin cures at sensor locations PS3 and PS5 first which are relatively close to the vent port, followed by PS2 and PS1. The maximum pressure observed for these sensors are exactly in the reverse order as shown in Figure 4.9. Thus a relationship exists between the cure gradient and the pressure variation measured by the sensors. This phenomenon can be explained by the LPA mechanism proposed in [20]. The LPA expansion is highly dependent on the visco-elastic properties of the materials. Since the cure progresses from vent port towards the injection port, the resin close to injection port is relatively less elastic compared with the resin close to the vent port. Hence, the stresses generated at the vent port due to the LPA action are dissipated since the material close to injection port is less elastic. Thus the pressure increase observed at the sensors locations close to injection port is higher compared with the sensors further away from the injection port. Cure gradient is also one of the reasons for the decrease in the maximum cure pressure observed during RTM cure cycle. The pressure variations of Figure 4.7 are plotted as a function of degree-of-cure in Figure 4.11. The pressure increase for all the sensors starts in a degree-of-cure range of 0.4-0.5. The pressure increase curves follow similar trends; however their elevations are between 0.9 and 1.6 MPa. The difference in the elevation of these curves is due to the cure gradient discussed earlier.

4.4.1 Effect of LPA on Resin Pressure

The graph in Figure 4.12 shows pressure variations at sensor location PS2 for different resin formulations (1, 14, 18) in Taguchi plan. The gel time was taken as one minute with a temperature gradient of 10°C. The only process parameter changed was the amount of LPA (between 0 and 40%), keeping all the other parameters at fixed levels. From Figure 4.12, the first three stages (injection, gelation and shrinkage) are similar for all the resin formulations, however the forth stage is different. Resins with 0 and 5% LPA show no pressure increase in Stage 4, which indicates that the resin is not expanding and

it is not pressing against the mold walls. The highest pressure increase (2.2 MPa) is observed for the resin with 20% LPA. Resins with 10% and 20% LPA reached the highest pressure level in approximately 15 minutes; however the resin with 40% LPA achieved the highest pressure level of 1.2 MPa in approximately 25 minutes after injection. As can be seen from Figure 4.12, not only the maximum pressure achieved with the 40% LPA is lower but also the time taken by this resin to achieve that pressure level is much longer compared with other two formulations. This is due to relatively slower reaction rate observed for resin formulation with 40% LPA [20] as shown in Figure 4.13.

The pressure data was also integrated with the degree-of-cure variations obtained from DSC. The data is plotted in Figure 4.14. As can be seen from Figure 4.14, the variation in pressure as a function of degree-of-cure is almost identical for all the formulations having LPA above 10%. Three stages can be identified from the graph in Figure 4.14. The pressure variations below a degree-of-cure of 0.1 are due to the injection pressure and gelation. The second stage is from a degree-of-cure of 0.1 to 0.5, where no pressure is observed. This stage represents shrinkage in the resin. Then the LPA expansion starts at an approximately 0.5 degree-of-cure. The same phenomenon was observed during dimensional change studies with rheology and is reported in [20]. The pressure increase as a function of degree-of-cure for all the formulations with LPA levels higher than 10% has the same trend; however the maximum pressure is highest for 20% formulation following by 10% and 40% formulations.

LPA expansions measured as percent of sample dimensions with a rheometer [20] and pressure variations observed during RTM processing of polyester resins with 10% LPA under 80°C and 90°C processing temperatures are plotted in Figure 4.15. Net LPA expansion and pressure curves are similar. LPA can be seen to stay inactive until a degree-of-cure of 0.5 and then expansion starts. Same trend is observed for pressure curves. Hence, it can be deduced from the graph in Figure 4.15 that the pressure variations observed during RTM manufacturing are mainly due to the LPA expansion and are independent of the processing temperature in the range tested. Hence, the procedure

developed for resin shrinkage-expansion measurements [20] is quite accurate for shrinkage-expansion characterization and LPA expansion mechanism proposed [20] is valid as can be seen from pressure variation curves in Figure 4.15.

Hence, to compensate shrinkage and get enough pressure for pushing the material against the mold cavity and to reduce cost, LPA can be added at an optimum level of 10%. Adding more LPA does not help to attain relatively higher pressure levels and higher LPA levels add more to the manufacturing cost. In addition, higher LPA levels slow down the reaction rate. The higher injection pressures are also recommended to reduce the cure gradient along the length of the test sample.

4.4.2 Statistical Analysis

Table 4.6 summarizes the effects of the processing conditions (for the test matrix of Table 4.5) on the resin pressure and process cycle time. Later, this data was used in carrying out Analysis of Variance (ANOVA) to study the effect of each process parameter on maximum pressure observed during manufacturing and the process cycle times. Table 4.7 shows the effects of processing parameters on the process cycle times obtained with Analysis of Variance (ANOVA). The values used for ANOVA are taken from the last column of Table 4.6. As expected, the gel time (which represents the cure rate) had the most significant effect (96%) on the process cycle time. It is also apparent from Table 4.7 that all the other process parameters are statistically insignificant and had no effect on the process cycle time.

Analysis of Variance (ANOVA) was also carried out for maximum pressure observed during Stage 4 of RTM manufacturing. Table 4.7 presents the effect of each processing parameter on the maximum pressure. As expected and as discussed earlier, the most influential parameter on maximum pressure is the LPA content and had an effect of 86% or maximum pressure. It is interesting to note that only one factor, which is the amount of LPA is statistically significant for resin pressure and only gel time (cure rate) is

significant for process cycle time. Since the effects of other factors are less than 10% of the size of most significant factor, it makes them relatively insignificant.

4.4.3 Resin Pressure and Cure Shrinkage Relationship

The average effects of the LPA content on the maximum pressure are plotted in Figure 4.16. This Figure also plots the effects of LPA content on final cure shrinkage measured with a rheometer [20]. It is interesting to note that the final cure shrinkage and maximum pressure curves are exactly opposite to each other. The final cure shrinkage is similar for LPA content between 0-5% and there is no pressure observed during RTM manufacturing with these formulations. When the LPA level is increased from 5% to 10%, the cure shrinkage drop from 10% to -2% which represents an expansion in the resin. Subsequently, a huge increase (from 0 to 1.4 MPa) in the pressure is observed. After this critical amount, adding more LPA does not help in getting more expansion and higher pressure. Hence, 10% LPA concentration is the minimum amount required for shrinkage compensation. The graph in Figure 4.16 also proves the fact that the pressure increase observed is solely due to the amount of LPA.

Figure 4.17 shows the effects of LPA content on the roughness measured for a cutoff wavelength of 25 mm taken from [39]. This Figure shows that the pressure and roughness curves are exactly opposite to each other. When LPA level is increased from 5% to 10%, pressure increases (from 0-1.4 MPa) and roughness decreases (from 3.4-0.4 μm). However the surface roughness does not decrease any further when LPA level is increased from 10-20%. Hence, it can be deduced that LPA level at 10% is the optimum amount of LPA that can be used for a reasonable pressure, good surface finish quality and minimum shrinkage.

Figure 4.18 shows the effects of gel time (cure rate) on the process cycle time and maximum pressure. Table 4.7 shows that the gel time has a minor effect (3.4%) on the maximum pressure. The maximum average pressure decreases with increase in gel time, however the decrease is not that significant (from 1.2 MPa to 0.9 MPa) when gel time is

increased from 1 – 10 minutes as can be seen from Figure 4.18. However, the gel time is the most influential factor affecting the process cycle time. The process cycle time increases from 15 minutes to 25 minutes when gel time is increased from 1 to 3 minutes. The increase in the process cycle time is even higher (from 25 to 70 minutes) when the gel time is increased from 3 to 10 minutes. This can also be seen from the pressure data obtained during RTM manufacturing for three formulations. Figure 4.19 shows the pressure variation curves for 10% LPA resin (experiment 4, 5 and 6) with different gel times. As it is apparent from this Figure that when the gel time is reduced from 10 minutes to 3 minutes the maximum pressure increases from 0.94 MPa to 1.33 MPa. By reducing gel time even further (3 to 1 minute), the maximum pressure increases from 1.33 MPa to 1.77 MPa. The time to achieve maximum pressures also decreased from (77 minutes to 15 minutes) by decreasing gel time from 10 minutes to 1 minute.

4.4.4 Processing Window for Class A Panels

Based on this analysis, a processing window can be defined for the proper mold filling without leaving any free spaces in the mold cavity and getting enough pressure to result in a good contact between the part and the mold. The graph in Figure 4.20 shows the relationship between maximum pressure and gel time of all the formulations of the Taguchi test matrix (Table 4.5). In a manufacturing environment faster cure rates are required for meeting production demands. Hence, a processing window is required to result in minimum gel times and process cycle times without sacrificing the resin pressure in Stage 4 during RTM manufacturing. Figure 4.21 presents the maximum resin pressure plotted as a function of process cycle time. From Figure 4.20, two process conditions (6, 18) meet the requirement of minimum gel time of approximately 1 minute, whereas four process conditions (6, 7, 14, 18) meet the requirements of minimum process cycle times. These four formulations also result in relatively higher resin pressures ranging from 1.8 MPa to 2.1 MPa. A high class surface finish is also measured for these process conditions. Some other process conditions (4, 8, 15, 16) although result in higher resin pressures; however their process cycle times are relatively longer (from 27-42

minutes). Rest of all the process conditions either result in low resin pressures or have long process cycle times and hence are not feasible for mass production. In short, any process condition can be chosen from (6, 7, 14, 18) for minimum cycle time and maximum resin pressure; however process conditions containing 10% LPA resin are preferred over 20% LPA resin due to lower cost.

4.5 Conclusion

The pressure increase observed during Stage 4 in RTM manufacturing was mainly due to the LPA content in the resin. Resin with LPA content less than 10% showed no pressure increase. The highest pressure was observed for resin formulations with 20% LPA resin following by 10% and 40% LPA resins. The pressure variation as a function of time were similar for 10 and 20% LPA formulations, however 40% resin took much longer time to reach the maximum pressure level due to slow cure rates observed for this resin formulation. The pressure variations plotted as a function of degree-of-cure had similar curves for all resin formulations (>10%) which means that pressure increase is solely dependent on the cure rate and degree-of-cure. No pressure increase was observed below a degree-of-cure of 0.5 which proves that fact that LPA action starts only after resin has become fully elastic as discussed in [20].

Injection pressure was observed to have a significant effect on the cure gradient. The injections at high pressure levels (> 400 kPa) showed no significant cure gradient because of short injection times, however injections at low pressure levels (< 400 kPa) had a significant cure gradient along the length of the part which resulted in relatively smaller pressure increase at locations away from the injection port. The cure gradient was also seen to have a significant effect on the maximum pressure observed at different sensors locations. The sensors close to injection ports showed much higher pressures compared with sensors further away due to cure gradient.

The maximum pressure, final cure shrinkage and roughness were mainly dependent on the LPA content and closely related to each other. Higher LPA contents (0-20%)

resulted in higher pressures, lower final cure shrinkage and lower roughness values. Resin formulations with 40% LPA resulted in lower pressure levels, longer time to reach maximum pressure level and no further improvement in surface roughness compared with 10% and 20% LPA formulations. The gel time (cure rate) had the most significant effect on the process cycle time. Resin formulations with shorter gel times resulted in short process cycle times. A linear relationship was observed between the gel time and process cycle time. Gel times had a minor affect on the maximum pressure with longer gel times resulting in relatively lower pressure levels. Based on short cycle times and maximum pressures a processing window was defined for the resin formulations and process parameters. LPA content of 10% was found to be the optimum amount of LPA needed for cure shrinkage compensation and to cause enough pressure for making a good contact between the part and the mold. Techniques developed earlier in this work to predict resin shrinkage and expansion [20] were verified with experimental data and were found to be accurate.

4.6 Acknowledgements

Ford Motor Inc. and Auto21 Network of Centers of Excellence are gratefully acknowledged for their financial and technical support. We would also like to thank Dr. Michael Debolt of Ford motors for the technical advice and support during this study. Eric St-Amant and Ronnie Lawand of McGill Composite Materials and Structures Laboratory are acknowledged for their help with injections.

References

1. Ludick J. Resin Transfer Molding for Missile Shroud Production, Proceedings of ICCM-11, Gold Coast, Australia, July 14-18, 1997.
2. Niu, MC. Composites Airframe Structures Practical Design Information and Data, Conmilit Press Ltd., Hong Kong, 1993.
3. Morrison G. The Art of Aerospace Composites: Keeping the Pressure on the Resin Transfer Molding Process for Manufacturing Flight Critical Carbon Fiber Parts. Mechanical Engineering 1999;121(4):58-61.
4. Holmberg JA, Berglund LA. Manufacturing and Performance of RTM U-beams. Composites Part A 1997;28A:513-521.
5. Thuis HGS, Biemans C. Design, Fabrication and Testing of a Composite Bracket for Aerospace Applications. Composite structures 1997;38(1):91-98.
6. Potter KD. The Early History of Resin Transfer Molding Process for Aerospace Applications. Composites Part A 1999;30:619-621.
7. Chen SC, Chen YC, Cheng NT, Huang MS. Simulations and Applications of Injection-Compression Molding. Journal of Reinforced Plastics and Composites 1999;18(8):724-734.
8. Rudd CD, Long AC, Kendall KN, Mangin CGE. Liquid Molding Technologies, Woodhead Publishing Limited, 1997, Cambridge, UK.
9. Potter K. Resin Transfer Moulding, Chapman and Hall, 1997, London, UK.
10. Brooks N. Is RTM Ready for Mass Production. Reinforced Plastics 1995;39(1):26-31.
11. Advani SG, Bruschke MV. Flow and Rheology in Polymer Composites Manufacturing. Elsevier Science BV, 1994, Amsterdam.
12. Kinekelaar M, Wang B, Lee LJ. Shrinkage behavior of low profile unsaturated polyester resins. Polymer 1994;35(4):3011-3022.
13. Hill RR, Muzumdar SV, Lee LJ, Analysis of volumetric changes of unsaturated polyester resins during curing. Polymer Engineering and Science 1995;35(10):852-859.
14. Liu CJ, Kiasat MS, Nijhof AHJ, Blokland H, Marissen R. The effect of the addition of a low profile additive on the curing shrinkage of an unsaturated polyester resin. Polymer Engineering and Science 1999;39(1):18-25.
15. Bucknall, CB, Partridge IK, Phillips MJ. Mechanism of shrinkage control in polyester resins containing low profile additives. Polymer 1991;32(4):636-640.
16. Wang K, Wang JH, Zhu YD, Xia Y. The effect of low profile additives on unsaturated polyester resins during curing at low/medium temperature: shrinkage behavior study. Key Engineering Materials 2003;249:351-354.
17. Cao X, Lee LJ. Control of shrinkage and residual styrene of unsaturated polyester resins cured at low temperatures: I. Effect of curing agents. Polymer 2003;44(6):1893-1902.
18. Ryan ME, Dutta A. Kinetics of epoxy cure: a rapid technique for kinetic parameter estimation. Polymer 1979;20(2):203-206.
19. Vilas JL, Laza, JM, Garay MT, Rodriguez M, Leon LM. Unsaturated polyester resins cure: Kinetic, rheologic, and mechanical-dynamical analysis. I. Cure kinetics by DSC and TSR. Journal of Applied Polymer Science 2001;79(3):447-457.
20. Haider M, Hubert P, Lessard L. Characterization and cure shrinkage modeling of a polyester resin with low profile additives. Composites Part A. (submitted).
21. Li W, Lee LJ. Shrinkage control of low profile unsaturated polyester resins cured at low temperature. Polymer 1998;39(23):5677-5687.
22. Li W, Lee LJ. Low Temperature Cure of Unsaturated Polyester Resins with Thermoplastic Additives. I. Dilatometry and Morphology Study. Polymer 2000;41:685-696.

23. Li W, Lee LJ. Low temperature cure of unsaturated polyester resins with thermoplastic additives II. Structure formation and shrinkage control mechanism. Polymer 2000;41:697-710.
24. Cao X, Lee LJ. Effect of Co-promoter and Secondary Monomer on Shrinkage Control of Unsaturated Polyester (UP)/Styrene (St)/Low-Profile Additive (LPA) Systems Cured at Low Temperatures. Journal of Applied Polymer Science 2001;82:738-749.
25. Kinkelaar P, Hsu CP, Lee LJ. Effects of Thermoplastic Additives on the Cure of Unsaturated Polyester Resins. Polymer Engineering and Science 1991;31(20):1450-1460.
26. Boyard N, Vayer M, Sinturel C, Delaunay D. Modeling PVTX Diagrams: Application to Various Blends Based on Unsaturated Polyester—Influence of Thermoplastic Additive, Fillers, and Reinforcements. Journal of Applied Polymer Science 2004;92:2976-2988.
27. Huang Y, Liang C. Volume Shrinkage Characteristics in the Cure of Low Shrink Unsaturated Polyester Resins. Polymer 1996;37(3):401-412.
28. Xu L, Lee LJ. Effect of Nanoclay on Shrinkage Control of Low Profile Unsaturated Polyester (UP) Resin Cured at Room Temperature. Polymer 2004;45:7325-7334.
29. Chan-Park MB, McGarry FJ. Tough Low Profile Additives in Sheet Molding Compound. Polymer Composites 1996;17(4):537-547.
30. Lebrun G, Gauvin R, Kendall KN. Experimental Investigation of Resin Temperature and Pressure During Filling and Curing in a Flat Steel RTM Mould. Composites Part A 1996;27A:347-355.
31. Lynch C, Hubert P, Poursartip A. Use of a Simple Inexpensive Pressure Sensor to Measure Hydrostatic Resin Pressure During Processing of Composite Laminates. Polymer Composites 1999;20(4):581-593.
32. Olivero KA, Barraza HJ, O'Rear EA, Altan MC. Effects of Injection Rate and Post Fill Cure Pressure on Properties of Resin Transfer Molding Disks. Journal of Composite Materials 2002;36(16):2011-2028.
33. Olivero KA, Hamidi YK, Aktas L, Altan MC. Effects of Preform Thickness and Volume Fraction on Injection Pressure and Mechanical Properties of Resin Transfer Molded Composites. Journal of Composite Materials 2004;38(11):937-957.
34. Scott Bader, Provisional Data Sheet PD9551 - R&D Group, Fax transmission, August 2002.
35. Specification Sheet, 2100cc Pneumatic RTM Injector, Radius Engineering, Utah USA, 2004.
36. Roy RK. Design of Experiments using the Taguchi Approach, John Wiley and Sons, New York, 2001.
37. Karbhari VM, Slotte SG, Steenkamer DA, Wilkins DJ. Effect of Material, Process and Equipment Variables on the Performance of Resin Transfer Molded Parts. Composite Manufacturing 1992;3(3):143-151.
38. Dutiro C, Alaka RN, and Matthews FL. Factors Controlling Surface Finish in Resin Transfer Molding Process. SAMPE Journal 1997;33(5):19-23.
39. Haider M, Hubert P, Lessard L. Optimization of Processing parameters for class A RTM manufacturing through design of experiments and multiple regression analysis, Composites Part A (submitted)

Table 4.1 Weight fractions of the materials based on resin weight.

Materials	Type (Manufacturer)	Weight Fraction (wt. %)
Resin	PD9551 (Scott Bader)	-----
LPA	PD9419 (Scott Bader)	0 - 40%
Filler	Calcium carbonate (Omya)	0 – 40%*
Catalyst	Tert-Butyl peroxybenzoate (Akzo Chemicals)	0.4 – 3%*
Accelerator	Cobalt 2-ethylhexanoate (Akzo Chemicals)	0.05 – 1%*
Fiber preform	F3P glass fibers preform (Ford Motors)	35
Mold release agent	41-90 Chemlease	1 layer
Mold sealant	Gore-tex gasket material	1 layer

* based on the weight of the resin and LPA.

Table 4.2 Process parameters and their levels used in DOE test matrix

Processing Parameters	Level 1	Level 2	Level 3
LPA (%)	5	10	20
Styrene (%)	0	4	8
Filler (%)	0	20	40
Target gel time (min)	1	3	10
Temperature gradient (°C)	5	10	15
Injection pressure (kPa)	207	414	621

Table 4.3 Definition of resin formulations tested for gel time variations with 10% LPA resin

Formulation	Accelerator (%)	Catalyst (%)	Experiment # (Table 4.5)
1	0.05	0.4	3,5,9,10,13,17
2	0.1	0.8	----------
3	0.15	1.2	----------
4	0.2	1.6	2,4,8,12,15,16
5	0.25	2	----------
6	1	3	1,6,7,11,14,18

Table 4.4 Measured resin gel time (min) for formulations at various isothermal temperatures

Temperature (°C)	Formulation					
	1	2	3	4	5	6
80	29	14	8.8	5.9	3.5	1.8
90	9.9	4.7	3.4	2.6	1.55	1.2
100	3.7	2.75	1.85	1.5	1.3	0.8

Table 4.5 Eighteen experiment L_{18} Taguchi test matrix

Exp. #	LPA level (%)	Styrene (%)	Filler (%)	Gel time (min)	Temperature gradient (°C)	Pressure (kPa)
1	5	0	0	1	5	207
2	5	4	20	3	10	414
3	5	8	40	10	15	621
4	10	0	0	3	10	621
5	10	4	20	10	15	207
6	10	8	40	1	5	414
7	20	0	20	1	15	414
8	20	4	40	3	5	621
9	20	8	0	10	10	207
10	5	0	40	10	10	414
11	5	4	0	1	15	621
12	5	8	20	3	5	207
13	10	0	20	10	5	621
14	10	4	40	1	10	207
15	10	8	0	3	15	414
16	20	0	40	3	15	207
17	20	4	0	10	5	414
18	20	8	20	1	10	621

Table 4.6 Pressure and cycle times for each experiment of Taguchi test matrix

Exp. #	Injection time (sec)	Measured injection pressure (kPa)	Gel time (min:sec)	Time at minimum pressure (min:sec)	Time at maximum pressure (min)	Max. pressure observed (kPa)	Process cycle time (min)
1	45	255	2	13	----	0	15
2	15	462	3	22	----	0	25
3	9	656	14	51	----	0	65
4	10	662	4:30	5	17	1325	27
5	30	262	9	18:30	47	938	77
6	15	414	1:15	3:45	10	1773	15
7	15	469	3	2:15	10	1829	15
8	10	669	3:30	8	18	1725	29
9	35	255	13	24	50	1235	87
10	24	324	13	47	----	0	60
11	9	683	1:10	21	----	0	22
12	20	221	5:30	20:30	----	0	26
13	10	573	13	25	42	1145	80
14	35	207	2:20	2	10	1780	14
15	10	483	3:40	11	21	1691	36
16	46	235	4:45	13	24	1139	42
17	16	518	11	23	40	1835	74
18	8	676	1:20	4	10	2132	16

Table 4.7 Analysis of Variance (ANOVA) in process cycle times and maximum pressure

Factors	**Percent Effect (cycle times)**	**Percent Effect (maximum pressure)**
LPA	0	86.5
Styrene	0	0.5
Filler	0.5	0
Gel time	96	3.4
Temperature gradient	0.25	0
Injection pressure	0.65	2.2
Other/Error	2.6	7.4

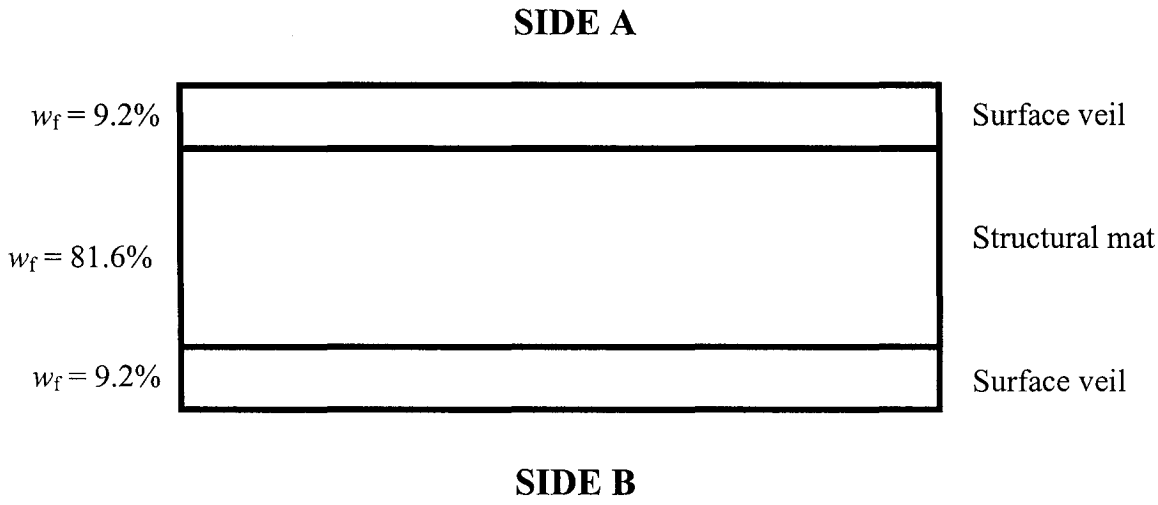

Figure 4.1 Through thickness structure of the F3P glass fiber preform.

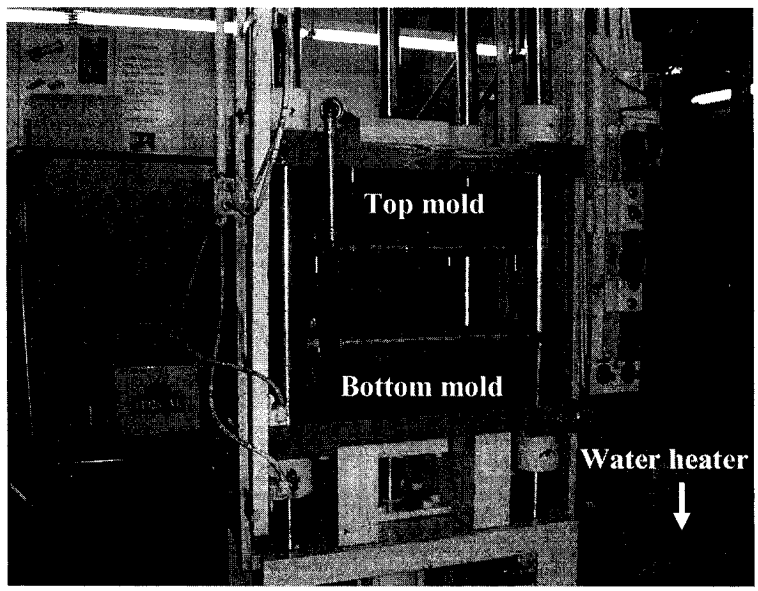

(a)

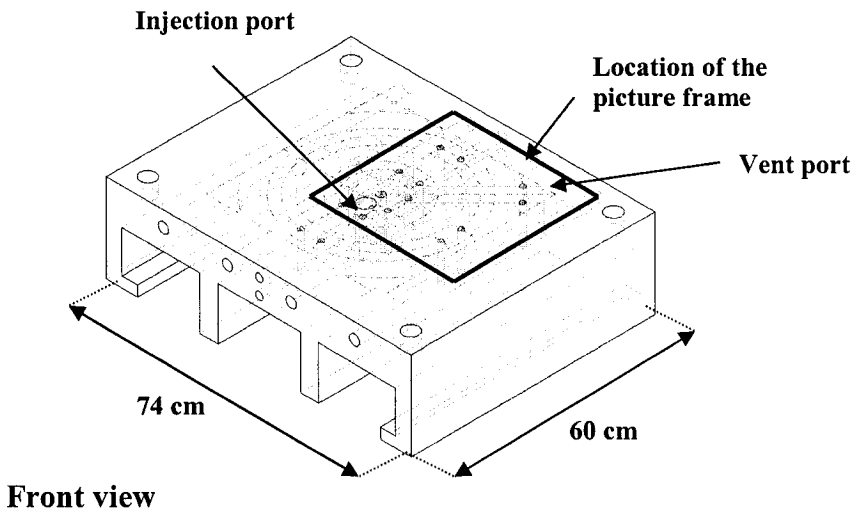

(b)

Figure 4.2 (a) Mold mounting on the press, (b) Diagram of the mold

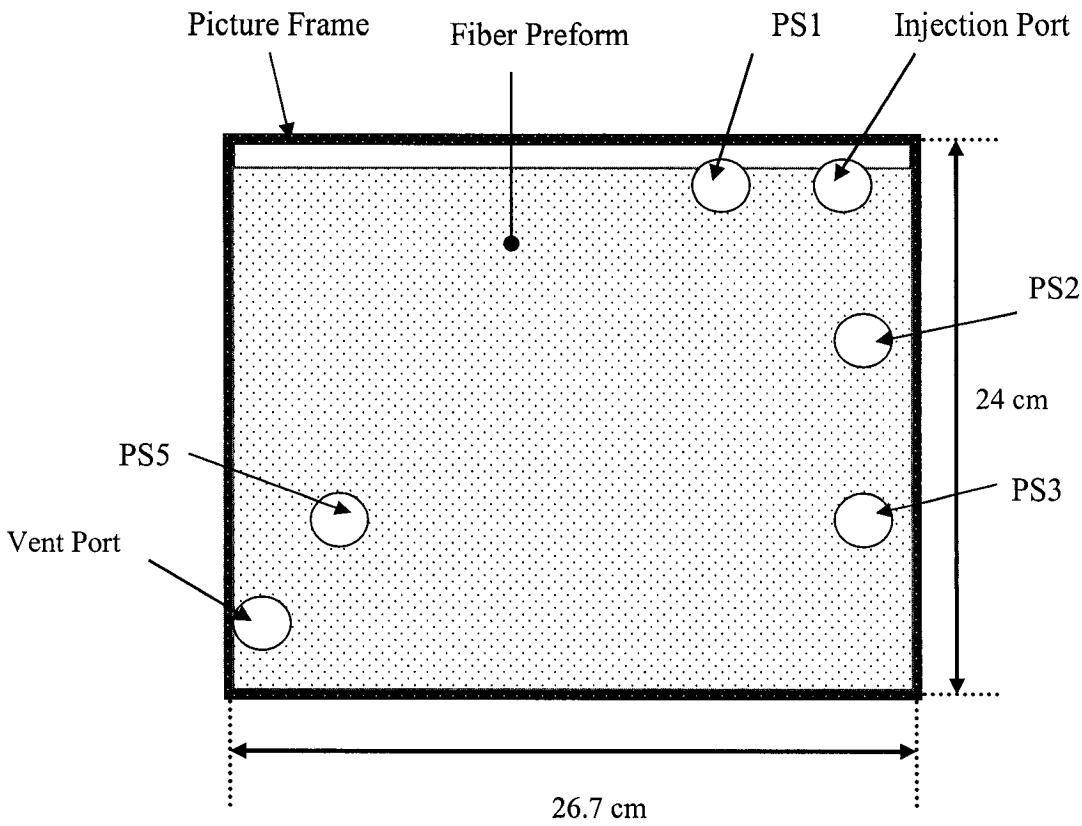

(a)

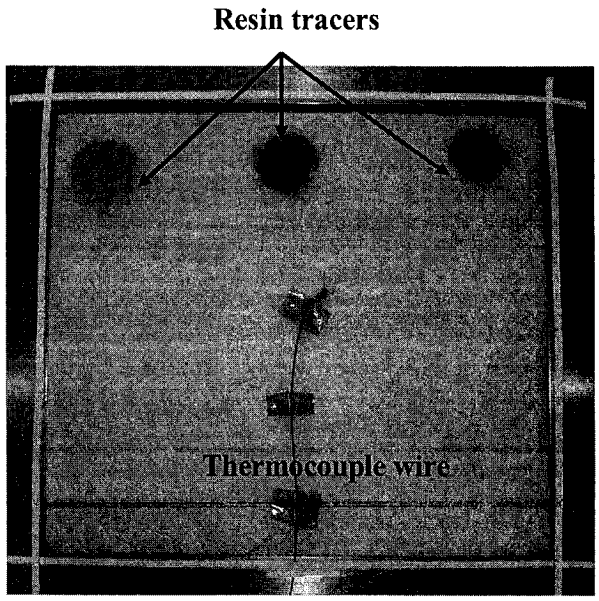

(b)

Figure 4.3 (a) Schematics of the picture frame, injection port, vent port and location of pressure sensors, (b) photograph of the picture frame with preform and sealant

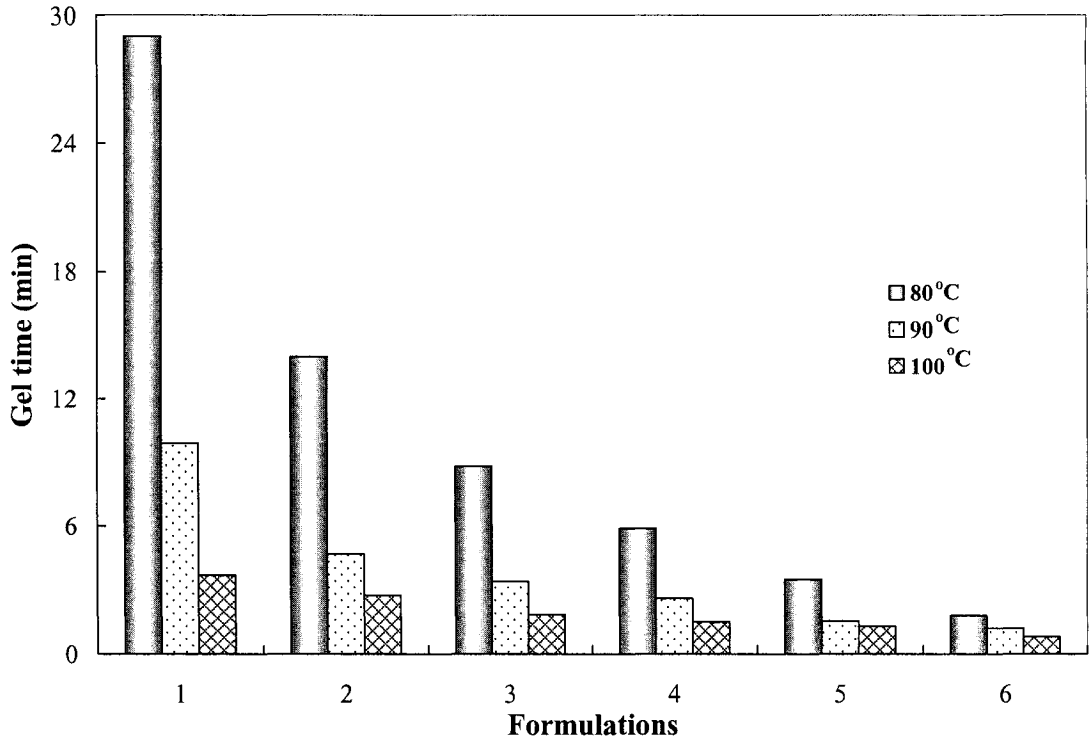

Figure 4.4 The variation in gel time at different isothermal temperatures for the formulations of Table 4.3.

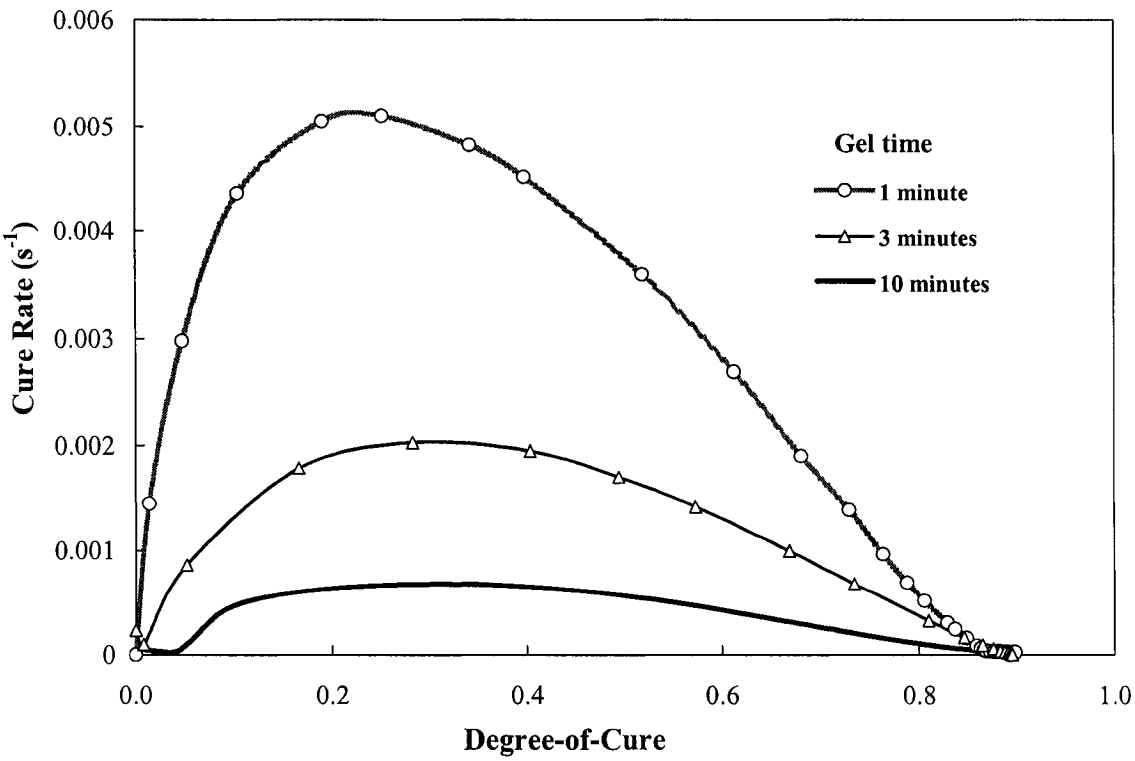

Figure 4.5 The variation in cure rate as a function of degree-of-cure for the formulations to be used in Taguchi Plan under 90°C isothermal cure conditions.

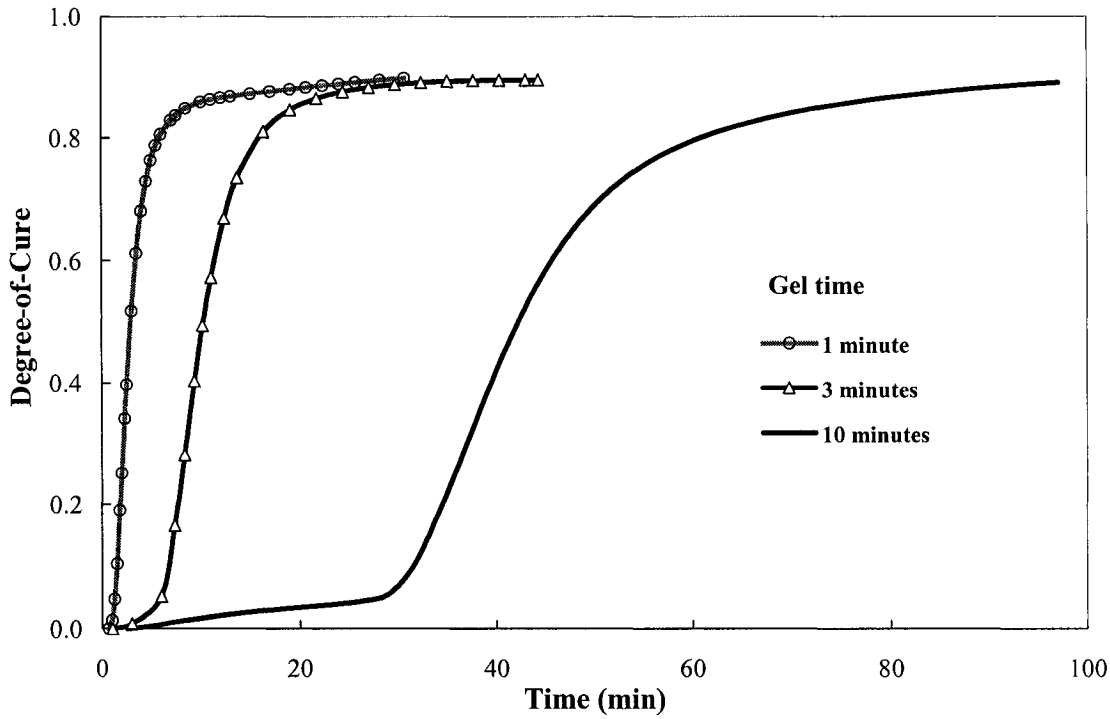

Figure 4.6 The variation in degree-of-cure for the formulations to be used in Taguchi test matrix under 90°C isothermal cure conditions.

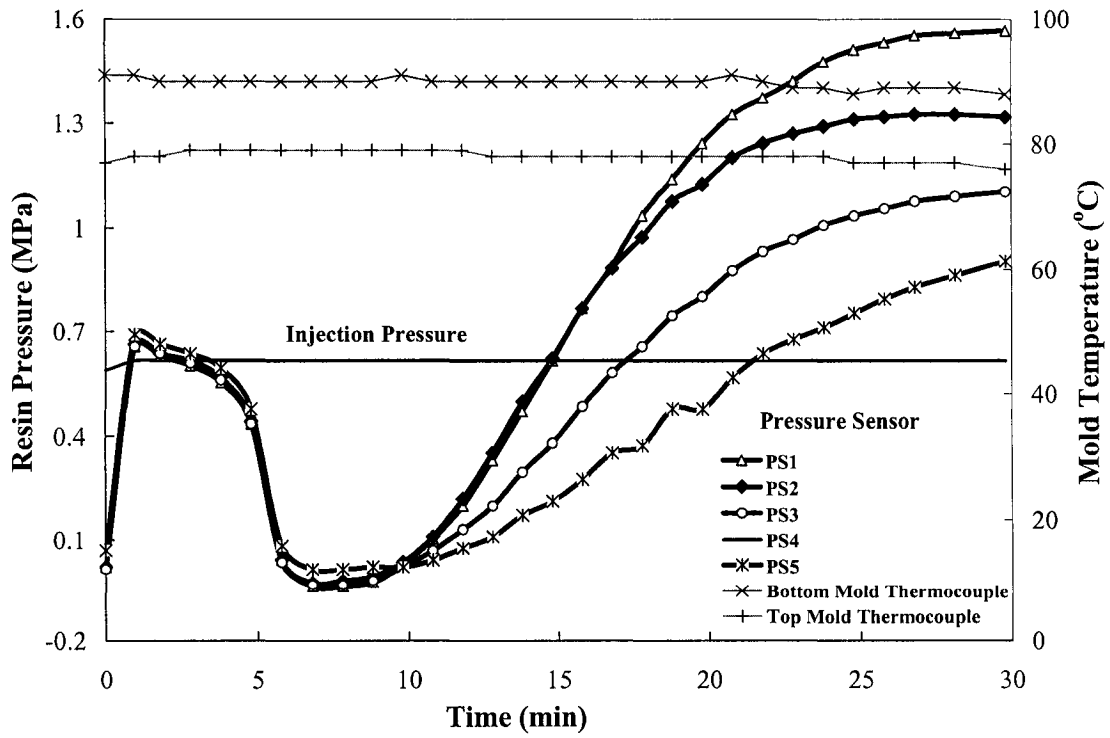

Figure 4.7 Pressure variations during RTM processing with resin containing 10% LPA (experiment # 4).

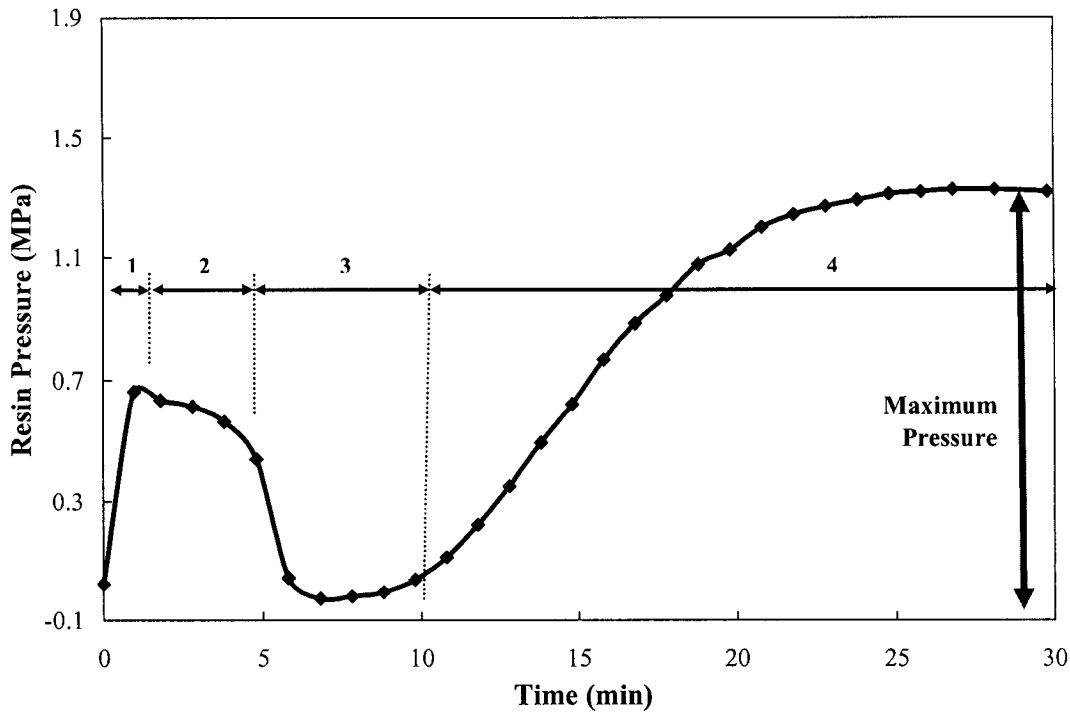

Figure 4.8 Pressure variations during resin injection, clamping, gelation and subsequent curing at sensor location PS2 during experiment # 4.

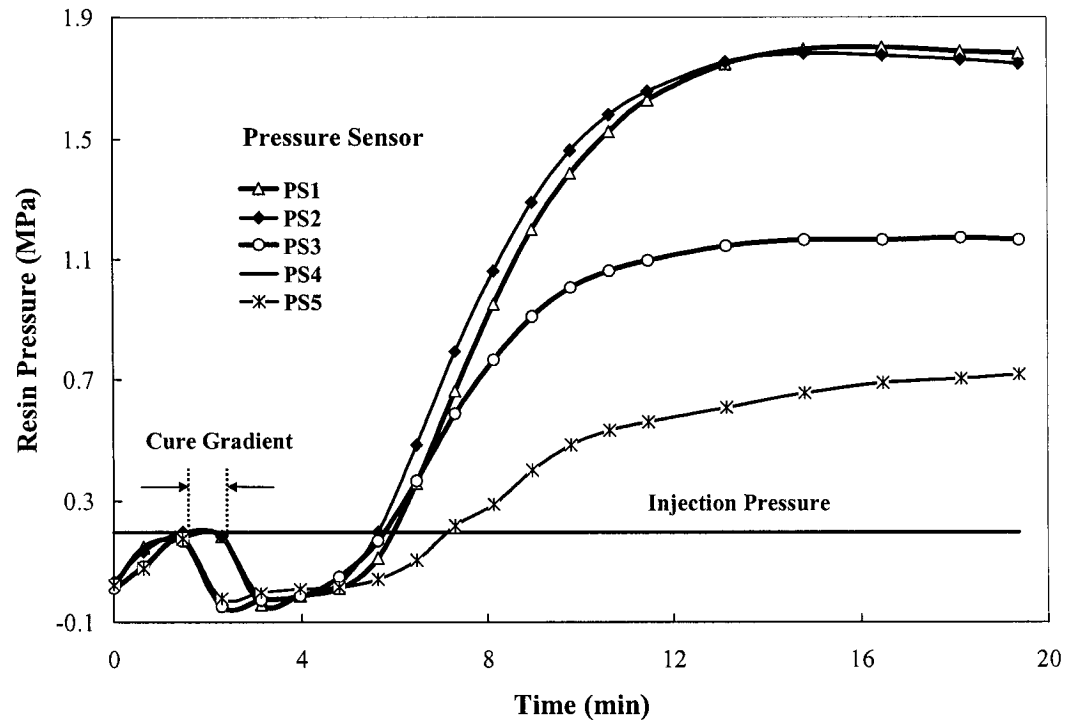

Figure 4.9 Pressure variations during resin injection, clamping, gelation and subsequent curing at all pressure sensor locations during processing of 10% LPA resin with a gel time of 1 minute (experiment # 14).

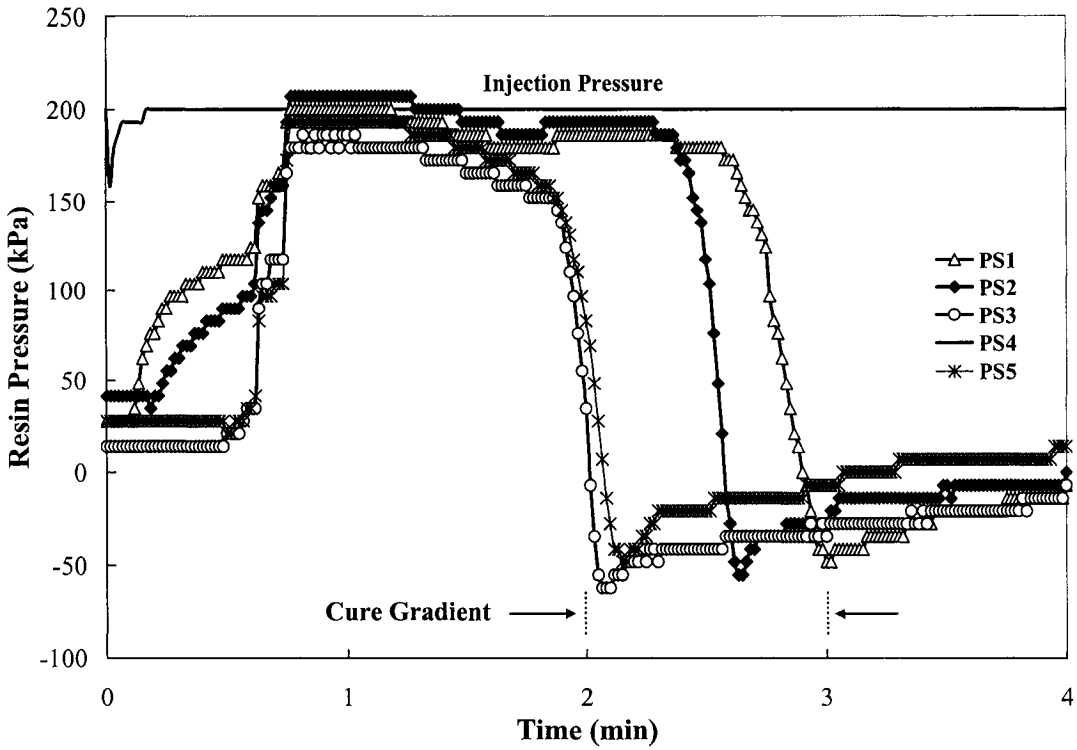

Figure 4.10 Variation in degree-of-cure at different sensor location at low injection pressures for experiment # 14.

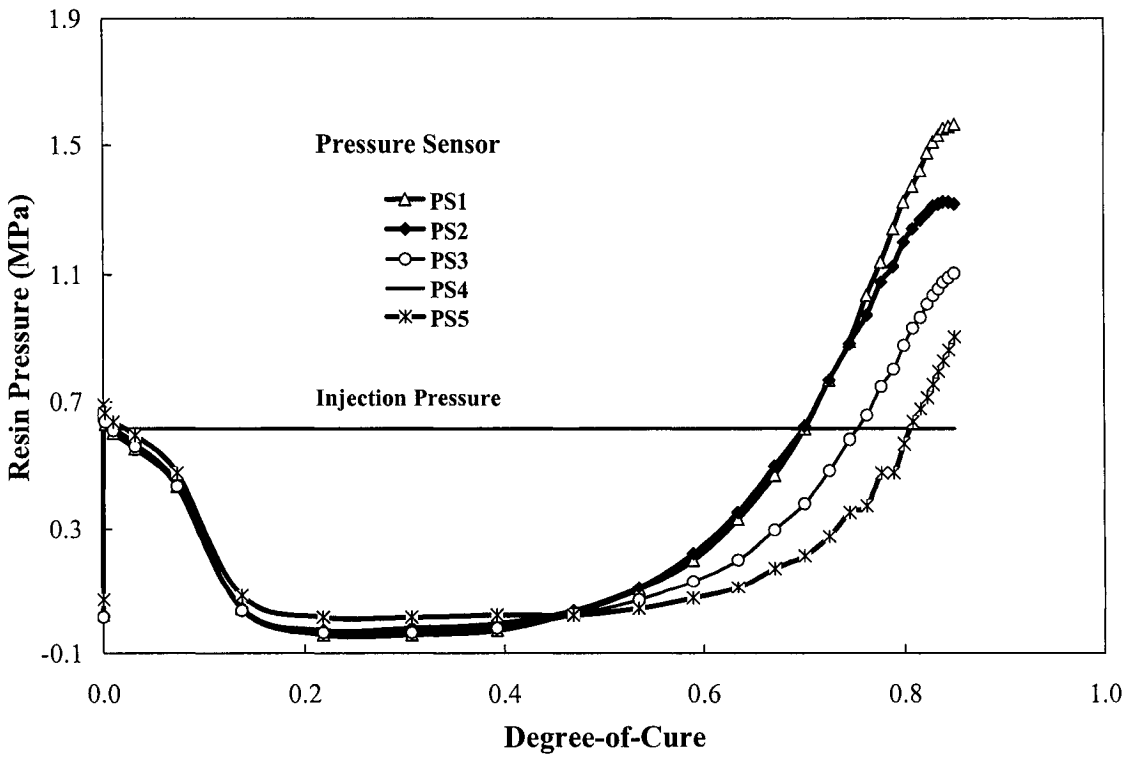

Figure 4.11 Pressure variations at different sensor locations as a function of degree of cure during experiment # 4.

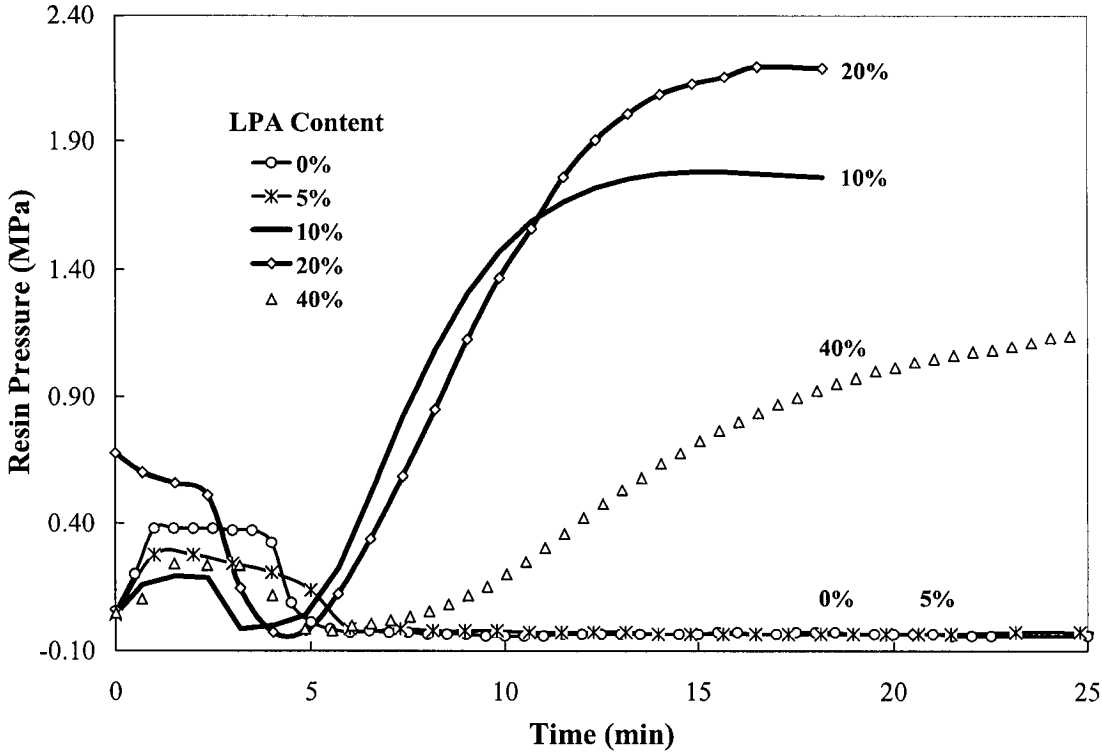

Figure 4.12 Resin pressure variations in different formulations during complete manufacturing cycle.

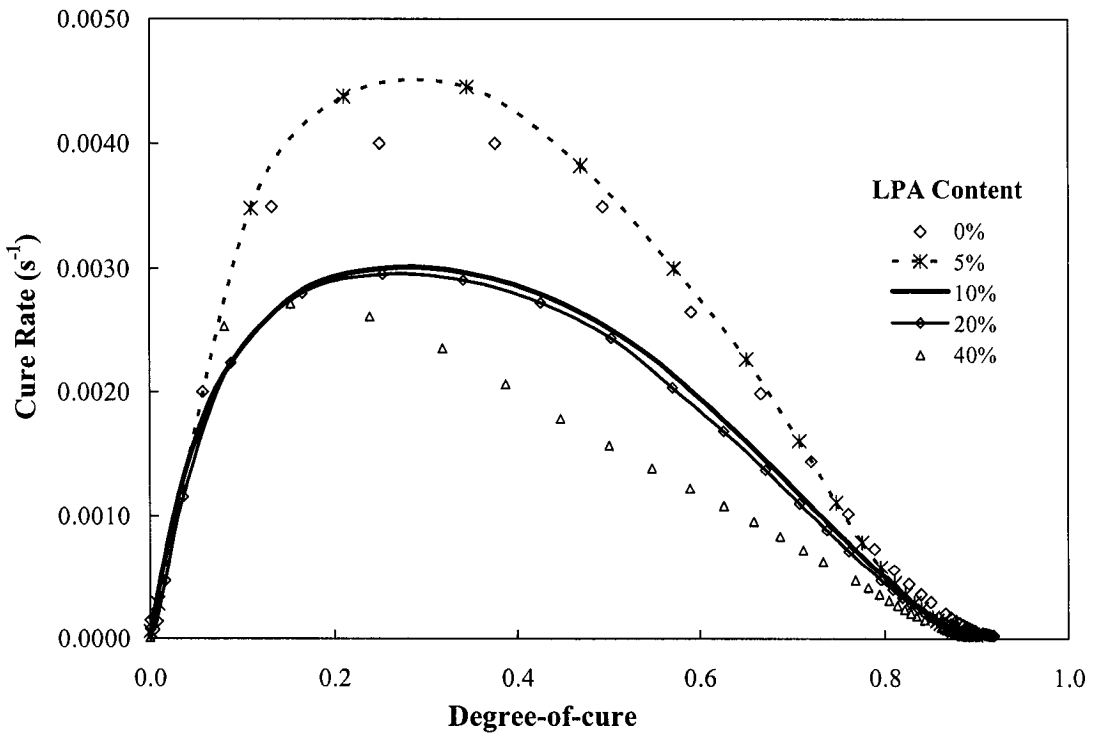

Figure 4.13 Variation in cure rate as a function of degree-of-cure under 90°C isothermal cure adapted from [20].

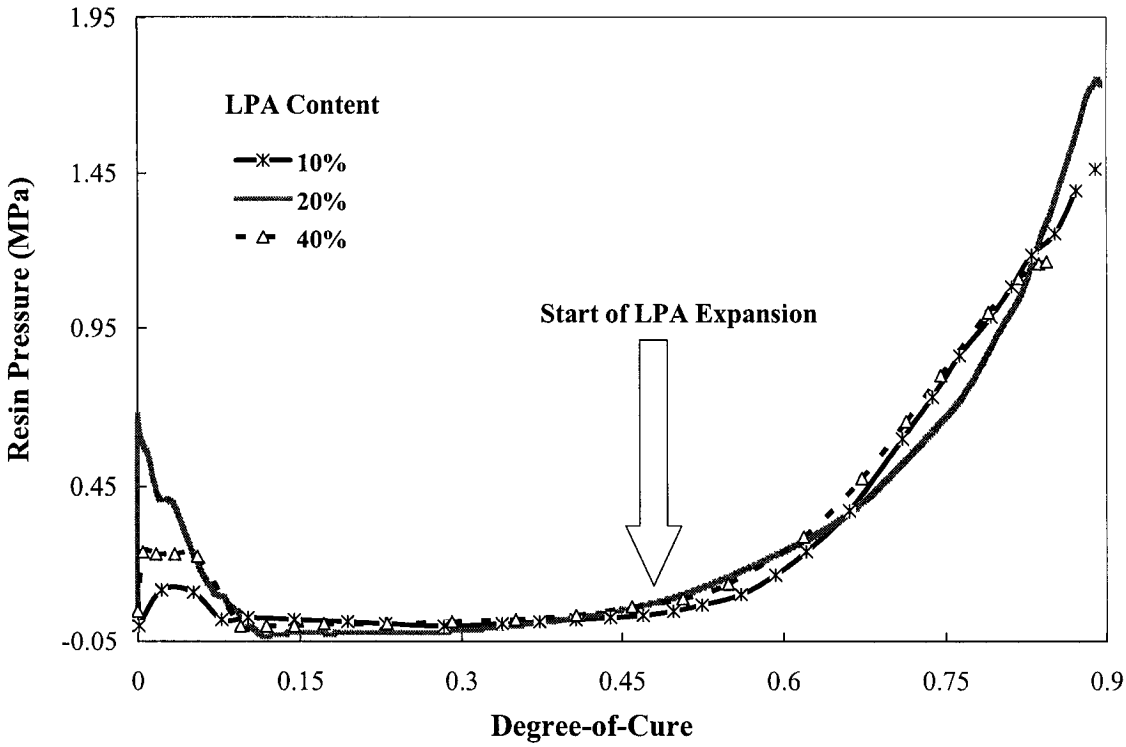

Figure 4.14 Resin pressure variations (in resins with 10, 20 and 40 % LPA) as a function of degree-of-cure for 90oC isothermal temperatures.

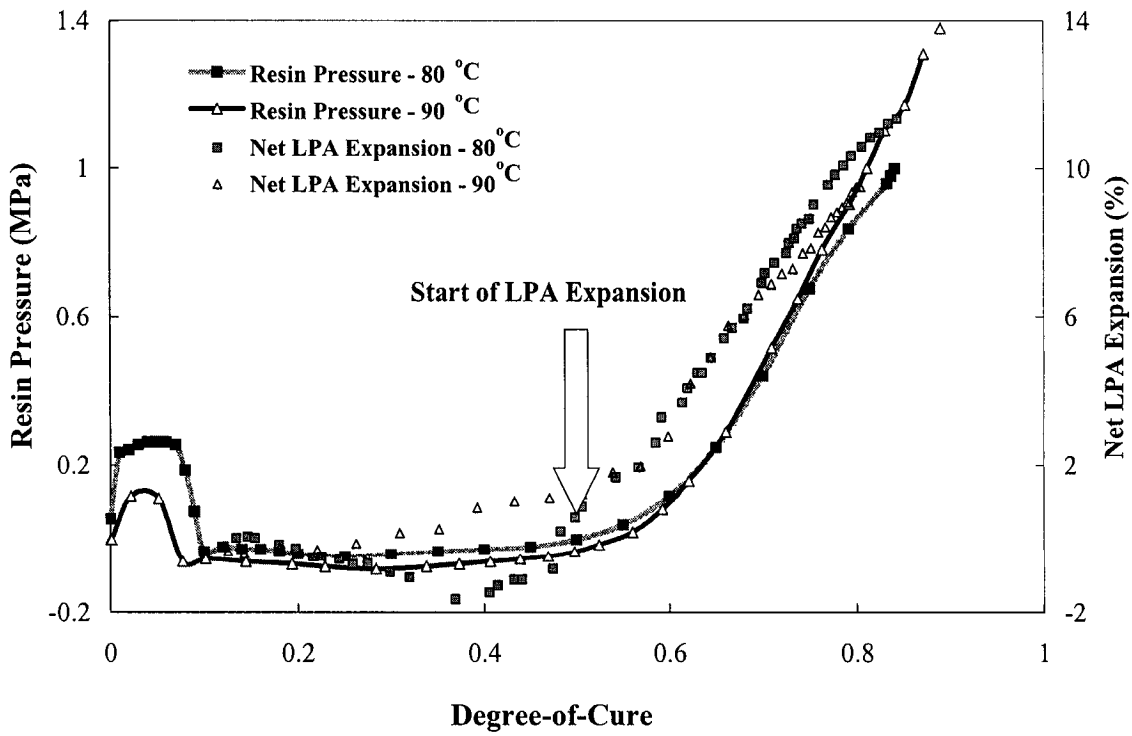

Figure 4.15 Comparison between % dimensional change due to net LPA expansion and pressure variations in 10% LPA resin.

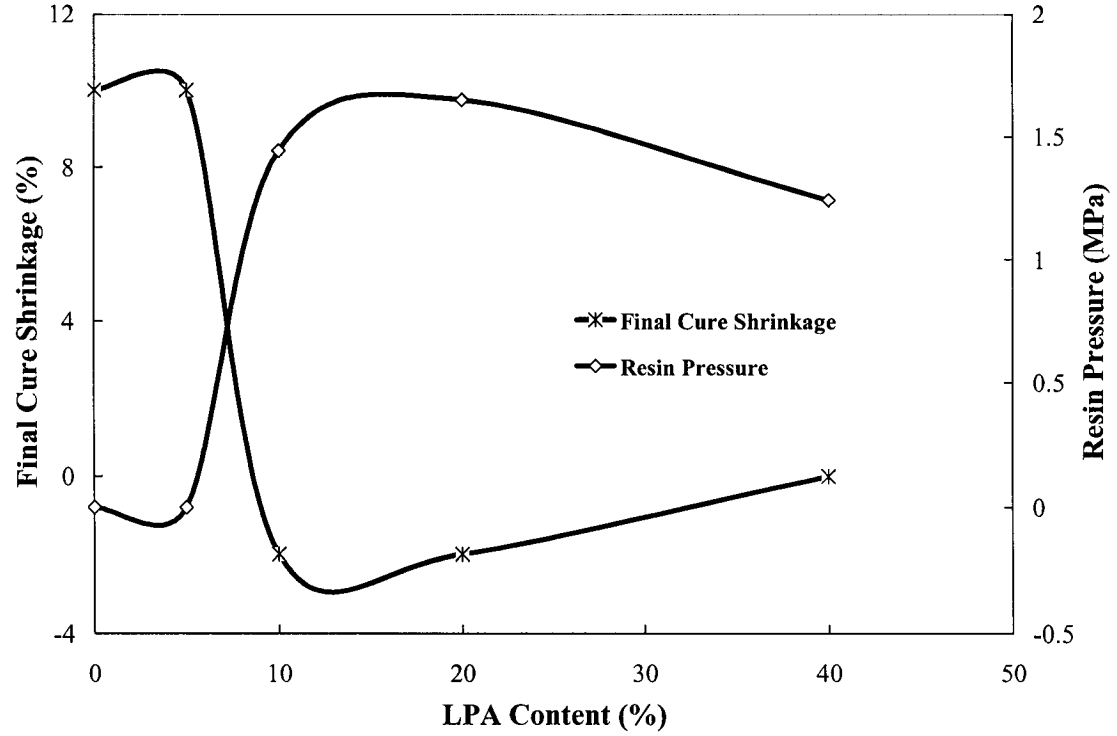

Figure 4.16 Variation in final cure shrinkage and maximum cure pressure as a function of LPA content.

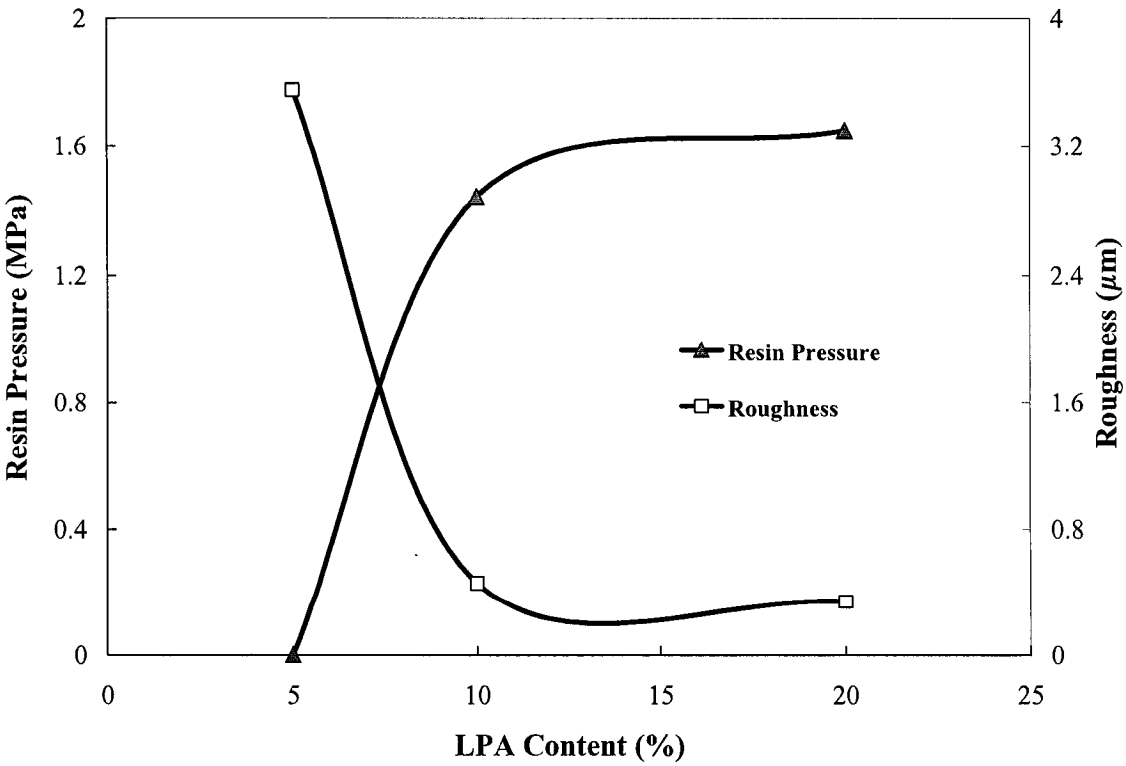

Figure 4.17 The effects of LPA content on the maximum cure pressure and roughness during RTM manufacturing [39].

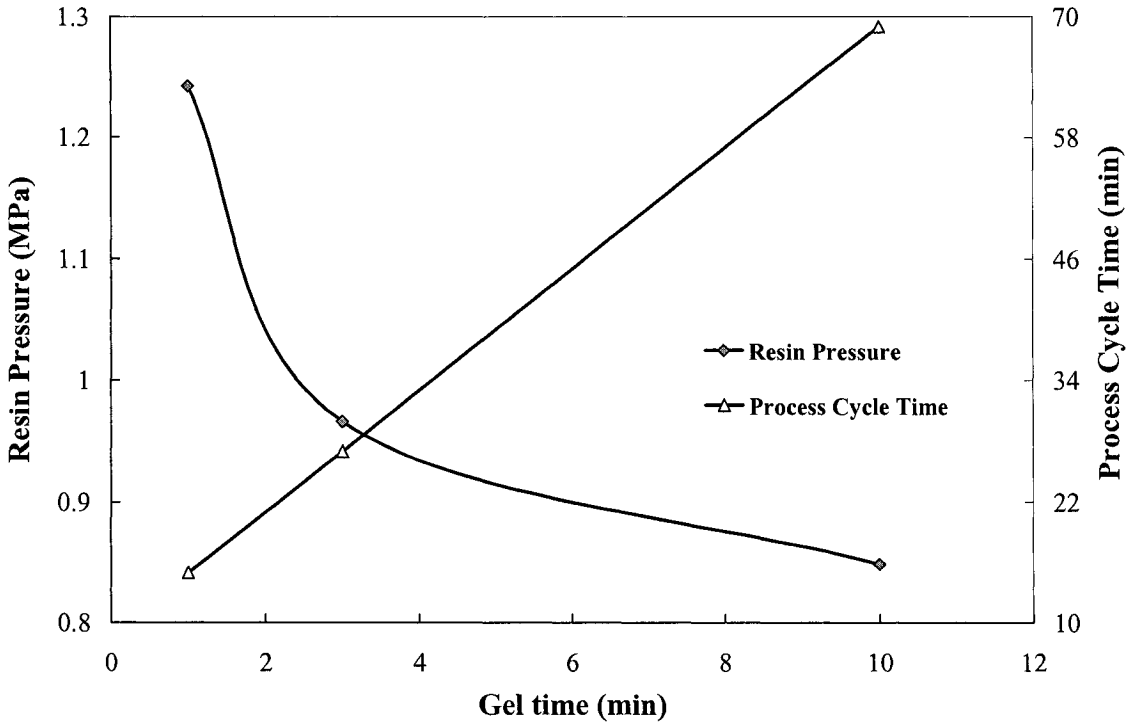

Figure 4.18 The effects of gel time levels on the maximum pressure and process cycle time.

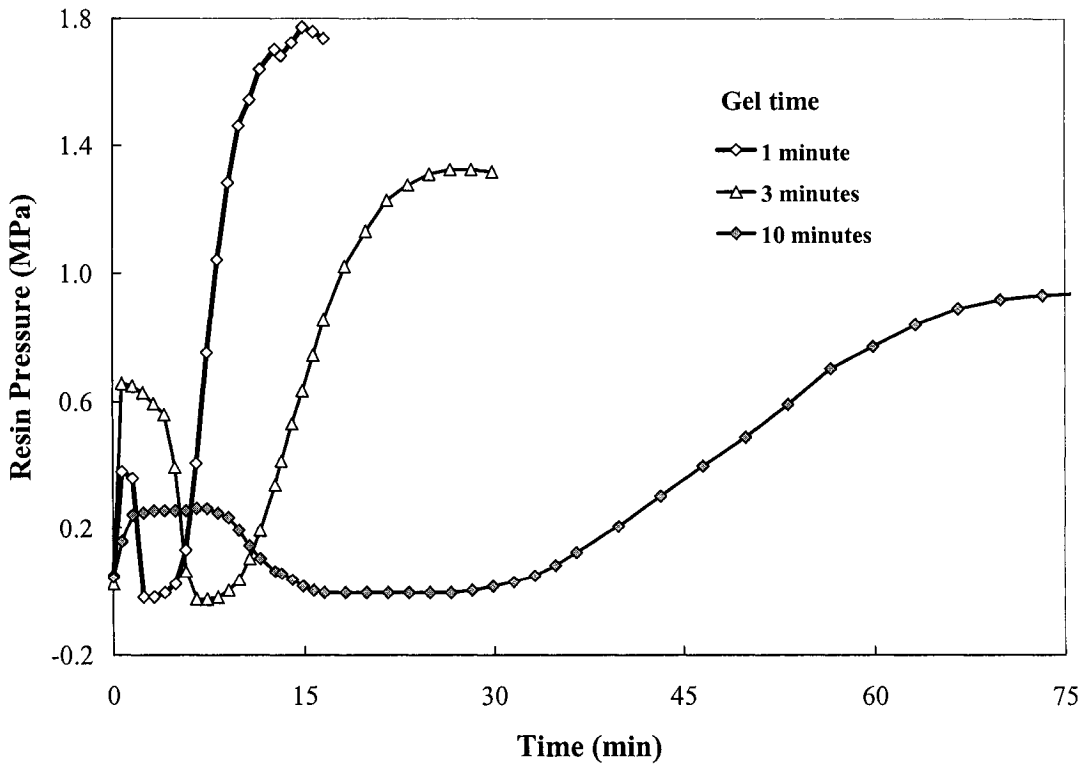

Figure 4.19 The effects of gel time levels on the pressure variations during RTM manufacturing.

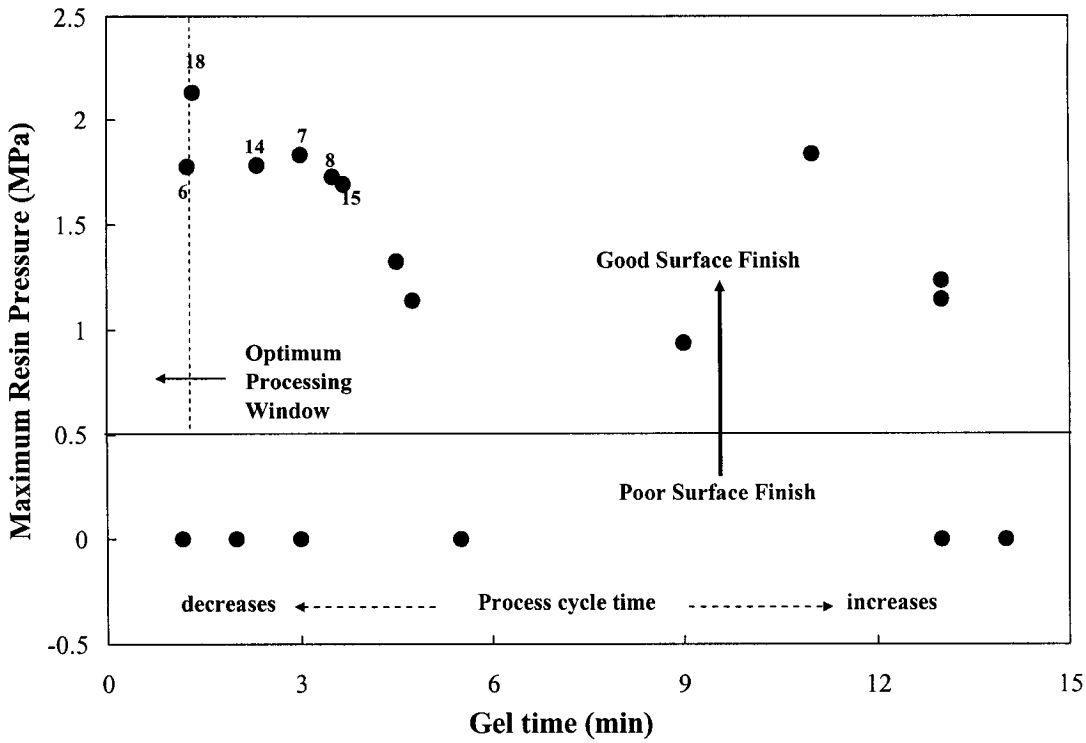

Figure 4.20 Optimum processing window based on the minimum gel times and maximum resin pressures.

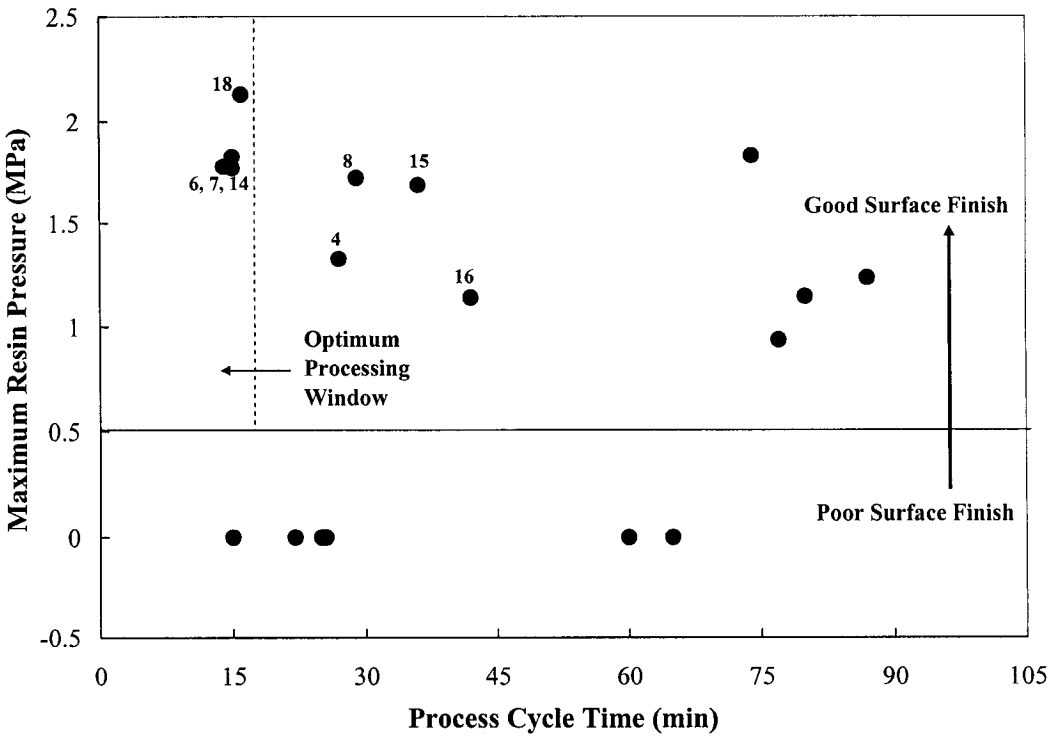

Figure 4.21 Optimum processing window based on the minimum process cycle time and maximum resin pressures.

Link between Material Characterization (chapter 3) and Numerical Simulations (chapter 5)

Based on the analysis of material parameters (chapter 3), models are developed to predict resin flow, resin cure, viscosity variations, resin shrinkage and expansion during processing. These models are then used in RTM numerical simulations to predict resin flow and cure inside the mold cavity. Simulations results are used to design molds and picture frames such that the flow inside the picture frames is uniform and does not result in dry spots and free spaces in the molded components, which potentially affect the surface quality.

Link between RTM Manufacturing (chapter 4) and Numerical Simulations (chapter 5)

RTM manufacturing and numerical simulation chapters of this thesis compliment each other. Numerical simulations predict mold pre-heating, mold filling and resin curing inside the mold cavity. These numerical results are verified with experimental data. Mold pre-heating is monitored by placing thermocouples inside the mold. Resin flow is monitored through pressure sensors and by placing colored tracers on the preform and resin cure is also monitored using pressure transducers. Experimental and numerical results are then compared. The pressure variations observed with resin formulations containing low profile additives during manufacturing are then modeled to predict pressure increase during the cure of resins containing low profile additives. Pressure levels in the experimental test matrix of chapter 4 are chosen based on the flow simulations of chapter 5.

CHAPTER 5

NUMERICAL SIMULATIONS FOR CLASS A SURFACE FINISH IN RESIN TRANSFER MOLDING PROCESS

Mohsan Haider, Eduardo Ruiz, Pascal Hubert*, Larry Lessard

Department of Mechanical Engineering, McGill University

817 Sherbrooke Street West, Montreal H3A 2K6, Quebec, Canada

(Prepared for Composite Science and Technology)

ABSTRACT

During recent years, Liquid Composite Molding (LCM) processes have been widely developed for aerospace, marine, transportation and sporting goods industries. Simulation tools for LCM processes are a key to predict and solve manufacturing issues. Despite the fact that numerical process analyses are commonly used to predict mold filling, resin cure and exothermic temperatures, more comprehensive computational tools are still required. Recent advances in resin additives such as Low Profile Additives (LPA) show a significant impact on process performance and part quality. Modeling of LPA resins and the integration of such models into numerical tools is a key to broaden the scope of computational analyses of LCM processes. In this work, mold pre-heating experiments were compared to numerical predictions using a commercial simulation software.

* Corresponding author:
E-mail: pascal.hubert@mcgill.ca
Tel.: 1(514) 398-6303

Colored tracers were used to follow the resin flow evolution along the mold cavity. Non-isothermal simulations were then carried out and the predicted flow evolution was compared to experiments. Numerical and experimental resin degree-of-cure evolution was also compared. Finally, a volume change model, previously developed, was implemented in this work to calculate mold pressure increases in RTM with low profile resins. Numerical predictions were compared to the results from the mold pressure transducers in the mold cavity. Results showed that the numerical code could be used accurately to predict mold pre-heating, cavity filling and curing behavior of low profile resins during RTM processing. Simulation results matched closely with the experimental results. Pressure evolution of low profile resins was found to be very sensitive to the model parameters.

Keywords: B. Modeling B. Rheological properties, E. Resin transfer molding, E. Computational simulation

---

5.1 Introduction

Advanced composite materials are well known for their superior structural performance. Potential benefits are lightweight, superior stiffness, strength, corrosion resistance and good design flexibility. Liquid Composite Molding (LCM) manufacturing techniques, which include Resin Transfer Molding (RTM), are attractive to the automotive industry because of low cost, good mechanical performance and part reproducibility in relatively short cycle times. However, there are several process-related problems associated with the use of these manufacturing techniques. Improper mold filling because of inadequate mold design can result in dry spots, void formation and poor surface quality. Lack of knowledge about cure kinetics results in longer cycle times, higher manufacturing costs and poor part quality. Numerical simulations of LCM processes, which can predict mold pre-heating, cavity filling and resin curing during isothermal and non-isothermal cycles,

have great potential to reduce and even eliminate process related problems, and reduce costs by avoiding tedious trial-and-error methods.

RTM process simulation issues have been addressed by many researchers. Martin et al. [1] modified a finite element code to develop a computer model for simulating resin flow front progression inside a 2D RTM mold. Based on this work many researchers have researched mold filling and pressure distribution under isothermal conditions for complex geometries, including 2D and 3D. Bruschke et al. [2] developed a numerical code based on finite elements and control volume to predict the flow pattern in anisotropic media. They also studied the effect of an anisotropic preform, inserts in the mold cavity and mold thickness on the flow pattern. A computer code was developed by Friedrichs et al. [3-4] to simulate 2D resin flow based on boundary-fitted finite difference techniques and a stream function formulation. Dessenberger and Tucker [5] also simulated the non-isothermal filling process of center-gated disk shape mold. Numerical simulation of 3D mold filling in RTM was carried out through quasi-steady state and partial saturation formulations by Shojaei [6]. Numerical schemes were evaluated by comparison with analytical solutions for simple geometries and good agreement was observed. A semi-empirical model was suggested for macro and micro impregnation of fibers during filling based on Darcy's law and capillary effects by Lekakou and Bader [7].

The effect of stacking sequence of the fiber mat and inlet pressure on the flow front position and its comparison with experimental results was done by Young et al. [8] with 2D and 3D numerical models based on control volume and finite element methods. A good agreement was reached between numerical and experimental results in two-dimensional models; however imperfections were observed for thick parts. This research also established the relationship between position of injection port and vent port with flow fronts and maximum pressures observed during injection. Boccard et al. [9] also developed models to determine optimum gate location and predict filling time for the RTM process. Young [10] also attempted to optimize the location of the inlet gate based on a generic algorithm to minimize the mold filling pressure, uneven filling pattern and temperature difference during the filling process. Another study from the same author

[11] was performed to simulate flow, heat and mass models in a three-dimensional space and obtain conversion, temperature and pressure distributions in all three directions.

PAM-RTM [12] previously known as RTMFLOT is a numerical code developed by Trochu et al. [13-14] based on non-conforming finite element methods. This method simplified the numerical calculation procedure. Gauvin et al. [15] used this code to study the position of flow front through multi-layer fiber reinforcement for 3D isothermal flow and reasonable agreement was obtained with experimental results. Recent efforts in the area of RTM simulations include prediction of edge effects. Hammami [16] developed geometric models to predict edge effects based on Navier-Stokes equations and equations based on Poiseuille flow. Lin et al. [17] simulated a cycle of the RTM process and found that heat conduction from the mold wall had a significant effect on temperature and conversion distributions in the mold filling and curing stages. They also observed that conversion near the mold wall was higher than that of the nearby center during filling stage and the early part of the curing stage. At a later time in the curing, the conversion near the wall was observed to become lower due to lower temperature. Mathematical modeling and numerical simulation of the RTM process cycle was also carried out by Antonelli and Farina [18] based on Lagrangian formulation and saturation functions. The code was found to be very effective in predicting injection time, injection pressure and residual strains in the preform. A review of RTM modeling and simulation approaches present in the literature is given by Shojaei et al. [19].

Despite the great deal of existing work in the area of LCM numerical simulations, there is need for more detail-oriented studies and development of computational tools for the resin transfer molding (RTM) process since a comprehensive and complete numerical simulation software for RTM is still absent. Advancements in resin technology and particularly the introduction of resins with low profile additives (LPA) have strengthened this need. LPA are thermoplastic additives, which are added to styrene-based polyester and vinylester resins. LPA compensate for resin shrinkage by phase separation and micro-void formation. This mechanism is reported in detail elsewhere [20]. Low profile based resin systems are increasingly used in the RTM process and hence the development

of mathematical and numerical tools to predict shrinkage-expansion behavior of these resin systems during curing and their integration with already existing numerical codes has become an essential objective to widen the scope of numerical modeling and simulation of RTM by including a broader range of resin systems. Also, there is a need to validate already existing numerical codes with the experimental data for the mold pre-heating, filling and curing stages. Unfortunately, the behavior of low profile resins is not well understood and models to predict low profile resin behavior are non-existent. The purpose of this study is to incorporate mathematical models, developed in a previous study [20], into an already existing software to simulate LPA behavior during actual manufacturing

In this paper, PAM-RTM software was used to study the pre-heating behavior of a steel RTM mold. Simulated and experimental results were compared to validate the numerical predictions. The resin flow during injection was observed by placing traces on the dry fiber preform. Numerical and experimental resin flow patterns, injection times as well as pressure variations during injection were compared. Variations in degree-of-cure, temperature and pressure during the cure cycle were also studied during non-isothermal processing. Finally, volume change models developed in a previous work [20] to predict the low profile resin shrinkage-expansion behavior during cure were incorporated into the software to predict pressure variations caused by LPA action during cure. Finally, a comparison was carried out between measured and predicted mold pressure variations during the cure of a low profile resin.

5.2 Manufacturing Setup

Composite plates were manufactured using a heated steel mold mounted on a hydraulic press. The mold had a mirror like polished finish and was instrumented with type J thermocouples and Dynisco PT422 pressure sensors connected to a Vishay's System 6000 data acquisition system. The mold platens were heated to the required temperatures with a Conair circulating water heating system. The picture of the mold with its mounting on the press is shown in Figure 5.1. The resin at room temperature was injected into the

mold cavity with a Radius Engineering constant pressure pneumatic-controlled injector. The 3.175 mm thick picture frame was sealed using a Gore-Tex joint sealant gasket. A temperature gradient was created by moving the top and bottom platens away from each other and setting them at two different temperatures (in a range from 75°C to 90°C). The bottom mold was always kept at 90°C whereas the temperature of the top mold was adjusted to achieve the required gradient. The 24 cm by 26 cm F3P glass fiber preform was cut and placed inside the mold just before injection. Side-A of the preform was placed towards the hottest mold platen. The injection and vent ports were designed to create a uniform linear flow front though the fiber preform. The pressure sensors (referred as PS1, PS2, PS3 and PS5) were located near the injection and vent ports and PS4 was mounted on the injection pump to measure injection pressure. The injections were performed at different injection pressure levels ranging from 200 to 650 kPa. The mold surfaces were cleaned with acetone and coated with a single layer of Chemlease 41-90 mold release agent. Manufactured composite panels were kept inside the mold until the resin achieved the maximum pressure level. A schematic and photograph of the picture frame, fiber preform, injection port, vent port and location of the pressure sensors (PS) is given in Figure 5.2. Resin tracers were used to verify the uniformity of the flow front.

5.2.1 Permeability Measurements

The permeability of the F3P preform was measured experimentally. Figure 5.3 shows a typical experimental setup for unidirectional permeability measurement. A layer of fiber preform was cut with a length of 40 cm, a width of 10 cm and a mass of 70 grams. Mold spacers were placed at a thickness of 3.2 mm to obtain a fiber volume fraction of 0.21. Surface density of the mat was calculated based on the mass and area of the fiber mat. The cavity was transparent and photo cells were used to record the flow front positions. Silicone oil was pumped into the mold cavity at a constant pressure of 39 kPa. Other process parameters are given in Table 5.1. Precautions were taken to ensure a constant cavity thickness and to prevent edge-flow racing effects. The oil took an estimated 400 seconds to flow through the fibers which resulted in an average velocity of

1mm/sec. Darcy's flow equation (Equation 5.1) was used to calculate permeability of the fiber preform:

$$[K] = \frac{\mathbf{V}\mu}{\Delta P} \tag{5.1}$$

where V is the velocity of resin flow front, K is the permeability, ΔP is the pressure gradient and μ is the resin viscosity. Pressure gradient is a measured quantity, whereas resin viscosity and velocity are found experimentally. A nominal value of 4.163×10^{-10} m^2 was found for in-plane permeabilities K_1 and K_2 through this experimental procedure by taking into account small pressure variations during this experiment.

5.2.2 Material Properties

The RTM mold used in this work was made of 1.5% carbon steel. Thermal and physical properties of the mold used in numerical analysis are given in Table 5.2. Scott Bader's PD9551 polyester resin [21] with and without LPA was used for RTM manufacturing. Thermal and physical properties of the resin used in simulations are given in Table 5.3. A glass fiber mat preform was used for which permeabilities were measured in a previous work [22]. The fiber properties used in the computational analysis are given in Table 5.4. A kinetic model of resin cure was also developed for a low profile polyester resin [20]. The cure kinetics model is given in Equation 5.2 and the model parameters are listed in Table 5.5.

$$\frac{d\alpha}{dt} = \left(K_1 + K_2 \alpha^m\right)\left(\alpha_{\max} - \alpha\right)^n \tag{5.2}$$

$$K_i = A_i \exp\left(-\frac{E_i}{RT}\right) \quad i = 1,2$$

where α is the degree-of-cure, α_{max} is the maximum degree-of-cure achieved in an isothermal scan, R is the ideal gas constant, T is the temperature, E_1 and E_2 are activation energies, A_1 and A_2 are the Arrhenius constants and m and n are kinetic exponents. The model parameters presented in Table 5.5 were obtained from fitting the measured rate of cure using a linear regression. Viscosity variation models were also developed and were used in simulations to predict changes in resin viscosity during resin filling and curing. Viscosity variation model is given in Equation 5.3 and its estimated parameters are listed in Table 5.6.

$$\eta(\alpha,T)=\eta_O(T)\left(\frac{\alpha_G}{\alpha_G-\alpha}\right)^{(C_1+C_2\alpha)} \tag{5.3}$$

where $$\eta_O(T)=B\exp\left(\frac{T_b}{T}\right)$$

where $\eta_O(T)$ is the viscosity at a given temperature, T is temperature in Kelvin, α is the degree-of-cure, α_G is the degree-of-cure at gelation, and T_b, B, C_1 and C_2 are model parameters obtained from linear regression techniques. The shrinakge of the neat polyester resin was also measured through a procedure presented in [20]. Models were developed to predict resin shrinkage behavior as a fuction of degree-of-cure. The shrinkage model is given in Equation 5.4.

$$\begin{aligned}\left(\frac{\Delta V}{V}\right)_{Shrinkage}&=\left(\frac{\alpha-\alpha_G}{\alpha_M-\alpha_G}\right)\left(\frac{\Delta V}{V}\right)_{Total}\left(1-V_{Filler}\right) \quad \alpha_G<\alpha<\alpha_M\\ \left(\frac{\Delta V}{V}\right)_{Shrinkage}&=\left(\frac{\Delta V}{V}\right)_{Total}\left(1-V_{Filler}\right) \quad \alpha\geq\alpha_M\end{aligned} \tag{5.4}$$

where α is the resin degree-of-cure, α_G is the degree-of-cure at gelation; α_M is the degree-of-cure corresponding to the total cure shrinkage and V_{filler} is the volume fraction of filler in the resin. For the neat resin α_G is 0.05, α_M is 0.8 and $(\Delta V/V)_{Total}$ is 0.095.

Low profile additives are usually added to polyester resins to compensate the polymerization shrinkage. A certain amount of LPA is needed to compensate the chemical shrinkage of the resin [20]. The shrinkage-expansion behavior of low profile resin was modeled using rheological techniques. The model of combined shrinkage-LPA action is given by Equation 5.5. This model was seen to adequately predict the shrinkage and expansion behavior of a low profile resin as a function of degree-of-cure. The model parameters are obtained from experimental values. The model is given in Equation 5.5 and its parameters are listed in Table 5.8.

$$
\begin{aligned}
\left(\frac{\Delta V}{V}\right)_{Shrinkage} &= 0 \quad \alpha \le \alpha_G \\
\left(\frac{\Delta V}{V}\right)_{Shrinkage} &= \left(\frac{\alpha - \alpha_G}{\alpha_C - \alpha_G}\right)\left(\frac{\Delta V}{V}\right)_{TSH} \quad \alpha_G < \alpha < \alpha_C \\
\left(\frac{\Delta V}{V}\right)_{Shrinkage} &= \left(\frac{\alpha - \alpha_C}{\alpha_M - \alpha_C}\right)\left(\frac{\Delta V}{V}\right)_{TEX} + \left(\frac{\Delta V}{V}\right)_{TSH} \quad \alpha_C < \alpha < \alpha_M \\
\left(\frac{\Delta V}{V}\right)_{Shrinkage} &= \left(\frac{\Delta V}{V}\right)_{TEX} + \left(\frac{\Delta V}{V}\right)_{TSH} \quad \alpha \ge \alpha_M
\end{aligned}
\tag{5.5}
$$

$(\Delta V/V)_{TSH}$ corresponds to the shrinkage of this resin and $(\Delta V/V)_{TEX}$ corresponds to the gross LPA expansion. α_C is the degree-of-cure of low profile resin at the point where resin shrinkage stops and expansion starts. Parameters in Equation 5.5 are estimated from experimental results and are listed in Table 5.8. This combined model predicts resin's shrinkage and expansion behavior as a function of degree-of-cure.

5.3 Results and Analysis

5.3.1 Pre-heating simulations

As shown in Figure 5.4, a detailed 3D CAD model was created with I-DEAS to the same dimensions as that of the actual mold. The water channels, shown by four holes, were set at the experimental temperature for each mold platen. The bottom mold platen was heated at relatively higher temperature than the top mold platen to induce a temperature gradient though the part thickness. Figure 5.5 shows the meshed model of both mold platens including the composite plate. A forced convective heat transfer coefficient of 12455 $W/m^{2o}C$ was used for heating channels. This coefficient was calculated based on the flow rate and diameter of the channels. A free convective heat transfer coefficient of 7 $W/m^{2o}C$ was used for all the nodes in contact with free air. The four boundary conditions applied for the pre-heating simulation are shown in Figure 5.6. As shown in Figure 5.7, four thermocouples were placed in the experimental set-up in order to follow the temperature gradients. The bottom mold platen was heated at 80°C and the top platen at 70°C. In the experiment both mold platens were heated for two hours before injection, however a uniform temperature distribution was observed after one hour. Pre-heating simulations were carried out under identical boundary conditions. Figure 5.8 shows experimental and numerical results of thermocouples 1 and 2 located at the bottom mold platen. Since thermocouple 1 was placed on the heating channels of the bottom mold, it showed a relatively faster increase in temperature compared with thermocouple 2; whereas thermocouple 2 took longer time to reach an equilibrium state. The same phenomenon was observed for the thermocouple on the top mold platen. As can be seen from Figure 5.8 and 5.9, the temperature evolution is almost identical for the sensors on both mold platens, which means that temperature evolution depends only on the location of the sensor irrespective of the isothermal temperature level. The fluctuations in the experimental temperature values in early stages of mold heating arise from minute variations in the water temperature and flow rate. Figure 5.10 depicts the simulated unsteady temperature distribution during pre-heating. As can be seen from Figure 5.10 (h), the whole mold does not reach the desired temperature after one hour, however since

the picture frame is placed between the four heating channels, it is not necessary for the rest of the mold to reach isothermal temperature level.

5.3.2 Non-Isothermal Filling Simulations

A non-isothermal filling simulation was carried out for the square picture frame shown in Figure 5.2. The purpose of filling simulations is to predict resin flow pattern inside the fiber preform, predict filling times and provide initial conditions for a hydrostatic cure pressure simulation. Figure 5.11 depicts the finite element mesh used for this simulation showing the injection port, vent gate, the resin channel and the placement of the fiber preform. The resin channel (with a width of 8 mm) was designed in the picture frame to obtain a linear resin flow through the fibers. Non-isothermal injections were done under constant injection pressures (in a range from 200-650 kPa). A temperature gradient of $10^{o}C$ was also considered between the top and bottom mold platens. Material properties listed in section 5.2.2 were used for filling and resin curing simulations. In the experimental set-up, colored tracers (represented by colored spots on the preform in Figure 5.2) were used to monitor the resin flow evolution during injection. As the resin passed through these colored spots, the tint particles also flew with the resin and left a trace on the surface of the cured composite plate. A straight line flow pattern was observed on all the tested injections as can be seen in Figure 5.12. The simulated resin flow during a non-isothermal injection at an injection pressure of 345 kPa is shown in Figure 5.13. As can be seen from Figure 5.13, the resin flows through the preform in a linear fashion. The flow front was found to be a straight line for low pressure injections. The flow pattern is also similar to that of the one shown in Figure 5.12. Hence, it can be deduced from this Figure that the flow front predictions obtained with the simulation software are quite accurate.

Various injections were performed at different injection pressures from 200 to 700 kPa. Filling simulations were also carried out for each injection pressure level. The measured and predicted injection times are plotted in Figure 5.14. An error of less than 10% was found between the predicted and measured filling times. As can be seen from this graph,

the injection time decreases (from 50 to 10 seconds) with increasing injection pressure levels (from 200 to 700 kPa). As the resin flows through the fibrous reinforcement, the mold pressure on a fixed location in the mold cavity rises after the resin passage. Three pressure transducers were placed into the mold cavity to record the resin pressure evolution (see Figure 5.2(a)). In Figure 5.15, a comparison between experimental and numerical pressure evolutions is presented for an injection pressure level of 345 kPa. A close match between measured and predicted values can be observed at the three positions along the mold cavity. As can be seen from Figure 5.15, the pressure at sensor locations (PS1 and PS2) closer to the injection port increases gradually; whereas the pressure at sensor locations (PS3) closer to vent ports increases sharply. This is due to the fact that no pressure is sensed by the sensors until the flow front reaches the sensor location. Shortly after the flow front reaches sensor locations PS3, it flows out of the vent port. The vent port is then closed and a sharp increase in pressure can be observed on the sensor locations. As can be seen from Figure 5.15, the simulation software gave a satisfactory prediction of the pressure increase during RTM manufacturing.

5.3.3 Curing Simulations

In the selected manufacturing process, a temperature gradient was set between the upper and the lower mold platens. This temperature variation induces a curing gradient through the part thickness. In Figure 5.16, the simulated resin degree of cure is plotted at 3 positions through the thickness of the mold cavity (i.e., top surface, part core and bottom surface) closer to the vent port. The surface of the part that is adjacent to the hottest mold platen starts to cure first and then a through-thickness cure gradient is observed. Due to the temperature differences between the mold and the resin prior to injection, the cure gradient is not only observed through the thickness but also along the length of the part. Non-isothermal filling and curing analyses were carried out to simulate the curing process on the test plate. Figure 5.17 shows the simulated evolution of the resin cure over the part area. A cure gradient can be observed between the vent gate and the injection port. It is also seen that the resin near the injection port (the latest resin to enter into the mold cavity) is the last resin to cure. This phenomenon is plotted in Figure 5.18. The

degree-of-cure evolution at sensor locations close to the injection port and vent port is plotted in Figure 5.18. As can be seen from this Figure, a cure gradient is present at two sensor locations. The resin at sensor 5 which is close to the vent port starts curing first followed by the resin further away from the vent port. The degree-of-cure evolution curves for the two locations are identical; however they are separated by a time lag of approximately one minute. If the time difference between the two curves is removed, they fall perfectly onto each other. This in-plane cure gradient can also be experimentally verified by the pressure drops along the part surface (see Figure 5.19). Initially, a constant pressure level is seen at all sensors locations because of the hydrostatic pressure when the mold vents are clamped at the end of injection. A pressure drop is then observed at the sensor because of the resin gelation and shrinkage. However, the pressure drop at those locations does not occur at the same time, which is due to the cure gradient along the part. The sensors closer to the vent port show gelation and shrinkage earlier compared with the sensors closer to the injection port. As can be seen from Figure 5.19, a time lag of approximately one minute is present between sensor 5 and sensor 1, which is consistent with the degree-of-cure evolution lag at two locations presented in Figure 5.18.

5.3.4 Pressure Simulations

It was observed that low profile resins shrink at the beginning and expand at the later stage of the cure cycle [20]. This resin expansion during polymerization causes an increase of the mold pressure [22]. During the cure of LPA resins, mold pressure indicates an intimate contact between the part and the mold surface. This wall-to-wall contact guaranties a good surface finish of the composite part. Hence, the monitoring of the mold pressure is a key to successful molding conditions for class A parts. In this work, a numerical model was developed to predict the pressure variations during the cure of LPA resins. Based on C. D. Rudd et al. [23], the mold pressure (M_p) can be calculated in the following way:

$$M_P = \Delta V \cdot \left(E_m + \frac{1}{\frac{\phi}{E_r} + \frac{1-\phi}{G_f}} \right) (1 + \nu_r) + H_P \tag{5.6}$$

where

ΔV is the total volume change of the composite part (i.e., thermal and chemical volume changes).

E_m is the mold elastic modulus (representative modulus)

E_r is the resin elastic modulus (bulk modulus) that evolves during cure

G_f is the shear modulus of the fibers

ν_r is the Poisson's ratio of the composite

ϕ is the porosity of the reinforcement

H_p is the initial hydrostatic pressure (i.e., the pressure at the end of injection)

E_m, ϕ and H_p are constant quantities and listed in Table 5.7; whereas ΔV, Er, G_f, and ν_r, are functions of degree-of-cure. The evolution of E_r, G_f, and ν_r during cure is discussed in detail by Ruiz and Trochu [24]. The volume change (ΔV) during cure was characterized for a LPA resin system in [20]. Two sources were identified for the volume changes: thermal expansion/contraction and chemical shrinkage/expansion (see Figure 5.20). The model of volume change during cure can be expressed as follows:

$$\Delta V = \Delta V_{thermal} + \Delta V_{chemical} \tag{5.7}$$

where

$$\Delta V_{thermal} = CTE_{comp} \cdot \Delta T$$

$$\Delta V_{chemical} = \text{Equations 5.4 and 5.5}$$

where:

CTE_{comp} is the coefficient of thermal expansion of the composite

ΔT is the temperature increment or decrement

$\Delta V_{chemical}$ is represented by Equations 5.4 and 5.5.

$\Delta V_{chemical}$ for neat polyester resin is given by Equation 5.4 and for an LPA based resin is given by Equation 5.5. These models are also plotted in Figure 5.20 along with the experimental data. Equation 5.6 was solved at each time step during the curing simulation to calculate the mold pressure using the volume change model of Equation 5.7. Two lists of parameters for the volume change model were tested. Parameters obtained from rheology experiments, referred to as Model 1, are listed in Table 5.8 and modified values, referred to as Model 2, are listed in Table 5.9. The difference between these two parametric models is show in Figure 5.21. These two kinds of parameters were used for the calculation of pressure variations during curing of low profile polyester resin.

Figure 5.22 shows a comparison of the measured mold pressure versus the numerically predicted pressures with the two models. Model 1, whose values were obtained from rheology experiments, seems to be appropriate at the beginning of the polymerization until resin gelation and shrinkage (0-5 minutes). However, calculated shrinkage compensation (i.e., pressure increments after gelation) seems to be too small compared to the experimental values. When the second model is applied, the predicted mold pressure agrees with the experiments. Although model 1 and 2 use the same Equation 5.5; however their parameters are different. As can be seen from Table 5.8 and 5.9, the difference between the model parameters was relatively small ($\Delta V/V_{TSH}$) 3 instead of 4.8, $\Delta V/V_{TEX}$) -6 instead of -6.8), however it had a large effect on the pressure evolution in the last stages of curing as can be seen from Figure 5.22. This means the model in Equation 5.5 is very sensitive to the model parameters and a small change in parameters translates into relatively large variation in the predicted pressure.

Mold pressure distribution over the part area is also shown in Figure 5.23 for various curing times. A pressure gradient along the part, from the vent gate to the injection port is observed in the numerical simulations. The pressure variations at sensor location 1, 2 and 3 are plotted in Figure 5.24. Since pressure sensor 1 and 2 are relatively close to each other and to the injection port, the pressure variations observed at these two locations are almost identical. However, sensor 3 and 5 are farther away but at equidistance from the

injection port. Hence, the pressure variations at these two sensor locations are identical. The pressure variations observed at different sensor locations are identical; however the maximum pressure during processing is different due to the cure gradient. This phenomenon is discussed in detail in [22]. Numerical and experimental pressure variations during injection, gelation and subsequent curing agree well with each other. A relatively lower maximum pressure is observed for the sensors away from the injection port. Overall, a good agreement is observed between the modified expansion model and the experimental pressure variations during cure of the LPA resin tested.

5.4 Conclusion

Mold pre-heating, filling, curing and pressure-variation simulations closely matched with the experimental results. Temperature variations recorded by thermocouples during mold pre-heating were verified by the simulations. Temperature gradients observed along the geometry of the mold during simulations and actual pre-heating suggested that the mold needed to be heated at least for an hour before injection to induce a uniform temperature distribution along the geometry of the mold platens. Flow patterns made by marked tracers on the surface of the preform matched closely with the filling simulations. These results were further confirmed by the similarity between measured and predicted filling times and pressure variations observed during filling on the pressure sensor locations. Also as expected, a cure gradient was observed along the length of the part. The resin close to the vent port, which entered in the mold earliest, started curing first followed by the resin which came after, as confirmed by experiments in Figure 5.19. This resulted in the cure gradient along the length of the part. A lag time of one minute between degree-of-cure evolution at injection and vent ports was predicted by the numerical code and almost same amount of lag time was recorded during experiments. Resin pressure variation modeling is very important for the class A RTM processing. A pressure increase in the later stages of resin cure predicts a good contact between the composite and the mold which ultimately helps in getting good surface finish on RTM molded parts by reproducing the mold's finish. A close match was found for the pressure variations

observed during the curing of low profile unsaturated polyester resins. Simulation of pressure variations were also seen to be very sensitive to the parameters of the resin expansion model. Overall RTM simulations were found to be very useful and quite accurate in predicting mold pre-heating, filling, curing and pressure variation behavior of a low profile polyester resin.

5.5 Acknowledgements

The Auto21 Network of Centers of Excellence and Ecole Polytechnique de Montreal are gratefully acknowledged for their financial and technical support. We would also like to thank Dr. Michael Debolt from Ford Motors for his technical advice and support during this research. Help from Eric St-Amant of McGill Composite Materials and Structures Laboratory is gratefully appreciated.

REFERENCES

1. Martin GQ, Son SI. Proceedings of Second conference on Advanced Composites, 1986, pp. 186
2. Bruschke MV, Advani SG. A Finite Element/Control Volume Approach to Mold Filling in Anisotropic Porous Media. Polymer Composites 1990;11(6):398-405.
3. Freidrichs B, Guceri S. A Hybrid Numerical Technique to Model 3-D Flow Fields in Resin Transfer Molding Processes. Polymer Engineering and Science 1995;35(23):1834-1851.
4. Friedrichs B, Guceri SI, Subbiah S, Altan MC. Simulation and Analysis of Mold Filling Processes with Polymer-Fiber Composites: Proceedings of ASME Polymer-Polymer Composites 1990: 73-90.
5. Dessenberger RB, Tucker CL. Thermal Dispersion in Resin Transfer Molding. Composite 1995;16(6):495-506.
6. Shojaei A, Ghaffarian SR, Karimian SMH. Numerical Modeling of Three-Dimensional Mold Filling Process in Resin Transfer Molding using Quasi Steady State and Partial Saturation Formulations. Composites Science and Technology 2002;62(6):861-869.
7. Lekakou C, Bader MG. Mathematical Modeling of Macro and Micro Infiltration in Resin Transfer Molding. Composites Part A 1998; 29A: 29-37.
8. Young WB, Han K, Fong LH, Lee LJ. Flow Simulation in Molds with Pre-placed Fiber Mats. Polymer Composites 1991;12(6):391-403.

9. Boccard A, Lee WI, Sprinager GS. Model for Determining the Vent Locations and the Fill Time for Resin Transfer Molds. Journal of Composite Materials 1995;29(3):306-333.
10. Young WB. Journal of Composite Materials 1994;28:1098.
11. Young WB. Three-dimensional Non-isothermal Mold Filling Simulations in Resin Transfer Molding. Polymer Composites 1994;15(2):118-127.
12. PAM-RTM by ESI Group, www.esi-group.com
13. Trochu F, Gauvin R, Gio DM. Numerical Simulation of the Resin Transfer Molding Process by the Finite Element Method. Advances in Polymer Technology 1993;12(4):329-342.
14. Gauvin R, Trochu F. Key Issues in Numerical Simulation for Liquid Composite Molding Processes. Polymer Composites 1998;19(3):233-240.
15. Gauvin R, Trochu F, Lemenn Y, Diallo L. Permeability Measurement and Flow Simulation through Fiber Reinforcement; Polymer Composites 1996;17(1):34-42.
16. Hammami A, Gauvin R, Trochu F. Modeling the Edge Effect in Liquid Composite Molding. Composites Part A 1998; 29(5):603-610.
17. Lin RJ, Lee LJ, Liou ML. Mold Filling and Curing Modeling of RTM and SRIM Processes, Proceedings of 7th Annual ASM/ESD Advanced Composite Conference, 165-174, 1991.
18. Antonelli D, Farina A. Resin Transfer Moulding: Mathematical Modeling and Numerical Simulations. Composites Part A 1999;30:1367-1385.
19. Shojaei A, Ghaffarian SR, Karimian SMH. Modeling and Simulation Approaches in the Resin Transfer Molding Process: A Review. Polymer Composites 2003;24(4):525-544.
20. Haider M, Hubert P, Lessard L. Cure Shrinkage Characterization and Modeling of a Polyester Resin Containing Low Profile Additives. Composites Part A, (submitted)
21. Cooper M. Scott Bader PD9551 Polyester Resin Safety Data Sheet, 2002.
22. Haider M, Hubert P, Lessard L. An Experimental Investigation for Class A Surface Finish in Resin Transfer Molding Process. Composite Science and Technology, (submitted).
23. Rudd CD, Long AC, Kendall K. Mangin CGE. Liquid Moulding Technologies, SAE books, Woodhead Publishing Limited, Cambridge, England, May 1997.
24. Ruiz E, Trochu F. Thermo-mechanical properties during cure of glass-polyester RTM composites: elastic and viscoelastic modeling. Journal of Composite Materials 2005;39(10): 881-916.

Table 5.1 Processing parameter for permeability measurements

Fiber volume fraction	Surface density	Fiber density	Thickness	Oil viscosity	Injection time
0.20	1.75 kg/m^2	2550 kg/m^3	0.0032 m	0.105 Pa.s	411 sec

Table 5.2 Properties of the mold

Mold Material	Thermal Conductivity (W/m ^{0}K)	Specific Heat (J/kg ^{0}K)	Density (kg/m^3)
1.5% Carbon Steel	36	500	6850

Table 5.3 Properties of the polyester resin

Thermal Conductivity (W/m ^{0}K)	Reaction Enthalpy (kJ/kg)	Specific Heat (J/kg ^{0}K)	Density (kg/m^3)
0.25	400	1600	1260

Table 5.4 Properties of the glass fiber preform

Permeabilities (m^2) $K_1 = K_2$	Thermal Conductivity (W/m ^{0}K)	Specific Heat (J/kg ^{0}K)	Density (kg/m^3)
4.163 x 10^{-10}	0.1	700	2500

Table 5.5 Parameters for the cure kinetics model (Equation 5.2).

Parameters	A_1 (sec^{-1})	E_1 (kJ mol^{-1})	A_2 (sec^{-1})	E_2 (kJ mol^{-1})	m	n	α_{max}
Values	$1.07x10^{13}$	149.7	$7.20x10^{10}$	87.54	0.711	1.464	0.9

Table 5.6 Parameters for the viscosity variation model (Equation 5.3).

Parameters	C_1	C_2	α_G	B (Pa.s)	T_b (°K)
Values	1.502	1.01	0.055	$1.51x10^{-4}$	2701

Table 5.7 Parameters for mold pressure model (Equation 5.6).

Parameters	E_m (N/m^2)	ϕ	H_p (kPa)
Values	$8x10^7$	0.8	200-650

Table 5.8 Parameters for LPA shrinkage-expansion model (Equation 5.5)

Parameters	α_G	α_C	α_M	$\left(\frac{\Delta V}{V}\right)_{TSH}$	$\left(\frac{\Delta V}{V}\right)_{TEX}$
Values	0.05	0.5	0.9	4.8	-6.8

Table 5.9 Modified parameters for LPA shrinkage-expansion model (Equation 5.5)

Parameters	α_G	α_C	α_M	$\left(\frac{\Delta V}{V}\right)_{TSH}$	$\left(\frac{\Delta V}{V}\right)_{TEX}$
Values	0.05	0.5	0.9	3	-6

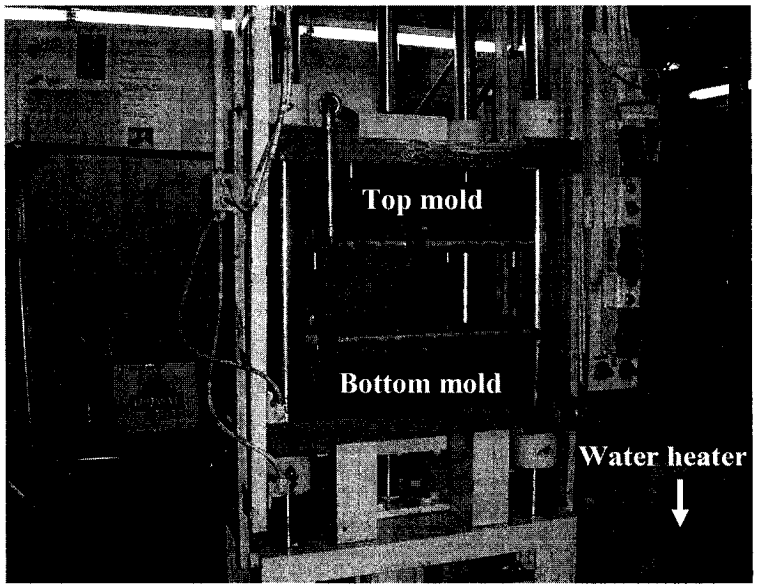

(a)

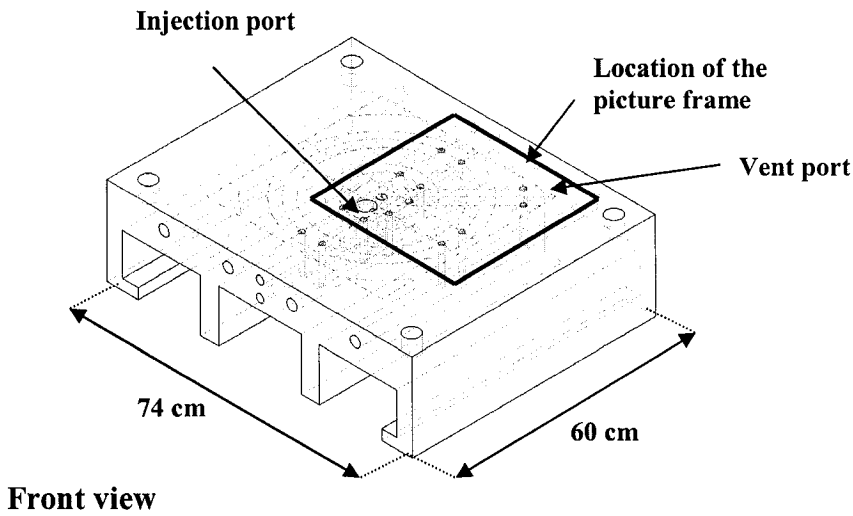

(b)

Figure 5.1 (a) Mold mounting on the press, (b) bottom mold platen

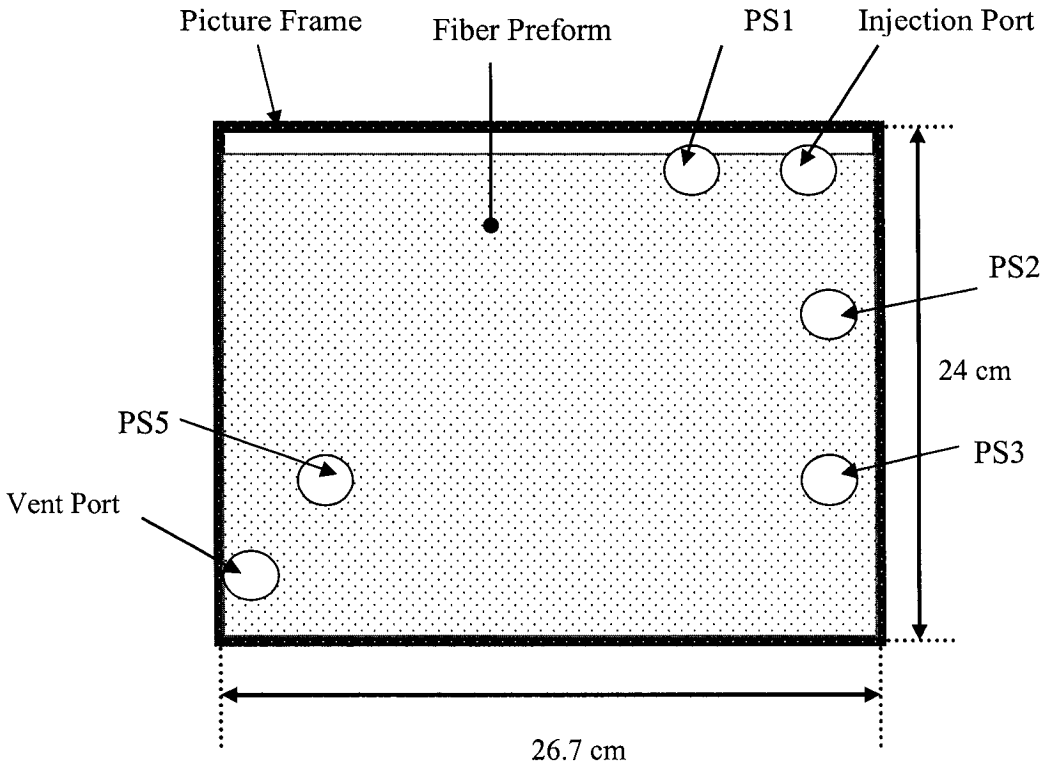

(a)

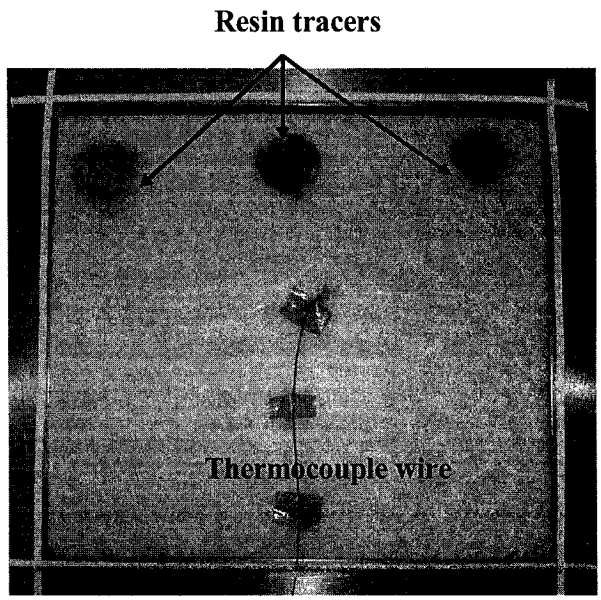

(b)

Figure 5.2 (a) Schematics of the picture frame, injection port, vent port and location of pressure sensors (PS), (b) Snapshot of the picture frame with preform, colored tracers, thermocouple and mold sealant.

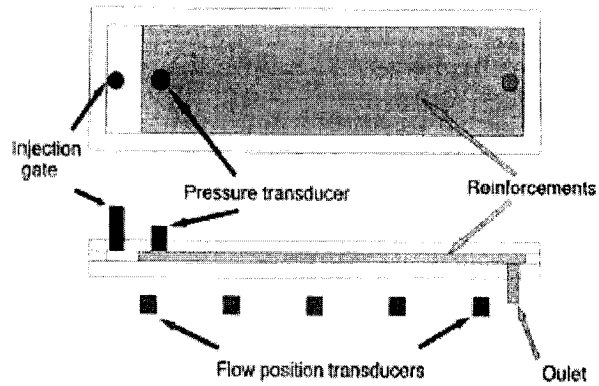

(a)

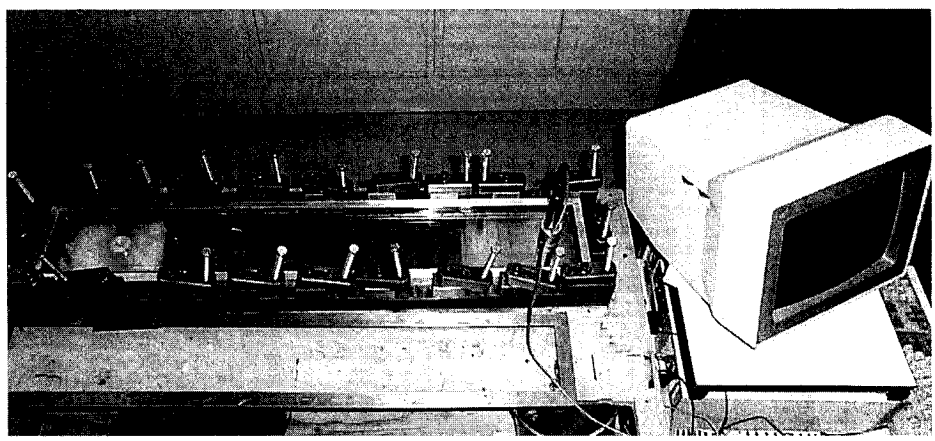

(b)

Figure 5.3 Experimental setup for permeability measurements (a) block diagram (b) picture of the setup.

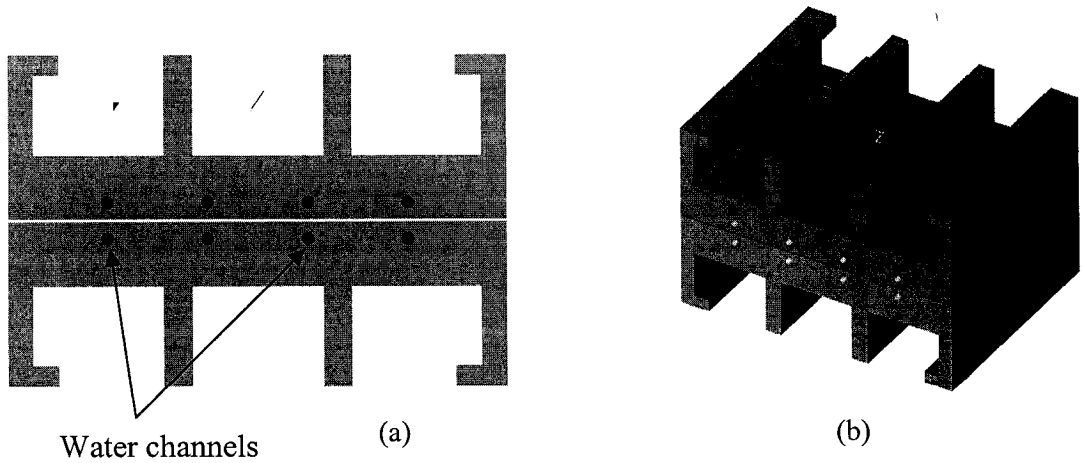

Figure 5.4 (a) Front view of the mold geometry (b) Isometric view of the mold

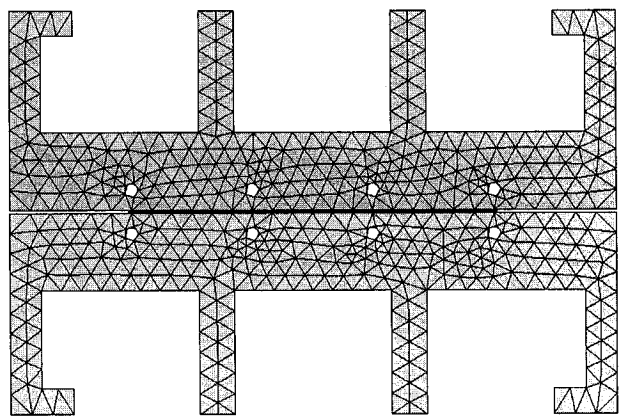

Figure 5.5 Finite element model of the test mold

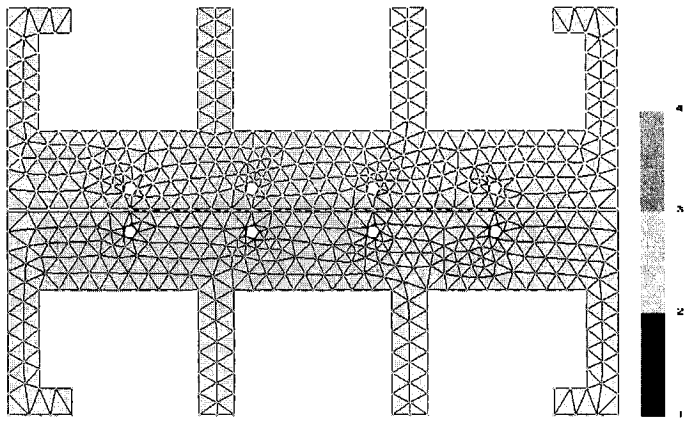

Figure 5.6 Groups of nodes for applying boundary conditions

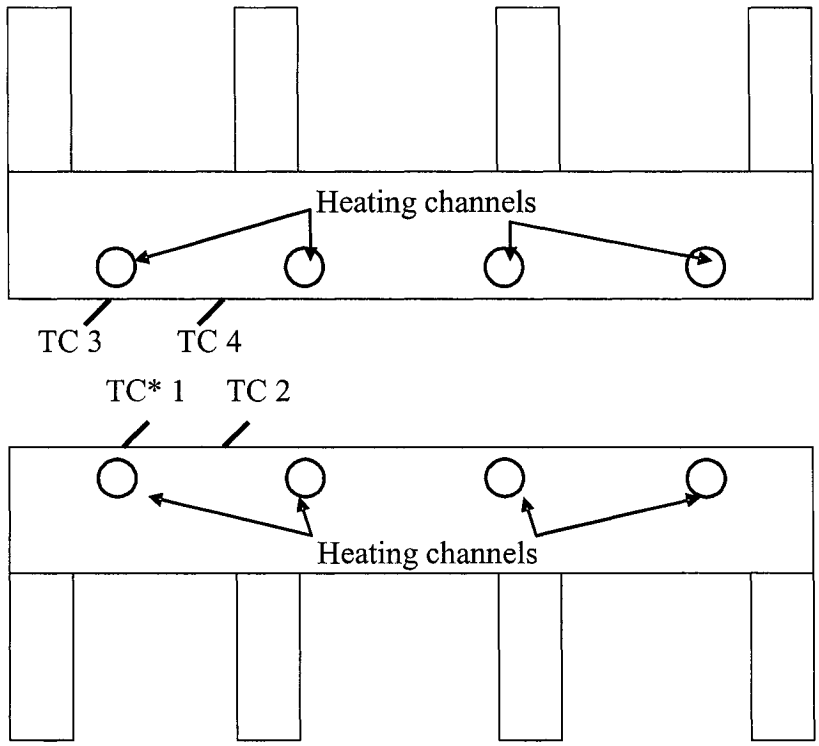

* *TC refers to thermocouples*

Figure 5.7 Placement of the thermocouples on the top and bottom mold platen surfaces for pre-heating simulations

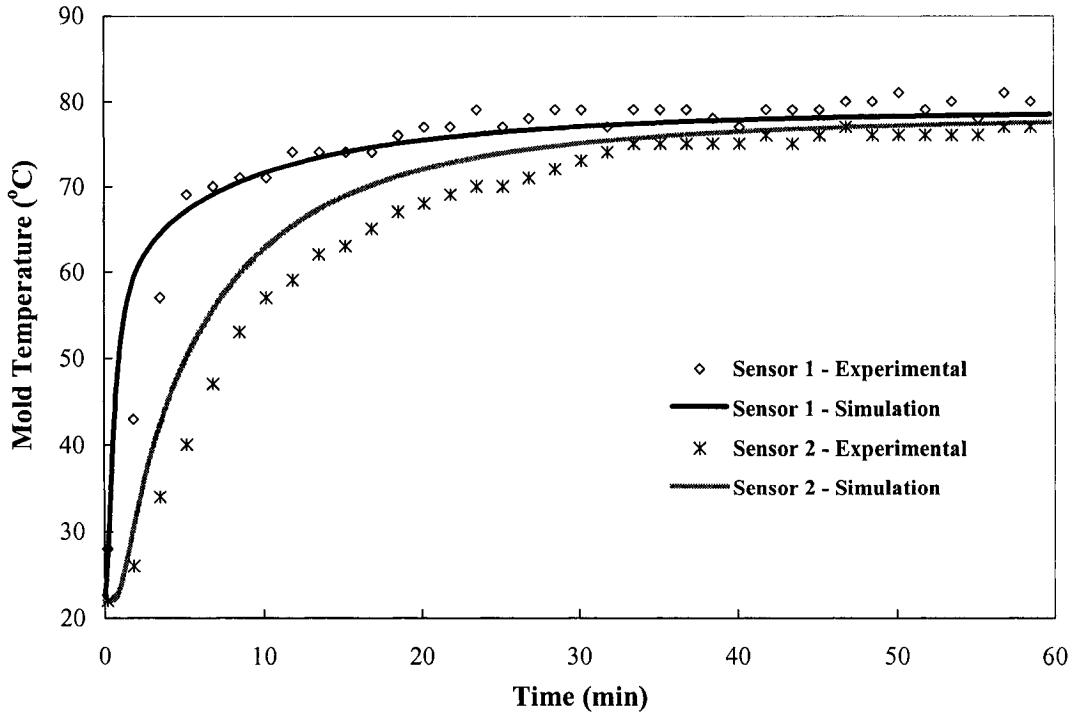

Figure 5.8 Temperature variation at thermocouple sensors 1 and 2 during mold heating: experimental and computational results

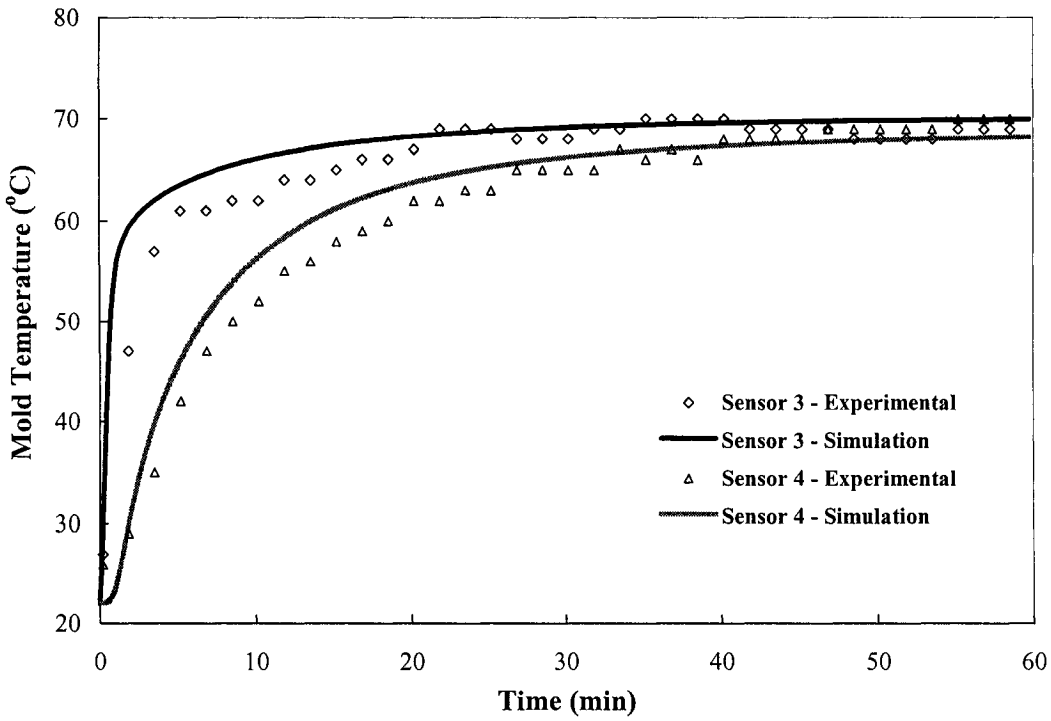

Figure 5.9 Temperature variation at thermocouple sensors 3 and 4 during mold heating: experimental and numerical results

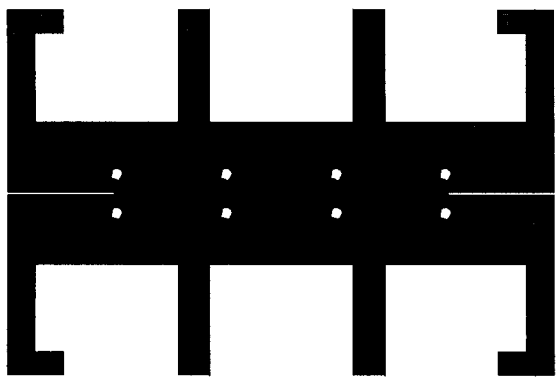

(a) t = 0

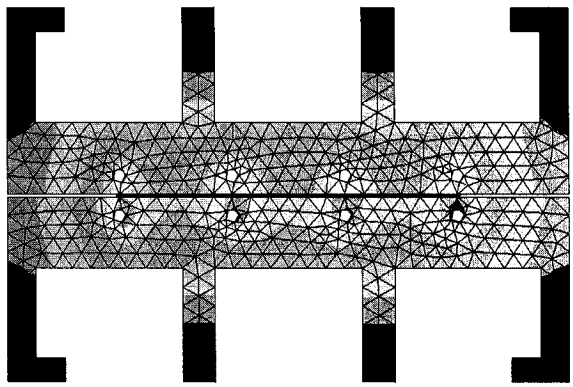

(b) t = 5 minutes

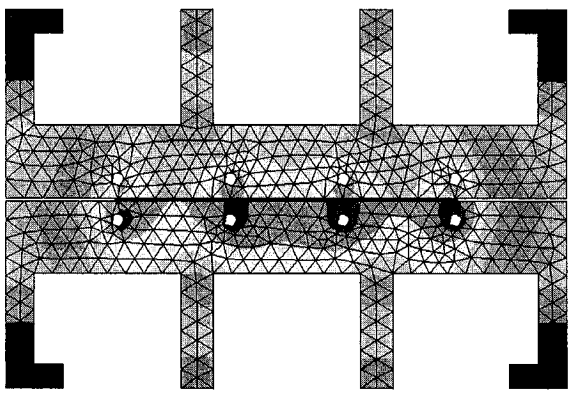

(c) t = 10 minutes

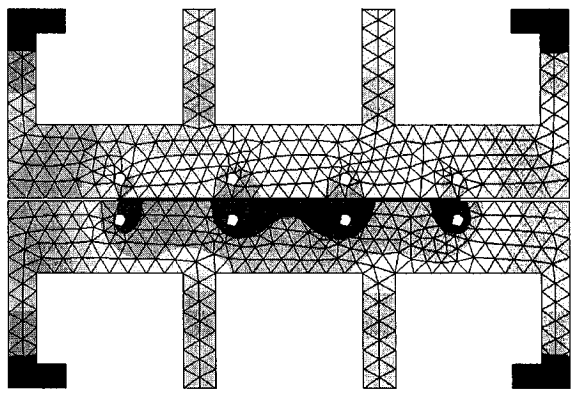

(d) t = 15 minutes

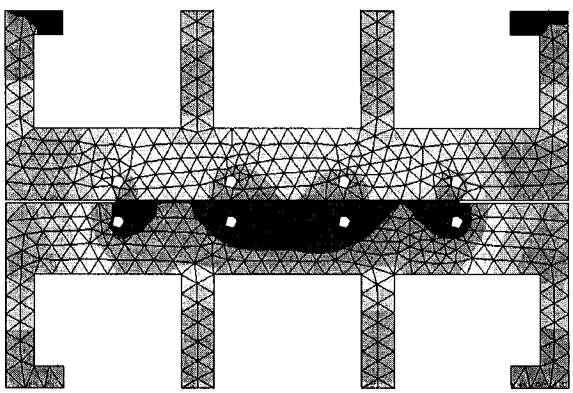

(e) t = 20 minutes

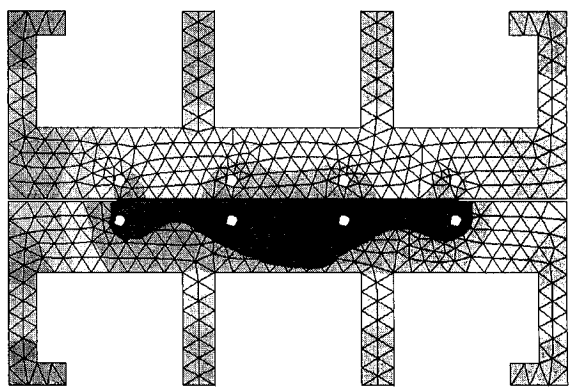

(f) t = 30 minutes

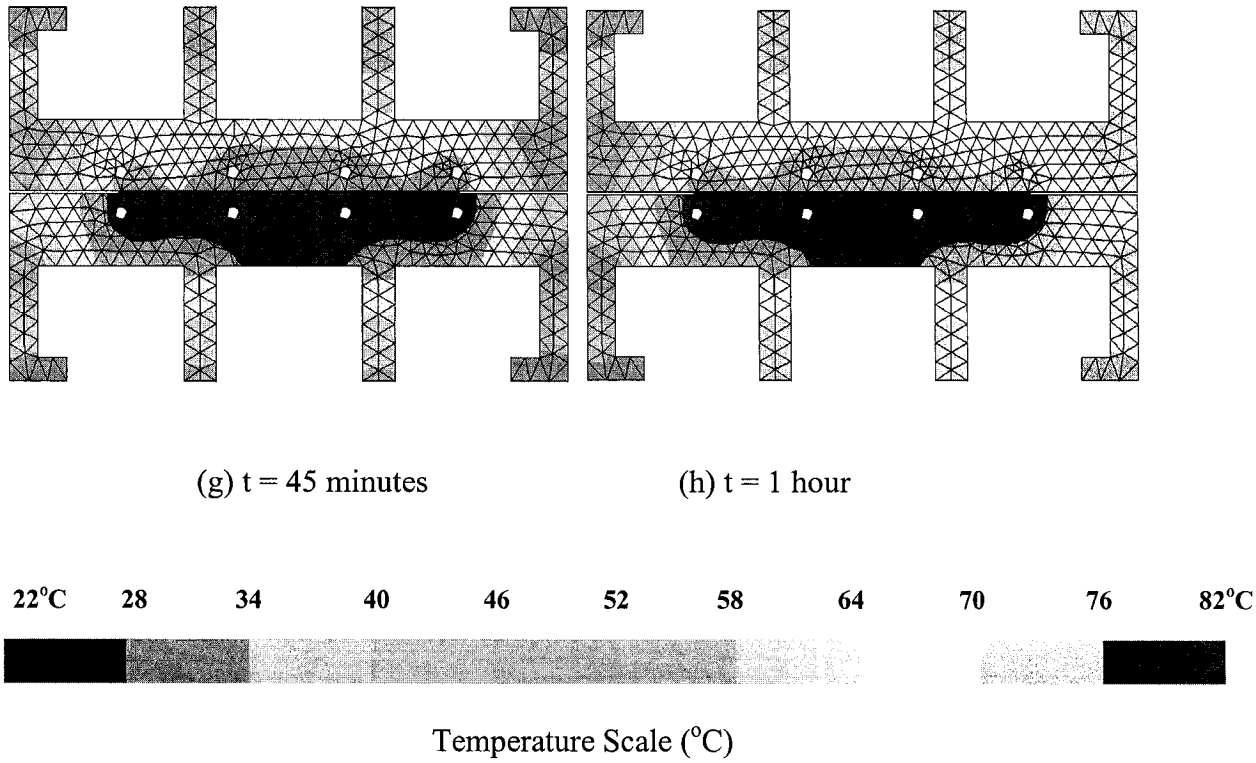

Figure 5.10 Thermal gradient along the mold geometry at different stages in pre-heating simulations (a) in the beginning (b) after 5 minutes (c) after 10 minutes (d) after 15 minutes (e) 20 minutes (f) half an hour (g) 45 minutes (h) one hour

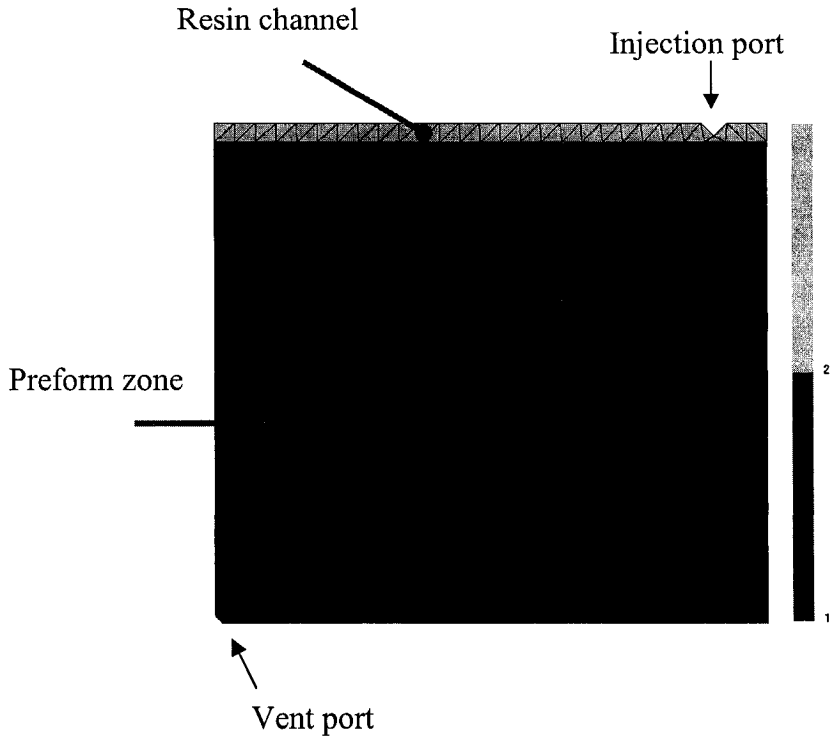

Figure 5.11 Position of the injection and vent ports along with 2 zones. Blue zone represents fibers and green zone represents resin channel without fibers.

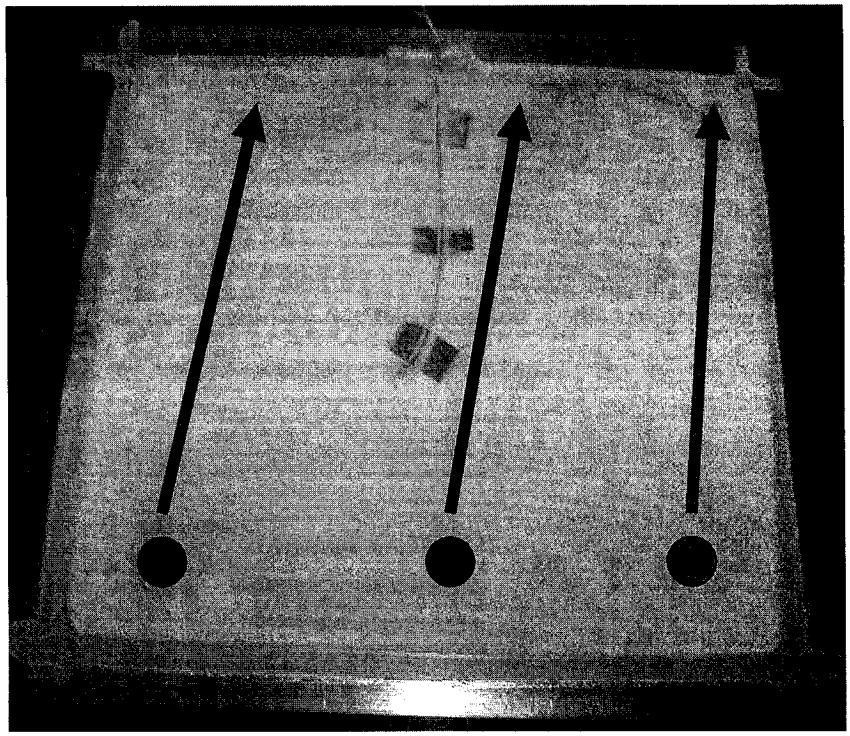

Figure 5.12 Tracers and their respective flow lines as the resin flows through the preform

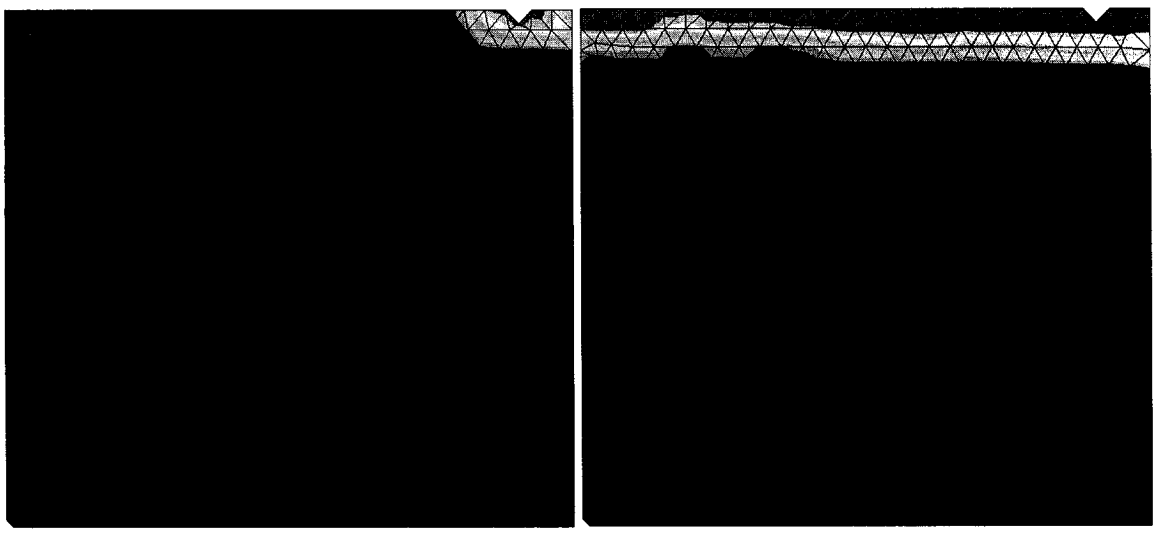

(a) t = 0 seconds (b) t = 3 seconds

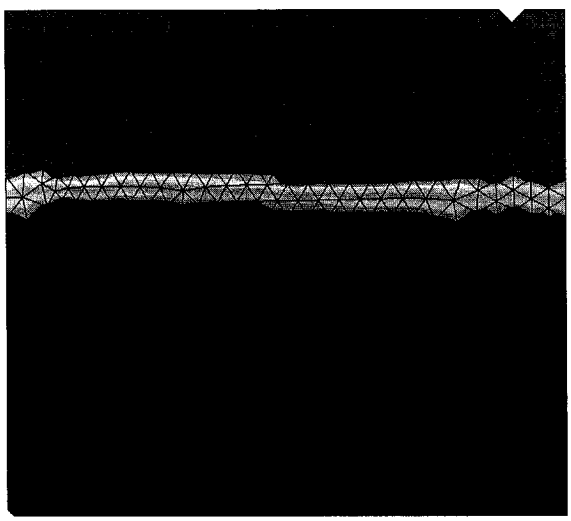

(c) t = 10 seconds

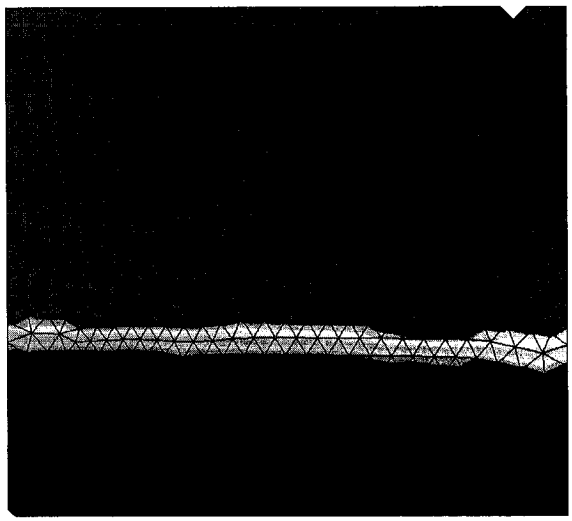

(d) t = 15 seconds

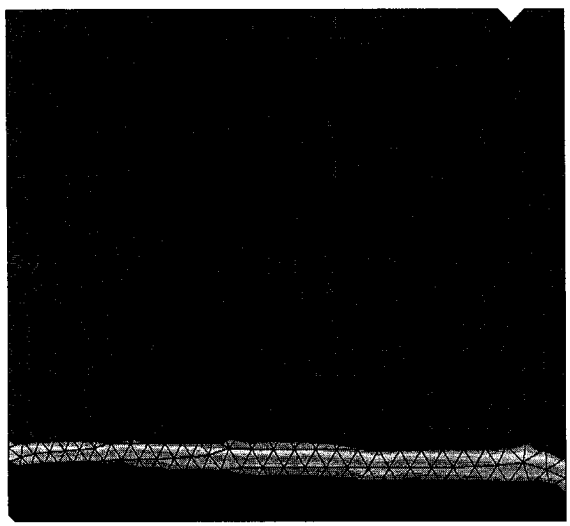

(e) t = 20 seconds

(f) t = 30 seconds

Figure 5.13 Flow front movements for an injection pressure of 345 kPa (a) after 0 seconds (b) after 3 seconds (c) after 10 seconds (d) after 15 seconds (e) after 20 seconds (f) after 30 seconds

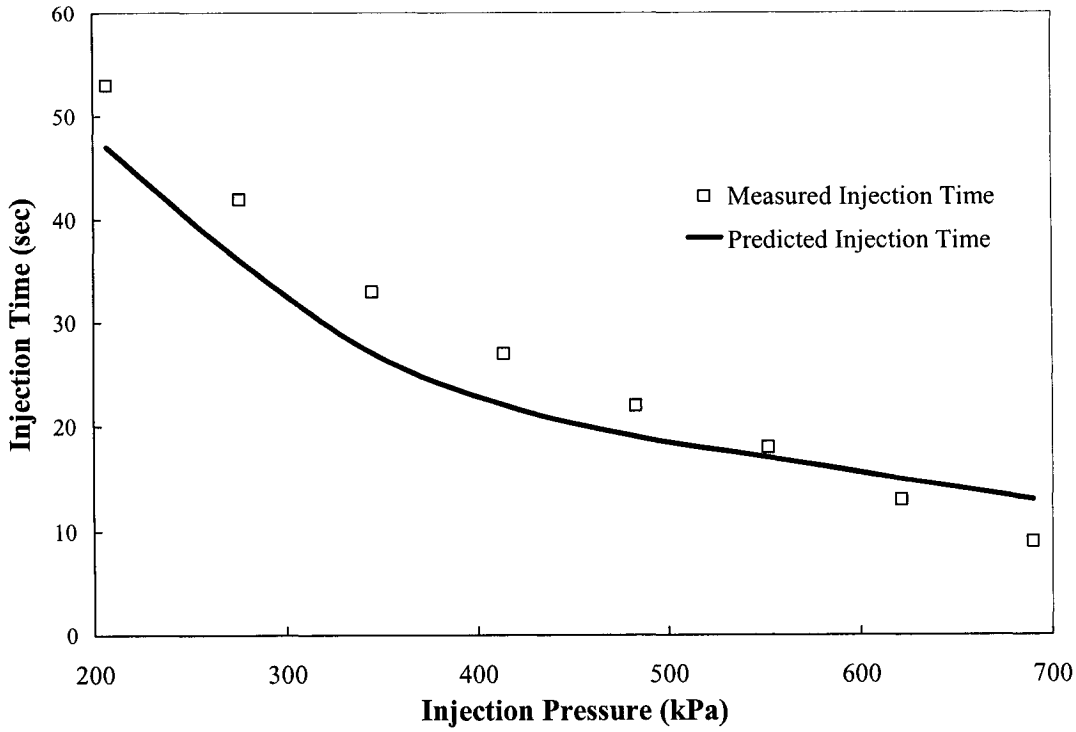

Figure 5.14 Injection time measured during actual manufacturing and predicted by simulation

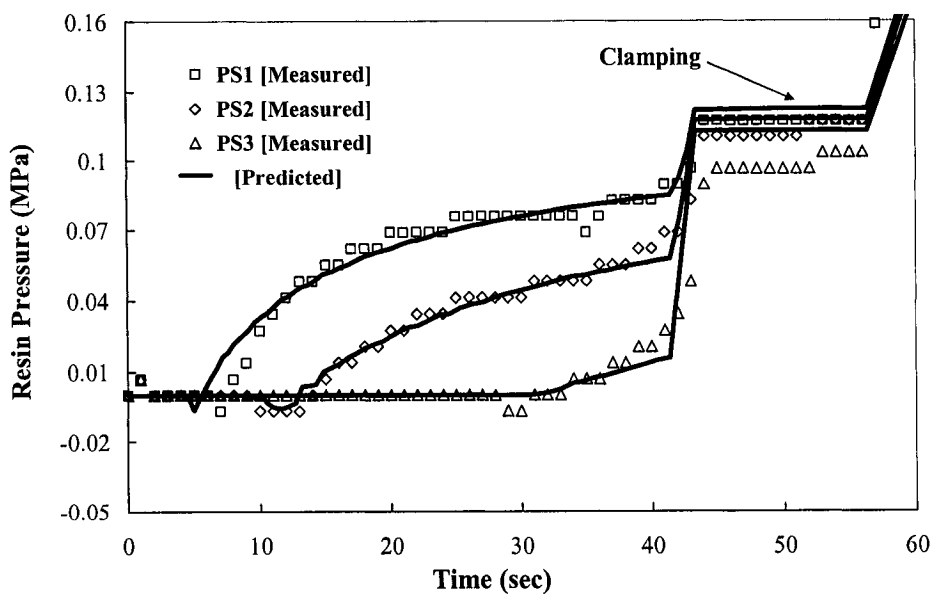

Figure 5.15 Pressure variation at sensor locations shown in Figure 5.2(a) during injection: measured and simulated results.

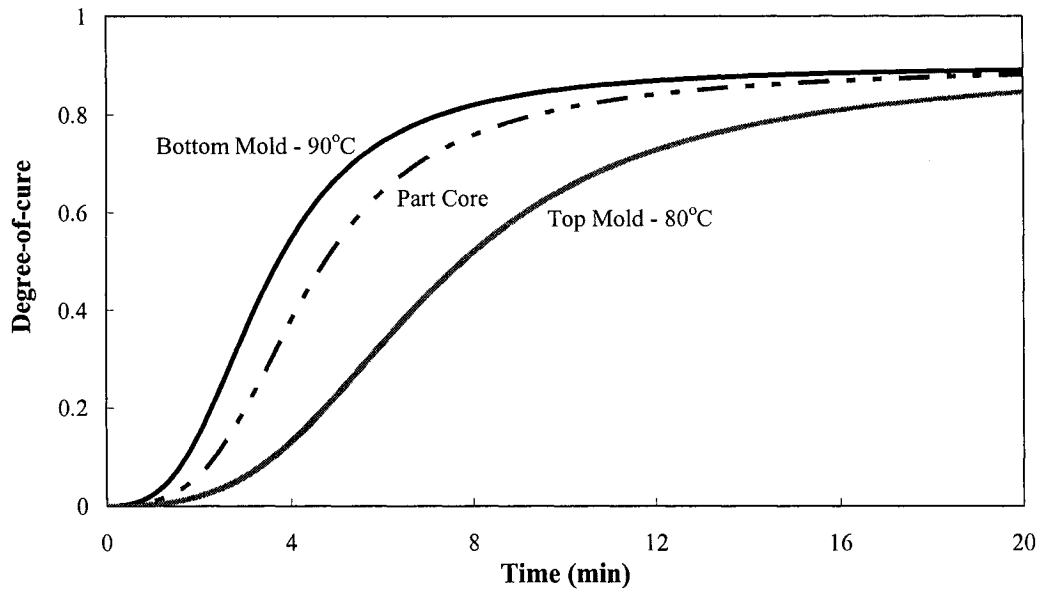

Figure 5.16 Through thickness degree-of-cure variations (on the top, bottom and middle of the part) close to the vent port when manufactured with a temperature gradient of 10°C.

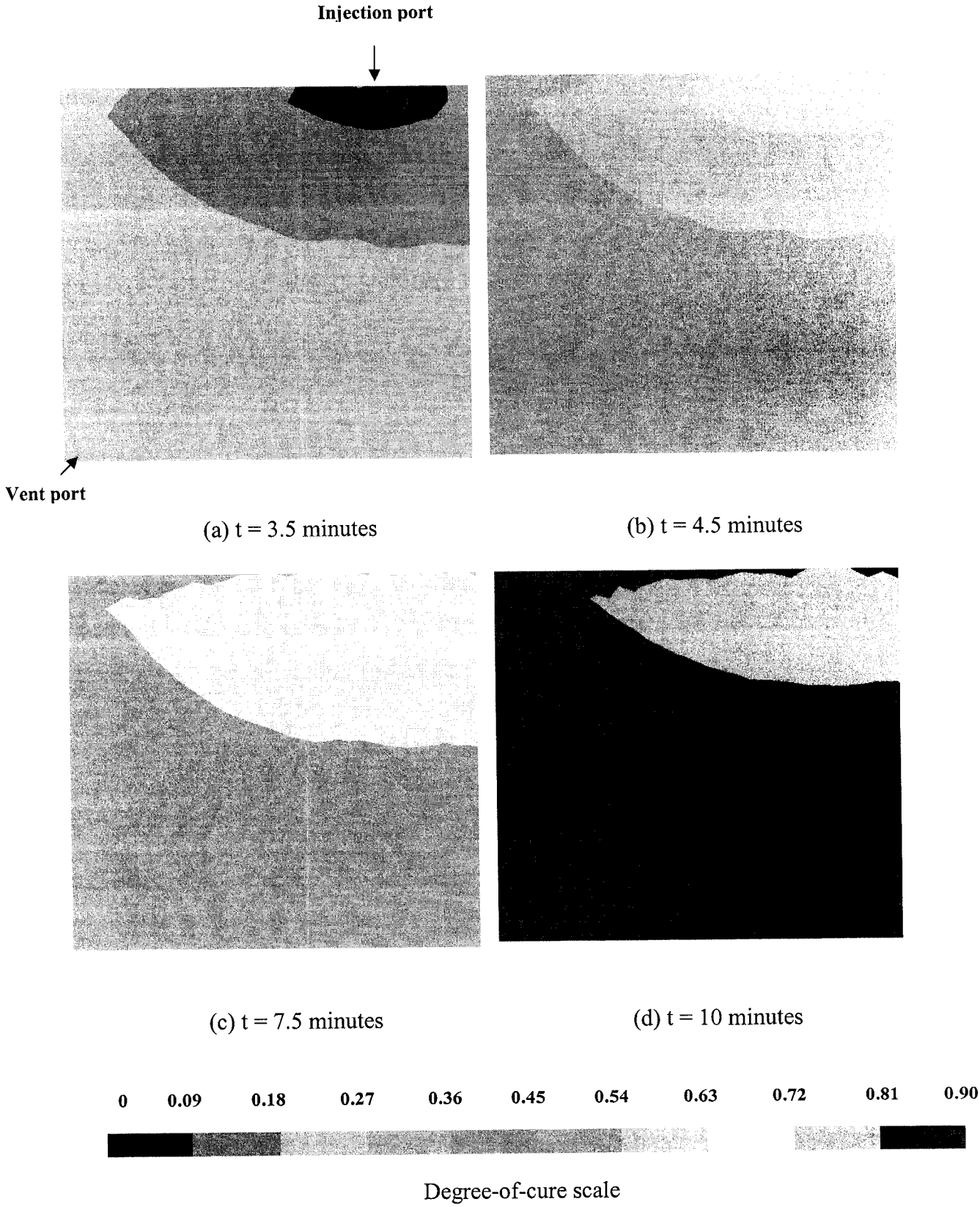

Figure 5.17 Simulated evolution of the resin degree-of-cure along the part (a) 3.5 minutes (b) 4.5 minutes (c) 7.5 minutes (d) 10 minutes

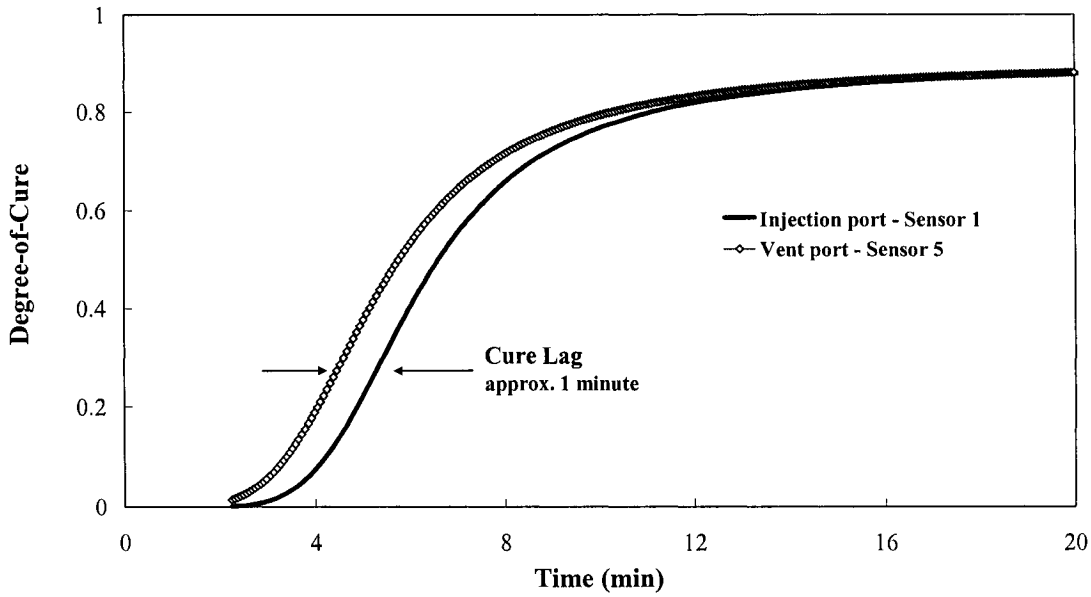

Figure 5.18 Cure gradient between the injection and vent ports

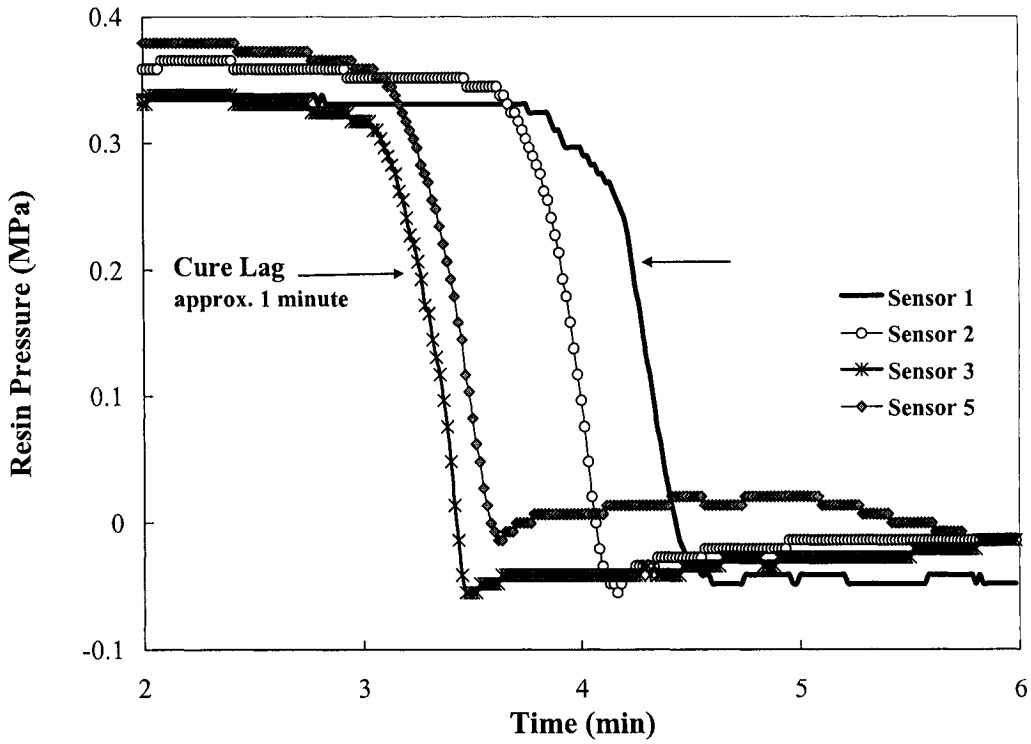

Figure 5.19 Pressure drop at different sensor locations representing the in-plane cure gradients and gelation of a polyester resin (sensor locations shown in Figure 5.2(a)).

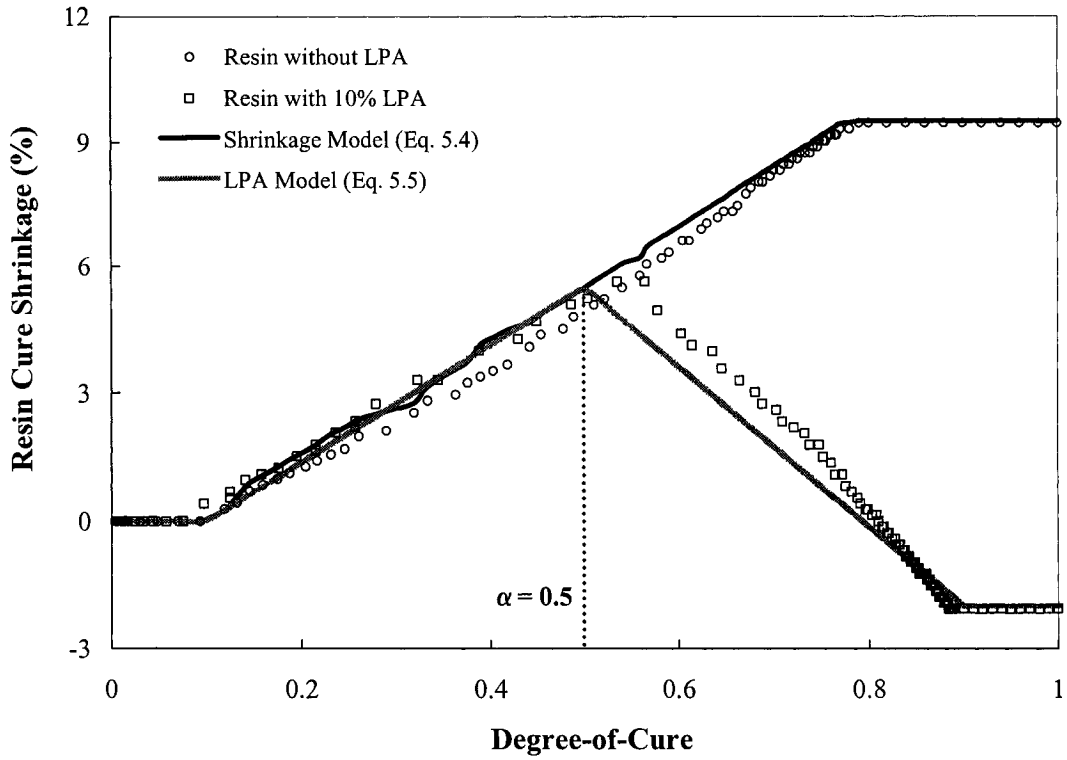

Figure 5.20 Volume change during cure of a resin with and without LPA (a) chemical shrinkage below $\alpha < 0.5$ and (b) chemical expansion (LPA compensation) above $\alpha > 0.5$.

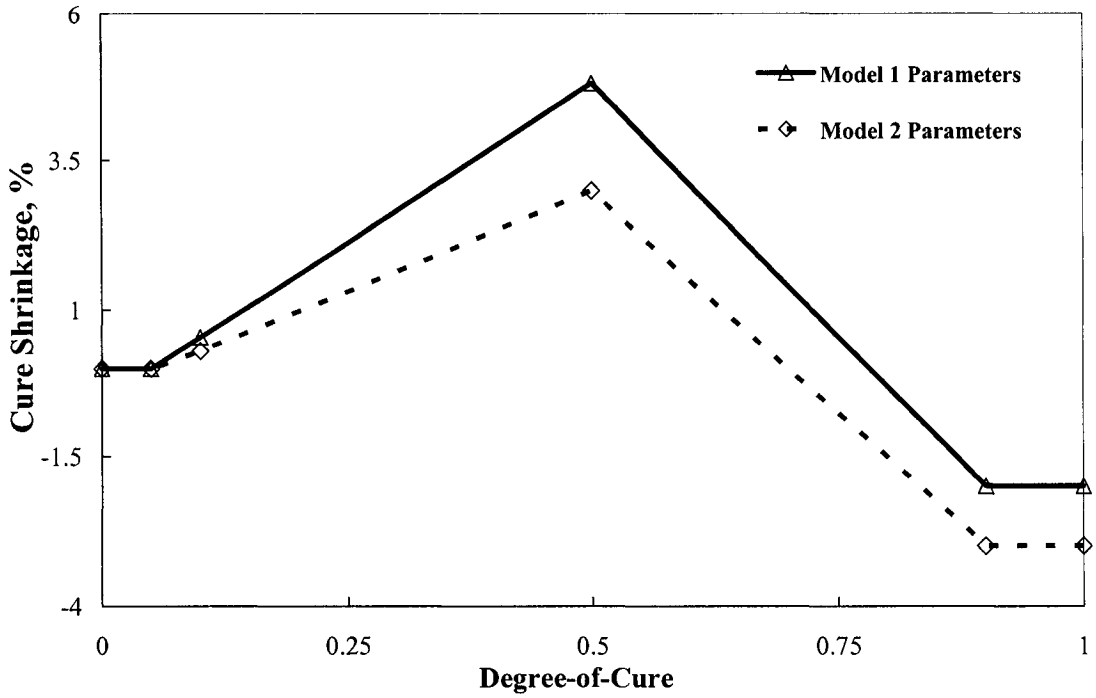

Figure 5.21 Dimensional change as a function of degree-of-cure for a low profile resin under two parametric models.

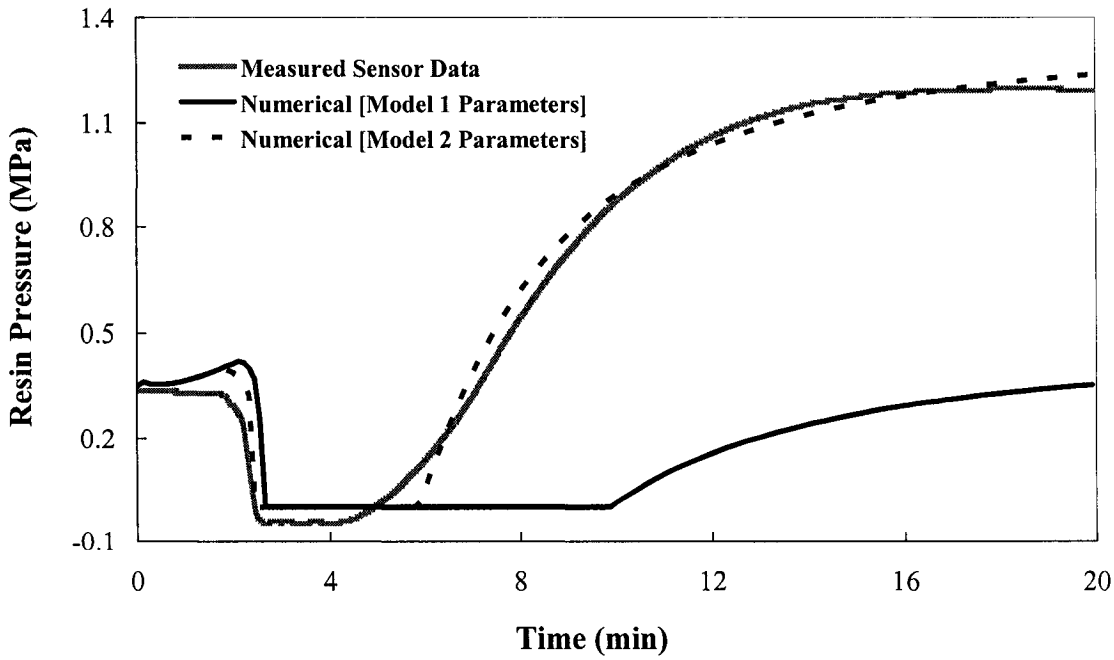

Figure 5.22 Dimensional change as a function of degree-of-cure for a low profile resin for two parametric models

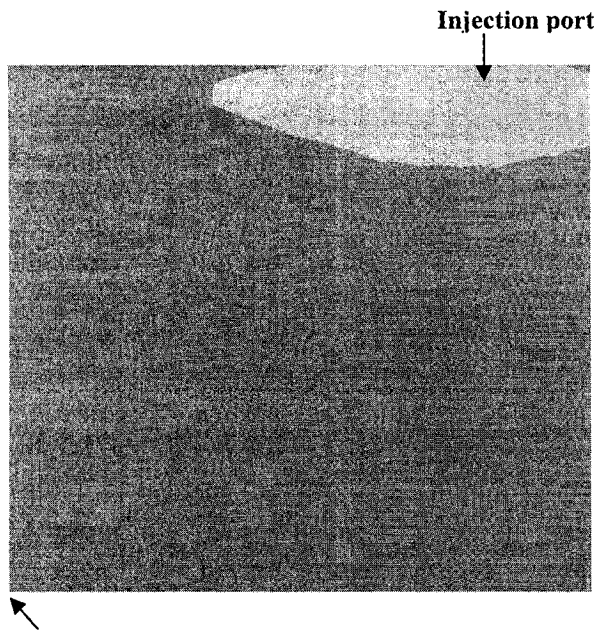

(a) t = 2 minutes

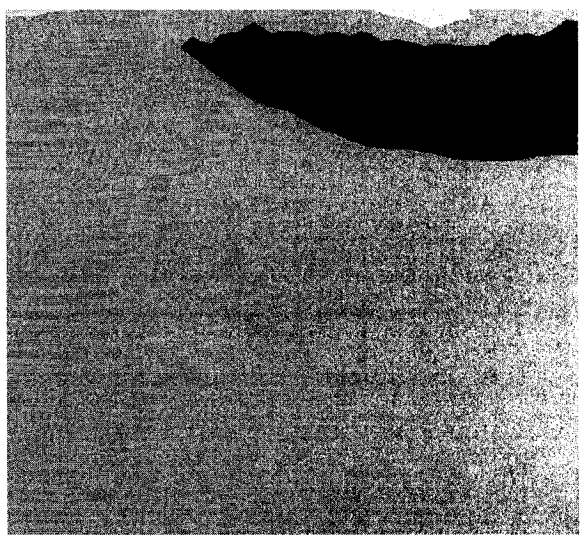

(b) t = 6.5 minutes

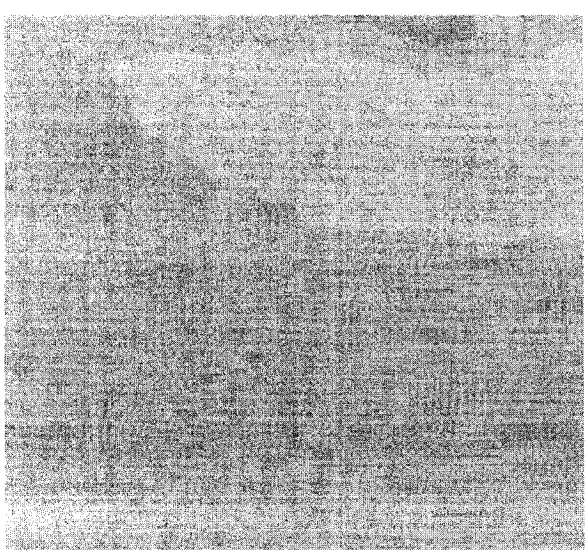

(c) t = 7.5 minutes

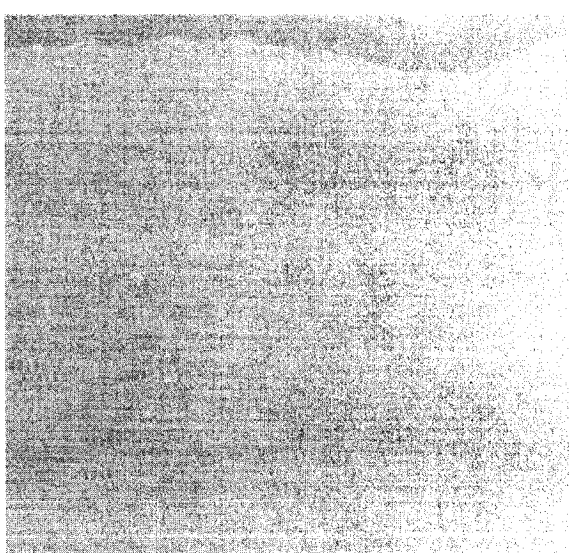

(d) t = 9 minutes

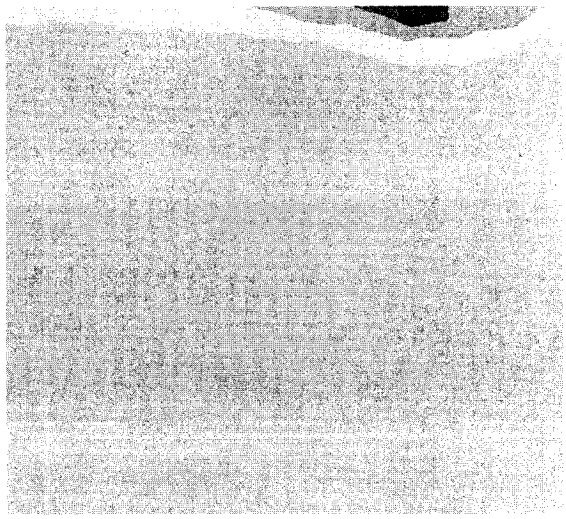

(e) t = 20 minutes

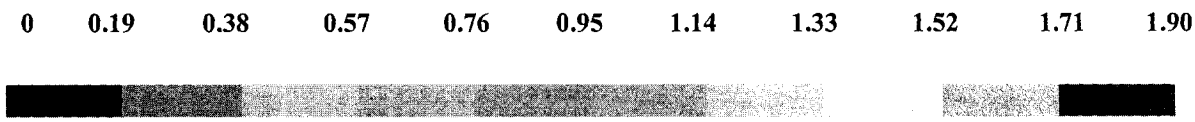

Pressure Scale (MPa)

Figure 5.23 Pressure along the length of the part after (a) 2 minutes (b) 6.5 minutes (c) 7.5 minutes (d) 9 minutes (e) 20 minutes

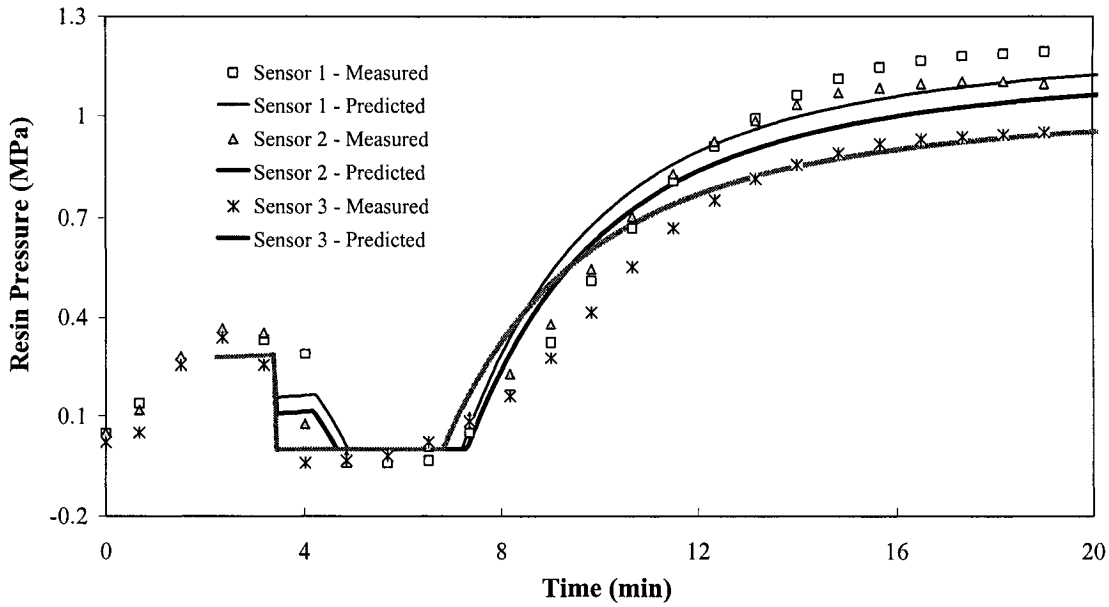

Figure 5.24 Measured and predicted pressure evolutions during the cure of a low profile resin at various sensor locations.

Link between RTM Manufacturing (chapter 4) and Process Optimization (chapter 6)

Chapter 6 of this thesis presents the surface profilometer data for the test panels manufactured for the processing conditions of the test matrix listed in chapter 4. Chapter 6 also integrates shrinkage measurement data (chapter 3) and pressure variation data (chapter 4) with surface roughness data (chapter 6). This chapter presents an overall picture of the whole optimization process. Chapter 4 and 6 use the same test matrix; however the focus of chapter 4 is on pressure variations whereas the focus of chapter 6 is the surface finish characterization and statistical analysis. It can be seen from Figure 2.10 that the all the components of this research are well integrated with each other.

Link between Numerical Simulations (chapter 5) and Process Optimization (chapter 6)

Mold pre-heating, mold filling and resin curing simulations (chapter 5) help in setting the levels of process parameters used in the test matrices of chapter 6. Numerical simulations eliminate costly trial-and-error experimentation for finding the appropriate levels of process parameters.

CHAPTER 6

OPTIMIZATION OF RTM PROCESSING PARAMETERS FOR CLASS A SURFACE FINISH

Mohsan Haider, Pascal Hubert*, Larry Lessard

Department of Mechanical Engineering, McGill University
817 Sherbrooke Street West, Montreal H3A 2K6, Quebec, Canada

(Prepared for Composites Part A: Applied Science and Manufacturing)

Abstract

Resin transfer molding (RTM) has great potential to become an efficient and economical process for fabricating large and complicated composite structural components. One of the challenges facing the automotive field is to obtain class A surface finish for RTM manufactured exterior car body components. There are several material and process parameters, which severely affect the surface quality. In this research, material and processing parameters were optimized for class A surface finish using design-of-experiments (DOE) and multiple regression analyses. Processing windows obtained for different process parameters based on analytical and numerical analyses were used in the test matrices designed through the Taguchi method. Analysis of variance (ANOVA) and multiple regression analyses were carried out on the surface roughness of test samples molded under varying processing conditions to determine the relative significance of

* Corresponding author:
E-mail: pascal.hubert@mcgill.ca
Tel.: 1(514) 398-6303

process parameters. The LPA content was found to be the most influential parameter affecting surface roughness and waviness. The roughness decreased non-linearly with increasing LPA content. However, an increase in filler content and injection pressure resulted in a linear decrease in surface roughness. LPA content at 10% was found to be the minimum amount required for class A surface finish. Post-cure shrinkage had no significant effect on short wavelength roughness; however it increased long wavelength roughness.

Keywords: B. Defects, B. Modeling, C. Statistics, E. Resin transfer molding

---

6.1 Introduction

The automotive industry is seen as one of the major potential consumers of advanced composite materials in the future. An estimated 8% of total domestic and engineering plastics manufactured worldwide are currently used in automotive applications and this consumption is expected to grow. Car manufacturers may favor composite materials for several reasons. In addition to being corrosion-resistant, they can be used with different production processes, making it possible to develop new techniques and produce more complex and larger parts, resulting in time and money savings. Composite materials are also light, which allows manufacturers to reduce transportation and storage costs, while reducing fuel consumption. End-users also benefit from lighter and faster vehicles. Other factors that make plastics and composites suitable candidates for replacing conventional materials are economy, styling potential, functional design and reduced maintenance. In the automobile industry today, composite materials are used in applications as varied as car body panels (doors, roofs), semi-structural parts (front bumpers) and engine parts (cylinder-head covers) [1-3]. Structural parts for front-ends and tailgate frames, mainly molded through the injection-compression or other injection technology, have also benefited from the advantages provided by composites.

Definition of Class A Surface Finish

Surface finish also known as surface texture or roughness is a quality characteristic, which represents the degree-of-smoothness of a surface. The achievement of high class surface finish on polymer composites is very important for their wide spread use in the manufacturing of exterior car body panels due to aesthetic appeal and surface quality requirements. The term used for acceptable surface roughness in the auto industry is known as class A surface finish. Unfortunately, a clear definition of class A surface finish is absent in the literature. In practice, class A surface finish is referred as a perfectly polished, high luster surface which is free of porosity and scratches of any kind. The term originated from the marine and automotive industries. Examples of such a finish can be found on high quality boat hulls and automobiles. Dutiro [4] and Bayldon [5] define class A finish as a surface which exhibits aspects of flatness, smoothness and light reflection similar to that of finished stamped steel sheeting, typically with a DORRI (Distinctness of Retro Reflective Image) values between 60 and 90, as measured with D-sight optical enhancement techniques. Neitzel et al. [6] define class A as: "a substrate made of composite material represents a class A surface, if its optical appearance is identical to an adjacent steel panel".

Unfortunately, due to the lack of a clear definition of class A surface finish in automotive applications, a standard method or procedure for class A surface finish measurement is absent from the literature. However, the work is in progress and researchers are trying to establish standards for class A surface finish characterization. Typical surface roughness measurement systems used in the automotive sector are quality measurement system (QMS), BYK wave-scan, D-sight and the ONDULO quality control systems [7]. The main drawback of all these techniques is that they can only be used with a high level of gloss, which is absent in most composite surfaces. Many of the RTM and sheet molding compound (SMC) surfaces do not have a high enough gloss to be measured with the techniques mentioned earlier [8]. However, contact and non-contact surface profilometry has the potential to be used as a standard method for the measurement of composite surfaces [7-8]. There are many parameters that can be defined from the surface profile obtained with a surface profilometer. One of the most common one-dimensional

parameters used for quantitative analysis of surface roughness is R_a [9-10], where R_a is defined as the arithmetical mean of the absolute values of the surface profile amplitude (Y_i) from the mean line [9-10]. R_a is represented by Equation 6.1.

$$R_a = \frac{1}{L}\int_{x=0}^{x=L} |Y_i| dx \tag{6.1}$$

where L is the scan length, x is the measurement direction and Y_i is the surface profile amplitude at the given location ($x = i$). However, the relationship between class A surface finish and R_a measurements is not available in the literature. Debolt [8] described a procedure to quantify surface roughness for class A finish. A non-contact profilometer was used and an analysis procedure was developed. This procedure employed band-pass filtering and Fourier Transforms for extracting regions of particular wavelengths. Calculations were performed to determine surface roughness for each of the wavelength regions. The method developed was found to be very efficient in quantifying the differences in plaques molded under varying processing conditions.

RTM for Class A Surface Finish

One low cost manufacturing process used to produce composite parts is the resin transfer molding (RTM) process. This process consists of injecting a thermoset resin at low pressure through a fibrous reinforcement (preform) placed in the mold cavity. Once the resin has impregnated the reinforcement, the composite part is cured and then de-molded at the end of this polymerization cycle. Although widely used in the aerospace industry, RTM is still not economically feasible for the high volume automobile industry. This is partly due to the difficulties related with process optimization, which requires an appropriate resin formulation for short cycle times, mold design and proper molding parameter selection. Also, for exterior car body panels it is difficult to achieve class A surface quality in compliance with the industry specifications and standards without sacrificing the stiffness and strength of the part.

There are numerous material and process variables which can potentially affect the surface quality in RTM molded components. Unsaturated polyester (UP) resins are the most common matrix materials used in automotive applications because of low cost and accelerated reaction rates, allowing faster and economical high volume production. However, a significant amount of shrinkage (7-10%) is common for UP resins, which results in components with inaccurate dimensions and poor surface finish. This shrinkage also results in fabric print through on the surface, which is another major contributing factor towards poor surface quality. Other common surface defects and possible contributing factors are listed in Table 6.1.

Low profile additives (LPA) are thermoplastic additives which are added to unsaturated polyester and vinyl ester resins to compensate for the cure shrinkage. Lucas et al. studied the effects of LPA and filler on polymerization reaction, mechanical properties and surface rugosities. Surface rugosity (surface quality) was measured using the Talysurf-120 device [11]. A glass plaque was used as a reference with R_a = 0.05 μm. No significant influence of LPA content was found on the cure kinetics. However, the filler decreased the induction time (time to start chemical reaction) and increased the rate of cure. Without the addition of LPA, the rugosity was measured to be R_a = 0.29 μm in the neat resin. For PVAc concentrations that resulted in shrinkage compensation, the measurements were reported between R_a = 0.06-0.08 μm. By adding both filler and PVAc, there was an improvement in surface finish. The surface finish was reported in the following order (neat resin < neat resin + filler < neat resin + filler+ LPA). Lucas et al. also found a critical concentration (8%) of LPA, which was needed for shrinkage compensation. No further improvement in the surface finish was observed when LPA level was increased above 8%. The effects of LPA content (between 0 and 40%) on cure kinetics, cure shrinkage, gel time, viscosity variations and morphological changes in Scott Bader PD9551 unsaturated polyester resin used in this research were studied and have been discussed in detail in [12]. It was observed that the LPA content had no significant affect on the cure kinetics and reaction rate in a range from 0-20%; however higher LPA content (40%) reduced the cure rate. A volumetric shrinkage of 9.5% was found in the polyester resin without LPA. A critical LPA amount of 10% was found for

complete shrinkage compensation. Resin formulations with less than 10% LPA showed a final shrinkage at the end of cure cycle. Resin formulations with LPA level higher than 10% showed a final expansion and had similar shrinkage-expansion behaviors. The shrinkage and shrinkage compensation was found to be a linear function of the degree-of-cure. Vallat et al. [13] reported on the effects of internal de-molding agents and $CaCO_3$ filler on the surface roughness of bulk molding compounds. No significant difference in the surface roughness was observed by increasing the amount of internal de-molding agent in the resin. The resin morphology was found to be different on the surface than in the bulk of the material. No LPA were found on the surface leaving a thin film of the resin; however filler and LPA were well dispersed through the thickness.

Kim et al. [14] investigated the effects of stacking sequence and fiber volume fraction of glass fiber mat on the surface quality of composite panels. Three different types of mats were used; however a satin weave on the outside gave the best finish. Ultimately, a composite bus housing panel was designed and manufactured by RTM and a stacking sequence for the fiber mat was determined which minimized fabric print through on the surface. Matthews et al. used statistical experimental design (SED) techniques to study the effect of various parameters on the degree of surface finish [15]. Gloss, surface roughness and mold filling times were taken as the response values. Roughness was measured using a laser profilometer. Fabric print through, shrinkage trenches, surface flow lines, filler filtration patches and pinholes were found to be the common problems contributing towards poor surface finish. This research established that gloss increased with the lower filler content, fiber volume fraction (V_f), mold temperature and higher injection pressure, whereas roughness reduced with higher filler content, injection pressure and with lower V_f and mold temperature. This work was further verified by Bayldon [5]. Higher filler content and injection pressures were confirmed to result in better surface finish.

The effect of LPA content and other process parameters on pressure variations during RTM manufacturing were investigated using design-of-experiments (the Taguchi

method) and are reported in [16]. A significant pressure increase was observed in the later stages of cure due to the LPA content in the resin. An optimum LPA concentration of 10% was found for the pressure increase which confirmed the results observed in [12]. An LPA content higher than 20% resulted in slower reaction rates. The measured pressure increase was a function of degree-of-cure. No pressure increase was observed below a degree-of-cure of 0.5 which proved the fact that LPA action started only after resin had become fully elastic as discussed in [12]. Injection pressure was found to have a significant effect on the cure gradient. The injections at high pressure levels (> 400 kPa) showed no significant cure gradient because of short injection times; however injections at low pressure levels (< 400 kPa) had a significant cure gradient along the length of the part which resulted in relatively smaller pressure increase at locations away from the injection port. The cure gradient was also seen to have a significant effect on the maximum pressure observed at different sensors locations. The sensors close to injection ports showed much higher pressures compared with sensors further away due to cure gradient. The gel time had the most significant effect on the total processing time. Resin formulations with shorter gel times resulted in short processing times. The total processing time increased linearly with increasing gel time. Karbhari et al. [17] studied the effect of material and process variables on the mechanical performance of RTM molded parts using the Taguchi method. Eight experiments were carried out to check the effect of seven 2-level factors. Parts were analyzed based on tensile failure stress; shear strength and maximum stress quality characteristics. Optimum levels of process parameters were determined and set, and validation experiments were carried out. The quality characteristics were found to be very close to theoretical values at optimum levels of process parameters. The Taguchi method was found to be an efficient and economical method for evaluating the relative importance and interaction of both process and performance related parameters.

The Taguchi method has also been applied successfully in various other fields of study, including all branches of engineering, along with applied and pure sciences. However, industrial and manufacturing product-and-process improvement has been the focal point of the Taguchi method's application. As an example, Jean et al. reported the

application of the Taguchi method for process optimization in high energy electron beam case hardening of cast iron [18]. The Taguchi method was compared with multiple regression techniques in predicting the response values. Both methods were found to be compatible; however multiple regression analysis resulted in less average error. The most significant factors were identified by using the Taguchi method. Predicted signal-to-noise ratios (SNR) was very close to the measured ratios [18]. Tsai et al. [19] investigated the application of the Taguchi method in simulation and optimization of a manufacturing system. Most recently, the Taguchi method has been successfully applied in process parameter optimization of a welding process [20], coil spring manufacturing process [21], hot forming process [22], injection molding process [23], die casting process [24], blow molding process [25], turning [26] and drilling operations [27]. Regression is also one of the most widely used statistical tools because it provides simple methods for establishing functional relationship among variables. It can be employed to develop a suitable model for predicting dependent variables from a set of independent variables.

Low profile additives show promises for cure shrinkage compensation of polyester resins. Previous research has shown that low profile additives, filler and higher injection pressures improve surface quality. Low profile additives used in this work have shown pressure increase in the later stages of the cure reaction; however the effects of LPA content and pressure increase on the surface quality still need to explored. Hence, the research efforts need to be focused on addressing the issue of class A surface finish in RTM which is very important to promote the wide spread use of low cost fiber glass composites in the automotive industry.

The objective of this paper is to investigate the effects of material and process parameters on the surface quality of RTM molded components. Several key parameters including LPA, styrene, filler, gel time, temperature gradient and injection pressure identified in a previous research [12,16] are used in test matrices designed through experimental design techniques to evaluate their relative influence on the surface finish of RTM panels. Test matrices are designed through the Taguchi method with parameters at both 2 and 3 levels. Levels are chosen based on the processing windows obtained through

analytical and numerical methods for different processing parameters reported elsewhere [12, 16, 28]. Analysis of variance (ANOVA) and multiple regression analyses are carried out on the surface roughness of test samples molded under varying conditions to evaluate the relative influence of each parameter. The most significant parameters which influence surface finish in RTM molded components are then characterized and empirical models are developed. The effects of post-cure shrinkage on the roughness of test samples are also investigated through oven post-curing. Process reproducibility is determined by manufacturing several test samples under optimum processing conditions.

6.2 Materials

Scott Bader PD9551 unsaturated polyester resin [29] was used in this work. The resin was supplied with a standard amount of LPA (10% wt. of resin). The low profile additive used in the resin was Scott Bader PD9419 polymer solution which contained poly vinyl-acetate (PVAc) and poly methyl-methylacrylate (PMMA) low profile additives. OMYA BLR2 calcium carbonate filler was added to the resin and standard accelerator (cobalt 2-ethylhexanoate) and catalyst (tert-butyl peroxybenzoate) were used. Composite panels were manufactured by RTM with F3P glass fiber preforms. The preform structure consisted of three layers of glass fibers as shown in Figure 6.1. The top layer (side-A) had a surface veil consisting of thin continuous glass fibers of an average diameter of 20 μm. The center layer consisted of chopped fiber bundles and the bottom layer (side-B) also had thin continuous individual glass fibers of an average diameter of 20 μm. The difference between side-A and side-B was that relatively higher binder concentration was present on side-B of the preform which could potentially affect the surface quality of the test samples. Hence, side-A was used for all the surface finish measurements. The weight fraction (w_f) of surface veil (9.2%) was much smaller compared to the weight fraction of structural mat (81.6%). The resin was mixed with the accelerator first and then the filler was added into it. The filler was mixed well with the resin mixture. At the end, the catalyst was added into the resin-filler mixture and mixed again. At this point the resin was ready for injection.

6.3 RTM Setup and Test Matrix

Composite test samples were manufactured using a heated steel mold mounted on a hydraulic press. The mold had a mirror like polished finish (class A finish) and was instrumented with type J thermocouples and Dynisco PT422 pressure sensors connected to a Vishay's System 6000 data acquisition system. The mold platens were heated to the required temperatures with a Conair circulating water heating system. The picture of the mold with its mounting on the press is shown in Figure 6.2. The resin at room temperature was injected into the mold cavity with a Radius Engineering constant pressure pneumatic-controlled injector [30]. The 3.175 mm thick picture frame was sealed using a Gore-Tex joint sealant gasket. A temperature gradient was created by moving the top and bottom platens away from each other and setting them at two different temperatures (from 75°C to 90°C). The bottom mold was kept at 90°C and top mold was heated at different temperatures based on the required gradient. The 24 cm by 26 cm F3P glass fiber preform was cut and placed inside the mold just before injection. Side-A of the preform was placed towards the hottest mold platen. The injection and vent ports were designed to create a uniform linear flow front though the fiber preform. The pressure sensors (PS1, PS2, PS3 and PS5) were located near the injection and vent ports and PS4 was mounted on the injection pump to measure injection pressure. The injections were performed at different injection pressure levels ranging from 200 to 650 kPa. The mold surfaces were cleaned with acetone and coated with a single layer of Chemlease 41-90 mold release agent. Manufactured composite panels were kept inside the mold until the resin achieved the maximum pressure level. A schematic and photograph of the picture frame, fiber preform, injection port, vent port and location of the pressure sensors is given in Figure 6.3. Resin tracers were used to verify the uniformity of the flow front.

6.3.1 Surface Roughness Measurement Procedure

A Taylor Hobson's Form Talysurf Series 2 stylus profilometer [31] was used to measure the roughness profile of the plaques. All the test samples were measured for surface finish at the same location. The location of the roughness measurement area on the test samples and direction of the scan lines is shown in Figure 6.4. Eight measurements were taken on each sample. Each scan was analyzed and the averages and standard deviations were calculated. The scan length was set at 100 mm. The distance between two consecutive scan lines was fixed at 10 mm. The speed of the stylus was kept at 1 mm/sec with a data sampling interval of 1 micron. Ultra Surface Finish software [31] was employed to calculate the roughness parameter R_a.

ISO 4287:96 standard was followed for surface finish measurements. A typical raw roughness profile is shown in Figure 6.5(a). The method for analyzing the surface scan consisted of leveling the raw data with the software to remove curvature and tilt effects from the raw data profile. A mean line was fitted in the data (Figure 6.5(b)) and five regions of wavelengths were then filtered from the leveled data. Standard cutoff wavelengths (ISO standard 4287:96) of 0.25 mm, 0.8 mm, 2.5 mm, 8 mm and 25 mm were used to filter out the wavelength regions. Each wavelength was then used to calculate the roughness parameter R_a. Using the cutoff wavelengths (λ_c) allowed for the calculation of the surface roughness for a specific wavelength region. Figure 6.5(c) shows the roughness profile obtained when mean line is subtracted from the raw profile. The roughness profile consists of several waveforms of different wavelengths superimposed on each other. Hence, cutoff wavelengths (based on ISO 4287:96) are used to extract various wavelength waveforms from the roughness profile as shown in Figure 6.5(d). The roughness waveform (Figure 6.5(d)) when added with the mean line (waviness profile Figure 6.5(b)) would result in the raw data profile.

6.3.2 Experimental Test Matrix

The parameters that can affect surface finish quality during RTM are divided in two categories: material parameters (e.g. LPA, styrene, filler and catalyst) and processing parameters (e.g. mold temperature, injection pressures and injection rates). In this study, LPA, styrene, filler, accelerator and catalyst (combined as gel time), injection pressure, and temperature gradient are considered. These six parameters are thought to be the most important in terms of their effect on surface finish, cost and cycle times.

A first test matrix with four experiments (L_4 test matrix) was designed with the Taguchi method to investigate the effects of three material parameters (LPA, styrene, filler) at two levels (Table 6.2). The four experiments and their respective conditions are presented in Table 6.3. LPA, styrene and filler added to the resin are based on the weight of the resin. The results of L_4 matrix were used to define a second test matrix of eighteen trials (L_{18} test matrix) with six parameters at three levels (Table 6.4). In L_{18} test matrix the maximum level of LPA was reduced from 40% to 20% and a broader range of filler from 0 to 40% was tested. Styrene can not be added more than 10% since it has detrimental effect on mechanical properties of composites so lower levels of styrene (0-8%) were used in the L_{18} test matrix. The levels of gel times were chosen to investigate the effects of reaction rate on the surface finish of molded test panels. Injection pressure levels were chosen to determine the effect of flow rate on the surface quality of the molded components. Table 6.5 tabulates all the experiments with each process parameter at a given level. The test panels were manufactured using the experimental setup discussed earlier. The fiber volume fraction for all the experiments was kept constant at 0.2.

6.3.3 Taguchi Analysis Procedure

As discussed earlier, roughness is characterized by the parameter R_a. A minimum value of R_a is desired for a good surface finish; hence the quality characteristic for

Taguchi analysis is "smaller-the-better". Since several measurements were taken on the single plaque, Taguchi's mean squared deviation (MSD) values need to be calculated to account for the variability in the measured data. The MSD formula for smaller-the-better quality characteristics is given in Equation 6.2.

$$MSD = \frac{1}{n}\sum_{i=1}^{n} R_{a,i}{}^{2} \tag{6.2}$$

where n is the number of trials or measurements under same conditions, $R_{a,i}$ is the roughness value obtained from each scan. MSD values are then used to calculate the signal-to-noise ratio (SNR). SNR is a crucial parameter for data analysis to take into account the variability arising from uncontrollable factors. SNR is used in the Taguchi method as a performance measure to choose control levels that best cope with noise. It takes both mean and variability into account. SNR is further used in Taguchi analysis to determine the percent effect of each input parameter on the output parameters. SNR for the smaller-the-better quality characteristic is given in Equation 6.3.

$$SNR = -10\log_{10}(MSD) \tag{6.3}$$

The multiplier 10 in Equation 6.3 is a scale factor and has no effect on the conclusions derived from the results. The negative sign in SNR formulation is used so that SNR always increases for decreasing MSD. For analysis purposes lower MSD and higher SNR values are desirable for minimum variability. SNR values are further used in Analysis of Variance (ANOVA) to determine the relative influence of process parameters on the output. A detailed description of ANOVA strategy and calculations is given by Roy [32]. In brief, ANOVA determines the variance caused by each parameter relative to the total variance observed in the results. The objective of ANOVA is to determine the most influential parameters on the surface roughness. Those parameters can then be used to model the behavior of output parameter (surface roughness R_a) as a function of the most influential input parameters using multiple regression techniques.

6.4 Results and Discussion

A typical raw data profile for experiments 1 and 4 (Table 6.5) is given in Figure 6.6. These two samples are chosen because visually the sample from experiment 1 had a very rough and poor surface quality, whereas the sample from experiments 4 was very shiny and smooth. This can be verified from the graph in Figure 6.6 where the raw profiles for the two samples are very different in terms of smoothness and fluctuations in the signal. Although there is long wavelength waviness associated with the signal yet it is very smooth with minimum fluctuations for the good finish sample (experiment 4), whereas the roughness signal for the test sample in experiment 1 is very noisy and full of disturbances and fluctuations. These signals are transformed into roughness and waviness values based on the procedure discussed in Section 6.3.1. The waviness and roughness profiles are plotted for experiment 1 (poor finish) in Figure 6.7. The raw data is plotted in Figure 6.7(a). The data is leveled to remove the tilt effects and is plotted in Figure 6.7(b). The long wavelength waviness is removed from the raw profile and the waviness profile is plotted in Figure 6.7(c). This waviness is basically the mean line in the plotted data. The waviness profile is subtracted from the leveled data and an overall roughness profile is obtained. This overall roughness profile is then separated into various profiles based on the cutoff wavelengths. The roughness profiles for 0.8, 2.5 and 8 mm cutoff wavelengths are plotted in Figure 6.7(d-f). Similarly, the roughness and waviness profiles for experiment 4 are plotted in Figure 6.8. For each of the roughness and waviness profile, parameters R_a and W_a are calculated. Roughness and waviness profiles completely describe the raw data profile of the test sample. R_a and W_a values are then used in ANOVA calculations to determine the effect of each input parameter on the surface roughness.

6.4.1 L_4 Test Matrix

Average roughness (R_a) and waviness (W_a) values for each experiment in L_4 test matrix and reference painted steel sample are given in Table 6.6 and plotted in Figure 6.9. The roughness values of all test samples (experiment 1-4) are very close (between 0.05-

0.1 μm) for short wavelength (between 0.25-2.5 mm). However, for longer wavelength region (between 8-25 mm) sample 1 and 2 (values between 0.11-0.27 μm) perform better than sample 3 and 4 (values between 0.18-0.42 μm). For short wavelength region (< 2.5 μm) all test samples are of the same order of magnitude as that of the reference sample whereas for long wavelength regions (> 2.5 μm including waviness) the test samples perform even better than the reference sample. The roughness values are higher for test samples in the short wavelength region compared with reference sample due to an even paint layer on the surface of the steel sample. Since long wavelength roughness and waviness is produced by the manufacturing process, the paint layer is unable to remove it. This analysis also shows that change in process parameter levels in the range tested has no significant effect or short wavelength roughness; however statistically significant effect can be observed for long wavelength roughness and waviness values.

Analysis of variance (ANOVA) is performed on SNR values calculated from roughness (R_a) and waviness (W_a) values for all cutoff wavelength regions to determine the effects of process parameters on surface roughness and waviness. ANOVA for all wavelength regions is presented in Table 6.7. The influence of different process parameters varies based on the wavelength region chosen which signifies the importance of other parameters for certain regions of interest. Overall, the most influential parameter is the LPA content followed by the filler content. Styrene although does not effect roughness, it has a significant influence on the waviness in the test samples. The effect of process parameters on average roughness values are plotted in Figures 6.10 and 6.11 for cutoff wavelengths of 2.5 and 25 mm. The roughness increases slightly (0.091-0.099 μm) when LPA level is increased from 10% to 40%; whereas roughness decreases slightly (0.1-0.09 μm) when filler level is increased from 20-30% for a cutoff wavelength of 2.5 mm. However, the roughness increases significantly (0.24-0.42 μm) with increasing LPA content when measured for a cutoff wavelength of 25 mm. Filler and styrene content has no significant effect on the surface roughness for this wavelength region. Based on these results, it can be deduced that the roughness increases with increasing LPA content and reduces with increasing filler content. This result is consistent with the findings of Dutiro

[4] and Matthews et al. [15]. The LPA content at 40% does not produce as good finish as that of 10%.

6.4.2 L_{18} Test Matrix

The manufactured test samples (Table 6.5) were characterized based on the visual inspection. Table 6.8 presents the relative evaluation of the samples based on the shine, degree of smoothness and the amount of dimples and pinholes on the surface. The samples are evaluated based on a scale of 1 to 7, 1 being the worst and 7 being the best. Based on this criteria, six samples (1,2,3,10,11,12) are easily distinguished from the rest due to the poor surface quality (Table 6.8); however rest all the samples are very shiny and smooth and it is difficult to differentiate among those samples through visual inspection. Hence, quantitative measurements are needed to distinguish between those samples. A comparison of visual inspection and surface roughness measurements show that the degree of smoothness and shine in the sample is related to the roughness at short wavelength ($\lambda_c < 2.5$ mm). The dimples and orange peel was related to the intermediate wavelengths ($0.25 < \lambda_c < 8$ mm), whereas the ripple was associated with the long cutoff wavelengths ($\lambda_c > 8$ mm).

Average roughness and waviness values for all wavelengths regions and for each test condition are presented in Table 6.9. Relatively much higher roughness and waviness values can be seen for experiment number 1, 2, 3, 10, 11 and 12. These six experiments are done with low profile additives at 5%. This can further be seen from Figure 6.12, where roughness values are plotted for each experiment of L_{18} matrix at a cutoff wavelength of 8 mm. A reference line is also drawn based on the roughness of reference steel sample at a cutoff wavelength of 8 mm. Samples 1-3 and 10-12 stand out and their roughness values are much higher than the reference sample, however all the other samples are quite close to the reference line. Same trend is observed for other cutoff wavelengths as shown in Figure 6.13. The samples can be divided into four categories based on their closeness to the reference. Sample # 8, 16 and 18 are included in category # 1, which are the best in terms of surface finish; however the samples in category # 2

(4,5,6,7,14,17) closely follow the first category. Samples in category # 3 (9,13,15) have relatively higher roughness values than category 1 and 2 and the roughness of samples in category # 4 (1-3,10-12) are way off from the other categories.

Roughness and waviness values for all wavelengths are further used to calculate signal-to-noise ratio (SNR). ANOVA is performed on SNR values and percent effect of each parameter is calculated. Table 6.10 presents the percent effect of each parameter on the surface roughness and waviness. The most significant parameters that influence surface roughness are LPA content, filler content and injection pressure. The variation in roughness as a function of the levels of most significant parameters for a cutoff wavelength of 2.5 mm is plotted in Figure 6.14. The results are also plotted for cutoff wavelength of 8mm and 25 mm in Figures 6.15 and 6.16 respectively. The interesting thing to note is the similarity between these graphs irrespective of the cutoff wavelength. The variation in roughness as a function of levels of LPA, filler and injection pressures are identical for all wavelengths. In fact, identical trends were observed for other cutoff wavelengths. The cutoff wavelengths above 2.5 mm are chosen for the analysis because they represent dimples and orange peel in the panel which severely affect the surface finish.

There is a significant decrease (0.9 to 0.1 μm for cutoff wavelength of 2.5 mm, 1.85 to 0.15 μm for cutoff wavelength of 8 mm and 3.6 to 0.46 μm for cutoff wavelength of 25 mm) in the roughness when the LPA content is increased from 5% to 10%. However, the decrease is relatively insignificant (0.1 to 0.095 μm for cutoff wavelength of 2.5 mm, 0.15 to 0.14 μm for cutoff wavelength of 8 mm and 0.46-0.34 for cutoff wavelength of 25 mm) when LPA content is increased from 10% to 20%, which suggests that LPA content at 10% is the critical amount needed for the shrinkage compensation and transition from rough to a smooth surface. After this critical amount relatively less improvement is observed in the surface quality. This result is consistent with the shrinkage-expansion behavior of low profile resin observed with rheology experimentation and pressure variations observed during RTM manufacturing [12, 16]. Filler and Injection pressure also affect surface finish and a linear relationship is observed for their amounts, which

means adding more filler improves surface finish and maintaining higher pressure also improves surface finish. This result is consistent with the findings of other researchers, who observed an improvement in surface finish by adding $CaCO_3$ filler and increasing injection pressure [4,5,11,15]. Lower injection pressures were seen to induce a cure gradient along the geometry of the sample which resulted in lower resin pressures away from the injection port [16]. Hence, there is a relationship between the cure gradient and surface roughness. Styrene content, gel time and temperature gradient have minimum effect on surface roughness as shown in Table 6.10. It can also be seen from this table that as the measurement wavelength increases, LPA becomes more influential, suppressing other parameters.

The most significant parameters that influence waviness are LPA content, styrene content and gel time (Table 6.10). The variation in waviness as a function of levels of the most influential parameters is plotted in Figure 6.17. It is interesting to note that the LPA content (most influential parameter) has similar effect on waviness as that of roughness. A significant decrease (from 14 to 2.84 μm) in waviness is observed when LPA level is increased from 5% to 10%; however relatively insignificant decrease (from 2.84 to 1.94 μm) occurs when LPA level is further increased from 10% to 20%. The styrene content has a significant influence (15%) on waviness. The waviness decreases with increasing styrene content. This result is consistent with the observation made with L_4 test matrix. The gel time has a non-linear effect on the waviness. The waviness decreases (from 6-3.6 μm) when the gel time is increased from 1-3 minutes; however waviness increases (from 3.6-9 μm) when gel time is further increased from 3-10 minutes.

Based on this analysis, 20% LPA, 4% styrene, 40% filler, 621 kPa injection pressure and a gel time at 3 minutes are the optimum conditions which would result in a minimum roughness and waviness in the test samples. However, the decrease in surface roughness and waviness is insignificant when LPA content is increased from 10% to 20% as shown in Figures 6.14-6.17. Hence, to reduce the material cost, 10% is considered to be the optimum LPA content that can be added into the resin to compensate for shrinkage and get good surface finish compared with a resin without LPA or resin with 5% LPA. In a

previous study, resin with 5% LPA showed no expansion behavior [12] and later no pressure increase was observed during manufacturing for this resin formulation [16]. A poor surface quality is visually observed and measured for the samples manufactured with this resin formulation, which means there is a direct relationship between the LPA content, expansion behavior of the resin, pressure variations and surface quality. This can be further verified from Figures 6.18 and 6.19.

The effects of LPA content on surface roughness and maximum pressure observed during RTM manufacturing [16] are plotted in Figure 6.18. It is interesting to note that the roughness and maximum pressure curves are exactly opposite to each other. The resin formulation with 5% LPA shows no pressure increase and a very rough surface (with an average roughness of 3.55 μm) is observed. When the LPA content is increased from 5-10%, pressure increases from 0-1.45 MPa and roughness decreases from 3.45-0.46 μm. By increasing LPA level from 10-20%, pressure further increases from 1.45-1.65 MPa and roughness decreases from 0.46-0.34 μm. However pressure reduces from 1.65-1.25 MPa and roughness increases from 0.34-0.41 for an LPA increase of 20-40%. This means that the LPA content has a significant effect on the pressure increase and surface roughness. Surface roughness and final cure shrinkage plotted on relative scales show that the curves are identical to each other as presented in Figure 6.19. The roughness and final cure shrinkage decrease with increasing LPA content (0-20%). However no significant decrease in roughness and final cure shrinkage is observed for the LPA content of 10-40%. Hence, it can be deducted that there is a direct relationship between LPA content, resin pressure, final cure shrinkage and surface roughness.

6.4.3 Multiple Regression Analysis

Multiple regression analysis fits a line to a series of points between values of one dependent variable and multiple independent variables. The method of least squares is used for curve fitting to reduce the sum of all squared deviations between measured and predicted results. A general regression model is given in Equation 6.4.

$$R_i = \beta_0 + \beta_1 x_{1i} + \beta_2 x_{2i} + \ldots\ldots\ldots + \beta_p x_{pi} \qquad (6.4)$$

$$i = 1,2,\ldots\ldots\ldots\ldots, n$$

where R_i is the response (roughness) corresponding to the i^{th} level of input variables (x_j) and β_j are regression constants. In the present study, multiple regression analysis was employed to predict surface roughness values based on the given parameter levels. Regression constants were estimated by least squares criterion and coefficients were tested using the following hypotheses.

$H_0 : \beta_1 = \beta_2 = \ldots\ldots\ldots\ldots\ldots = \beta_p = 0$

H_1 : at least one $\beta_j \neq 0$ for j = 0, 1, 2, ……., p

where H_0 refers to the null hypothesis where the response is independent of all input variables, hypothesis H_1 test the significance of input variables on the response and p is the total number of input variables. When all the regression constants are zero, the response is independent of the input variables.

STATGRAPHICS 5.0 was employed to analyze the data obtained with L_{18} experimental test matrix of the Taguchi method. An analysis of variance (ANOVA) is carried out based on multiple regression technique on the data for 8 mm cutoff wavelength which is converted into natural log scale. ANOVA is presented in Table 6.11. In this table, SS refers to the sum of squares, DOF refers to the degree of freedom and MS refers to the mean squares. These parameters are calculated through standard formulation given by Roy [32]. Based on mean squares, F-ratios and P-values are calculated. P-values are further used to test the significance of parameters based on the confidence interval. For example, when a confidence level of 95% is chosen for the analysis, all the parameters with P-values >0.05 become insignificant. In Table 6.11, the effect of squared term of LPA and interaction between injection pressure and filler level are also included. Since P-values of most of the parameters in Table 6.11 are <0.05, it means these parameters are significant parameters at 95% confidence interval. The P-values in Table 6.11 test the null hypothesis H_0: $\beta_j = 0$, j = 0, 1, 2……., p against an

alternative H_1: $\beta_j \neq 0$. The data from Table 6.11 shows that B and D which represent amount of styrene and gel time are insignificant since their P-values are greater than 0.05 at 95% confidence interval; however for further analysis temperature gradient is also neglected since it was found an insignificant parameter for other wavelengths. The same parameters were found to be insignificant for 2.5 and 25 mm cutoff wavelengths. These parameters can be excluded from the analysis. ANOVA table is modified and is presented in Table 6.12. P-values of all the parameters shown are below 0.05, which means that all these parameters are significant at 95% confidence level which rejects the null hypothesis H_0. An empirical model can be developed based on the significant parameters and interactions. STATGRAPHICS software is used to model the input and output behavior. The general form of the model is given in Equation 6.5.

$$R_a = e^{\left(\beta_0+\beta_1 A^2+\beta_2 A+\beta_3 C+\beta_4 F+\beta_5 CF\right)} \tag{6.5}$$

where R_a refers to the surface roughness in μm, β_0, β_1, β_2, β_3, β_4, β_5 are constants and are estimated by the least squares method. Variable A refers to the amount of LPA, C refers to the amount of filler and F refers to the injection pressure. Since the P-values in the ANOVA Table 6.12 are less than 0.05, there is a statistically significant relationship between the variables at 95% confidence level. Similar analysis is carried out for 2.5 and 25 mm cutoff wavelengths. Tables 6.13-6.15 present the estimated parameters of roughness model (Equation 6.5) for 2.5, 8 and 25 mm cutoff wavelengths, respectively.

The adjusted R-squared statistic indicates that the model as fitted explains 96% of the variability in $Ln(R_a)$. A graph is plotted between the measured and predicted roughness values based on Equation 6.5 for 8 mm cutoff wavelength. A very close match can be seen in the graph shown in Figure 6.20, which means the model closely predicts roughness of composite samples based on the levels of significant parameters. The same trend is observed for 2.5 and 25 mm cutoff wavelengths.

6.4.4 Optimum Process Conditions and Model Verification

Material and process parameters can be selected based on the previous analyses to reduce cost, cycle time and achieve high finish quality. As was seen previously, increasing the amount of filler and higher injection pressure resulted in better surface finish, so the filler level was selected at 40% and injection pressure was set at 621 kPa. Although 20% LPA resin resulted in slightly better surface quality, however this LPA level was not used for optimal results. LPA are expensive additives and increasing the amount of LPA twofold would double the cost of the resin which is not worthwhile considering the improvements it gives. Accelerator and catalyst were added into the resin for a gel time range of 3 minutes and temperature gradient was set at 15°C with the bottom mold at 90°C and the top mold at 75°C. Five injections were done under identical conditions. The roughness values for 0.25 and 25 mm wavelength regions for all samples are shown in Figure 6.21. Roughness values for both wavelengths for all samples are very close to each other; hence a straight line can be drawn through all the data points. This shows that the manufacturing system is very stable and capable of reproducing same results under identical processing conditions.

The surface roughness of the reference sample and the composite sample is presented in Table 6.16. As seen in an earlier study [12], the maximum degree-of-cure achieved during resin processing was about 0.9, which means these composite samples need post-curing before they could be used in actual applications. Hence, all the samples were post-cured at 110°C for two hours and their roughness was measured again. The roughness results of post-cures samples are also presented in Table 6.16. The roughness values of composite sample with and without post cure are very close to each other and are of the same order of magnitude for small wavelength measurements (wavelengths < 2.5 mm) as that of the reference sample as shown in Figure 6.22. However, at higher wavelengths, composite samples without post-curing resulted in even better surface finish than the reference sample. When the composite sample went through post-curing, its short wavelength roughness was not significantly affected by the post curing. However at longer wavelengths, it showed more waviness compared to the sample without post-curing. The roughness R_a values of post-cured composite samples were still close to the

reference sample in the high cutoff wavelength region, which means that even after post-curing, the composite sample was in class A region for higher wavelength measurements. Based on the analysis of all the test samples from the L_{18} test matrix and the reference sample, R_a values can be set for class A surface finish when measured with a stylus profilometer for different cutoff wavelength regions. The values are shown below;

$R_a \leq 0.1$ μm for $\lambda_c \leq 2.5$ mm

$R_a \leq 0.25$ μm for 2.5 mm $< \lambda_c \leq 8$ mm

$R_a \leq 0.6$ μm for 8 mm $< \lambda_c \leq 25$ mm

It was impossible to distinguish between different samples whose R_a values were less than 0.1 μm for smaller cutoff wavelength regions through visual inspection. However the breakdown of roughness R_a values based on different cutoff wavelength regions provided a good measure of differences among various samples. Based on these criteria, five test conditions (6, 8, 14, 16 and 18) from Table 6.5 and 6.9 would result in class A surface finish at every cutoff wavelength.

Figure 6.22 also presents a comparison between the measured and predicted R_a values for the composite plate without post-cure. The measured R_a values (0.07, 0.1, 0.34 μm) and predicted (0.07, 0.12, 0.40 μm) are very close for cutoff wavelengths of 2.5, 8 and 25 mm with an error of about 11%. Hence, the model is quite accurate and can be used to adequately predict the roughness of manufactured panels for different wavelengths. A close match between the measured and predicted (Equation 6.5) R_a values is also obtained for different levels of parameters in L_{18} matrix as shown in Figures 6.14-6.16.

6.5 Conclusion

The Taguchi method and multiple regression analysis techniques were employed successfully to sort out parameters based on their significance on the output parameter. The most significant parameter affecting surface roughness was found to be the LPA content. There was a significant improvement observed in roughness when LPA level was increased from 5% to 10%. However, the improvement in surface roughness was not

significant between 10% and higher LPA levels. This inference is consistent with the shrinkage-expansion data obtained from rheometer [12] and pressure increases observed during RTM manufacturing [16]. Surface finish also improved with increasing amounts of filler and injection pressures but to a least degree as compared to the effect of LPA. Roughness R_a limits were set for class A surface finish based on the measurements of a standard painted steel sample. Based on these criteria, only six samples showed a class A surface finish. To reduce cost and process cycle time, a minimum amount of LPA (10%) can be added to the resin. The higher levels of filler are also beneficial for getting good surface quality as well as for reducing costs. Post-curing did not affect short wavelength roughness however it had a significant affect on long wavelength waviness. The composite sample was still considered to be in the class A surface finish region even after post-curing. The empirical model developed with a multiple regression technique was found to be quite accurate in predicting surface roughness values in the range of the parameters tested. The Taguchi method and multiple regression both resulted in same set of significant parameters.

6.6 Acknowledgements

This work was made possible with the financial support from the Auto21 Network of Centers of Excellence and Ford Motors. Dr. Helmi Attia and Danen Chellan of AMTC-NRC are gratefully acknowledged for equipment and technical support. The authors would also like to thank Dr. Michael Debolt of Ford motor company and Mr. Eric St-Amant of McGill Composite Materials and Structure Laboratory for technical input on this project.

References

1. Kendall K, Johnson K. Composite Applications for the Aston Martin DB9. JEC Composites 2004;11:50-52.
2. Strong A. Fundamentals of Composite Manufacturing: Materials, Methods and Applications. Society of Manufacturing Engineers, 1989, Michigan, USA.
3. Tari MJ, Bals A, Park J, Lin MY, Hahn HT. Rapid Prototyping of Composites Parts using Resin Transfer Molding and Laminated Object Manufacturing. Composites Part A 1998;29A: 651-661.
4. Dutiro C. Factors affecting Surface Finish of RTM Products. M.Sc. Thesis, Imperial College of Science Technology and Medicine, University of London, September 1995.
5. Bayldon JM. An in-depth Study of Surface Finish in Resin Transfer Moulding, M.Sc. Thesis, Imperial College of Science Technology and Medicine, University of London, September 1996.
6. Neitzel M, Blinzler M, Edelmann K, Hoecker F. Surface Quality Characterization of Textile-Reinforced Thermoplastics. Polymer Composites 2000;21(4):630-635.
7. Whitefield RJ. Non-Contact Optical Profilometer. Applied Optics;14(10): 2480-2485.
8. Debolt MA. Surface Finish Evaluation Method for Class A Composite Substrates. Proceedings of 36th International SAMPE technical conference, 2004, San Diego, USA.
9. SURFPAK-SV/PRO/SJ Surface Texture Parameter User's Manual, Mitutoyo Corporation, Japan.
10. Gong H, Shushan M. Measurement of Surface Roughness, China Measurement Publisher, 1998.
11. Lucas J, Borrjo J, Williams R. Cure of Unsaturated Polyester Resins: 2. Influence of Low Profile Additives and Fillers on the Polymerazation Reaction, Mechanical Properties and Surface Rugosities. Polymer 1993;34(9):1886-1890.
12. Haider M, Hubert P, Lessard L. Cure Shrinkage Characterization and Modeling of a Polyester Resin Containing Low Profile Additives, Composites Part A, (submitted).
13. Vallat MF, Schultz J, Mauzac C, Jacquin M. Characterization of the Surface of Bulk Molding Compounds. Polymers for Advanced Technologies 1999;10(1):237-243.
14. Kim PJ, Lee DG. Surface Quality and Shrinkage of the Composite Bus Housing Panel Manufactured by RTM. Composite Structures 2002;57(1):211-220.
15. Matthews FL, Dutiro C, Alaka RN. Factors Controlling Surface Finish in Resin Transfer Molding. SAMPE Journal 1997;33(5):19-24.
16. Haider M, Hubert P, Lessard L. An Experimental Investigation for Class A Surface Finish in Resin Transfer Molding Process, Composite Science and Technology (submitted).
17. Karbhari VM, Slotte SG, Steenkamer DA, Wilkins DJ. Effect of Material, Process and Equipment Variables on the Performance of Resin Transfer Molded Parts. Composites Manufacturing 1992;3(3):143-152.
18. Jean MD, Tzeng Y-F. Use of Taguchi Methods and Multiple Regression Analysis for Optimal Process Development of High Energy Electron Beam Case Hardening of Cast Iron. Surface Engineering 2003;19(2):150-156.
19. Tsai CS, Mort N. Simulation and Optimization in Manufacturing Systems using Taguchi Methods, Proceedings of UKACC International Conference on Controls, 1996, UK, 467-472.
20. Tarng YS, Juang SC, Chang CH. The Use of Grey-Based Taguchi Methods to Determine Submerged Arc Welding Process Parameters in Hard-facing. Journal of Materials Processing Technology 2002;128:1-6.
21. Caporaletti L, Gillenwater E, Jaggers J. The Application of Taguchi Methods to a Coil Spring Manufacturing Process. Production and Inventory Management Journal 1993;34(4):22-27.

22. Anthony J, Warwood S, Kernandes K, Rowlands H. Process Optimization using Taguchi Methods of Experimental Design. Work Study 2001;50(2):51-57.
23. Huang MC, Tai CC. The Effective Factors in the Warpage Problem of an Injection Molded Part with a thin Shell Feature. Journal of Materials Processing Technology 2001;110:1-9.
24. Syrcos GP. Die Casting Process Optimization using Taguchi Methods. Journal of Materials Processing Technology 2003;135:68-74.
25. Cheng YJ, Xiang C, Tsung H, Francis T. Optimization of Extrusion Blow Molding Processes using Soft Computing and Taguchi Method. Journal of Intelligent Manufacturing 2004;15(5):625-634.
26. Lin CL. Application of the Taguchi Method and Grey Relational Analysis to Optimize Turning Operations with Multiple Performance Characteristics. Materials and Manufacturing Processes 2004;19(2):209-220.
27. Huang MF, Lin TR. Application of Grey-Taguchi Method to Optimize Drilling of Aluminum Alloy 6061 with Multiple Performance Characteristics. Materials Science and Technology 2004;20(4):528-532.
28. Haider M, Ruiz E, Hubert P, Lessard L. Numerical Simulations for Class A Surface Finish in Resin Transfer Molding Process, Composite Science and Technology (submitted).
29. Scott Bader, Provisional Data Sheet PD9551 - R&D Group, Fax transmission, August 2002.
30. Specification Sheet, 2100cc Pneumatic RTM Injector, Radius Engineering, Utah USA, 2004.
31. User Manual, Taylor Hobson Series 2 Surface Profilometer, 2004.
32. Roy RK. Design of Experiments using the Taguchi Approach: 16 steps to Product and Process Improvement, 2001, John Wiley and Sons, New York, USA.

Table 6.1 Common surface defects and possible causes

Defects	Possible Contributing Factors
Pinholes	Coarse particles, particle agglomeration
Ripple or long range waviness	Resin shrinkage, glass fiber dispersion
Sink marks	Resin shrinkage, fiber distribution, fiber length, fiber orientation
Fabric print through	Resin shrinkage, fiber bundle integrity, strand dimensions, fiber distribution, high fiber volume fraction
Variable localized fiber volume fraction	Fiber washout due to high flow rates and injection pressures
Dark areas	Styrene loss from the surface
Pop up blisters in painted surfaces	Subsurface voids due to trapped air and volatiles
Dimensional inaccuracy	Warpage and resin shrinkage
Dry spots	Poor resin flow and impregnation, race tracking and edge flow, sharp corners in the mold
Resin overflow	Irregular resin film on the surface due to cure gradient
Rough surfaces	Poor mold finish
Dull surfaces	Mold coated with too much release agent or mold sealant

Table 6.2 Parameters and levels for L_4 matrix

Parameters	Level 1	Level 2
LPA (%)	10	40
Filler (%)	20	30
Styrene (%)	0	10

Table 6.3 L_4 experimental test matrix

Experiment #	LPA (%)	Filler (%)	Styrene (%)
1	10	30	0
2	10	20	10
3	40	30	10
4	40	20	0

Table 6.4 Parameters and levels for L_{18} matrix

Parameters	Symbol Used	Level 1	Level 2	Level 3
LPA (%)	A	5	10	20
Styrene (%)	B	0	4	8
Filler (%)	C	0	20	40
Gel time (min)	D	1	3	10
Temperature gradient (°C)	E	5	10	15
Injection pressure (kPa)	F	207	414	621

Table 6.5 L_{18} experimental test matrix

Exp. #	LPA (%)	Styrene (%)	Filler (%)	Gel time (min)	Temperature gradient (°C)	Injection pressure (kPa)
1	5	0	0	1	5	207
2	5	4	20	3	10	414
3	5	8	40	10	15	621
4	10	0	0	3	10	621
5	10	4	20	10	15	207
6	10	8	40	1	5	414
7	20	0	20	1	15	414
8	20	4	40	3	5	621
9	20	8	0	10	10	207
10	5	0	40	10	10	414
11	5	4	0	1	15	621
12	5	8	20	3	5	207
13	10	0	20	10	5	621
14	10	4	40	1	10	207
15	10	8	0	3	15	414
16	20	0	40	3	15	207
17	20	4	0	10	5	414
18	20	8	20	1	10	621

Table 6.6 Average roughness and waviness values for L_4 matrix at all cutoff wavelengths

Experiment No.	Average Roughness (μm)					Average Waviness (μm)
	0.25	0.8	2.5	8	25	
1	0.0736	0.0729	0.0826	0.1097	0.2251	1.5331
2	0.0775	0.0835	0.1009	0.1441	0.2689	1.3197
3	0.0618	0.0701	0.0963	0.1790	0.4012	0.8119
4	0.0564	0.0692	0.1036	0.2047	0.4226	1.7217
Reference steel sample	0.0101	0.0198	0.0607	0.2281	0.5666	3.9115

Table 6.7 Effects on roughness (%) obtained from ANOVA for L_4 matrix at all cutoff wavelengths

Parameters	Roughness (%)					Waviness (%)
	0.25	0.8	2.5	8	25	
LPA	89	57	25	78	94	20
Filler	1	16	60	19	5	19
Styrene	10	27	13	2	1	61

Table 6.8 Visual inspection data for L_{18} matrix

Exp. #	Sink Marks	Print through	Shine	Pin holes	Dimples	Ripple	Degree of smoothness
1	1	1	1	1	1	3	1
2	2	2	1	2	2	4	2
3	1	2	2	2	2	4	3
4	6	5	5	4	4	6	6
5	6	5	6	6	5	6	6
6	6	6	6	6	6	5	7
7	4	5	4	5	5	6	6
8	5	5	5	5	6	6	6
9	5	6	4	5	4	6	5
10	2	3	1	3	2	3	2
11	2	2	1	3	2	3	2
12	2	2	1	3	2	2	2
13	6	6	6	5	6	5	6
14	6	6	6	5	6	6	6
15	5	6	5	4	5	5	5
16	6	6	7	6	6	6	7
17	6	6	5	5	5	5	5
18	5	5	6	6	6	6	6

SCALE

1---- worst
2---- worse
3---- bad
4---- fair
5---- good
6---- better
7---- best

Table 6.9 Average roughness and waviness values for L_{18} matrix at all cutoff wavelengths

Experiment No.	Average Roughness (μm)					Average Waviness (μm)
	0.25	**0.8**	**2.5**	**8**	**25**	
1	0.5790	1.3232	2.2928	4.1193	7.6500	22.9940
2	0.3693	0.6025	1.0054	2.2981	4.2273	8.5707
3	0.1687	0.2153	0.3125	0.7588	1.8851	12.4354
4	0.0872	0.0978	0.1160	0.1716	0.3712	1.6744
5	0.1091	0.1679	0.0766	0.1388	0.4477	3.0375
6	0.0862	0.0806	0.0837	0.1340	0.3722	2.2379
7	0.1377	0.0670	0.0831	0.1425	0.3374	2.4704
8	0.0853	0.0706	0.0721	0.1142	0.2602	1.7371
9	0.1791	0.1378	0.1266	0.2055	0.6080	4.1327
10	0.1801	0.2366	0.4187	1.1949	2.5742	29.3598
11	0.1950	0.2802	0.4700	1.0167	1.7916	4.4125
12	0.2973	0.4447	0.7174	1.7579	3.1797	5.5559
13	0.1056	0.0891	0.0865	0.1481	0.5130	3.9771
14	0.0650	0.0645	0.0796	0.1513	0.3908	3.4729
15	0.1841	0.1507	0.1387	0.2039	0.6776	2.6368
16	0.0816	0.0709	0.0671	0.0947	0.2579	1.2894
17	0.2081	0.1512	0.1241	0.1890	0.3592	1.1874
18	0.0764	0.0780	0.0812	0.1064	0.2049	0.7909
Reference steel sample	0.0101	0.0198	0.0607	0.2281	0.5666	3.9115

Table 6.10 Effects on roughness (%) obtained from ANOVA for L_{18} matrix at all wavelengths

Parameters	Roughness (%)					Waviness (%)
	0.25	0.8	2.5	8	25	
LPA	70	88	92	91	96	80
Styrene	0	0	0	0	0	15
Filler	19	6	2	1	0	0
Gel time	0	0	0	0	0	5
Temperature gradient	4	0	3	4	1	0
Injection pressure	7	6	3	4	3	0

Table 6.11 ANOVA for average roughness (R_a) values of 8 mm wavelength roughness based on multiple regression analysis

Variables	SS	DOF	MS	F-Ratio	P-Value
A	14.099	1	14.099	480.47	0.000
A^2	8.617	1	8.617	293.65	0.000
B	0.047	1	0.047	1.60	0.240
C	0.938	1	0.938	31.97	0.000
D	0.042	1	0.042	1.43	0.260
E	0.462	1	0.462	15.74	0.003
F	0.529	1	0.529	18.03	0.002
C*F	0.223	1	0.223	7.60	0.022
Errors	0.2641	9	0.029		

Table 6.12 Updated ANOVA based on multiple regression analysis

Variables	SS	DOF	MS	F-Ratio	P-Value
A	14.099	1	14.099	203.939	0.000
A^2	8.617	1	8.617	124.643	0.000
C	0.938	1	0.938	13.568	0.003
F	0.529	1	0.529	7.652	0.017
C*F	0.208	1	0.208	3.006	0.044
Errors	0.830	12	0.069		

Table 6.13 Estimated parameters of roughness model for 2.5 mm wavelength

Constants	β_0	β_1	β_2	β_3	β_4	β_5
Values	3.7691	0.0243	-0.7436	-0.0343	-0.0017	4.097×10^{-5}

Table 6.14 Estimated parameters of roughness model for 8 mm wavelength

Constants	β_0	β_1	β_2	β_3	β_4	β_5
Values	5.1038	0.0282	-0.8675	-0.0312	-0.0018	4.162×10^{-5}

Table 6.15 Estimated parameters of roughness model for 25 mm wavelength

Constants	β_0	β_1	β_2	β_3	β_4	β_5
Values	5.1878	0.02058	- 0.6667	- 0.0394	- 0.00254	6.7318×10^{-5}

Table 6.16 Roughness comparison between composite sample with and without post-cure and reference steel sample

Cutoff Wavelength (mm)	Reference Steel Sample (μm)	Composite Sample (μm)	
		Before post-cure	After post-cure
0.25	0.0101	0.0738	0.0873
0.8	0.0198	0.0661	0.0841
2.5	0.0607	0.0692	0.1370
8	0.2281	0.1097	0.2606
25	0.5666	0.3425	0.5661

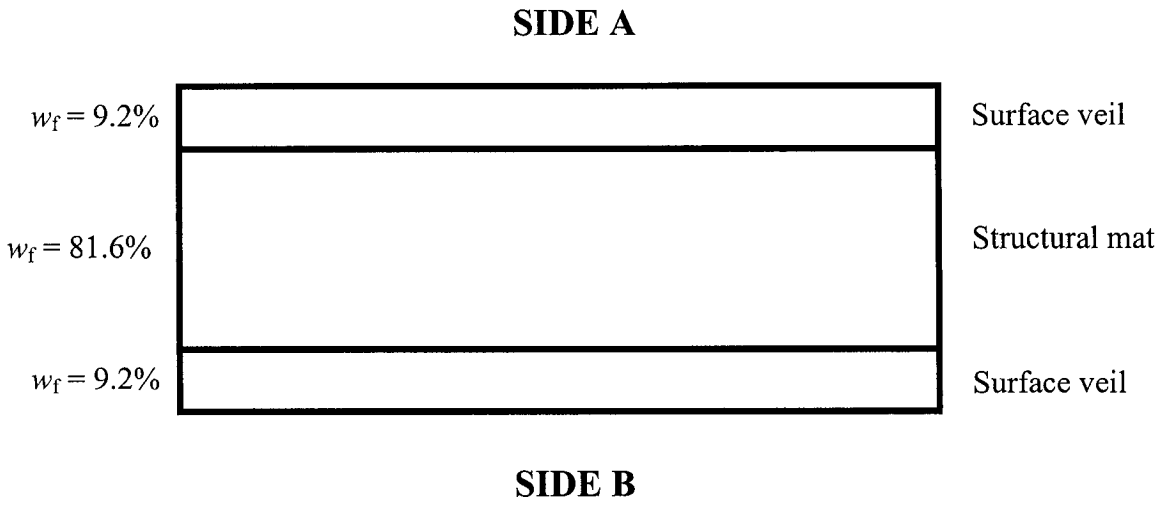

Figure 6.1 Through thickness structure of the F3P glass fiber preform

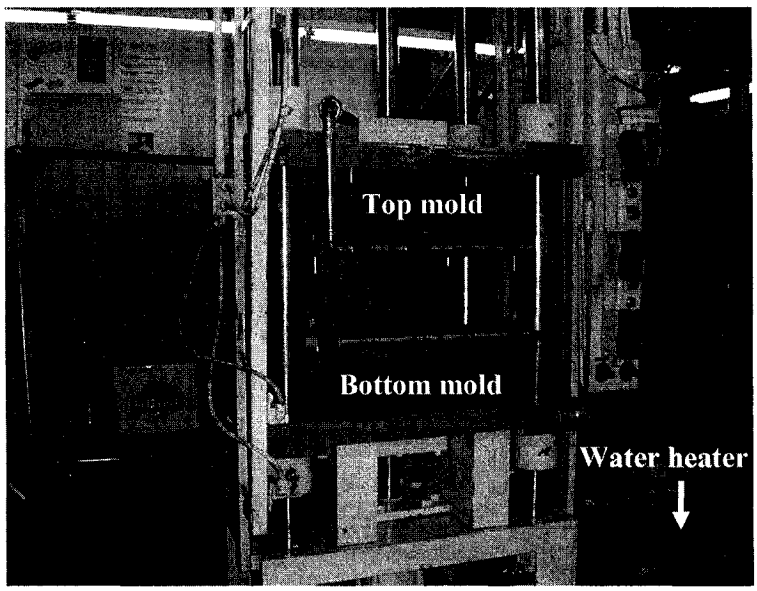

(a)

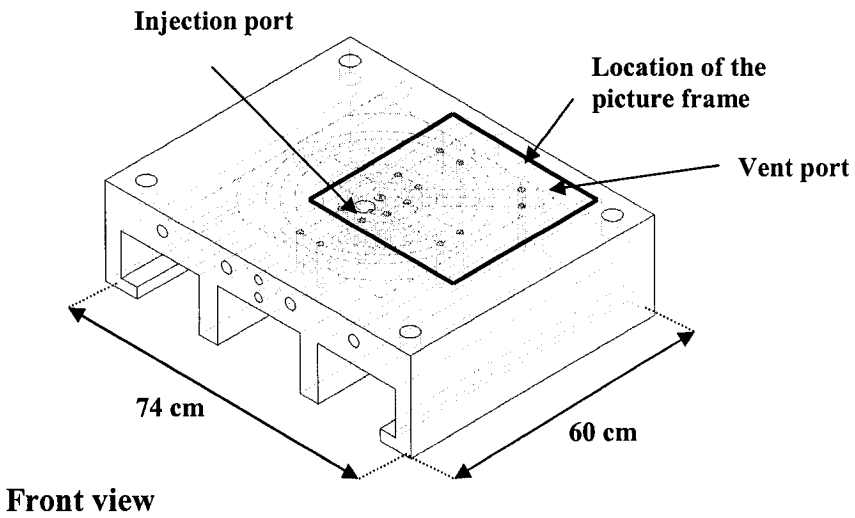

(b)

Figure 6.2 (a) Mold mounting on the press, (b) Diagram of the mold

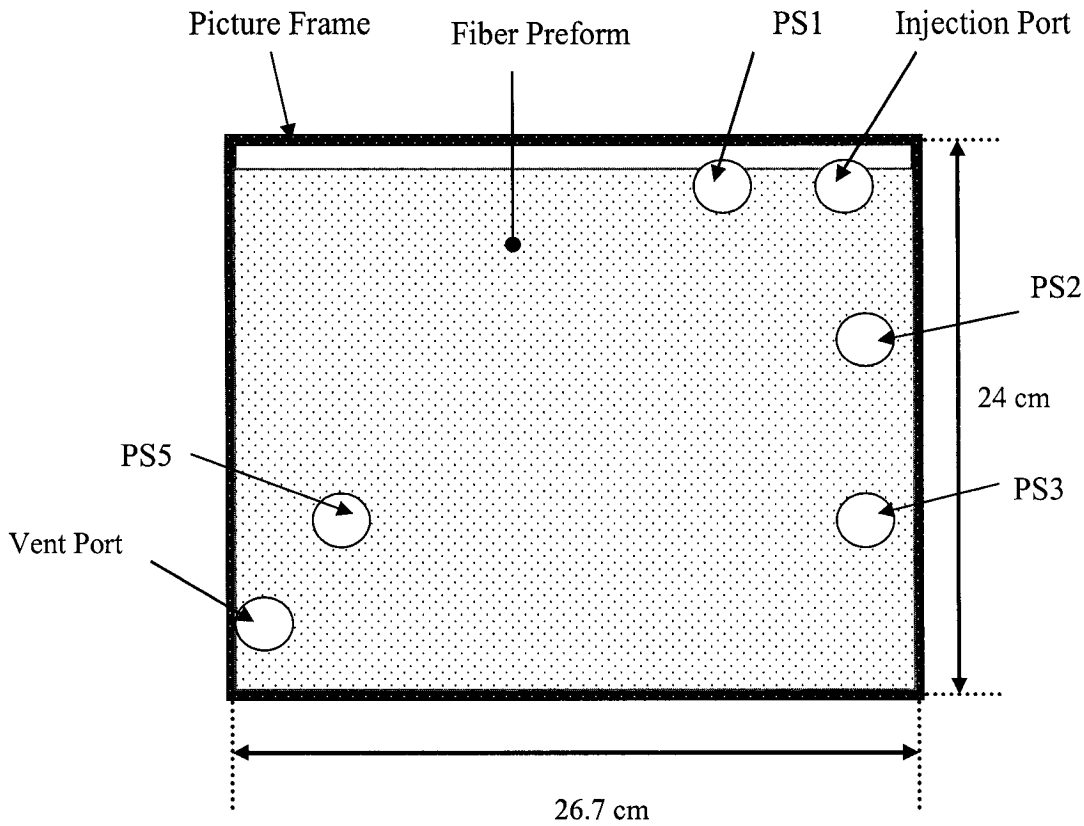

(a)

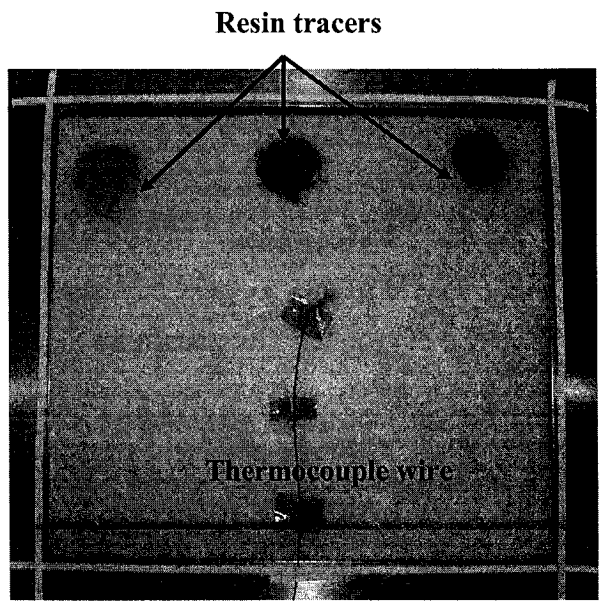

(b)

Figure 6.3 (a) Schematics of the picture frame, injection port, vent port and location of pressure sensors (PS), (b) Snapshot of the picture frame with preform and sealant

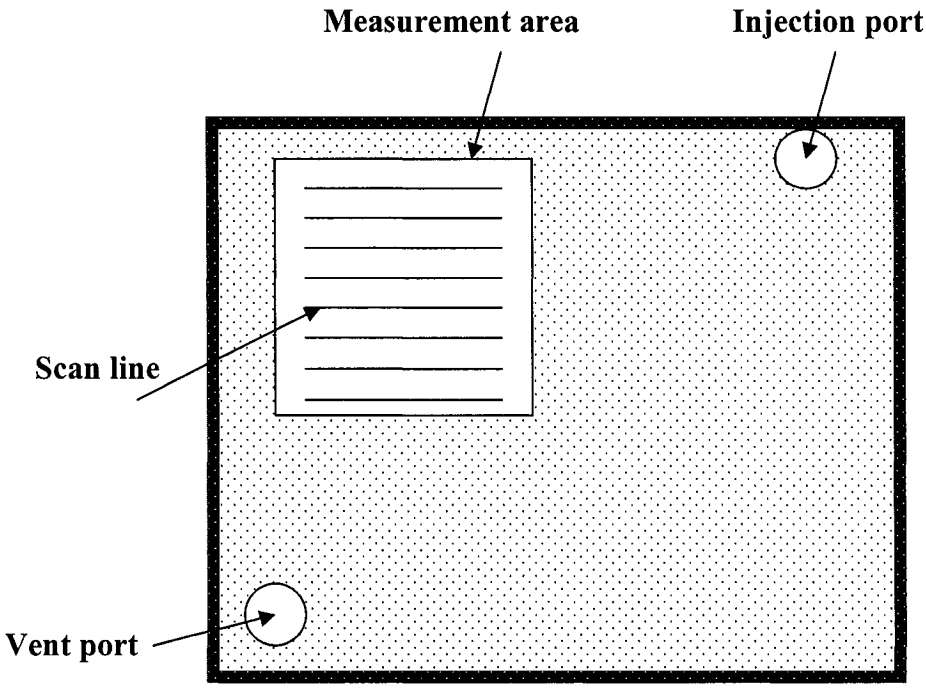

Figure 6.4 The location of the roughness measurement area and direction of the scan lines on the molded sample

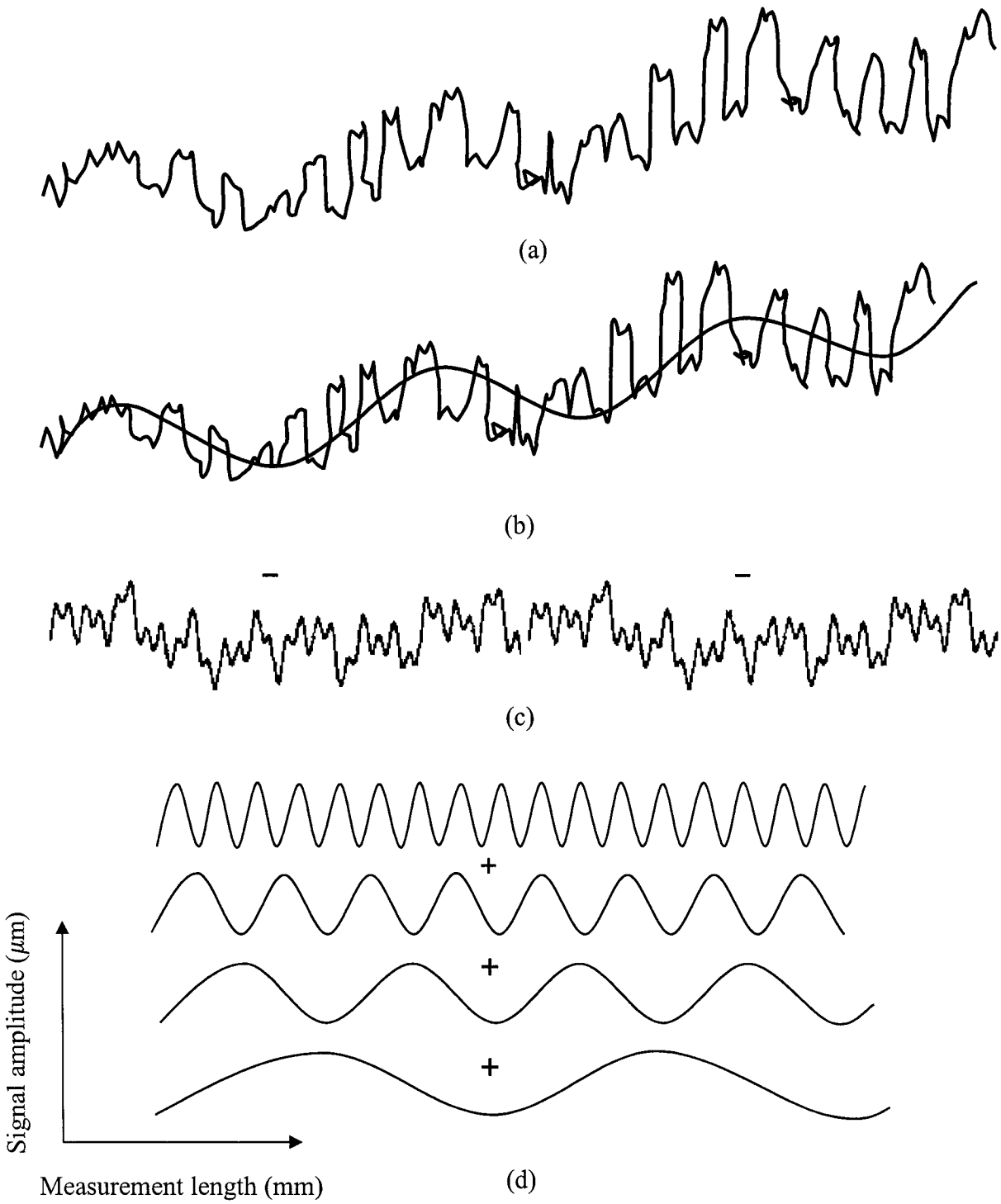

Figure 6.5 (a) A typical raw roughness profile (b) mean line in the raw profile to extract waviness (c) Roughness profile without waviness (d) division of the roughness profile into several wavelengths based on the cutoff wavelength

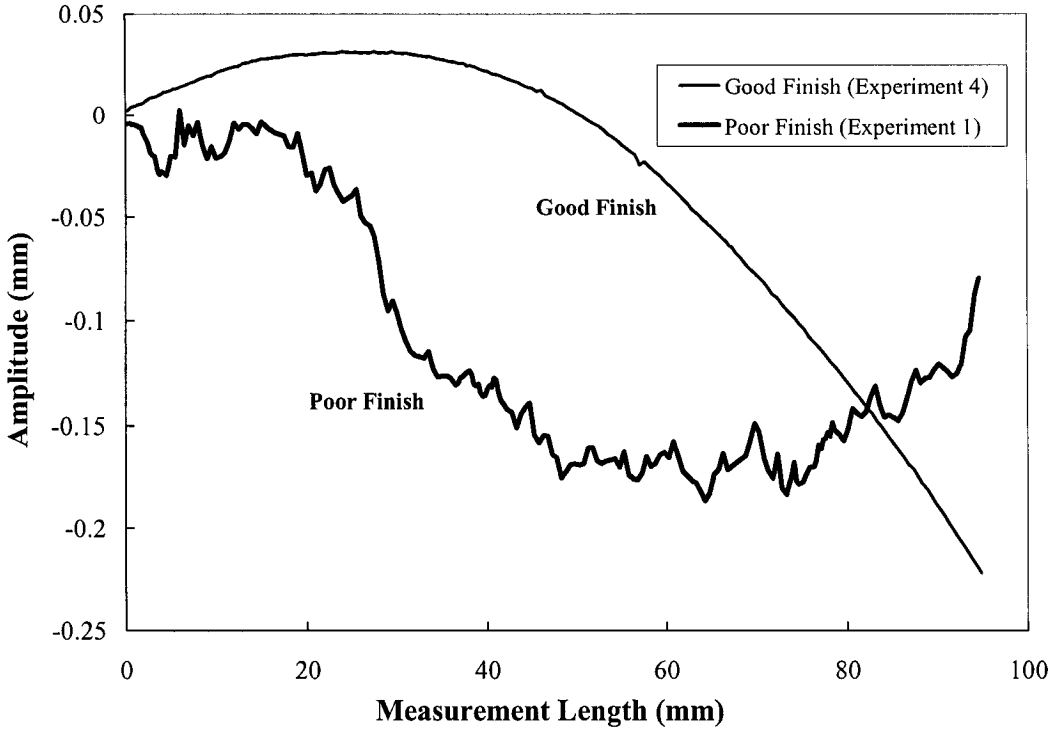

Figure 6.6 Raw roughness profile obtained for a very rough surface (experiment 1) and a very smooth surface (experiment 4)

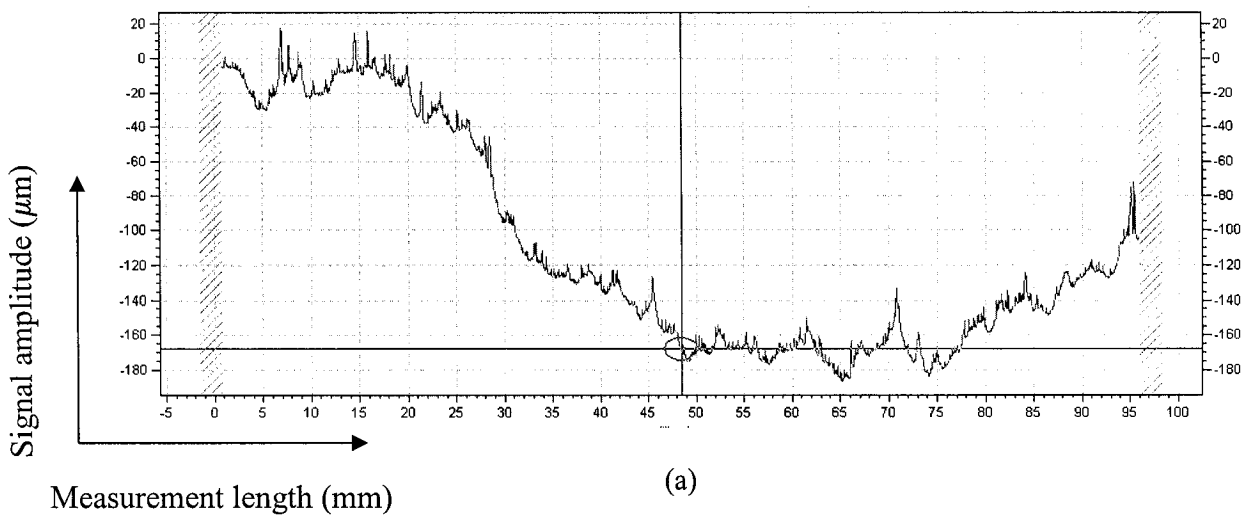

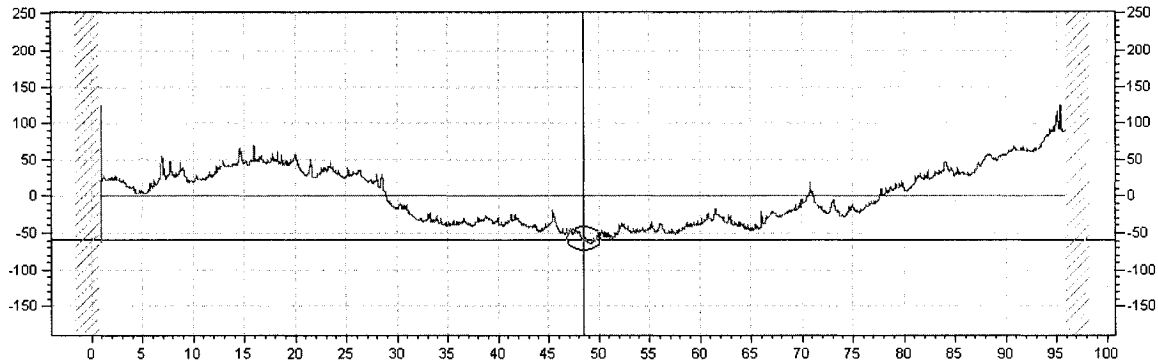
250
200
150
100
50
0
-50
-100
-150
0 5 10 15 20 25 30 35 40 45 50 55 60 65 70 75 80 85 90 95 100

(b)

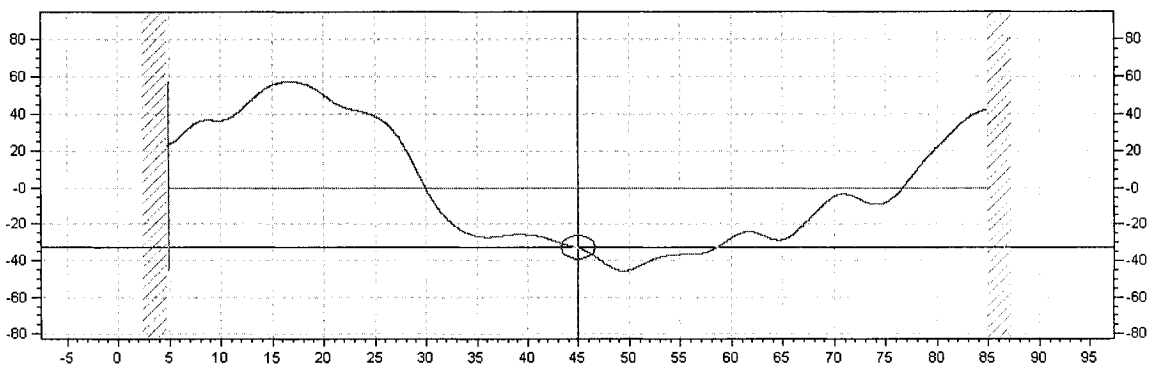
80
60
40
20
-0
-20
-40
-60
-80
-5 0 5 10 15 20 25 30 35 40 45 50 55 60 65 70 75 80 85 90 95

(c)

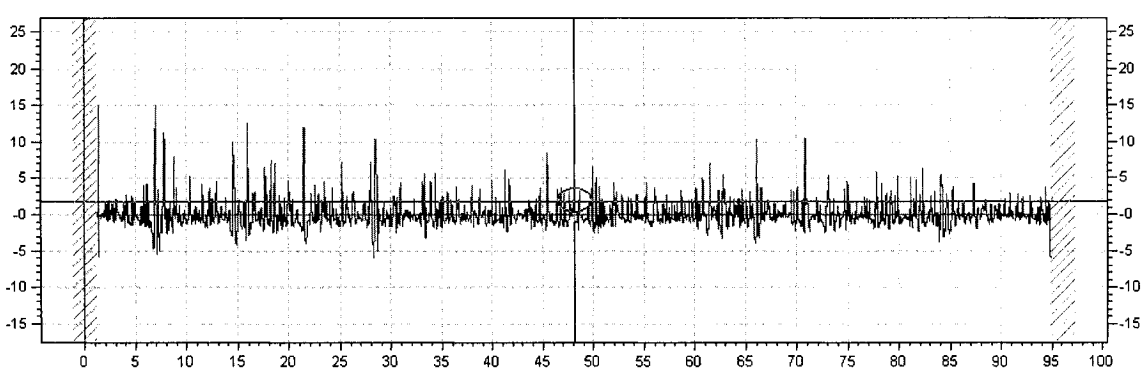
25
20
15
10
5
-0
-5
-10
-15
0 5 10 15 20 25 30 35 40 45 50 55 60 65 70 75 80 85 90 95 100

(d)

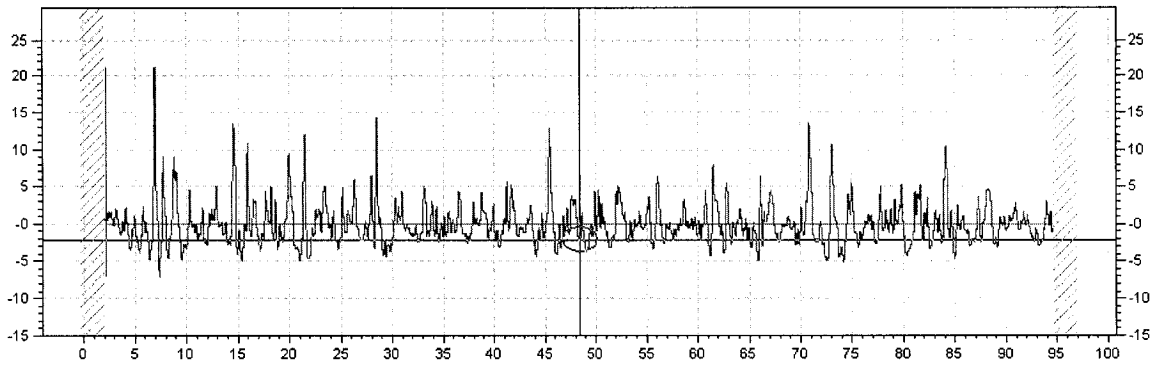

(e)

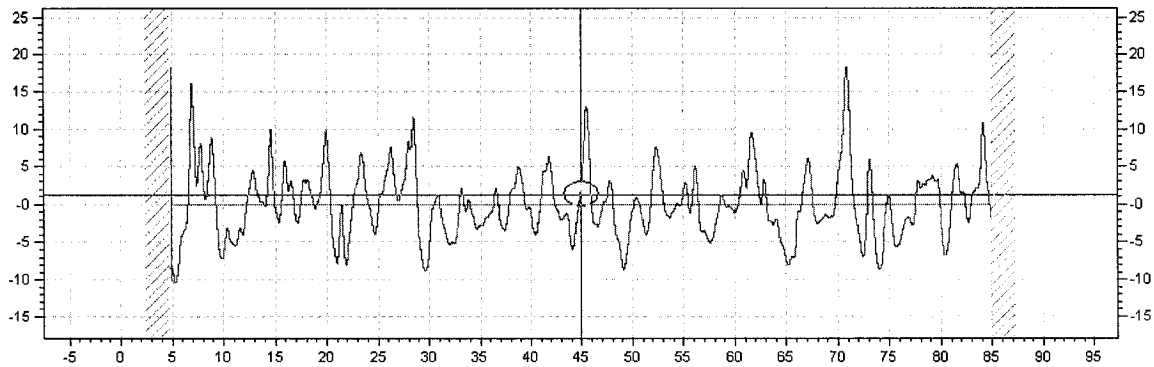

(f)

Figure 6.7 (a) Raw data profile of sample in experiment 1 (b) Leveled profile to remove tilt effects (c) long range waviness (d) Roughness at cutoff wavelength of 0.8 mm (e) Roughness at cutoff wavelength of 2.5 mm (f) Roughness at cutoff wavelength of 8 mm

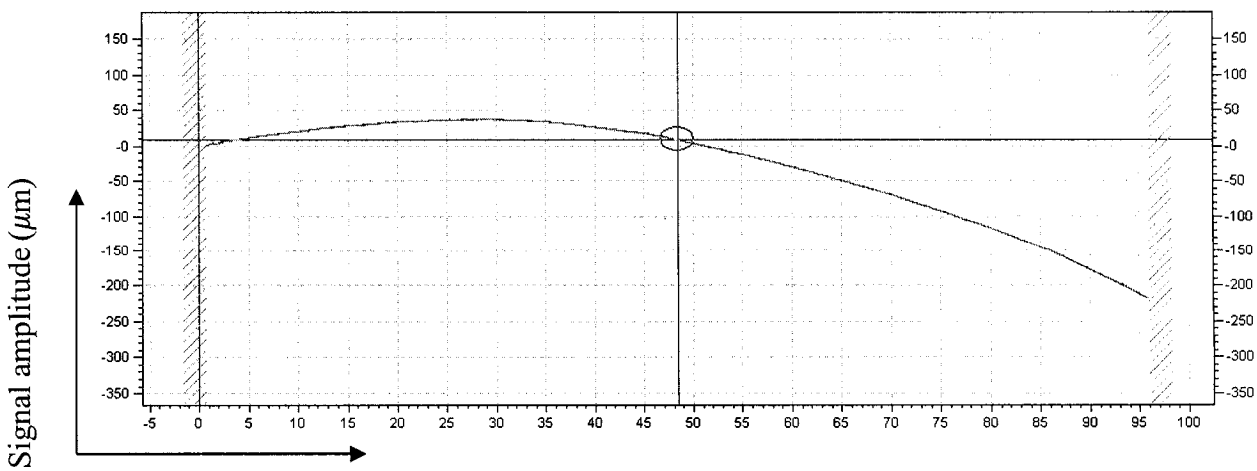

(a)

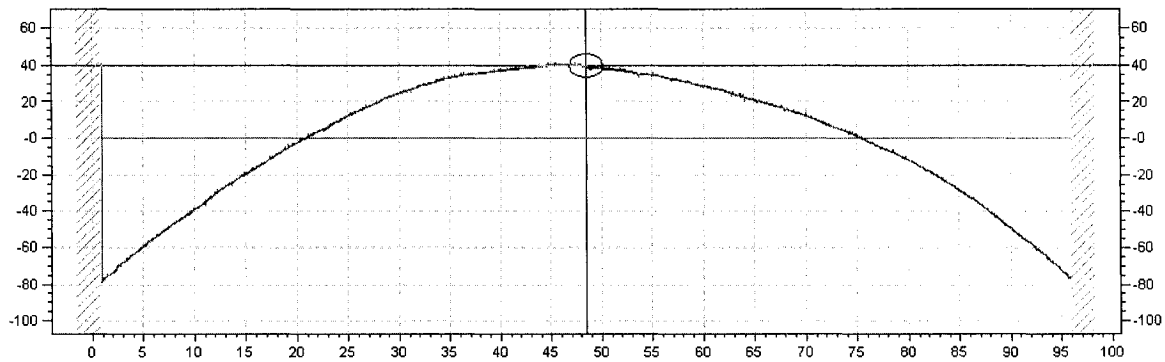
60
40
20
-0
-20
-40
-60
-80
-100
0 5 10 15 20 25 30 35 40 45 50 55 60 65 70 75 80 85 90 95 100

(b)

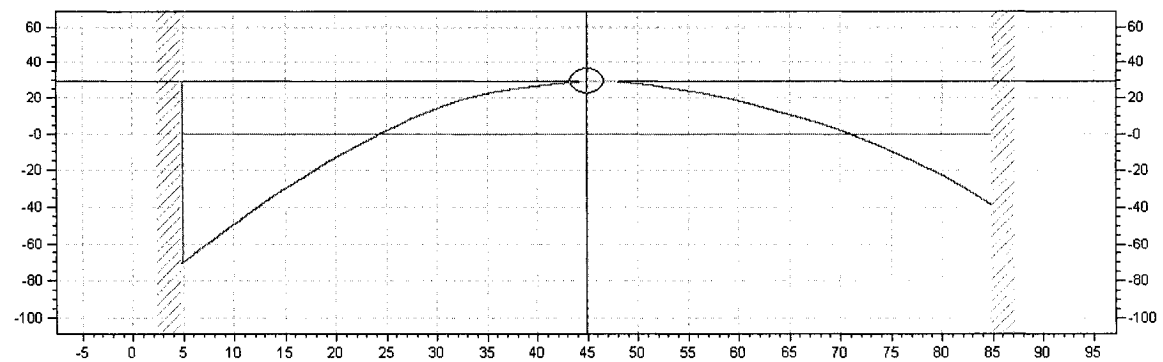
60
40
20
-0
-20
-40
-60
-80
-100
-5 0 5 10 15 20 25 30 35 40 45 50 55 60 65 70 75 80 85 90 95

(c)

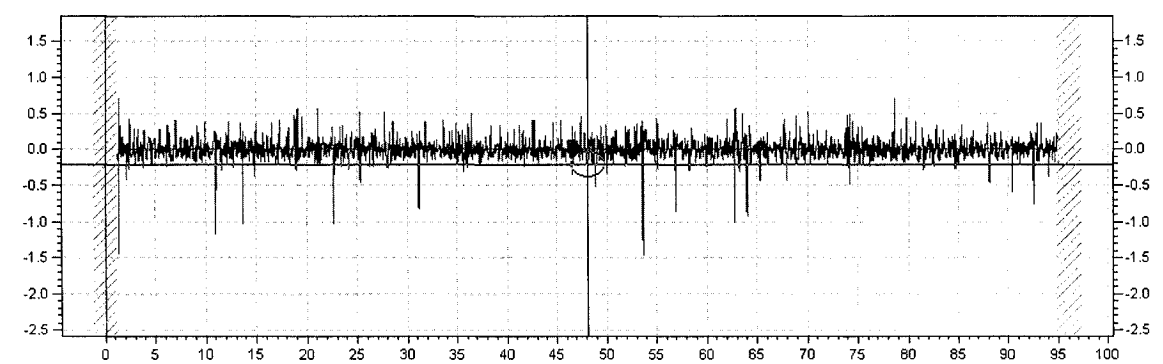
1.5
1.0
0.5
0.0
-0.5
-1.0
-1.5
-2.0
-2.5
0 5 10 15 20 25 30 35 40 45 50 55 60 65 70 75 80 85 90 95 100

(d)

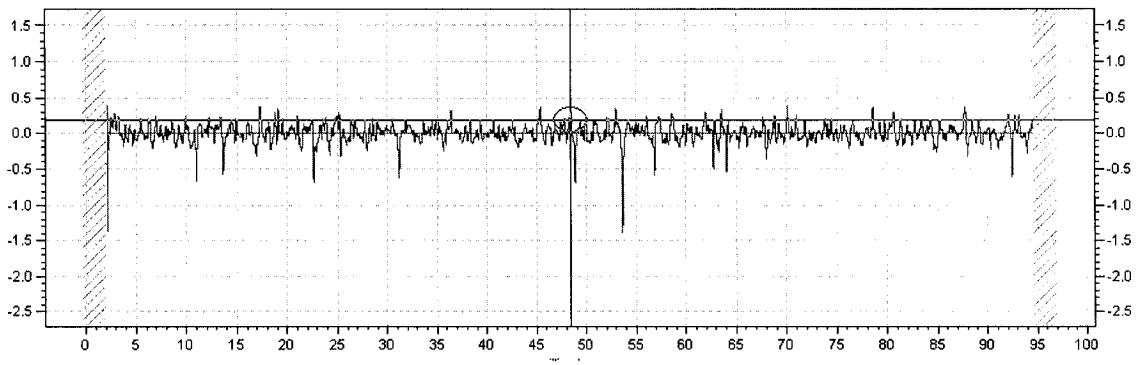

(e)

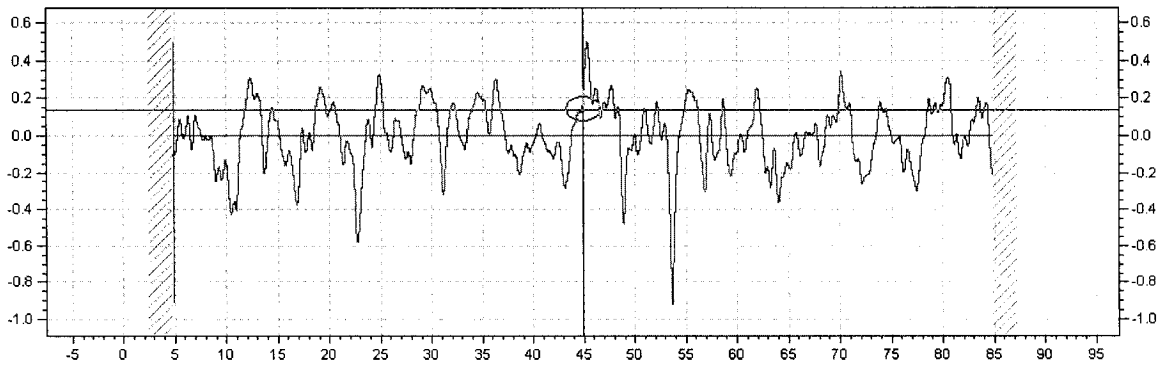

(f)

Figure 6.8 (a) Raw data profile of sample in experiment 4 (b) Leveled profile to remove tilt effects (c) long range waviness (d) Roughness at cutoff wavelength of 0.8 mm (e) Roughness at cutoff wavelength of 2.5 mm (f) Roughness at cutoff wavelength of 8 mm

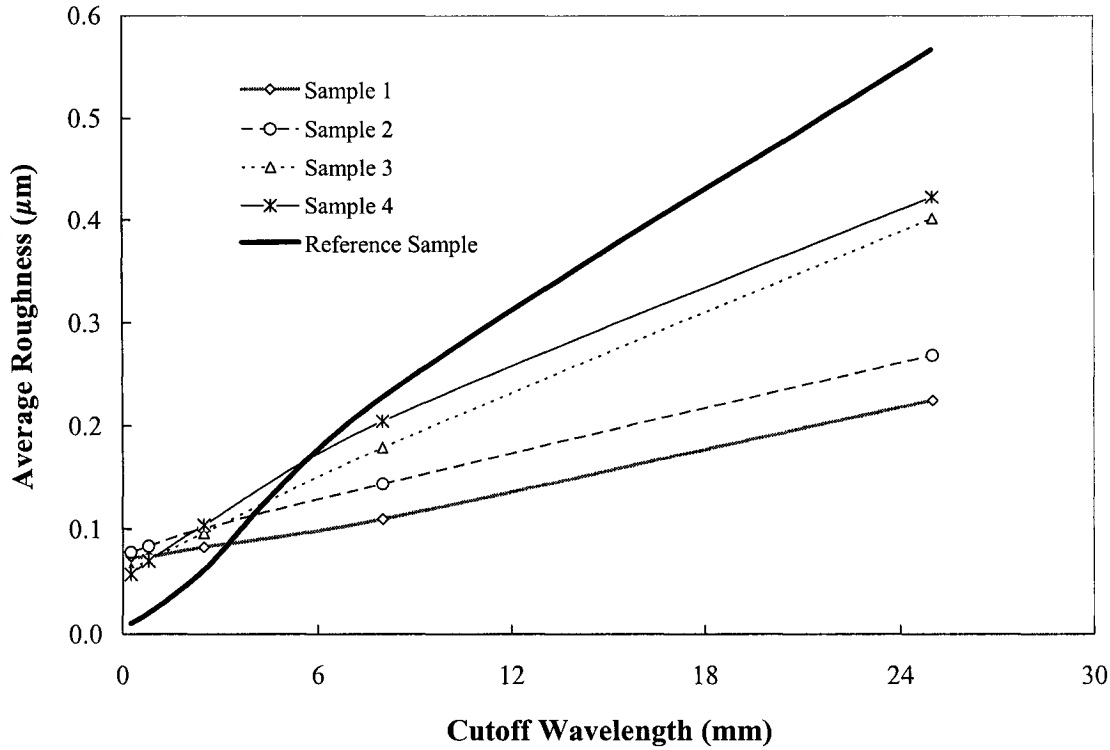

Figure 6.9 Variation in roughness (R_a) as a function of cutoff wavelength for L_4 matrix.

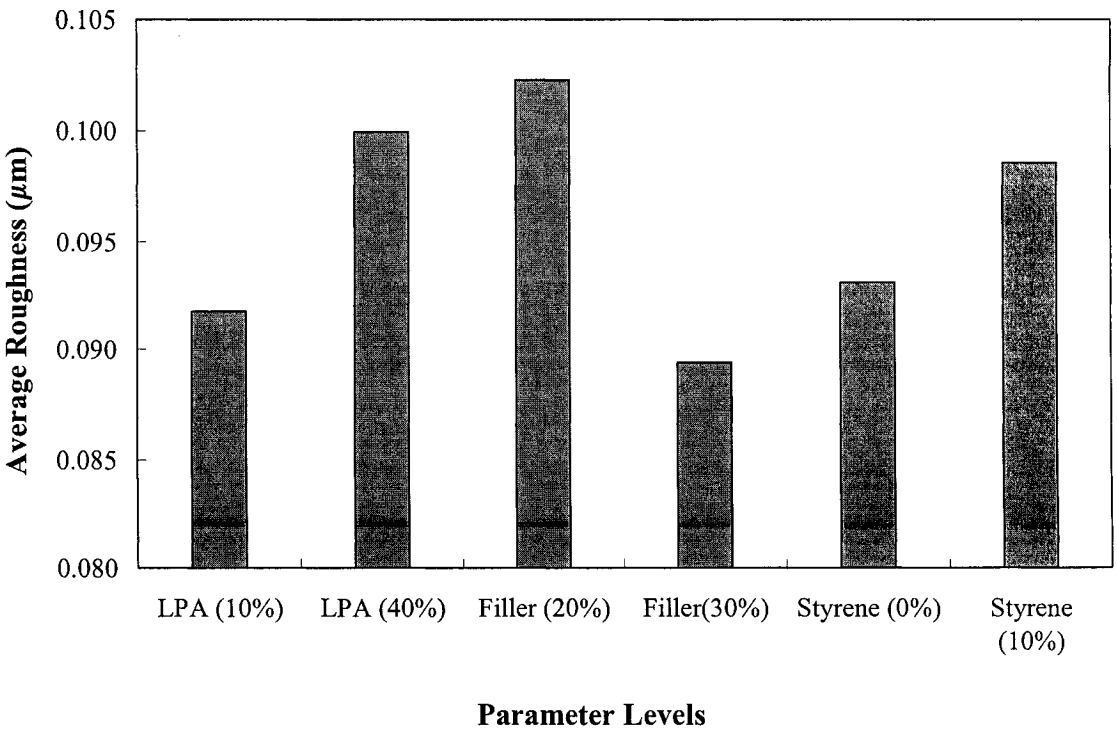

Figure 6.10 The effects of process parameter levels on R_a at 2.5 mm cutoff wavelength

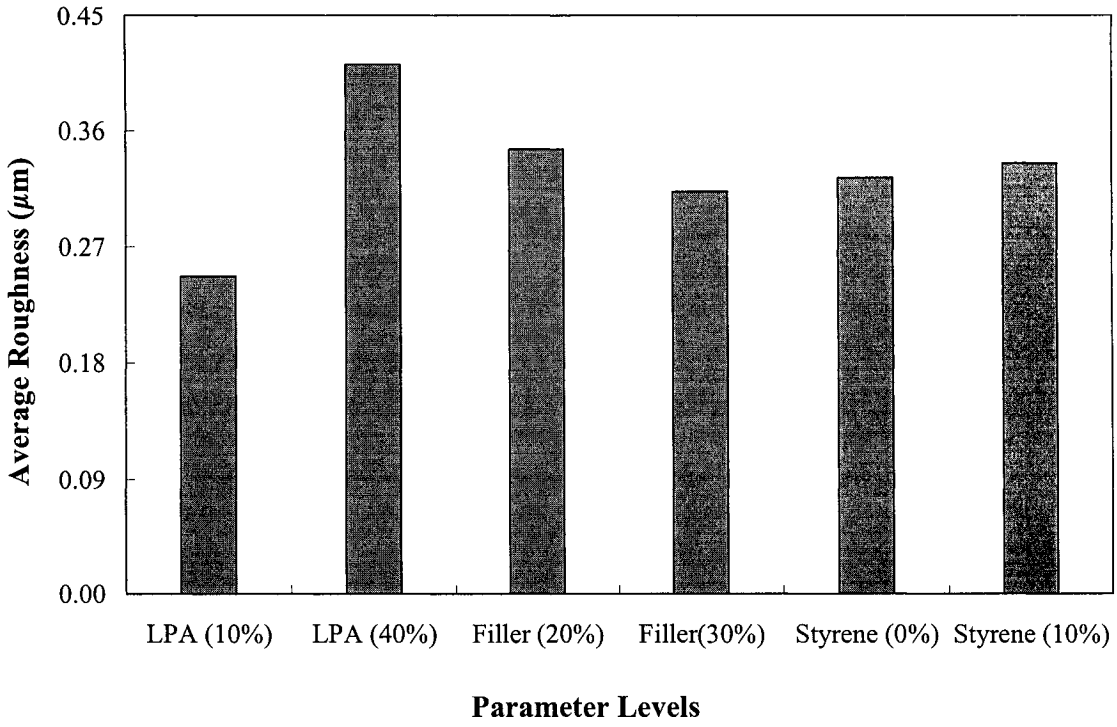

Figure 6.11 The effects of process parameter levels on R_a at 25 mm cutoff wavelength

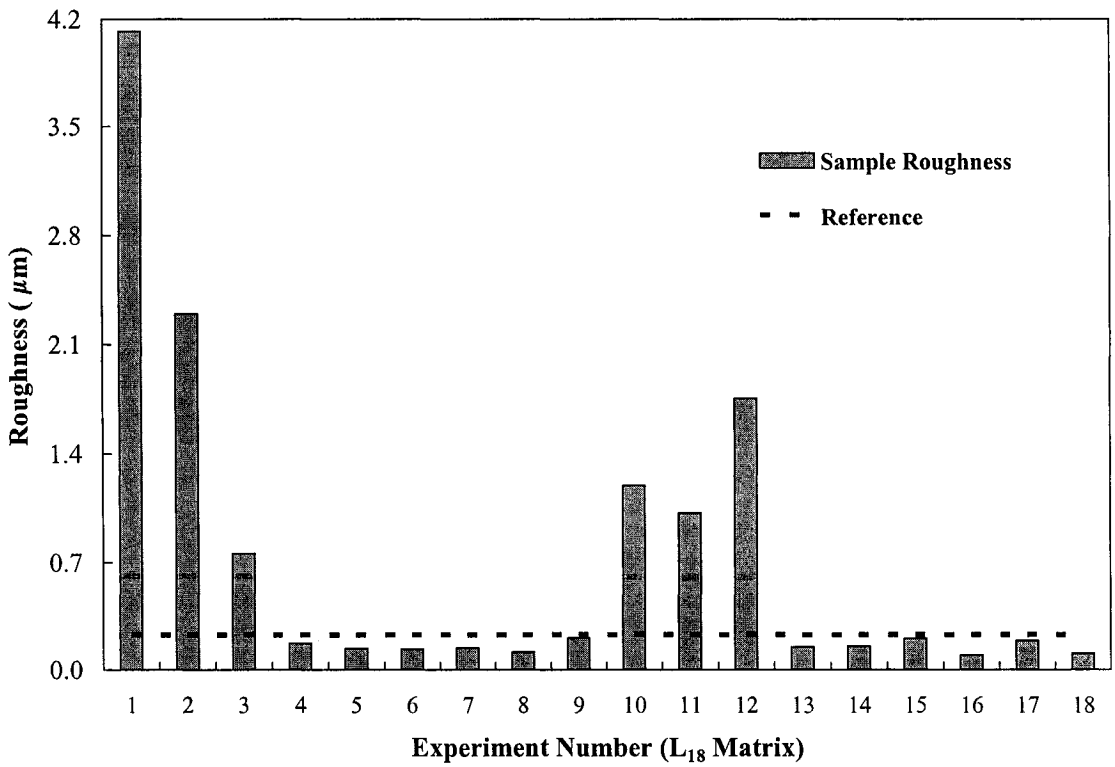

Figure 6.12 Roughness R_a at cutoff wavelength of 8 mm for all experiments in L_{18} matrix and reference sample

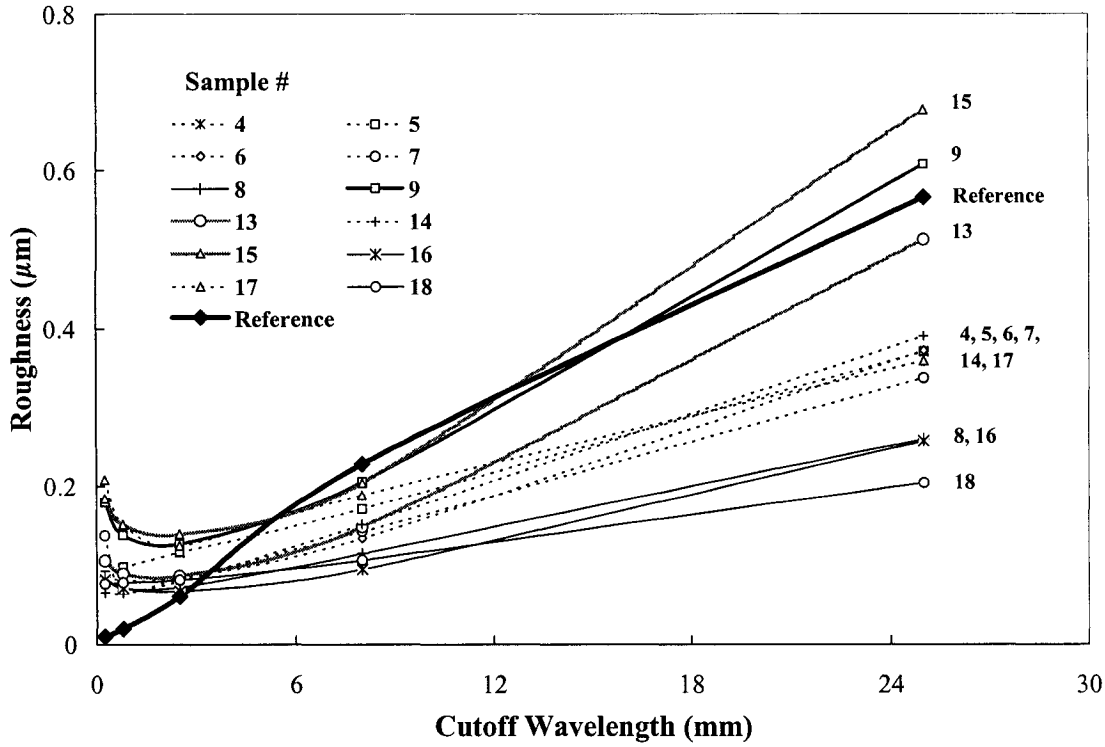

Figure 6.13 Variation in roughness (R_a) as a function of cutoff wavelength for L_{18} matrix

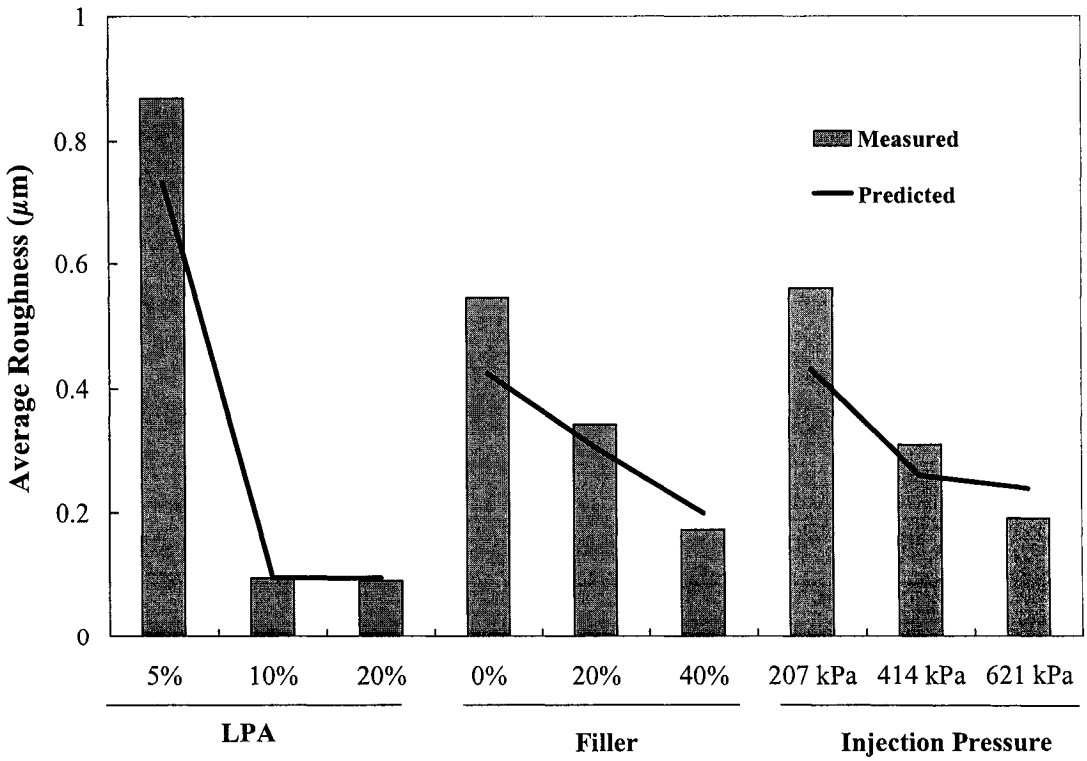

Figure 6.14 Variation in average roughness as a function of levels of significant parameters for a cutoff wavelength of 2.5 mm.

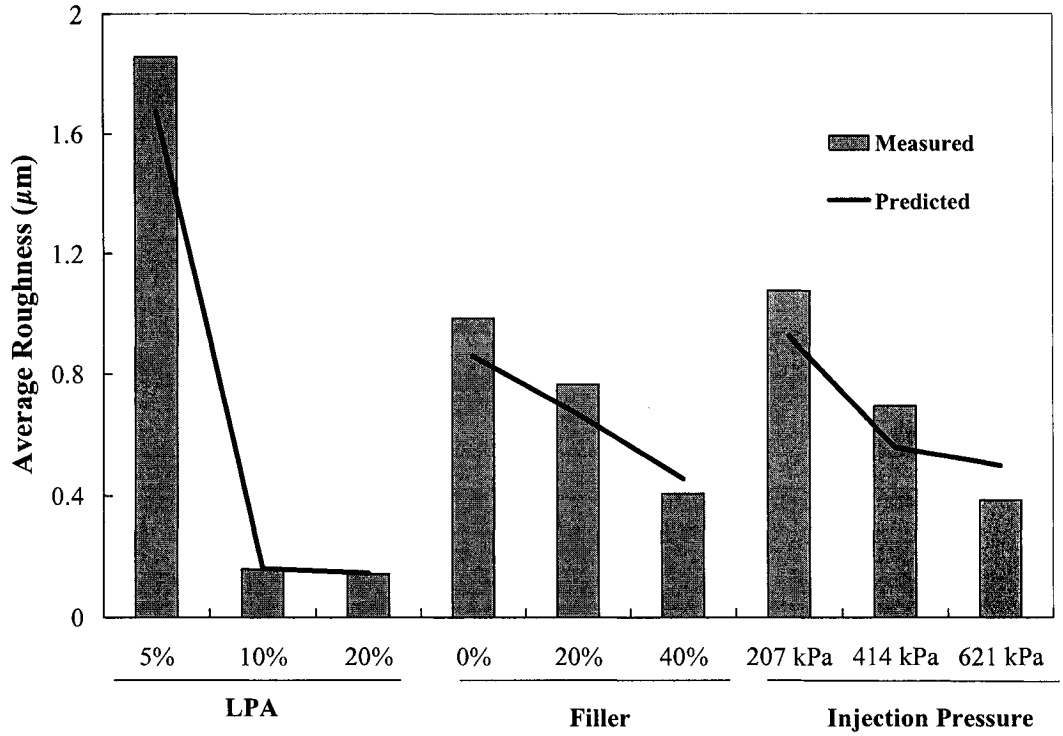

Figure 6.15 Variation in average roughness as a function of levels of significant parameters for a cutoff wavelength of 8 mm.

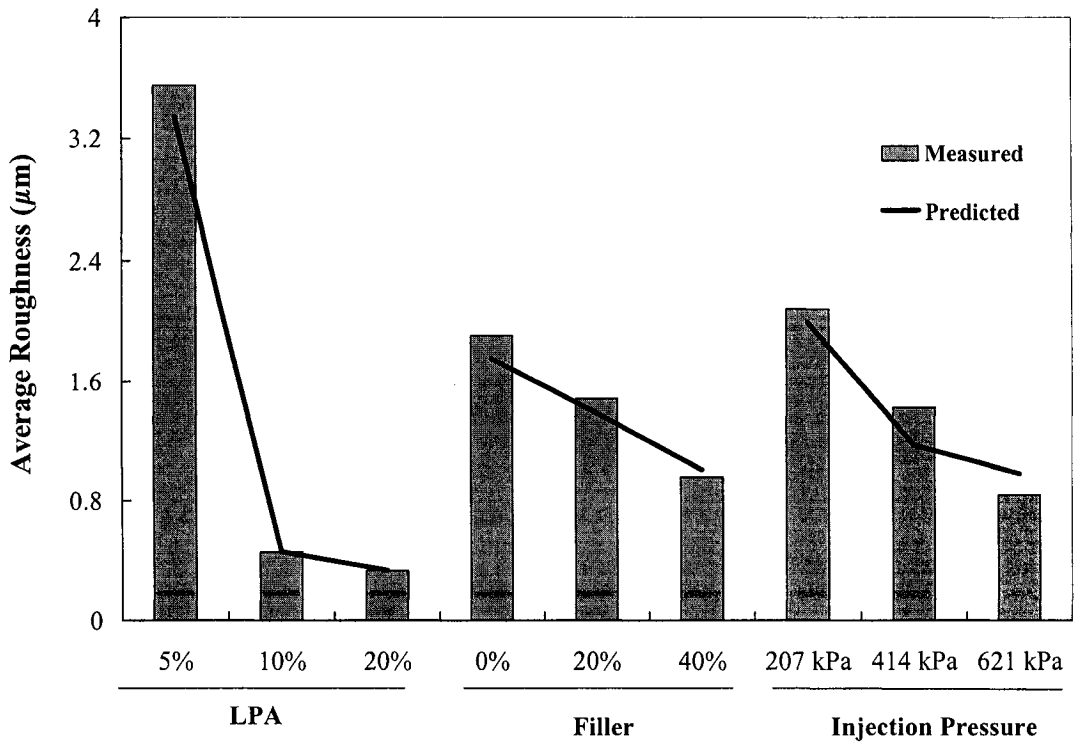

Figure 6.16 Variation in average roughness as a function of levels of significant parameters for a cutoff wavelength of 25 mm.

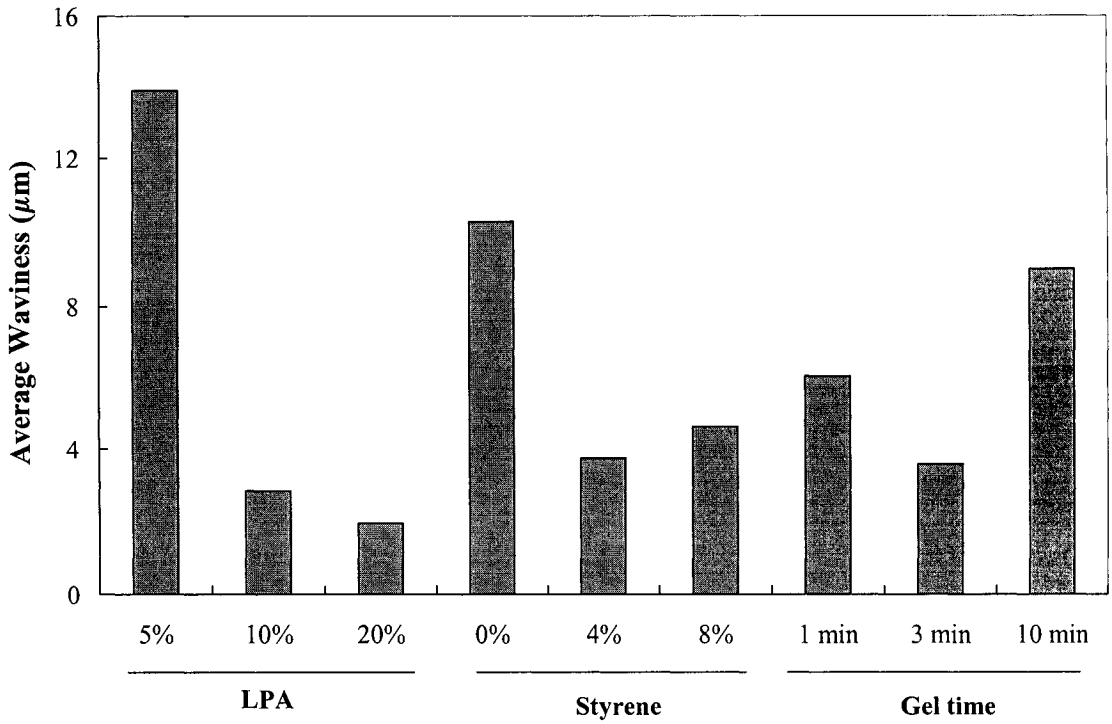

Figure 6.17 Variation in average waviness as a function of levels of significant parameters.

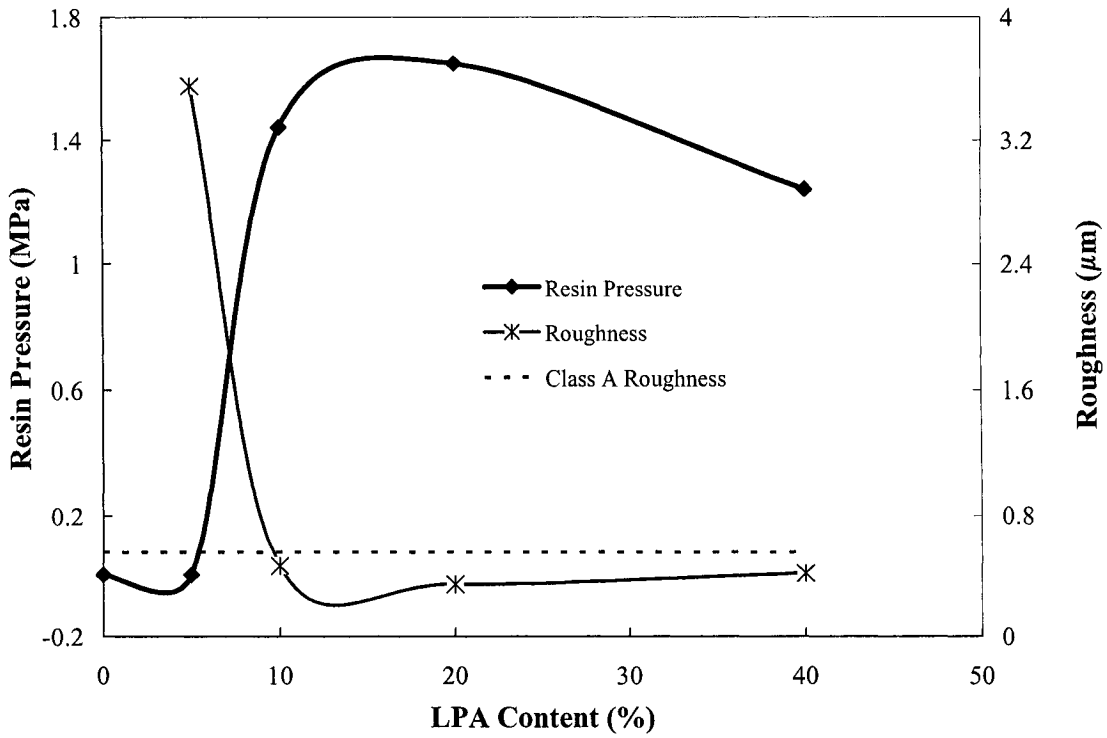

Figure 6.18 Relationship between LPA content, resin pressure and surface roughness.

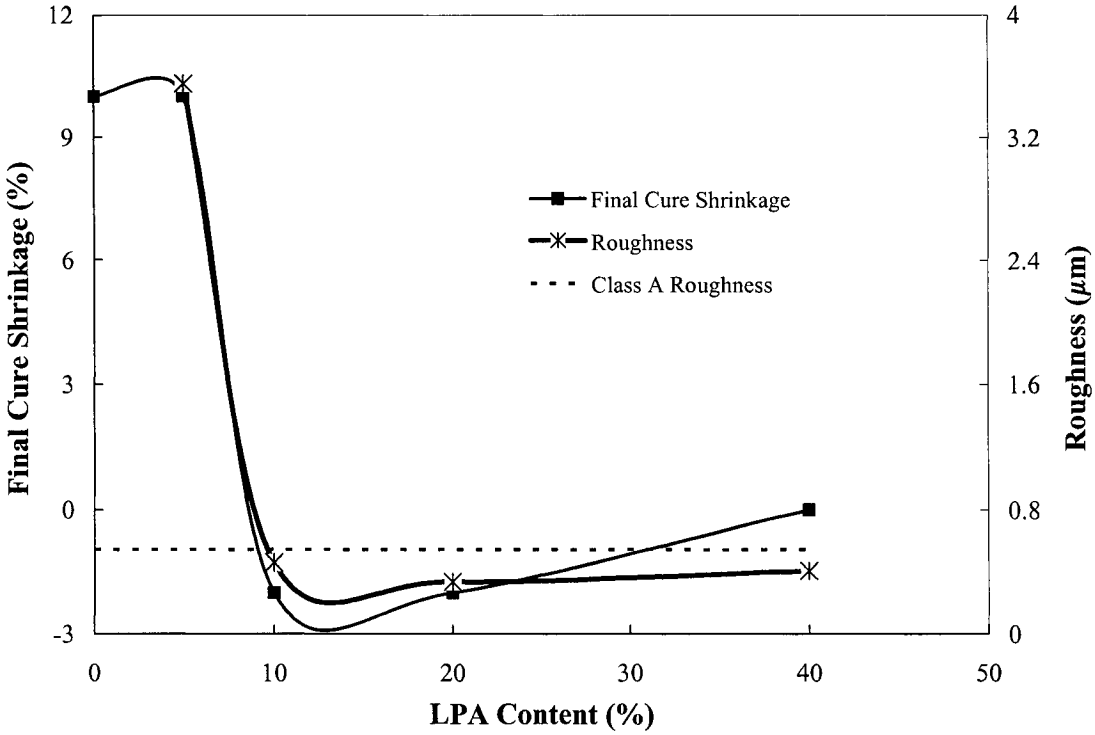

Figure 6.19 Relationship between LPA content, final cure shrinkage and surface roughness.

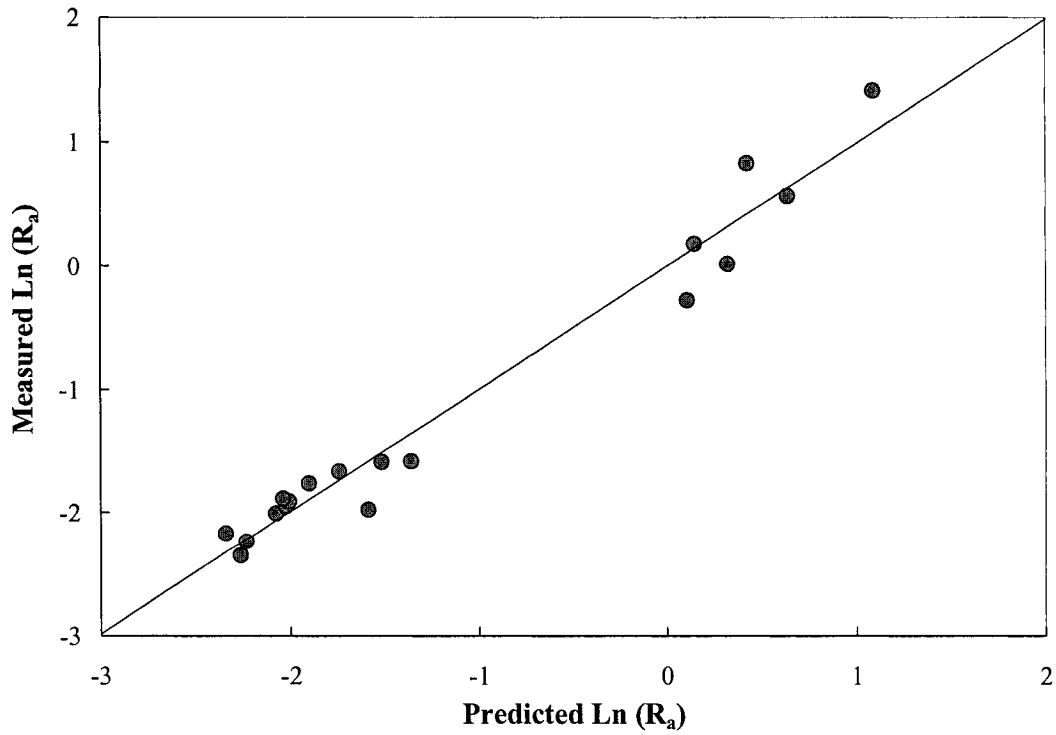

Figure 6.20 Measured and predicted roughness values

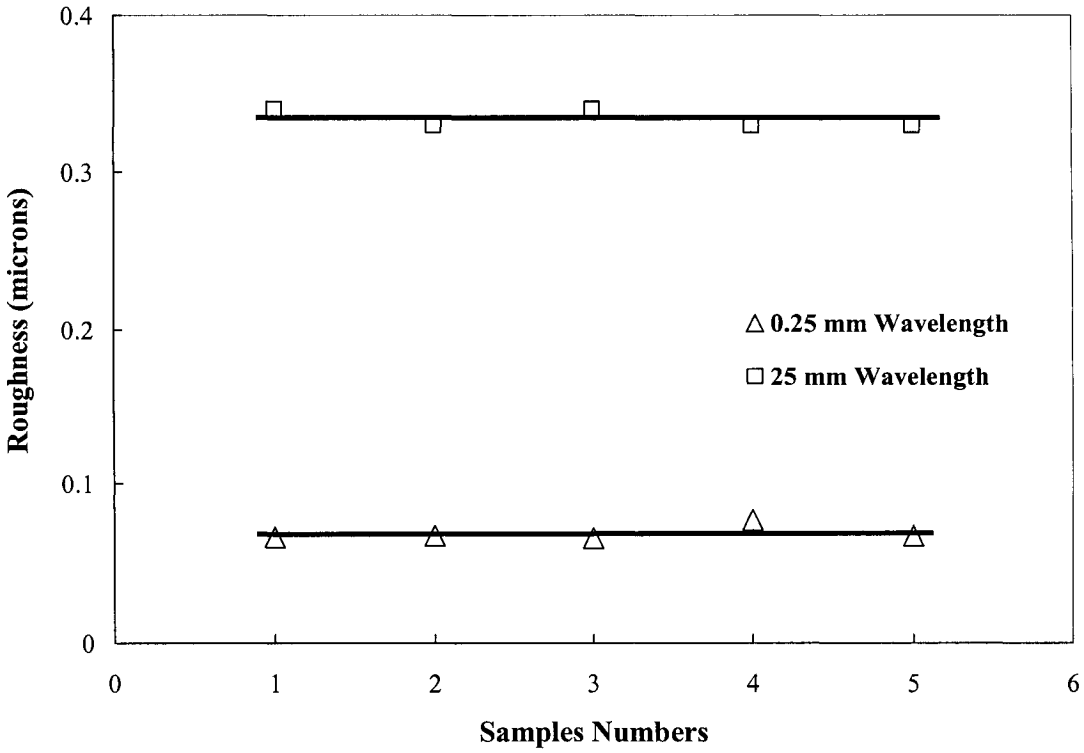

Figure 6.21 Roughness measurements for short (0.25 mm) and long (25 mm) wavelengths of all 5 samples.

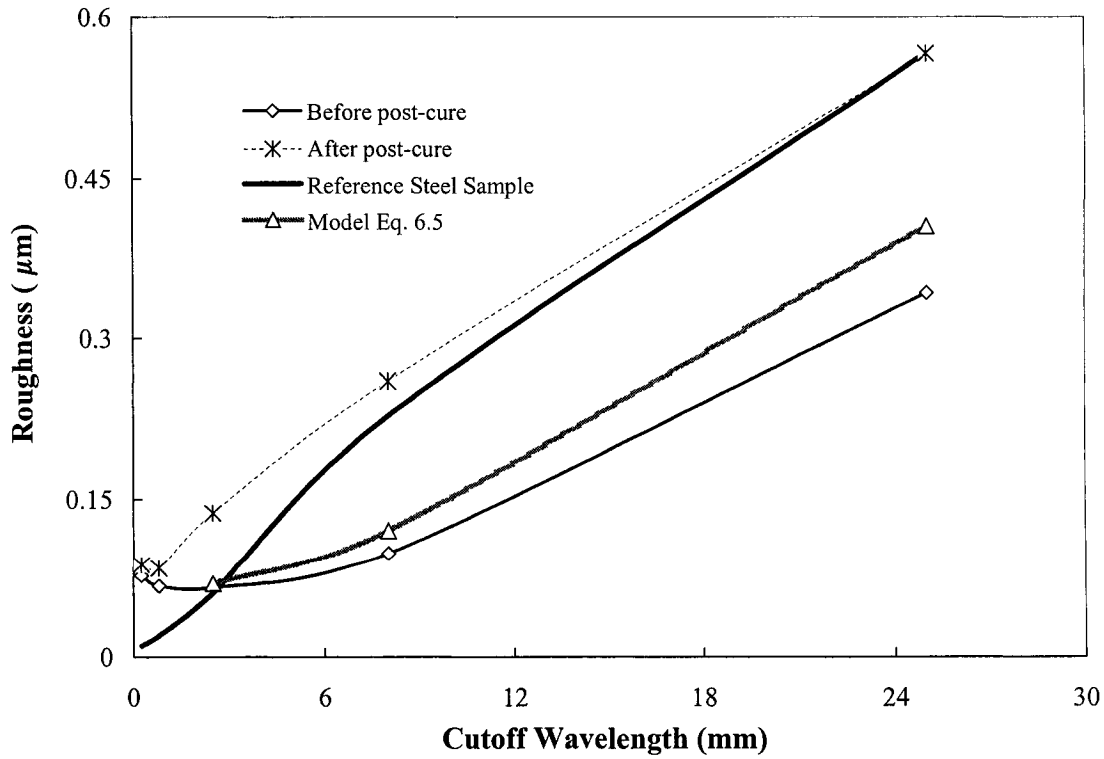

Figure 6.22 Effects of post-cure on surface roughness for all cutoff wavelengths.

CHAPTER 7

CONCLUSION

7.0 Conclusion

The objective of this study was to evaluate and optimize the influence of material and process parameters on the surface finish of RTM molded components for automotive applications. The problem was addressed experimentally using material characterization, RTM manufacturing, process simulations and validation, and statistical analysis. The following inferences can be drawn from this work.

1. The cure shrinkage is a non-linear function of the LPA content.

The LPA content (0-20%) had no significant effect on the cure kinetics and gel time of the polyester resin. However, higher LPA content (40%) reduced the cure rate. A volumetric shrinkage of 9.5% was found in the neat resin. The shrinkage decreased non-linearly with increasing LPA content. LPA content at 10% was found to be the minimum amount for shrinkage compensation. The shrinkage and shrinkage compensation were a linear function of the degree-of-cure. The LPA stayed inactive until a degree-of-cure of 0.5 and then expansion started. The results obtained, from cure shrinkage measurement procedure developed, were in good agreement with the published data.

2. **The LPA content has a significant effect on resin morphology.**

No change in the structure and transparency was observed for the resin without LPA; however resin with 10% LPA showed a co-continuous structure development during cure which turned the transparent resin into an opaque solid. Micro-cracking was observed in the resin with LPA at a later stage during cure due to the micro-void formation. The LPA expansion was highly dependent on the development of elastic modulus during cure. The LPA expansion started only after the resin became fully elastic (approximately at a degree-of-cure of 0.5).

3. **LPA expansion results in pressure increase during RTM manufacturing.**

A significant pressure increase was observed during RTM processing of resin formulations with at least 10% LPA. The highest pressure was observed for resin formulation with 20% LPA following by 10% and 40% LPA resins. The pressure curves were found to be a function of degree-of-cure irrespective of the LPA content (above 10%) and processing temperature in the range tested. Pressure started to increase after a degree-of-cure of 0.5. The pressure data and LPA expansion curves matched closely, which suggests that pressure increase is mainly due to the LPA expansion. No pressure increase or LPA expansion was observed for resin formulations with 0 and 5% LPA.

4. **A significant cure gradient along the part geometry is induced by low injection pressures.**

Injection pressure had a significant effect on the cure gradient. The injections at high pressure levels (> 400 kPa) showed no cure gradient due to shorter injection times, however low pressure (< 400 kPa) injections resulted in a significant cure gradient along the geometry of the part which reduced the resin pressure during curing at locations away from the injection port. The cure gradient was also seen to have a significant effect on the maximum pressure observed at various sensors locations. The sensors close to injection ports showed much higher pressures compared with sensors further away due to the cure gradient. Higher injection pressures (less cure gradient) resulted in better surface finish.

5. **Numerical simulations can be used successfully to predict pressure caused by LPA.**

RTM numerical simulations were found to be very useful and quite accurate in predicting mold pre-heating, flow and curing behavior of a polyester resin. Numerical modeling of the resin pressure during cure suggests that the analytical models can be incorporated in already existing codes to model the cure behavior of low profile resin systems; however accurate parameters are required since pressure variation model was found to be very sensitive to the parameters of the LPA expansion model.

6. **The most influential parameter affecting surface finish is the LPA content.**

LPA content had the most significant effect on the surface finish of RTM molded components. A significant improvement in the surface roughness was observed when LPA level was increased from 5% to 10%. However, the improvement was not significant between 10% and higher LPA levels. This result is consistent with the shrinkage-expansion data obtained with rheometer and pressure increases measured during RTM manufacturing. LPA content at 10% was found to the minimum amount for class A surface finish.

7. **Higher injection pressures and high filler content improve surface finish.**

A linear decrease in surface roughness was observed with increasing injection pressures and filler content. This result is consistent with the pressure data where low pressure injections induced cure gradients. This result is also consistent with the findings of other researchers. Styrene content, gel time (cure rate) and temperature gradient had no significant effect on the surface roughness in the range tested. Empirical model developed for surface roughness prediction was in good agreement with the experimental results.

8. **LPA content, resin shrinkage behavior, pressure increase and surface roughness are directly related to each other.**

The maximum pressure measured was exactly opposite to the final cure shrinkage and surface roughness when plotted as a function of LPA content. As the LPA content increased, the pressure increased whereas final cure shrinkage and surface roughness decreased. LPA content at 10% was found to be the minimum amount for a significant increase in pressure and consequently a significant decrease in final cure shrinkage and surface roughness.

9. **Optimum parameters for low cost, class A surface finish RTM manufacturing**

A minimum amount of LPA (10%) can be added to the resin to reduce cost without sacrificing the surface finish of RTM molded components. Higher filler content and injection pressures are also beneficial for getting good surface quality as well as for reducing costs. However, maximum filler content in the resin depends on the range of mechanical properties required for the components to be manufactured. Faster cure rates result in shorter process cycle times. Hence, processing temperature, amounts of accelerator and catalyst can be obtained through resin characterization to result in faster cure rates based on the processing window required for resin injection. Minimum styrene content and temperature gradient can be used to reduce cost and process cycle time, and to improve mechanical properties.

7.1 Contributions of This Dissertation

The purpose of this work was to further the study of the effects of material and processing parameters on the surface finish of fiber glass composite panels. Table 7.1 presents a summary of the previous research work in this area. As can be seen from Table 7.1, most of research efforts in the past were focused on the cure characterization and cure shrinkage measurements. However, not enough literature is available relating the effects of material and process parameters to the surface roughness. Work on

Table 7.1 Previous research work related to the optimization of process parameters.

RESEARCHER [reference], *year published*	**MATERIALS and PROCESS**				**PROPERTIES**				**ANALYSIS**	
	Resin System	LPA	Fibers	RTM	Cure Kinetics	Cure Shrinkage	Morphology	Surface Finish	Optimization	Modeling
Bucknall et al. [174], *1991*	Polyester	√			√	√				
Lucas et al. [178], *1993*	Polyester		√		√			√		
Huang et al. [180], *1995*	Polyester	√			√		√			
Dutiro et al. [188], *1997*	Polyester			√				√	√	
Vallat et al. [224], *1999*	BMC	√	√				√			
Liu et al. [182], *1999*	Polyester	√				√				
Lee et al. [170], *2000*	Polyester	√			√	√	√			
Gordon et al. [153], *2001*	Polyester	√				√				
Kim et al. [225], *2002*	Polyester		√	√				√		
Boyard et al. [185], *2004*	Polyester	√				√				√

the characterization and modeling of the behavior of low profile resins during processing and manufacturing and the cause-effect relationships of low profile resins and other processing parameters with the surface roughness aspects of RTM molded components is also scarce. This research addressed these issues by providing the following contributions to the knowledge:

1. A comprehensive study on the effects of LPA content on cure kinetics, cure shrinkage and resin morphology under isothermal and non-isothermal processing conditions.
2. The development of cure kinetics, viscosity variation and cure shrinkage models along with the development of a direct, time saving and cost effective cure shrinkage measurement procedure for polyester resins.
3. The integration of analytical models in a commercial software and experimental validation of predicted resin flow, cure and pressure variations during RTM manufacturing.
4. A study on the behavior of LPA based resins during RTM manufacturing, effects of process parameters on the curing behavior and experimental validation of LPA expansion during RTM cure cycle.
5. A basic understanding of the effects of material and processing parameters on the resulting surface finish and cycle times of glass fiber-polyester panels for automotive applications.

7.1.1 Publications

Four journal papers, four conference papers and two conference poster presentations have been produced from the results of this research. Publications are listed below:

Referred Journals

1. Haider, M., Hubert, P., Lessard, L., "Cure Shrinkage Characterization and Modeling of a Polyester Resin Containing Low Profile Additives", Composites Part A: Applied Science and Manufacturing, (submitted)

2. Haider, M., Hubert, P., Lessard, L., "An Experimental Investigation for Class A Surface Finish in Resin Transfer Molding Process", Composite Science and Technology, (submitted)

3. Haider, M., Ruiz, E., Hubert, P., Lessard, L., "Numerical Simulations for Class A Surface Finish in Resin Transfer Molding Process", Composite Science and Technology, (submitted)

4. Haider, M., Hubert, P., Lessard, L., "Optimization of RTM Processing Parameters for Class A Surface Finish", Journal of Composite Materials, (submitted)

Conference Papers

5. Haider, M., Ruiz, E., Hubert, P., Lessard, L., Cure Shrinkage and LPA Expansion Modeling of a Polyester Resin for Surface Quality Improvement, Proceedings of CANCOM 2005, Vancouver, Canada. August 16-19, 2005.

6. Haider, M., Hubert, P., Lessard, L., Trochu, F., Applications of Experimental Design Techniques for Surface Roughness Improvements in RTM Processing, Proceeding of SAMPE 2005, Long Beach, USA, May 1-5, 2005.

7. Haider, M., Hubert, P., Lessard, L., Trochu, F., Experiments and Procedures for Examination of RTM Process Parameters for obtaining Class A Surface Finish, Proceedings of ICCM-14, San Diego, USA, July 14-18, 2003.

8. Haider, M., Lessard, L., Trochu, F., Octeau, M-A., Experimental Optimization of Process Parameters to obtain Class A Surface Finish in Resin Transfer Molding", Proceedings of 4th Joint Canada-Japan Workshop on Composites, Vancouver, Canada, September 19-21, 2002.

Conference Proceedings (Poster Presentations)

9. Haider, M., Hubert, P., Lessard, L., Trochu, F., Process Parameter Optimization for Class A Surface Finish in Automotive Applications, Proceedings of Auto21 Student Conference, Oshawa, Canada, May 10-12, 2005.

10. Haider, M., Hubert, P., Lessard, L., Trochu, F., Application of Design of Experiments for RTM Process Optimization, Proceedings of Auto21 Student Conference, Windsor, Canada, May 4-6, 2004.

7.2 Future Work

To expand the range of understanding on surface finish aspects of RTM molded components, future research efforts can be focused to address following issues and problems:

1. In this work, the surface finish of RTM molded components was evaluated before and after post-curing. However, the effects of material aging and environmental conditions on class A surface finish are still unknown. Hence, research needs to be carried out to investigate the effects of material aging and environmental conditions on class A surface finish.

2. Mechanical performance of composite panels needs to be investigated under varying process conditions to study the effect of process parameters on mechanical properties. A flat steel mold was used to manufacture flat test samples in this research. The mold and part geometry can be changed to investigate the effect of complex geometries on the surface roughness of the part manufactured. An American Society for Testing and Materials (ASTM) standard for Class A surface finish, in terms of roughness parameters R_a, R_q and R_y, also needs to be established.

3. Levels of processing parameters were defined in collaboration with the industrial partner. For example, filler was tested at a maximum level of 40%. Future research work in this area may include even higher levels of some processing parameters. Also, only PD9419 LPA was characterized in this research. In future, other types of LPA can be studied for their effects on the shrinkage and surface finish aspects with the same resin system.

4. A detailed study needs to be conducted on the effects of post-curing on the surface finish of RTM molded test samples. After manufacturing composite car body panels

are normally painted at high temperatures above the T_g. Cause-effect relationship between high temperature painting process and surface roughness needs to be established.

5. Further research may include an investigation to verify the uniformity in chemical composition through the thickness of manufactured samples by employing scanning electron microscope (SEM) and Fourier transform infrared spectroscopy (FTIR).

6. The analytical and empirical models developed for shrinkage-expansion behavior of low profile resins and surface roughness can be incorporated in commercial software to broaden the scope of numerical simulations by including the shrinkage-expansion behavior and roughness predictions of RTM molded components.

7. This study was conducted from a mechanical engineering and manufacturing point of view; where the focus was on the overall effects of process parameters on the surface finish of RTM molded components. Future work may include a detailed understanding of the underlying physics and chemistry through which LPA, filler and injection pressure improve surface quality of RTM molded components.

REFERENCES

1. Kyoto Protocol, United Nations Framework Convention on Climate Change, Document # FCCC/CP/1997/L7/Add 1, December 1-10, 1997, Kyoto, Japan.

2. USCAR, United States Council for Automotive Research. www.uscar.org

3. Kendall, K., Johnson, K., "Composite Applications for the Aston Martin DB9", JEC Composites, No. 11, 2004, pp. 50-52.

4. Kendall, K., "Composite Materials in European Cars", JEC Composites, No. 11, 2004, pp. 38-40.

5. Renault Escape 1996, Volvo V70XC AWD 2000, Ford Thunderbird 2002, Aston Martin V12 Vanquish 2002, Ferrari Anzo 2003, BMW M3 Sport Coup 2003, Aston Martin DB9 2004.

6. Kenworth T2000, Chevrolet Silverado 2002, Compositttrailer 2004, HycoProd Composite Trailer 2002.

7. GM Ultralite 1992, BMW Z22 2000, Dodge Viper SRT-10 Carbon 2003

8. Chrysler Composite Vehicle 1998, Chevrolet Corvette Z06 2004, VW New Beetle, Audi A8 2003.

9. Hendrickson's composite bumper 2000, Saturn Coup 1997.

10. Ford Windstar Minivan 1998, Chrysler Dodge Dakota 1997, GM EV1.

11. Strong A., *Fundamentals of Composite Manufacturing: Materials, Methods and Applications*, Society of Manufacturing Engineers, 1989, Michigan, USA.

12. Tari, M.J., Bals, A., Park, J., Lin, M.Y., Hahn, H.T., "Rapid Prototyping of Composites Parts using Resin Transfer Molding and Laminated Object Manufacturing", Composites Part A, Vol. 29A, 1998, pp. 651-661.

13. Morrison, G., "The Art of Aerospace Composites: Keeping the Pressure on the Resin Transfer Molding Process for Manufacturing Flight Critical Carbon Fiber Parts", Mechanical Engineering, Vol. 121, No. 4, 1999, pp. 58-61.

14. Holmberg, J.A., Berglund, L.A., "Manufacturing and Performance of RTM U-beams", Composites Part A, Vol. 28A, 1997, pp. 513-521.

15. Thuis, H.G.S., Biemans, C., "Design, Fabrication and Testing of a Composite Bracket for Aerospace Applications", Composite structures, Vol. 38, No. 1, 1997, pp. 91-98.

16. Potter, K.D., "The Early History of Resin Transfer Molding Process for Aerospace Applications", Composites Part A, Vol. 30, 1999, pp. 619-621.

17. Andreas, T., Astrom, T., "Heat Transfer in Compression Molding of Thermoplastic Composite Laminates and Sandwich Panels", Journal of Thermoplastic Composite Materials, Vol. 5, No. 1, 2002, pp. 43-64.

18. Park, C.H., Lee, W.I., Yoo, Y.E., Kim, E.G., "A Study on Fiber Orientation in the Compression Molding of Fiber Reinforced Polymer Composite Material", Journal of Materials Processing Technology, Vol. 111 , No. 1 , 2001, pp. 233 -239.

19. Dweib, M.A., Bradaigh, C.M.O, "Compression Molding of Glass Reinforced Thermoplastics: Modeling and Experiments", Polymer Composites, Vol. 21, No. 5, 2000, pp. 832-845.

20. Chen, S.C., Chen, Y.C., Peng, H.S., "Simulation of Injection-Compression-Molding Process. Influence of Process Characteristics on Part Shrinkage", Journal of Applied Polymer Science, Vol. 75, No. 13, 2000, pp. 1640- 1654.

21. Chen, S.C., Chen, Y.C., Cheng, N.T., Huang, M.S., "Simulations and Applications of Injection-Compression Molding", Journal of reinforced Plastics and Composites, Vol. 18, No. 8, 1999, pp. 724-734.

22. Rudd, C.D., Long, A.C., Kendall, K.N., Mangin, C.G.E., *Liquid Molding Technologies*, Woodhead Publishing Limited, 1997, Cambridge, UK.

23. Potter, K., *Resin Transfer Moulding*, Chapman and Hall, 1997, London, UK.

24. Brooks, N., "Is RTM Ready for Mass Production", Reinforced Plastics, Vol. 39, No. 1, 1995, pp. 26-31.

25. Advani, S.G., Bruschke, M.V., *Flow and Rheology in Polymer Composites Manufacturing*, Elsevier Science BV, 1994, Amsterdam.

26. Nielsen, D., Pitchumani, R., "Intelligent Model-based Control of Preform Permeation in Liquid Composite Molding Processes, with Online Optimization", Composites Part A, Vol. 32, No. 12, 2001, pp. 1789-1803.

27. Long, A.C., "Process Modeling for Liquid Molding of Braided Preforms", Composites Part A, Vol. 32, No. 7, 2001, pp. 941-953.

28. Mantle, M.D., Bijeljic, B., Sederman, A.J., Gladden, L.F., "MRI velocimetry and lattice-Boltzmann simulations of viscous flow of a Newtonian liquid through a dual porosity fibre array", Magnetic Resonance Imaging, Vol. 19, No. 3-4, 2001, pp. 527-529.

29. Pillai, K.M., Tucker, C.L., Phelan, F.R., "Numerical Simulation of Injection/Compression Liquid Composite Molding. Part 2: Preform Compression", Composites Part A, Vol. 32, No. 2, 2001, pp. 207-220.

30. Saouab, A., Bréard, J., Lory, P., Gardarein, B., Bouquet, G., "Injection Simulations of Thick Composite Parts Manufactured by the RTM Process", Composites Science and Technology, Vol. 61, No. 3, 2001, pp. 445-451.

31. Lam, Y.C., Joshi S.C., Liu, X.L., "Numerical Simulation of the Mold-Filling Process in Resin-Transfer Molding", Composites Science and Technology, Vol. 60, No. 6, 2000, pp. 845-855.

32. Han, K., Jiang, S., Zhang, C., Wang, B., "Flow Modeling and Simulation of SCRIMP for Composites Manufacturing", Composites Part A: Applied Science and Manufacturing, Vol. 31, No. 1, 2000, pp. 79-86.

33. Antonelli, D., Farina, A., "Resin Transfer Molding: Mathematical Modeling and Numerical Simulations", Composites Part A, Vol. 30, No. 12, 1999, pp. 1367-1385.

34. Kang, M.K., Lee, W., "A Flow-Front Refinement Technique for the Numerical Simulation of the Resin-Transfer Molding Process", Composites Science and Technology, Vol. 59, No. 11, 1999, pp. 1663-1674.

35. Kanapady, R., Tamma, K.K., Baddourah, M., Mark, A., "High Performance Computing on a Symmetric Multiprocessor (SMP) Environment for RTM Process Modeling of Large Complex Structural Geometries", Advances in Engineering Software, Vol. 29, No. 3-6, 1998, pp. 399-408.

36. Lin, M.H., Hahn, T., Huh, H., "A Finite Element Simulation of Resin Transfer Molding based on Partial Nodal Saturation and Implicit Time Integration", Composites Part A, Vol. 29, No. 5-6, 1998, pp. 541-550.

37. Baichen, L., Bickerton, S., Advani, S.G., "Modeling and Simulation of Resin Transfer Molding (RTM)--Gate Control, Venting and Dry Spot Prediction", Composites Part A, Vol. 27, No. 2, 1996, pp. 135-141.

38. Shojaei, A., Ghaffarian, S.R., Karimian, S.M.H., "Modeling and Simulation Approaches in the Resin Transfer Molding Process: A Review", Thesis, Amirkabir University of Technology, 2002, Tehran, Iran.

39. Advani, S.G., Bruschke, M.V., Parnas, R.S., "Resin Transfer Molding Flow Phenomena in Polymeric Composites", in: S.G. Advani (Ed.), Flow and Rheology in Polymer Composite Manufacturing, Elsevier, Amsterdam, 1994, pp. 465–515.

40. Chan, A.W., Hwang, S.T., "Mold Filling Simulation for the Injection Molding of Continuous Fiber-Reinforced Polymer", Polymer Engineering Science, Vol. 28, 1988, pp. 333–339.

41. Mal, O., Couniot, A., Dupret, F., "Non-isothermal Simulation of the RTM Process", Composites Part A, No. 29, 1998, pp. 189–198.

42. Lin, R., Lee, L.J., Liou, M.J., "Non-isothermal Mold Filling in RTM and Structural Reaction Injection Molding", SPE ANTEC Technical Papers, Vol. 37, 1991, pp. 815–818.

43. Lin, R., Lee, L.J., Liou, M.J., "Non-isothermal Mold Filling and Curing Simulation in Thin Cavities with Pre-placed Fiber Mats", International Polymer Processing, Vol. 6, 1991, pp. 356–369.

44. Bruschke, M.V., Advani, S.G., "A Numerical Approach to Model Non-Isothermal Viscous Flow through Fibrous Media with Free Surfaces", International Journal of Numerical Methods in Fluids, Vol. 19, 1994, pp. 575–603.

45. Wang, T.J., Lin, R.J., Lee, R.J., "Tool Heat Transfer Analysis in RTM", International Polymer Processing, Vol. 4, 1995, pp. 364–373.

46. Dessenberger, R.B., Tucker III, C.L., "Thermal Dispersion in RTM", Polymer Composites, Vol.16, 1995, pp. 495–506.

47. Dessenberger, R.B., Tucker III, C.L., "Governing Equations for Flow and Heat Transfer in Stationary Bed", in: S.G. Advani (Ed.), Flow and Rheology in Polymer Composite Manufacturing, Elsevier, Amsterdam, 1994, pp. 257–323.

48. Antonucci, V., Giordano, M., DiVita, G., Nicolais, L., "A Simulation of the Non- Isothermal Resin Transfer Molding Process", Polymer Engineering Science, Vol. 40, No. 12, 2000, pp. 2471-2481.

49. Lim, S.T., Lee, W.I., "Analysis of the Three-Dimensional Resin Transfer Mold Filling Process", Composite Science Technology, Vol. 60, 2000, pp. 961–975.

50. Calado, V., Advani, S.G., "Thermoset Resin Cure Kinetics and Rheology", in: Transport Processes In Composites, A. Loos, R. Dave (Eds.), A Review of Cure Kinetics and Chemorheology for Thermoset Resins in Transport Processes in Composites, 2000, pp. 32–107.

51. Michaud, D., "Simulation-Based Design Optimization and Control of Thick Composite Laminates Manufactured by Resin Transfer Molding", Ph.D. Thesis, University of Delaware, Newark, DE, 2000.

52. Bogetti, T.A., Gillespie J.W. Jr., "Process-Induced Stress and Deformation in Thick-Section Thermoset Composite Laminates", Journal of Composite Materials, Vol. 26, 1992, pp. 626–660.

53. Tucker III, C.L., "Heat Transfer And Reaction Issues In Liquid Composite Molding", Polymer Composites, Vol. 17, 1996, pp. 60–72.

54. Ngo, N.D., Tamma, K.K., "Non-Isothermal Three-Dimensional Developments and Process Modeling of Composites: Flow/Thermal/Cure Formulations and Experimental Validations", Computer Modeling Engineering Science, Vol. 1, 2000, pp. 57–72.

55. Chang, W., Kikuchi, N., "Analysis of Non-Isothermal Mold Filling Process in Resin Transfer Molding (RTM) Structural Reaction Injection Molding (SRIM)", Composite Mechanics, Vol. 16, 1995, pp. 22–35.

56. Lee, L.J., Young, W.B., Lin, R.J., "Mold Filling and Cure Modeling of RTM and SRIM Processes", Composite Structures., Vol. 27, 1994, pp. 109–120.

57. Mohan, R.V., Ngo, N.D., Tamma, K.K., Fickie, K.D., "On a Pure Finite Element Based Methodology for Resin Transfer Mold Filling Simulations", Proceedings of the Ninth International Conference on Numerical Methods in Thermal Problems, Part 2, 1995, pp. 1287–1310.

58. Dessenberger, R.B., Tucker, C.L., "Heat Dispersion in Resin Transfer Molding", ASME Eng. Cong. Exposition, 1994, pp. 21–40.

59. Hsiao, K.-T., Laudorn, H., Advani, S.G., "Experimental Investigation of Heat Dispersion due to Impregnation of Viscous Fluids in Heated Fibrous Porous Media during Composites Processing", ASME Journal of Heat Transfer, Vol. 123, 2000, pp. 178–187.

60. Howe, C.A., Paton, R.J., and Goodwin, A.A.,"A Comparison between Voids in RTM and Prepreg Carbon/Epoxy Laminates", Composites Processing and Microstructures, Vol. 4, pp. 46-54.

61. Lundström, T.S., Gebart, B.R., Lundemo, C.Y., "Void formation in RTM", Journal of Reinforced Plastics and Composites, Vol. 12, No. 12, 1993, pp. 1339-1349.

62. Lundström, T.S., Gebart, B.R., "Influence from Process Parameters on Void Formation in Resin Transfer Molding", Polymer Composites, Vol. 15, No. 1, 1994, pp. 25-33.

63. Young, W.B., Tseng, C.W., "Study on the Pre-Heated Temperatures and Injection Pressures of the RTM Process", Journal of Reinforced Plastics and Composites, Vol. 13, 1994, pp. 467-475.

64. Hayward, J.S., Harris, B., "Effect of Process Variables on the Quality of RTM Mouldings", SAMPE Quarterly, Vol. 26, 1990, pp. 39-46.

65. Patel, N., Rohatgi, V., Lee, L.J., "Micro Scale Flow Behavior and Void Formation Mechanism during Impregnation through a Unidirectional Stitched Fiberglass Mat", Polymer Engineering & Science, Vol. 35, No. 10, 1995, pp. 837-851.

66. Chen, Y.T., Davis, H.T., Macosko, C.W., "Wetting of Fibers Mats for Composites Manufacturing: I. Visualization Experiments", AIChE Journal, American Institute of Chemical Engineers, Vol. 41, No, 10, 1995, pp. 2261-2273.

67. Mahale, A.D., Prud'Homme, R.K., Rebenfeld, L., "Quantitative Measurement of Voids Formed during Liquid Impregnation of Non-woven Multifilament Glass Networks using an Optical Visualization Technique", Polymer Engineering & Science, Vol. 32, No. 5, 1992, pp. 319-326.

68. Sadiq, T.A.K., Advani, S.G., Parnas, R.S., "Experimental Investigation of Transverse Flow through Aligned Cylinders", International Journal of Multiphase Flow, Vol. 21, No. 5, 1995, pp. 755-774.

69. Chan, A.W., Morgan, R.J., "Modeling Preform Impregnation and Void Formation in Resin Transfer Molding of Uni-Directional Composites," SAMPE Quarterly, No. 23, 1992, pp. 48-52.

70. Chan, A.W., Morgan, R.J., "Tow Impregnation during Resin Transfer Molding of Bi-directional Non-woven Fabrics", Polymer Composites, Vol. 14, No. 4, 1993, pp. 335-340.

71. Phelan, F. R. Jr., Leung, Y., Parnas, R., "Modeling of Microscale Flow in Unidirectional Fibrous Porous Media", Proceedings of the American Society for Composites, Technical Conference, No. 8, 1993, pp. 85-96.

72. Patel, N., Rohatgi, V., Lee, L.J., "Influence of Processing and Material Variables on Resin-Fiber Interface in Liquid Composite Molding", Polymer Composites, Vol. 14, No. 2, 1993, pp. 161-172.

73. Lebrun, G., Gauvin, R., Kendall, K.N., "Experimental Investigation of Resin Temperature and Pressure during Filling and Curing in a Flat Steel RTM Mould", Composite Part A, Vol. 27A, 1996, pp. 347-355.

74. Lebrun, G., Gauvin, R., "Heat Transfer Analysis in a Heated Mold during the Impregnation Phase of the Resin Transfer Molding Process", Journal of Materials Processing and Manufacturing Science, Vol. 4, 1995, pp. 81-103.

75. Dutiro, C., "Factors affecting Surface Finish of RTM Products", M.Sc Thesis, Imperial College of Science, Technology and Medicine, University of London, September 1995.

76. Bayldon, J.M., "An in-depth Study of Surface Finish in Resin Transfer Moulding", M.Sc Thesis, Imperial College of Science, Technology and Medicine, University of London, September 1996.

77. Neitzel, M., Blinzler, M., Edelmann, K., Hoecker, F., "Surface Quality Characterization of Textile-Reinforced Thermoplastics", Polymer Composites, Vol. 21, No. 4, 2000, pp. 630-635.

78. Gordon, S., Boukhili, R., Trochu, F., "The Effect of Low Profile Additives on the Surface Aspects of RTM Molded Composites" Proceedings of third Canadian International Composite Conference, Montreal, Canada, 21st –24th August, 2001.

79. Yu, T.L., Sun, "Effects of Low Profile Additives on the Curing Reaction of Unsaturated Polyester Resins", Journal of applied polymer science, Vol. 57, 1995, pp. 7-23.

80. Kinekelaar, M., Wang, B., Lee, L.J., "Shrinkage Behavior of Low Profile Unsaturated Polyester Resins", Polymer, Vol. 35, No. 14, 1994, pp. 3011-3032.

81. Huang, Y., Liang, C., "Volume Shrinkage Characteristics in the Cure of Low Shrink Unsaturated Polyester Resins", Polymer, Vol. 37, No. 3, 1996, pp. 401-412.

82. Hill, R.R. Jr., Muzumdar, S.V., Lee, L.J., "Analysis of Volumetric Changes of Unsaturated Polyester Resins During Curing", Polymer Engineering and Science, Vol. 35, No. 10, 1995, pp. 852-859.

83. Li, C., Potter, K., Wisnom, M.R., Stringer, G., "In-Situ Measurement of Chemical Shrinkage of MY750 Epoxy Resin by a Novel Gravimetric Method", Composite Science and Technology, Vol. 64, 2004, pp. 55-64.

84. Han, S., Wang, K.K., Hieber, C.A., "Characterization of the Rheological Properties of a Fast Curing Epoxy Molding Compound", Journal of Rheology, Vol. 41, No. 2, 1997, pp. 177-195.

85. Ninan, N.K., Reghunadhan, C.P., "Rheological Cure Characterization of Phosphate –Triazine Polymers", Journal of Applied polymer Science, Vol. 88, 2003, pp. 908-914.

86. Rocks, J., Halter, M., George, G., Vohwinkel, F., "Calorimetric and Rheological Characterization of a High Performance Epoxy Curable at Low Temperatures", Polymer International, Vol. 52, 2003, pp. 1749-1757.

87. Jiang, D., Zhang, C., Wang, B., "Optimum Arrangement of Gate and Vent Locations for RTM Process Design using a Mesh Distance based Approach", Composites Part A, Vol. 33, 2002, pp. 471-481.

88. Kang, M.K., Jung, J.J., Lee, W.I., "Analysis of Resin Transfer Molding Process with Controlled Multiple Gates Resin Injection", Composites Part A, Vol. 31, 2000, pp. 407-422.

89. Bickerton, S., Stadtfeld, H.C., Steiner, K.V., Advani, S.G., "Design and Application of actively Controlled Injection Schemes for Resin Transfer Molding", Composites science and technology 61, 2001, pp. 1625-1637.

90. Luo, J., Liang, Z., Zhang, C., Wang, B., "Optimum Tooling Design for Resin Transfer Molding with Virtual Manufacturing and Artificial Intelligence", Composites Part A, No. 32, 2001, pp. 877-888.

91. Rayle, J.W., and Cassil, D.W., "Advancements in Injection in-mold Coating Technology", Metal Finishing, Vol. 93, No. 9, 1995, pp. 41-46.

92. Matthews, F.L., Dutiro, C., Alaka, R.N., "Factors Controlling Surface Finish in Resin Transfer Molding", SAMPE Journal, Vol. 33, No. 5, 1997, pp. 19-24.

93. Lin, M.Y., Murphy, M.J., Hajn, H.T., "Resin Transfer Molding Process Optimization", Composites Part A, Vol. 31, No. 4, 2000, pp. 361-372.

94. Chang, J.C.I., "Aerospace Materials and Structural Research into the Next Millennium", Composites Applications and Design, Vol. 1, pp. 134-158.

95. Krenkel, W., Dollhopf, V., "RTM Processing of High Performance Composites", Proceedings of ICCM-11, 1997, Gold Coast, Australia.

96. Debolt, M.A., "Surface Finish Evaluation Method for Class A Composite Substrates", Proceedings of 36th International SAMPE Technical Conference, 2004, San Diego, USA.

97. Whitefield, R.J., "Non-Contact Optical Profilometer", Applied Optics, Vol. 14, No. 10, pp. 2480-2485.

98. SURFPAK-SV/PRO/SJ Surface Texture Parameter User's Manual, Mitutoyo Corporation, Japan.

99. Gong, H., Shushan, M., *Measurement of Surface Roughness,* China Measurement Publisher, 1998.

100. Hu, S., "Surface Finish of Automobile Composite Panels", Ph.D. Thesis, Concordia University, 2005.

101. Vilas, J.L., Laza, J.M., Garay, M.T., Rodriguez, M., Leon, L.M., "Unsaturated Polyester Resin Cure: Kinetic, Rheologic, and Mechanical-Dynamical Analysis. I. Cure Kinetics by DSC and TSR", Journal of Applied Polymer Science, Vol. 79, 2001, pp. 447-457.

102. Ramis, X., Salla, J.M., "Time-Temperature Transformation (TTT) Cure Diagram of an Unsaturated Polyester Resin", Journal of Polymer Science: Part B: Polymer Physics, Vol. 35, 1997, pp. 371-388.

103. Salla, J.M., Ramis, X., "Comparative Study of the Cure Kinetics of an Unsaturated Polyester Resin Using Different Procedures", Polymer Engineering and Science, Vol. 36, No. 6, 1996, pp. 835-851.

104. Yousefi, A., Lafleur, P.G., Gauvin, R., "Kinetic Studies of Thermoset Cure Reactions: A Review", Polymer Composites, Vol. 18, No. 2. 1997, pp. 157-168.

105. Halley, P.J., Mackay, M.E., "Chemo-rheology of Thermoset – An Overview", Polymer Engineering and Science, Vol. 36, No. 5, 1996, pp. 593-609.

106. Kamal, M.R., Sourour, S., "Kinetics and Thermal Characterization of Thermoset Cure", Polymer Engineering and Science, Vol. 13, No. 1, 1973, pp. 59-64.

107. Kamal, M.R., "Thermoset Characterization for Moldability Analysis", Polymer Engineering and Science, Vol. 14, No. 3, 1974, pp. 231-239.

108. Stevenson, J.F., "Free Radical Polymerization Models for Simulating Reactive Processing", Polymer Engineering and Science, Vol. 26, No. 11, 1986, pp. 746-759.

109. Atarsia, A., Boukhili, R., "Relationship between Isothermal and Dynamic Cure of Thermosets via iso-conversion Representation", Polymer Engineering and Science, Vol. 40, No. 3, 2000, pp. 607-620.

110. NG, H., Zloczower, I.M., "A Non-isothermal Differential Scanning Calorimetry Study of the Curing Kinetics of an Unsaturated Polyester System", Polymer Engineering and Science, Vol. 29. No. 16, 1989, pp. 1097-1102.

111. Han, C.D., Lee, D.S., "Analysis of the Curing Behavior of Unsaturated Polyester Resins Using the Approach of Free Radical Polymerization", Journal of Applied Polymer Science, Vol. 33, pp. 2859-2876.

112. Lee, D.S., Han, C.D., "The Effect of Resin Chemistry on the Curing Behavior and Chemo-rheology of Unsaturated Polyester Resin", Journal of Applied Polymer Science, Vol. 34, 1987, pp. 1235-1258.

113. Martin, J.L., Cadenato, J.M., Salla, J.M., "Comparative Studies on the Non-Isothermal DSC Curing Kinetics of an Unsaturated Polyester Resin Using Free Radicals and Empirical Models", Thermochimica Acta, Vol. 306, 1997, pp. 115-126.

114. Lee, L.J., "Curing of Compression Molded Sheet Molding Compound", Polymer Engineering and Science, Vol. 21, No. 8, 1981, pp. 482-492.

115. Hsieh, T.H., Su. A.C., "Cure Behavior of an Epoxy-Novolac Molding Compound", Journal of Applied Polymer Science, Vol. 44, No. 1, 1992, pp. 165-172.

116. Gonzales-Romero, V.M., Casillas, N., "Isothermal and Temperature Programmed Kinetic Studies of Thermosets", Polymer Engineering and Science, Vol. 29, No. 5, 1989, pp. 295-301.

117. Khanna, Y.P., Kumar, S.D., "Phenolic triazine (PT) Resins. II: Cure Characterization by Dynamic Melt Rheology and its Comparison to DSC", Polymer Engineering and Science, Vol. 30, No. 8, 1990, pp. 1171-1174.

118. Prime, R.B., "Differential Scanning Calorimetry of the Epoxy Cure Reaction", Polymer Engineering and Science, Vol. 13, No. 5, 1973, pp. 365-371.

119. Chiou, P., Letton, A., "Modeling the Chemo-rheology of an Epoxy Resin System Exhibiting Complex Curing Behavior", Polymer, Vol. 33, No. 18, 1992, pp. 3925-3931.

120. Ryan, M.E., "Rheological and Heat Transfer Considerations for the Processing of Reactive Systems", Polymer Engineering and Science, Vol. 24, No. 9, 1984, pp. 698-706.

121. Martin, G.C., Tungare, A.V., Gotro, J.T., "Modeling the Chemorheology of Thermosetting Resins during Processing", Polymer Engineering and Science, Vol. 29, No. 18, 1989, pp. 1279-1285.

122. Yang, Y.S., Suspene, L., "Curing of Unsaturated Polyester Resins: Viscosity Studies and Simulations in Pre-Gel State", Polymer Engineering and Science, Vol. 31, No. 5, 1991, pp. 321-332.

123. Roller, M.B., "A Critical Examination of the Prepreg Resin Flow Experiment", Polymer Engineering and Science, Vol. 16, No. 10, 1976, pp. 687-689.

124. Dusi, M.R., May, C.A., Seferis, J.C., "Predictive models as aids to thermoset resin processing", ACS Symposium Series, Chemorheology of Thermosetting Polymers, Vol. 47, 1983, pp. 301-318.

125. Vinogradov, G., Malkin, A.Ya., *Rheology of Polymers*, MIR Publishers, Moscow, 1977.

126. Lipshitz, S.D., Macosko, C.W., "Kinetics and Energetics of a Fast Polyurethane Cure", Journal of Applied Polymer Science, Vol. 21, No. 8, 1977, pp. 2029-2039.

127. Mijović, J., Lee, C.H., "A Comparison of Chemorheological Models for Thermoset Cure", Journal of Applied Polymer Science, Vol. 38, No. 12, 1989, pp. 2155-2170.

128. Castro, J.M., Lipshitz, S.D., Macosko, C.W., "Laminar Tube Flow with a Thermosetting Polymerization", AIChE Journal, Vol. 28, No, 6, 1982, pp. 973-980.

129. Castro, J.M., Macosko, C.W., "Studies of Mold Filling and Curing in the Reaction Injection Molding Process", AIChE Journal, Vol. 28, No. 2, 1982, pp. 250-260.

130. Kamal, M.R., "Thermoset Characterization for Moldability Analysis", Polymer Engineering & Science, Vol. 14, No. 3, 1974, pp. 231-239.

131. Mussati, F.G., Macosko, C.W., "Rheology of Network Forming Systems", Polymer Engineering and Science, Vol. 13, No. 3, 1973, pp. 236-240.

132. Martin, G.C., Tungare, A.V., Gotro, J.T., "Chemorheological Characterization of Thermoset Cure", Polymer Engineering and Science, Vol. 28, No. 16, 1988, pp. 1071-1075.

133. Pannone, M.C., Macosko, C.W., "Reaction Kinetics of a Polyurea Reaction Injection Molding System", Polymer Engineering and Science, Vol. 28, No. 10, 1988, pp. 660-669.

134. Martin, G.C., Tungare, A.V., Gotro, J.T., "Modeling Rheological and Dielectric Properties during Thermoset Cure", Advances in Chemistry Series, 1990, pp. 235-248.

135. Castro, J.M., Macosko, C.W., "Kinetics and Rheology of Polyurethane Reaction Injection Molding Systems", SPE Technical Papers, Vol. 26, 1980, pp. 434-438.

136. Lane, J.W., Seferis, J.C., Bachman, M.A., "Dielectric Modeling of the Curing Process", Polymer Engineering and Science, Vol. 26, No. , 1986, pp. 346-353.

137. Rocks, J., Halter, M., George, G., Vohwinkel, F., "Calorimetric and Rheological Characterization of a High Performance Epoxy Curable at Low Temperature", Polymer International, Vol. 52, No. 11, 2003, pp. 1749-1757.

138. Lane, J.W., Khattak, R. K., Dusi, M.R., "Evaluation of Dielectric Cure Models for an Epoxy-Amine Resin System", Polymer Engineering and Science, Vol. 29, No. 5, 1989, pp. 339-346.

139. Roller, M.B., "A Critical Examination of the Prepreg Resin Flow Experiment", Polymer Engineering and Science, Vol. 16, No. 10, 1976, pp. 687-689.

140. Castro, J.M., Macosko, C.W., "Kinetics and Rheology of Polyurethane Reaction Injection Molding Systems", SPE Technical Papers, Vol. 26, 1980, pp. 434-438.

141. Malkin A.Ya., Kulichikin, S.G., "Rheokinetics of Curing", Advances in Polymer Science, Vol. 101, 1991, pp. 217-257.

142. Lane, J.W., Seferis, J.C., Bachman, M.A., "Dielectric Modeling of the Curing Process", Polymer Engineering and Science, Vol. 26, No. , 1986, pp. 346-352

143. Kojima, C.J., Hushower, M.E., Morris, V.L., SPE ANTEC Technical Papers, Vol. 32, 1986, pp. 344-347.

144. Pahl, M.H., Hesekamp, D., "Curing Effects on Viscosity of Reactive Epoxy Adhesives" Rheology 93, 1993, pp. 97-104.

145. Han, C.D., Lem, K.W., "Chemorheology of Thermosetting Resins. I. The Chemorheology and Curing Kinetics of Unsaturated Polyester Resin", Journal of Applied Polymer Science, Vol. 28, 1983, pp. 3155-3183.

146. Han, C.D., Lem, K.W., "Chemorheology of Thermosetting Resins. 11. Effect of Particulates on the Chemorheology and Curing Kinetics of Unsaturated Polyester Resin", Journal of Applied Polymer Science, Vol. 28, 1983, pp. 3185-3206.

147. Han, C.D., Lem, K.W., "Chemorheology of Thermosetting Resins. 111. Effect of Low-Profile Additive on the Chemorheology and Curing Kinetics of Unsaturated Polyester Resin", Journal of Applied Polymer Science, Vol. 28, 1983, pp. 3207-3225.

148. Han, C.D., Lem, K.W., "Rheology of Unsaturated Polyester Resins. I. Effects of Filler and Low-Profile Additive on the Rheological Behavior of Unsaturated Polyester Resin", Journal of Applied Polymer Science, Vol. 28, 1983, pp. 743-762.

149. Tajima, Y.A., Crozier, D., "Thermokinetic Modeling of an Epoxy resin I. chemoviscosity", Polymer Engineering and Science, Vol. 23, No. 4, 1983, pp. 186-190.

150. Kenny, J.M., Trivisano, A., Berglund, L.A., SAMPE Journal, No. 27, 1991, pp. 39-45.

151. Park, S.J., Seo, M.K., Lee, J.R., Lee, D.R., "Studies on Epoxy Cured by Cationic Latent Thermal Catalysts: The effect of the Catalysts on the Thermal, Rheological and Mechanical Properties", Journal of Polymer Science Part A. Polymer Chemistry, Vol. 39, 2001, pp. 187-195.

152. Sundstrom, D.W., Burkett, S.J., "Rheology of Diallyl Phthalate Polymers below the Gel Point", Polymer Engineering and Science, Vo. 21, 1981, pp. 1108-1120.

153. Gordon, S., Boukhili, R., Trochu, F., "The Effect of Low Profile Additives on the Surface Aspects of RTM Molded Composites" Proceedings of third Canadian International Composite Conference, Montreal, Canada, 21st –24th August, 2001.

154. Yu, T.L., Sun, "Effects of Low Profile Additives on the Curing Reaction of Unsaturated Polyester Resins", Journal of applied polymer science, Vol. 57, 1995, pp 7-23.

155. Kinekelaar, M., Wang, B., Lee, L.J., "Shrinkage Behavior of Low Profile Unsaturated Polyester Resins", Polymer, Vol. 35, No. 14, 1994, pp. 3011-3032.

156. Huang, Y., Liang, C., "Volume Shrinkage Characteristics in the Cure of Low Shrink Unsaturated Polyester Resins", Polymer, Vol. 37, No. 3, 1996, pp. 401-412.

157. Bogetti, T.A., Gillespie J.W. Jr., "Process-Induced Stress and Deformation in Thick-Section Thermoset Composite Laminates", Journal of Composite Materials, Vol. 26, 1992, pp. 626–660.

158. Hill, R.R. Jr., Muzumdar, S.V., Lee, L.J., "Analysis of Volumetric Changes of Unsaturated Polyester Resins During Curing", Polymer Engineering and Science, Vol. 35, No. 10, 1995, 852-859.

159. Han, S., Wang, K.K., Hieber, C.A., "Characterization of the Rheological Properties of a Fast Curing Epoxy Molding Compound", Journal of Rheology, Vol. 41, No. 2, 1997, pp. 177-195.

160. Ninan, N.K., Reghunadhan, C.P., "Rheological Cure Characterization of Phosphate – Triazine Polymers", Journal of Applied polymer Science, Vol. 88, 2003; pp. 908-914.

161. Rocks, J., Halter, M., George, G., Vohwinkel, F., "Calorimetric and Rheological Characterization of a High Performance Epoxy Curable at Low Temperatures", Polymer International, Vol. 52, 2003, pp. 1749-1757.

162. Li, C., Potter, K., Wisnom, M.R., Stringer, G., "In-Situ Measurement of Chemical Shrinkage of MY750 Epoxy Resin by a Novel Gravimetric Method", Composite Science and Technology, Vol. 64, 2004, pp. 55-64.

163. Schoch, K.F., Panackal, P.A., Frank, P.P., "Real Time Measurement of Resin Shrinkage during Curing", Thermomechanica Acta, Vol. 417, 2004, 115-118.

164. Bartkus, E.J., Kroekel, C.H., "Low Shrink Reinforced Polyester Systems", Applied Polymer Symposia, No.15, 1970, pp.113-135.

165. Pattison, V.A., Hindersinn, R.R., Schwartz, W.T., "Mechanism of Low-Profile Behavior in Single-Phase Unsaturated Polyester Systems", Journal of Applied Polymer Science, Vol. 19, No. 11, 1975, pp. 3045-3050.

166. Atkins A.E., in Paul D.R., Newman, S., editors. *Polymer Blends*, Academic Press, New York, 1978, pp. 391-400.

167. Kinkelaar, M., Wang, B., Lee, L.J., "Shrinkage Behavior of Low Profile Unsaturated Polyester Resins", Polymer, Vol. 35, No. 14, 1994, pp. 3011-3022.

168. Li, W., Lee, J.L., "Shrinkage control of Low Profile Unsaturated Polyester Resins Cured at Low Temperatures", Polymer, Vol. 39, No. 23, 1998, pp. 5677-5687.

169. Li, W., Lee, J.L., "Low Temperature Cure of Unsaturated Polyester Resins with Thermoplastic Additives. I. Dilatometry and Morphology Study", Polymer, Vol. 41, 2000, pp 685-696.

170. Li, W., Lee, J.L., "Low Temperature Cure of Unsaturated Polyester Resins with Thermoplastic Additives II. Structure Formation and Shrinkage Control Mechanism", Polymer, Vol. 41, 2000, pp 697-710.

171. Cao, X., Lee, L.J., "Control of Shrinkage and Residual Styrene of Unsaturated Polyester Resins Cured at Low Temperature: I. Effects of Curing Agents", Polymer, No. 44, 2003, pp. 1893-1902.

172. Cao, X., Lee, L.J., "Effect of Co-promoter and Secondary Monomer on Shrinkage Control of Unsaturated Polyester (UP)/Styrene (St)/Low-Profile Additive (LPA) Systems Cured at Low Temperatures", Journal of Applied Polymer Science, Vol. 82, 2001, pp. 738-749.

173. Xu, L., Lee, L.J., "Effect of Nanoclay on Shrinkage Control of Low Profile Unsaturated Polyester (UP) Resin Cured at Room Temperature", Polymer, No. 45, 2004, pp. 7325-7334.

174. Bucknall, C., Davies, P. and Partridge, I., "Phase Separation in Styrenated Polyester Resin Containing a Poly (vinyl acetate) Low-Profile Additive", Polymer, Vol 26, No. 1, 1985, pp. 109-112.

175. Bucknall, C.B., Partridge, I.K., Phillips, M.J., "Mechanism of Shrinkage Control in Polyester Resins Containing Low Profile Additives", Polymer, Vol. 32, No. 4, 1991, pp. 636-640.

176. Zhang, Z., Zhu, S., "Microvoids in Unsaturated Polyester Resins containing Poly (vinyl acetate) and Composites with Calcium Carbonate and Glass Fibers", Polymer, Vol. 21, 2000, pp. 3861-3870.

177. Suspène, L., Fourquier, D., Yang, Y., "Application of Phase Diagrams in the Curing of Unsaturated Polyester Resins with Low-Profile Additives", Polymer, Vol. 32, No. 9, 1991, pp. 1593-1604.

178. Lucas, J., Borrjo, J., Williams, R., "Cure of Unsaturated Polyester Resins: 2. Influence of Low Profile Additives and Fillers on the Polymerazation Reaction, Mechanical Properties and Surface Rugosities", Polymer, Vol. 34, No. 9, 1993, pp. 1886-1890.

179. Hsu, C.P., Kinkelaar, P., Lee, L.J., "Effects of Thermoplastic Additives on the Cure of Unsaturated Polyester Resins", Polymer Engineering and Science, Vol. 31, No. 20, 1991, pp. 1450-1460.

180. Huang, Y.J., and Sue C.C., "Effect of Polyvinyl Acetate and Polymethyl Methacrylate Low Profile Additives on the Curing of Unsaturated Polyester Resins. Morphological Changes during Cure", Journal of Applied Polymer Science, Vol. 55, No. 2, 1995, pp. 323-342.

181. Huang, Y.J., and Sue C.C., "Effect of Polyvinyl Acetate and Polymethyl Methacrylate Low Profile Additives on the Curing of Unsaturated Polyester Resins. Curing Kinetics by DSC and FTIR", Journal of Applied Polymer Science, Vol. 55, No. 2, 1995, pp. 305-322.

182. Liu, C.J., Kiasat, M.S., Nijhof, A.H., Blokland, H.,Marissen, R., "The Effect of the Addition of a Low Profile Additive on the Curing Shrinkage of an Unsaturated Polyester Resin", Polymer Engineering and Science, Vol. 39, No. 1, 1999, pp. 18-25.

183. Kinkelaar, M., Muzumdar, S., Lee, L.J., "Dilatometric Study of Low Profile Unsaturated Polyester Resins", Polymer Engineering and Science, Vol. 35, No. 10, 1995, pp. 823-836.

184. Hsieh, Y.N., Yu, T.L., "Phase Separation of Unsaturated Polyester Resin Blended with Polyvinyl acetate", Journal of Applied Polymer Science, Vol. 73, 1999, pp. 2413-2428.

185. Boyard, N., Vayer, M., Sinturel, C., Delaunay, D., "Modeling PVTX Diagrams: Application to Various Blends Based on Unsaturated Polyester—Influence of Thermoplastic Additive, Fillers, and Reinforcements", Journal of Applied Polymer Science, No. 92, 2004, pp. 2976-2988.

186. Huang, Y., Liang, C., "Volume Shrinkage Characteristics in the Cure of Low Shrink Unsaturated Polyester Resins", Polymer, Vol. 37, No. 3, 1996, pp. 401-412.

187. Chan-Park, M.B, McGarry, F.J., "Tough Low Profile Additives in Sheet Molding Compound", Polymer Composites, Vol. 17, No. 4, 1996, pp. 537-547.

188. Dutiro, C., Matthews, F.L., Alaka, R.N., "Factors Controlling Surface Finish in Resin Transfer Molding", SAMPE Journal, Vol. 33, No. 5, 1997, pp. 19-24.

189. Meisel, R.M., "A planning Guide for More Successful Experimentation", ASQC Quality Congress Transaction, 1991, pp. 174-179.

190. Anthony, J., Kaye, M., *Experimental Quality*, Kluwer Academic Publishers, 1999, Massachusetts, USA.

191. Fisher, R.A., *Statistical Methods Experimental Design and Scientific Interface*, Oxford Science Publications, 1995, New York, USA.

192. Lucas, J., "How to Achieve a Robust Process using Response Surface Methodology", Journal of Quality Technology, Vol. 26, No. 4, 1994, pp. 248-260.

193. Box, G.E.P., Draper, N.R., *Empirical Model Building and Response Surfaces*, John Wiley and sons, 1987, New York, USA.

194. Baker, T.B., "The Evolution of a System for Teaching EVOP", ASQC Quality Congress Transactions, 1992, pp. 302-308.

195. Montgomery, D.C., "Using Factorial Design for Robust Process and Product Development", Quality Engineering, Vol. 3, No.2, 1991, pp. 193-205.

196. Sirvanci, M.B., Durmaz, H., "Variation Reduction by use of Designed Experiments", Quality Engineering, Vol. 5, No. 4, 1993, pp. 611-618.

197. Sheaffer, M., "How to Optimize and Control the Wire Bonding Process", Solid State Technology, 1990, pp. 119-123.

198. Bhote, K.R., "DOE – The Road to Quality", Management Review, 1988, pp. 27-33.

199. Bhote, K.R., "A Most Cost Effective Approach to DOE than Taguchi", ASQC Annual Congress Transactions, 1990, pp. 857-862.

200. Logothetis, N., "A Perspective on Shainin's Approach to Experimental Design for Quality Improvement", Quality and Reliability Engineering International, Vol. 6, 1990, pp. 195-202.

201. Amster, S., Tsui, K.L., "Counter Examples for the Component Search Procedure", Quality Engineering, Vol. 5, No. 4, 1993, pp. 545-552.

202. Bhote, K.R., "World Class Quality-Design of Experiments Made Easier, More Cost Effective than SPC", American Management Association, 1998, New York, USA.

203. Anthony, J., Cheng, A.H.Y., "Training for Shainin's Approach to Experimental Design using a Catapult", Journal of European Industrial Training, Vol. 27, No. 8, 2003, pp. 405-412.

204. ASI Publication, *Taguchi Methods: Implementation Manual*, American Supplier Institute, 1989, Michigan, USA.

205. Bendell, A., "Introduction to Taguchi Methodology", Proceedings of the 1988 European Conference, London, England, 1998, pp. 1-14.

206. Bryne, D., Taguchi, S., "The Taguchi Approach to Parameter Design", ASQC Quality Congress Transactions, 1986, pp. 168-178.

207. Phadke, S.M., *Quality Engineering Using Robust Design*, Prentice Hall, 1986, New Jersey, USA.

208. Taguchi, G., *Introduction to Quality Engineering*, Asian Productivity Organization, 1986, Michigan, USA.

209. Roy, R.K., *Design of Experiments using the Taguchi Approach: 16 Steps to Product and Process Improvement*, John Wiley and Sons, 2001, New York, USA.

210. Jean, M.D., Tzeng, Y.-F., "Use of Taguchi Methods and Multiple Regression Analysis for Optimal Process Development of High Energy Electron Beam Case Hardening of Cast Iron", Surface Engineering, Vol. 19, No. 2, 2003, pp. 150-156.

211. Tsai, C.S., Mort, N., "Simulation and Optimization in Manufacturing Systems using Taguchi Methods", Proceedings of UKACC International Conference on Controls, 1996, UK, pp.467-472.

212. Tarng, Y.S., Juang, S.C., Chang, C.H., "The Use of Grey-Based Taguchi Methods to Determine Submerged Arc Welding Process Parameters in Hard-facing", Journal of Materials Processing Technology, Vol. 128, 2002, pp. 1-6.

213. Caporaletti, L., Gillenwater, E., Jaggers, J., "The Application of Taguchi Methods to a Coil Spring Manufacturing Process", Production and Inventory Management Journal, Vol. 34, No. 4, 1993, pp. 22-27.

214. Anthony, J., Warwood, S., Kernandes, K., Rowlands, H., "Process Optimisation using Taguchi Methods of Experimental Design", Work Study, Vol. 50, No. 2, 2001, pp. 51-57.

215. Huang, M.C., Tai, C.C., "The Effective Factors in the Warpage Problem of an Injection Molded Part with a thin Shell Feature", Journal of Materials Processing Technology, Vol. 110, 2001, pp. 1-9.

216. Syrcos, G.P., "Die Casting Process Optimization using Taguchi Methods", Journal of Materials Processing Technology, Vol. 135, 2003, pp. 68-74.

217. Cheng, Y.J., Xiang, C., Tsung, H., Francis, T., "Optimization of Extrusion Blow Molding Processes using Soft Computing and Taguchi Method", Journal of Intelligent Manufacturing, Vol. 15, No. 5, 2004, pp. 625-634.

218. Lin, C.L., "The Taguchi Method and Grey Relational Analysis to Optimize Turning Operations with Multiple Performance Characteristics", Materials and Manufacturing Processes, Vol. 19, No. 2, 2004, pp. 209-220.

219. Huang, M.F., Lin, T.R., "Application of Grey-Taguchi Method to Optimize Drilling of Aluminum Alloy 6061 with Multiple Performance Characteristics", Materials Science and Technology, Vol. 20, No. 4, 2004, pp. 528-532.

220. Teicholz, E., Orr, J.N., *Computer Integrated Manufacturing Handbook*, McGraw-Hill, 1987, New York, USA.

221. Wille, R., 1990, "Landing Gear Weight Optimization using Taguchi Analysis", SAWE Journal, 1990, pp. 31-40.

222. Unal, R., Dean, E.B., "Taguchi Approach to Design Optimization for Quality and Cost – An Overview", Proceedings of 13th Annual Conference of the International Society of Parametric Analysts, New Orleans, LA, May 21-24, 1991.

223. Karbhari, V.M., Slotte, S.G., Steenkamer, D.A., Wilkins, D.J., "Effect of Material, Process and Equipment Variables on the Performance of Resin Transfer Molded Parts", Composites Manufacturing, Vol. 3, No. 3, 1992, pp 143-152.

224. Vallat, M.F., Schultz, J., Mauzac, C., Jacquin, M., "Characterization of the Surface of Bulk Molding Compounds", Polymers for Advanced Technologies, Vol. 10, 1999, pp. 237-243.

225. Kim, P.J., Lee, D.G., "Surface Quality and Shrinkage of the Composite Bus Housing Panel Manufactured by RTM", Composite Structures, Vol. 57, 2002, pp. 211-220.

APPENDIX A